Studies on cannabinoid effects in intestinal tissue and in neuroblastoma cells

William Rupert Sones

A thesis submitted in partial fulfilment of the requirements of the University of Hertfordshire for the degree of Doctor of Philosophy

April 2007

Abstract

The growing numbers of putative receptors and allosteric sites in which cannabinoids have been observed to act upon has called in to question the established action of cannabinoids through solely the CB_1 receptor.

CB_1 receptor mediated inhibition of electrically stimulated contraction of the guinea-pig ileum myenteric plexus-longitudinal muscle preparation (MPLM) has been elucidated but the influence of cannabinoids on chemically induced contraction has not been examined. Cannabinoids appeared to act through multiple pathways. Stimulus-evoked contractions by low concentrations of nicotine was blocked by a CB_1 receptor dependent mechanism while high nicotine concentrations showed CB_1 receptor independent blockade. Contraction evoked by stimulus of nicotinic receptors located at the nerve terminal of the excitatory motor neurones displayed CB_1 receptor independent inhibition while whole-cell electrophysiological recording showed a lack of WIN 55.212 stereoselectivity corroborating the suggested presence of a CB_1 receptor independent inhibitory pathway.

The intracellular mechanism through which cannabinoids modulate MPLM activity has yet to be established. Using whole-cell electrophysiological recordings in primary cultures of guinea-pig ileum myenteric AH neurones, cannabinoids appeared to inhibit Ca^{2+} currents through a $G_{i/o}$ coupled mechanism dependent upon either both CB_1 and CB_2 receptors or a novel receptor.

Guinea-pig ileum myenteric and NG108-15 neurones demonstrated interaction between cannabinoid and opioid signalling pathways in contractile and electrophysiological models. Interaction occurred at high agonist concentrations with data suggesting the existence of a more complex model than that of simply exhaustion of a shared intracellular messenger.

With the simultaneous abuse of multiple drugs of addiction becoming more common, investigation into the interaction of cannabinoids and other drugs of abuse in the reward pathway is needed. CP 55,940 induced no change in spontaneous action potential firing frequency in the ventral tegmental area (VTA) of rat coronal midbrain slices under blind whole cell patch clamp, suggesting cannabinoids may not act directly upon dopaminergic neurones within the VTA.

Acknowledgements

I would like to thank my supervisors, Areles Molleman and Mike Parsons, for their time, patience and constructive criticism throughout the past few years. I would also like to thank Iain Greenwood for his patience and continuous pestering, without which things would be very different.

Further thanks go to my fellow research students, Raj, Anita, Joanna and Dirk. You certainly made days in Hatfield much more colourful!

And finally, gratitude goes to Katy, for putting up with not having a daddy for far too long, and to my wife, for putting up with not having a husband.

Contents

Table of abbreviations

Δ^8-THC	Δ^8-Tetrahydrocannabinol
Δ^9-THC	Δ^9-Tetrahydrocannabinol
ω-CgTX	ω-Conotoxin
2-AG	2-Arachidonyl glycerol
5-HT	5-Hydroxytryptamine
Abn-CBD	Abnormal cannabidiol
AC	Adenylyl cyclase
ACh	Acetylcholine
ACSF	Artificial cerebral-spinal fluid
AM251	1-(2,4-Dichlorophenyl)-5-(4-iodophenyl]])-4-methyl-*N*-(1-piperidyl)pyrazole-3-carboxamide
AM281	*N*-(Morpholin-4-yl)-5-(4-iodophenyl)-1-(2, 4-dichlorophenyl)-4-methyl-1H-pyrazole-3-carboxamide
AM404	*N*-Arachidonoylphenolamine
AM630	6-Iodopravadoline
AMPA	α-Amino-3-hydroxy-5-methyl-4-isoxazole propionic acid
ANOVA	Analysis of variance
AP	Endogenous alkaline phosphatase
BK	Large conductance Ca^{2+}-activated K^+ channel
Calb	Calbindin
Calret	Calretinin
cAMP	Cyclic adenosine monophosphate

CBD	Cannabidiol
CCK	Cholecystokinin
cDNA	Complementary DNA
CGRP	Calcitonin-gene-related peptide
ChAT	Choline acetyltransferase
CHO cells	Chinese Hamster ovary cells
CNS	Central nervous system
CP 55,940	(-)-Cis-3-[2- hydroxy-4-(1,1-dimethylheptyl) phenyl]-trans-4-(3-hydroxypropyl) cyclohexanol
DALN	Desacetyl-levonantradol
DMEM	Dulbecco's modified Eagle's medium
EGTA	Ethylene glycol tetraacetic acid
ENK	Enkephalin
ERK	Extracellular signal-regulated kinases
FAAH	Fatty acid amide hydrolase
FAK	Focal adhesion kinase
FAN	Factor associated with neutral sphingomyelinase
FDA	U.S. Food and Drug Administration
GABA	γ-Amino butyric acid
GDP	Guanosine diphosphate
GIRK	G-protein coupled inwardly rectifying potassium channels
GlyR	Glycine receptor
GPRC	G-protein coupled receptor
GRP	Gastrin-releasing peptide
GTP	Guanosine triphosphate

GTPγS	Guanosine 5'-*O*-[γ-thio]triphosphate
HBSS	Hank's balanced salt solution
HEK 293	Human embryonic kidney cells
HU-210	11-Hydroxy-Δ^8-tetrahydrocannabinol-dimethylheptyl
HU-243	1,1-Dimethylheptyl-11-hydroxytetrahydrocannabinol
HVA	High voltage activated calcium current
ICC	Interstitial cells of Cajal
IK	Intermediate conductance Ca^{2+}-activated K^+ channel
IP_3	Inositol-1,4,5-triphosphate
JUN	Jun amino-terminal kinases
JWH-051	1-Deoxy-11-OH-Δ^8- tetrahydrocannabinol-dimethylheptyl
JWH-133	3-(1,1-Dimethylbutyl)-1-deoxy-Δ^8-tetrahydrocannabinol
K_{Ach}	Acetylcholine-evoked potassium current
K_{ir}	Ca^{2+}-activated, inwardly-rectifying potassium channel
L-NAME	N^G-Nitro-L-arginine methyl ester
LPS	Lipopolysaccharide
LY320135	4-[6-Methoxy-2-(4-methoxyphenyl)1-benzofuran-3-carbonyl]benzonitrile
MAPK	Mitogen-activated protein kinase
MEK	MAPK kinase
MEKK	MAPK kinase kinase
MPLM	Myenteric plexus-longitudinal muscle
mRNA	Messenger ribonucleic acid
MSNs	Medium-sized spiny neurones
NAcc	Nucleus accumbens

nAChR	Nicotinic acetylcholine receptor
NADA	*N*-Arachidonoyl-dopamine
NFP	Neurofilament protein triplet
NMDA	*N*-Methyl-D-aspartate
NMU	Neuromedin U
NO	Nitric oxide
NOS	Nitric oxide synthase
NPY	Neuropeptide Y
O-1918	1,3-Dimethoxy-5-methyl-2-[(1*R*,6*R*)-3-methyl-6-(1-methylethenyl)-2-cyclohexen-1-yl]benzene
O-2050	(6a*R*,10a*R*)-3-(1-Methanesulfonylamino-4-hexyn-6-yl)-6a,7 ,10,10a-tetrahydro-6,6,9-trimethyl-6H-dibenzo[b,d]pyran
PEA	Palmitoylethanolamide
PGE_1	Prostaglandin E_1
PI3K	Phosphatidylinositol-3-kinase
PKA	cAMP-dependent protein kinase A
PKC	Protein kinase C
PLA2	Phospholipase A2
PLC	Phospholipase C
PLD	Phospholipase D
PTX	Pertussis toxin
RT-PCR	Reverse transcription polymerase chain reaction
SAPK	Stress-activated kinases
S.E.M.	Standard error of the mean

SOM	Somatostatin
SP	Substance P
SR141716	Rimonabant; *N*-(piperidin-1-yl)-5-(4-chlorophenyl)-1-(2,4,-di-chlorophenyl)-4-methyl-1H-pyrazole-3-carboxamide hydrochloride
SR144528	5-(4-Chloro-3-methylphenyl)-1-[(4-methylphenyl)methyl]-*N*-[(1*S*,4*R*,6*S*)-1,5,5-trimethyl-6-bicyclo[2.2.1]heptanyl]pyrazole-3-carboxamide
TASK-1	Background (leak) K^+ channel
THC	Tetrahydrocannabinol
TRPV1	Transient receptor potential vanilloid 1
TTX	Tetrodotoxin
U-73122	1-[6-[[(17b)-3-Methoxyestra-1,3,5(10)-trien-17-yl]amino]hexyl]-1H-pyrrole-2,5-dione
VIP	Vasoactive intestinal polypeptide
VGCC	Voltage-gated calcium channels
VTA	Ventral tegmental area
WIN 54,461	6-Bromopravadoline
WIN 55,212-2	(*R*)-(+)-[2,3-Dihydro-5-methyl-3-(4-morpholinylmethyl)pyrrolo[1,2,3-de)-1,4-benzoxazin-6-yl]-1-napthalenylmethanone
WIN 55,212-3	(*S*)-(-)-WIN 55,212; [(3*S*)-2,3-Dihydro-5-methyl-3-(4-morpholinylmethyl)pyrrolo[1,2,3-de]-1,4-benzoxazin-6-yl]-1-naphthalenyl-methanone monomethanesulfonate

Table of figures

Figure 5.3 (b) Bar chart demonstrating modulation of spontaneous firing frequency in neurones within the VTA by dopamine and CP 55,940.

Chapter 1 - General Introduction

1. Chapter 1 - General Introduction

It is only recently with the discovery of cannabinoid receptors and endogenous ligands for these receptors that the importance of the endogenous cannabinoid system has come to be accepted in both physiological and pathophysiological conditions. Consequently, far greater understanding of the role that the cannabinoid system plays, and its interaction with other systems is required in order that full utilisation can be obtained in the treatment of pathological conditions.

1.1. Overview

Extracts from the hemp plant *Cannabis sativa* have been used for at least four thousand years for their therapeutic properties (reviewed by Mechoulam, 1986). The earliest of the Chinese pharmacopoeias, the Pên Ching, dating from the first century B.C., contained material describing the psychoactive properties of cannabis, while recommendations for relief from the symptoms of malaria, constipation, rheumatic pains and dysmenorrhoea have been found in a Chinese medical treatise dating from around 2600 B.C. (Abood and Martin, 1996; Grinspoon and Bakalar, 1993). Medicinal use in Europe did not emerge until the mid-nineteenth century when Irish scientist and physician W.B. O'Shaughnessy administered cannabis resin in an ethanolic solution to patients after observing its analgesic, antispasmodic, antiemetic and hypnotic properties with use in India. His report (O'Shaughnessy, 1843) generated considerable interest and use expanded rapidly with

full endorsement by one of Queen Victoria's physicians (Reynolds, 1890). However, variability in potency of preparations coupled with unpredictability in response and poor availability led to a steep decline in use. In 1925 the Geneva Convention on the manufacture, sale and movement of dangerous drugs imposed a limitation on the use of cannabis, restricting use for solely scientific and medicinal purposes. Prescription of cannabis in the UK was finally prohibited by the Misuse of Drugs Act (1971). Recreational use of cannabis developed a resurgence in the USA during the 1960's and 1970's, in a period of social turmoil, and illegitimate use has increased strongly since. Currently, cannabis is the most widely used recreational drug with 119,922 people in Britain charged with possession of cannabis in 2005/2006 (Thorpe and Robb, 2006).

Partly as a result of the discovery and appreciation of the endogenous cannabinoid system, a renewed interest has developed in the potential therapeutic use of cannabis and related compounds. Currently, Sativex, a blend of the entire aerial part of the cannabis plant formulated to contain tetrahydrocannabinol (THC) and cannabidiol (CBD) in a 1.08:1 ratio, was approved by Health Canada under a conditional licence for prescription use in April 2005 for the treatment of neuropathic pain in multiple sclerosis sufferers. Marinol (Dronabinol), a synthetic Δ^9-THC, was approved by the U.S. Food and Drug Administration (FDA) in 1985 for the treatment of nausea and vomiting associated with cancer chemotherapy. In 1992, the FDA approved the marketing of Marinol for the treatment of anorexia associated with weight loss in AIDS patients. The FDA has also approved nabilone (Cesamet), the synthetic (S,S) and (R,R) isomers of Δ^9-THC, for use in the prevention of nausea and vomiting that may occur after cancer treatments when other medicines are unsuccessful. Sanofi-Aventis have recently been granted permission

by the European Medicines Agency to market rimonabant (SR141716), the CB_1 cannabinoid receptor antagonist, within Europe for use as an anorectic anti-obesity drug. A large number of other potential therapeutic uses of cannabis and related compounds have been suggested including glaucoma, epilepsy, asthma and a number of psychiatric disorders.

Difficulties in medicinal use of these compounds do arise, with similar cognitive effects to recreational cannabis if taken in sufficient quantities. However, acute toxicity is low with the lethal dose to effective dose ratio, based upon extrapolation from mouse to man, of around 40,000:1 (Grinspoon and Bakalar, 1993). Large doses of cannabis have been linked with transient hallucination and delusion (Johns, 2001) but the effects on mental health of doses commonly taken are more debatable. Studies suggest a possible precipitation and exacerbation of schizophrenia and psychosis in vulnerable individuals (Hall *et al.*, 2004).

1.2. Cannabinoid receptor ligands

The term "cannabinoid" was originally given as a collective name for the C_{21} terpenophenolic compounds that naturally occur in *Cannabis sativa*, with (−)-Δ^9-*trans*-(6aR,10aR)-tetrahydrocannabinol (Δ^9-THC) being the most psychologically active constituent (Mechoulam and Gaoni, 1967). The development of synthetic compounds which closely mimicked the properties of these cannabinoids and the discovery of chemically different endogenous cannabinoid receptor ligands have prompted the use of the terms "phytocannabinoids" to describe plant-derived cannabinoids and "endocannabinoid" to describe endogenous cannabinoids (Pate, 1999). On the basis of chemical structure, cannabinoids have been divided into four main groups: classical, nonclassical, aminoalkylindole, and endocannabinoid.

1.2.1. Classical cannabinoids

Classical cannabinoids describe a group consisting of dibenzopyran derivatives and are either plant-derived or their synthetic analogues. These include the psychotropic ingredients in *C. sativa* (phytocannabinoids) notably Δ^9-tetrahydrocannabinol (Δ^9-THC), Δ^8-THC and cannabinol (Figure 1.1), and the synthetic cannabinoids. Notable examples of which include 11-hydroxy-Δ^8-THC-dimethylheptyl (HU-210) and desacetyl-L-nantradol (Gaoni and Mechoulam, 1964; Figure 1.2). Δ^9-THC, first isolated by Gaoni and Mechoulam (1964), is considered to be the predominant of at least 66 psychotropic constituents of cannabis (ElSohly, 2002). It undergoes significant binding to cannabinoid

receptors at submicromolar concentrations, with similar affinities for CB_1 and CB_2 receptors (CB_1 receptor K_i ranging between 35.3 and 80.3 nM, and CB_2 receptor K_i between 3.9 and 75.3 nM; Rinaldi-Carmona *et al.*, 1994; Felder *et al.*, 1995; Bayewitch *et al.*, 1996; Showalter *et al.*, 1996; Rhee *et al.*, 1997). At both cannabinoid receptors Δ^9-THC behaves as a partial agonist with the size of its maximal effect falling far below that of other CB_1 agonists, such as CP 55,940 and WIN 55,212-2 (Gérard *et al.*, 1991; Breivogel *et al.*, 1998; Griffin *et al.*, 1998). Δ^9-THC exhibits such reduced efficacy that it has been shown to behave as a cannabinoid receptor antagonist in a bioassay system and in hippocampal cultures, expressing an IC_{50} close to its K_i (Bayewitch *et al.*, 1996; Kelly and Thayer, 2004). A marked stereoselectivity has been demonstrated for Δ^9-THC and HU-210 with *cis* 6a,10a isomers displaying an activity less than 1% of that possessed by the *trans* isomer (Herkenham *et al.*, 1990; Matsuda *et al.*, 1990; Felder *et al.*, 1992). The first generation classical cannabinoids displayed a lack of CB_1/CB_2 selectivity. However, minor alterations to the THC molecule enabled the generation of CB_2-selective agonists, an example being 1-deoxy-11-OH-Δ^8-THC-dimethylheptyl (JWH-051; Huffman *et al.*, 1996), which retained affinity for the CB_1 receptor but gained a marked increase in affinity for the CB_2 receptor (CB_1 receptor K_i 1.2 nM, CB_2 receptor K_i 0.032 nM; Huffman *et al.*, 1996).

1.2.2. Nonclassical cannabinoids

The second group, developed by Pfizer, USA, possess a similar structure to classical cannabinoids, consisting of bicyclic and tricyclic analogues of Δ^9-THC but missing the dihydropyran ring (Johnson and Melvin, 1986). Examples include CP 55,940 that possesses less lipophilicity than THC, enabling Devane *et al.* (1988) to demonstrate specific binding sites within the rat brain that led to the discovery of the CB_1 receptor. CP 55,940 expresses the same low nanomolar range affinity for both CB_1 and CB_2 receptors (CB_1 receptor K_i ranging between 0.5 and 5 nM, and CB_2 receptor K_i between 0.69 and 2.8 nM; Ross *et al.*, 1999; Rinaldi-Carmona *et al.*, 1994; Felder *et al.*, 1995; Showalter *et al.*, 1996; Hillard *et al.*, 1999) and displays a relatively high efficacy *in vivo* being 10 to 50 times more active than Δ^9-THC in the mouse tetrad model (Johnson and Melvin, 1986; Little *et al.*, 1988). Like classical cannabinoids, nonclassical cannabinoids exhibit significant stereoselectivity (Little *et al.*, 1988; Herkenham *et al.*, 1990; Melvin *et al.*, 1993).

1.2.3. Aminoalkylindoles

Developed by Sterling Winthrop, USA, this group is structurally very different when compared with classical and nonclassical cannabinoids, being made up of a series of structurally constrained analogues of pravadoline (Bell *et al.*, 1991; Pacheco *et al.*, 1991). The frequently used cannabinoid agonist WIN 55,212-2 is a member of this group. WIN 55,212-2 displays a low nanomolar range affinity for both cannabinoid receptors,

although it possesses a slightly greater affinity for the CB_2 receptor (CB_1 receptor K_i ranging between 4.4 and 123 nM, and CB_2 receptor K_i between 0.28 and 16.2 nM; Rinaldi-Carmona *et al.*, 1994; Felder *et al.*, 1995; Showalter *et al.*, 1996; Hillard *et al.*, 1999; Shire *et al.*, 1996). It possesses a relatively high efficacy at both CB_1 and CB_2 receptors (Bouaboula *et al.*, 1997; Griffin *et al.*, 1998; Tao and Abood, 1998; Pertwee, 1999). Efficacy has been shown to be enantioselective with the *R*-(+)-enantiomer, WIN 55,212-2, being more active than the *S*(-)-enantiomer, WIN 55,212-3, in inhibiting adenylyl cyclase (EC_{50} 0.3 and 10 mM respectively; Pacheco *et al.*, 1991).

1.2.4. Endocannabinoids

With the discovery of mammalian cannabinoid receptors, the search began for the release of an endogenous receptor agonist. Arachidonyl ethanolamine amide (anandamide) was initially isolated from porcine brain by a team led by Prof. Mechoulam (Devane *et al.*, 1992). This lipophilic molecule was found to readily displace [^{3}H]-HU-243 from rat brain membranes with a K_i of 52 nM and inhibit electrically evoked contractions of the mouse isolated vas deferens with a similar EC_{50}. Anandamide possesses a slightly greater affinity for the CB_1 receptor (CB_1 receptor K_i ranging between 52 and 543 nM, and CB_2 receptor K_i between 279 and 1940 nM; Lin *et al.*, 1998; Showalter *et al.*, 1996; Felder *et al.*, 1995; Hillard *et al.*, 1999; Mechoulam *et al.*, 1995) and behaves as a partial agonist at cannabinoid receptors, inhibiting Ca^{2+} currents in whole-cell voltage clamped N18 neuroblastoma cells to an extent 55% less efficacious than that of WIN 55,212-2 (Mackie

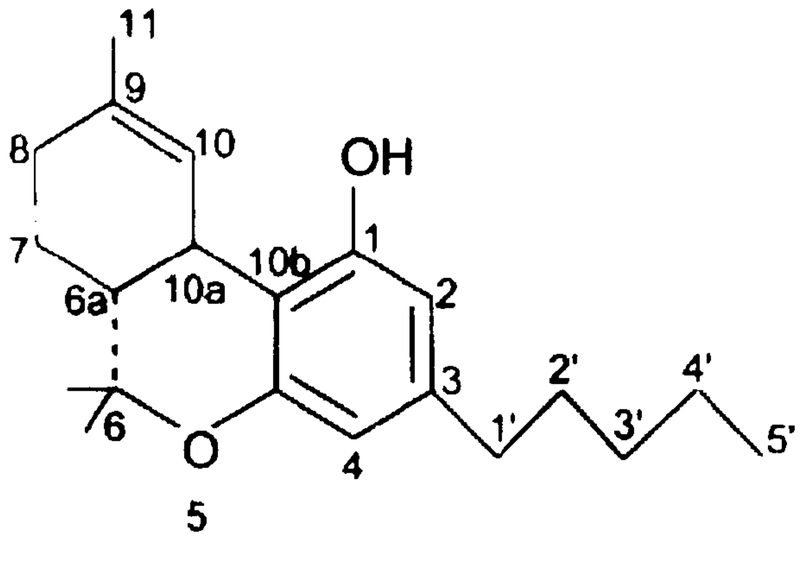

Δ^9-Tetrahydrocannabinol

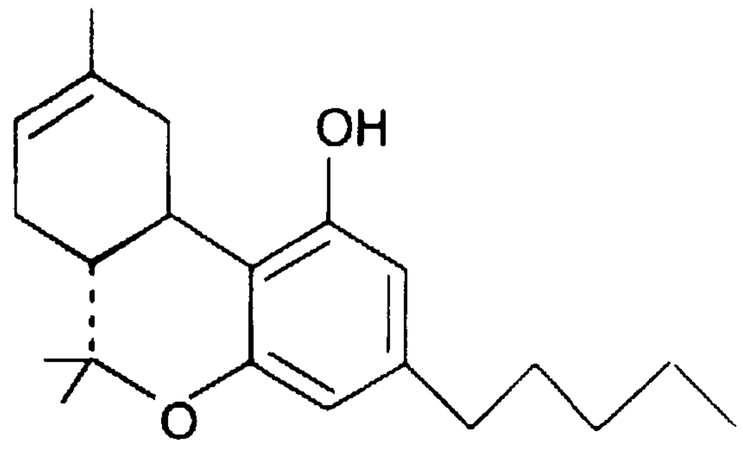

Δ^8-Tetrahydrocannabinol

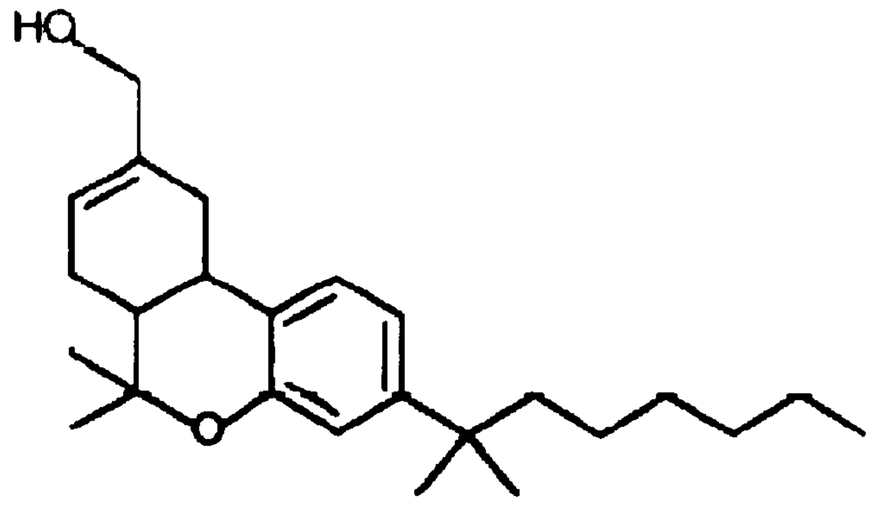

1-deoxy-11-OH-Δ^8-THC-dimethylheptyl
(1-deoxy-HU-210 or JWH-051)

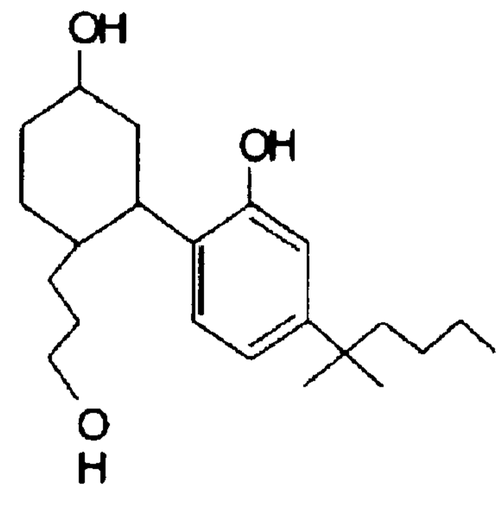

CP-55,940

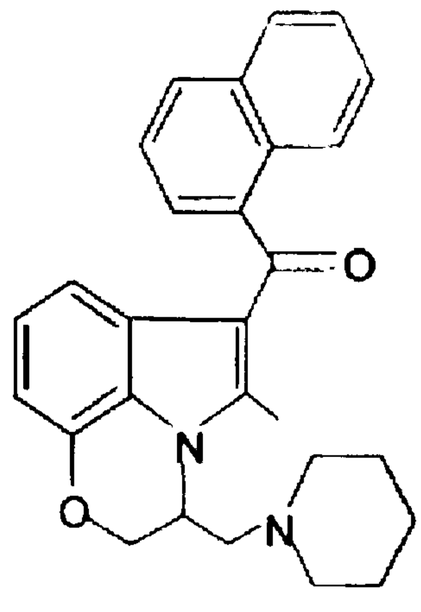

WIN 55,212-2

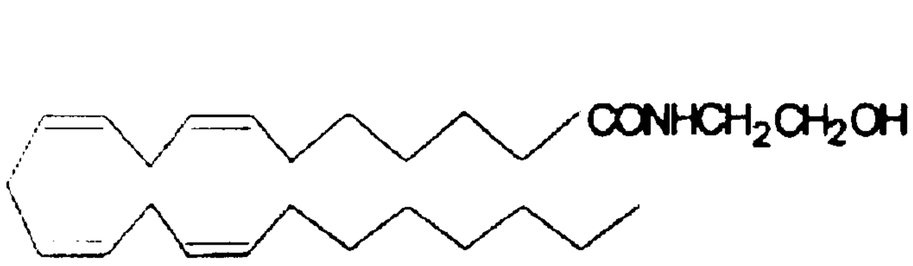

Anandamide

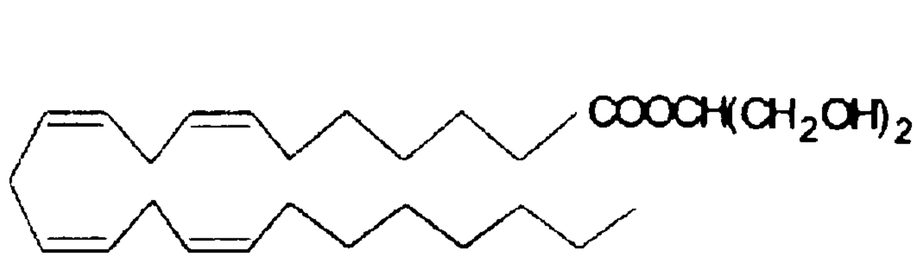

2-Arachidonylglycerol

Figure 1.1 Cannabinoid agonists.

et al., 1993). Anandamide has also been shown to activate the TRPV1 (vanilloid) receptor, as first noted by Di Marzo *et al.* (1998). 2-arachidonyl glycerol (2-AG), discovered in canine gut and rat brain in 1995, possesses a similar binding affinity for the CB_1 and CB_2 receptors (CB_1 receptor K_i ranging between 58.3 and 472 nM, and CB_2 receptor K_i between 145 and 1400 nM; Ben-Shabat *et al.*, 1998; Mechoulam *et al.*, 1995; Sugiura *et al.*, 1995) and exhibits a greater relative intrinsic activity than anandamide at both CB_1 and CB_2 receptors (Gonsiorek *et al.*, 2000; Savinainen *et al.*, 2001). Both endocannabinoids have displayed susceptibility to metabolism via hydrolysis and oxidation; the most studied being fatty acid amide hydrolase (FAAH)-mediated hydrolysis (McKinney and Cravatt, 2005). More recently an ether-linked analogue of 2-AG, 2-arachidonyl-glyceryl ether (noladin), was isolated from porcine brain. It differed from anandamide and 2-AG by expressing very little affinity for the CB_2 receptor (CB_1 receptor K_i 21.2 nM, and CB_2 receptor K_i >3000 nM; Hanus *et al.*, 2001) and possessed less relative intrinsic activity at the CB_1 receptor than 2-AG (Savinainen *et al.*, 2001). *O*-arachidonoyl-ethanolamine (virodhamine), discovered by Porter *et al.* (2002), displayed partial agonism at the CB_1 receptor and full agonism at the CB_2 receptor. The weak agonist efficacy enabled virodhamine to inhibit the action of anandamide at the CB_1 receptor, suggesting it may play a putative role as an antagonist within the endogenous system (Porter *et al.*, 2002). A recent study investigating activity cAMP formation at the human neocortical CB_1 receptor found virodhamine behaved as a antagonist/inverse agonist (Steffens *et al.*, 2005). The final member of this group, *N*-arachidonoyl-dopamine (NADA), was first detected in both rat and bovine brain, with highest concentrations in striatum and hippocampus (Huang *et al.*, 2002). Bisogno *et al.* (2000) demonstrated a

binding selectivity for the CB_1 receptor over the CB_2 receptor as well as greater efficacy than anandamide in stimulating intracellular Ca^{2+} mobilization in undifferentiated N18TG2 neuroblastoma cells. NADA has been shown to share ability with anandamide to activate TRPV1 receptors (Huang *et al.*, 2002). Palmitoylethanolamide (PEA), a shorter and fully saturated analogue of anandamide, is produced through a similar route to anandamide and can be co-released with anandamide from depolarised neurones (Di Marzo *et al.*, 1994; Izzo *et al.*, 2000). Unlike anandamide, PEA does not bind efficiently to the CB_1 and CB_2 receptors (Lambert and Di Marzo, 1999). PEA has been shown to exhibit antinociceptive activity in the mouse abdominal stretch test and formalin paw test in a mechanism susceptible to SR144528 antagonism (Calignano *et al.*, 1998; 2001). A putative "CB_2-like" receptor has been suggested to be responsible (Pertwee, 2004).

1.2.5. Cannabinoid receptor antagonists

Developed by Sanofi, the diarylpyrazole, SR141716 (rimonabant) was the first highly potent and selective CB_1 receptor antagonist (CB_1 receptor K_i ranging between 1.98 and 12.3 nM, and CB_2 receptor K_i between 702 and 13,200 nM; Felder *et al.*, 1998; Felder *et al.*, 1995; Showalter *et al.*, 1996; Rinaldi-Carmona *et al.*, 1994). It has been shown to readily displace CP 55,940 from selective binding sites and prevent typical cannabinoid effects both *in vivo* and *in vitro* (Rinaldi-Carmona *et al.*, 1994). Other diarylpyrazole CB_1 antagonists include AM251 and AM281 possessing minor structural differences from SR141716. SR144528, another diarylpyrazole developed by Sanofi, has demonstrated a greater binding affinity for the CB_2 receptor as opposed to the CB_1 (CB_1 K_i ranging

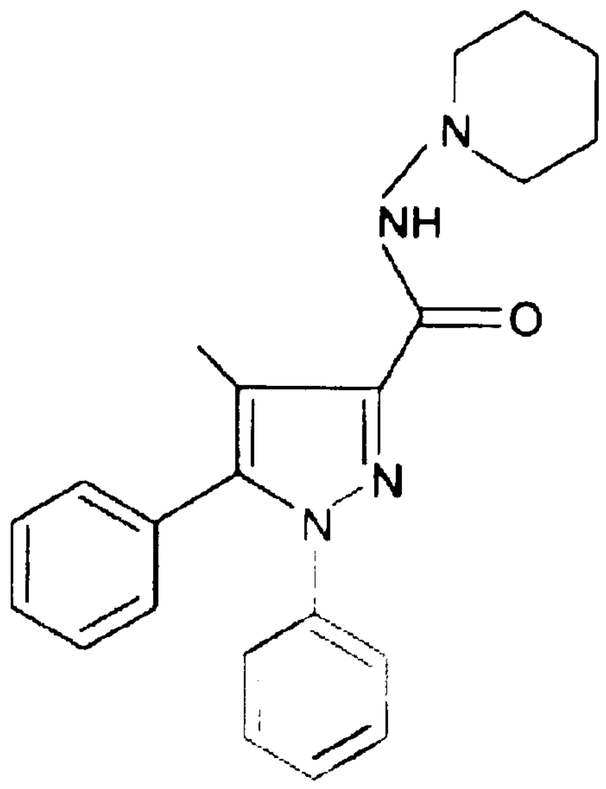

SR141716A

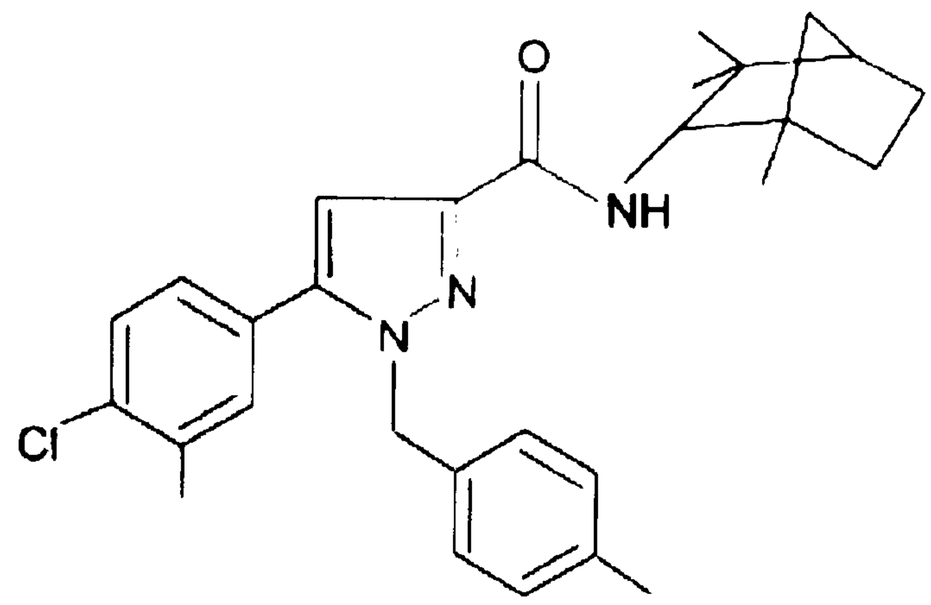

SR144528

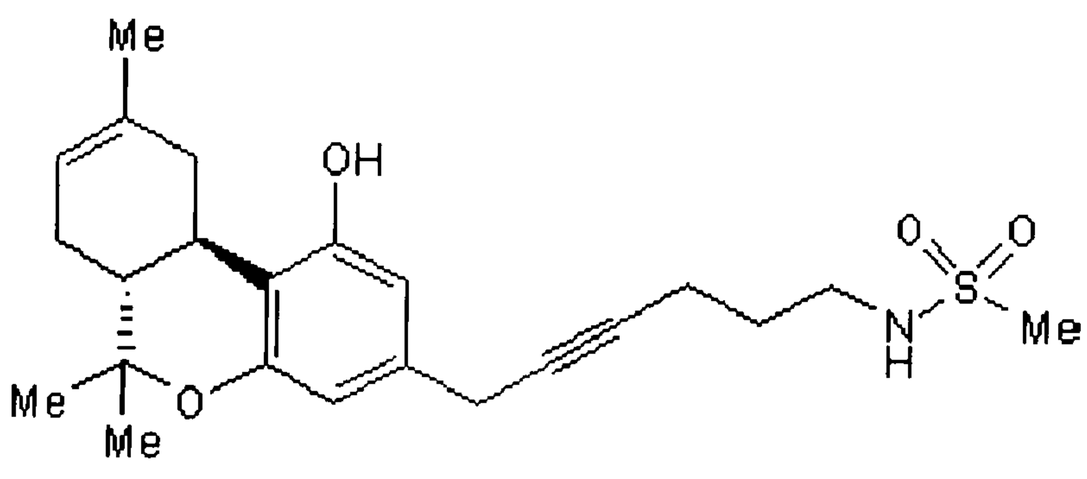

O-2050

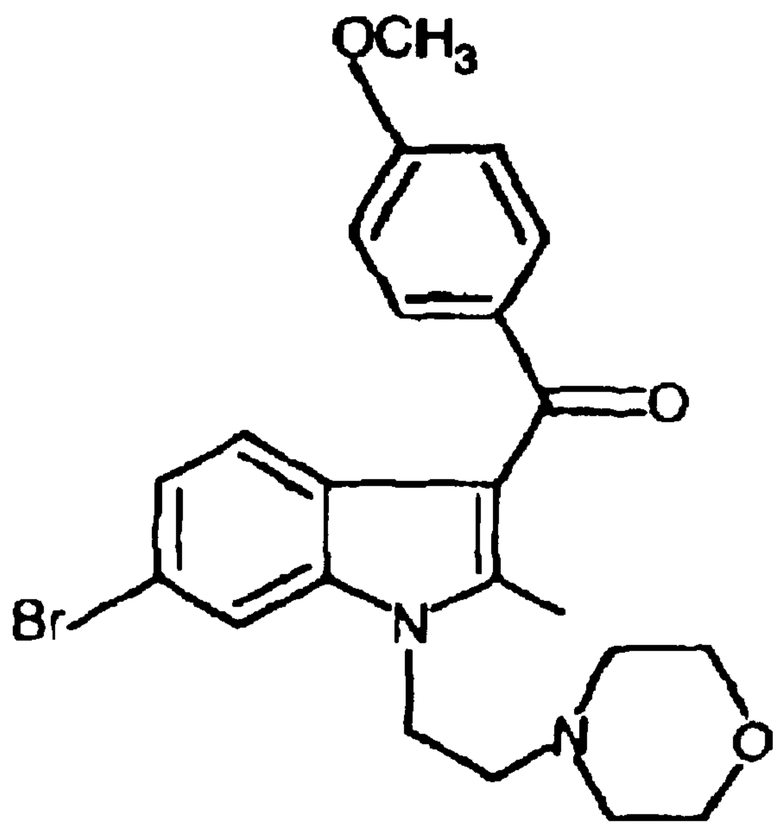

6-Bromopravadoline
(WIN 54,461)

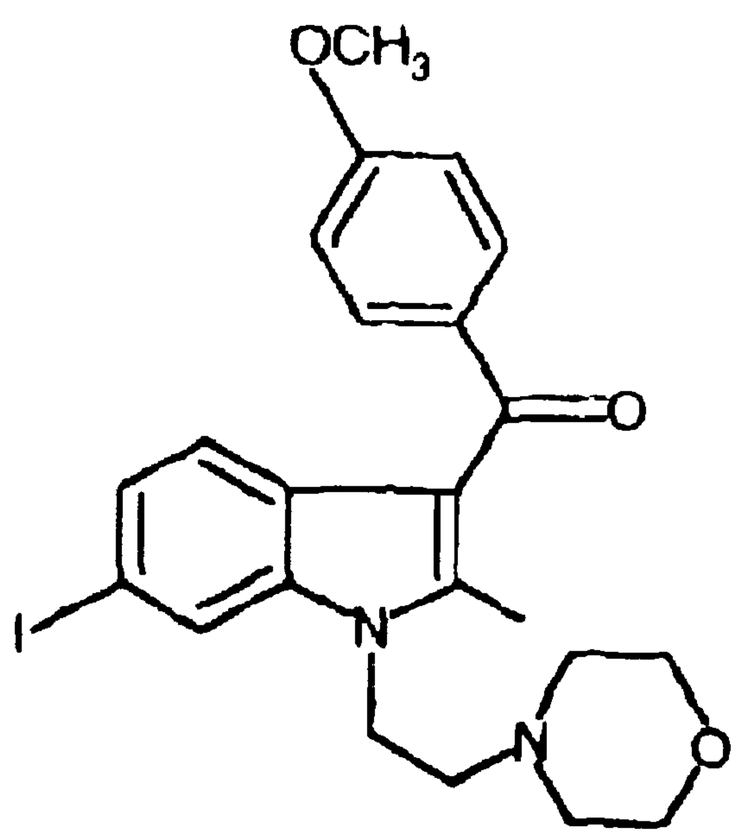

6-Iodopravadoline
(AM630)

Figure 1.2 Cannabinoid receptor antagonists.

between 305 and >10,000 nM, and CB_2 K_i between 0.30 and 5.6 nM; Rinaldi-Carmona *et al.*, 1998; Ross *et al.*, 1999). As well as attenuating the effects of cannabinoid agonists, these compounds have been found to produce opposing effects, at least in some preparations, to that produced by cannabinoid agonists (Bass *et al.*, 2002; Coutts *et al.*, 2000; MacLennan *et al.*, 1998; Pertwee, 2005). It has been postulated that this opposing action could be due to antagonism of cannabinoid receptor activity evoked by an endogenously released endocannabinoid. However, the observance of inverse cannabimimetic effects in the absence of any endogenous cannabinoid release prompted the hypothesis of 'inverse agonism' in which cannabinoid receptors exist in what can be described by a "two-state model". According to this model, receptors exist in a constitutively active state with some degree of coupling to effector mechanisms occurring in the absence of an agonist. The presence of a cannabinoid agonist would evoke a change in receptor state resulting in an increase in receptor activity whilst an 'inverse agonist' would induce the receptor to adopt a less active state resulting in a decrease in activity (Pertwee, 2005). Consistent with this hypothesis is the recent development of 'neutral' competitive CB_1 receptor antagonists. An example of this is O-2050, a sulphonamide analogue of Δ^8-tetrahydrocannabinol, which displayed high CB_1 receptor affinity (K_i 2.5 nM) and did not elicit any inverse agonism in mouse vas deferens (Martin *et al.*, 2002). Developed by Eli Lilly, the substituted benzofuran LY320135, although selective for the CB_1 receptor, possessed much lower affinity for the receptor than SR141716 (CB_1 *Ki* 141 nM, and CB_2 *Ki* 14.9 μM; Felder *et al.*, 1998) and showed binding at similar ranges to muscarinic and 5-HT_2 receptors. Like SR141716, LY320135 displayed inverse activity at some signal transduction pathways of the CB_1 receptor

(Felder *et al.*, 1998; Christopoulos *et al.*, 2001). The pravadoline analogues WIN 56,098, 6-bromopravadoline (WIN 54461), and 6-iodopravadoline (AM 630) were the first cannabinoid antagonists/inverse agonists to be discovered. AM 630 was shown to be a CB_2 receptor selective antagonist/inverse agonist in hCB_2-transfected CHO cells, reversing CP 55,940 inhibition of forskolin-stimulated cAMP production (EC_{50} 128.6 nM) and when administered alone, enhancing forskolin-stimulated cAMP production (EC_{50} 230.4 nM) and inhibiting [^{35}S]GTPγS binding (EC_{50} 76.6 nM; Ross *et al.*, 1999). At the CB_1 receptor AM 630 was shown through multiple investigations to possess mixed agonist/antagonist properties acting as a low-affinity partial agonist, and in one case, as a low-potency inverse agonist (Pertwee *et al.*, 1996; Hosohata *et al.*, 1997a; b; Ross *et al.*, 1999; Landsman *et al.*, 1998). WIN 56,098, discovered by Stirling Winthrop, possessed a weak disassociation constant against Δ^9-THC of 1.85 μM in the mouse isolated vas deferens (Pacheco *et al.*, 1991). 6-Bromopravadoline showed potency values of 159 and 251 nM against WIN 55,212-2 and Δ^9-THC respectively and an IC_{50} value of 515 nM for displacement of [^{3}H]-WIN 55,212-2 from rat cerebellar membranes (Eissenstat *et al.*, 1995).

1.3. Overview of cannabinoid receptors

Cannabinoid receptors are named based upon their response to cannabinoid drugs, ligands derived from *Cannabis sativa* and its biologically active synthetic analogues. Cannabinoid receptor types are denoted by the abbreviation CB and numbered in the order of their discovery by a subscript (CB_1, CB_2). Currently, two cannabinoid receptor types have been established, displaying differing predicted amino acid sequences, signalling mechanisms, and tissue distribution. Synthetic ligands have been developed displaying marked selectivity for CB_1 or CB_2 receptors (Section 1.2). Human cannabinoid receptors CB_1 and CB_2 exhibit 48% amino acid sequence identity (Sections 1.3.2 and 1.3.3). Both receptors possess a structure suggestive of a seven-transmembrane domain receptor, and express biochemical and cellular properties suggestive of signal transduction via G-proteins through modulation of adenylyl cyclase and mitogen-activated protein kinase. The CB_1 receptor has also been shown to couple via G-proteins to calcium and potassium channels (Section 1.3.1.3). CB_1 receptor mRNA and protein are found primarily in brain and neuronal tissue while the CB_2 receptor has been reported to be found primarily in immune tissue and, until recently, considered absent from normal nervous tissue (Sections 1.3.2 and 1.3.3).

1.3.1. The CB_1 receptor

Due to the highly lipophilic nature of cannabinoids, the elicited effects were originally thought to be due to a non-specific interaction with membrane lipids and alteration of membrane fluidity. However, Howlett and Flemings' observation of functional inhibition

of adenylyl cyclase in a neuroblastoma cell line following addition of Δ^9-THC (Howlett and Fleming, 1984) coupled with GTP dependency and pertussis toxin blockade (Howlett *et al.*, 1986) suggested effects might be mediated by a $G_{i/o}$-protein coupled receptor. Demonstrations of stereoselectivity of the (-)-enantiomers of Δ^9-THC (Dewey, 1986) and specific radiolabelled CP 55,940 binding in rat brain membranes (Devane *et al.*, 1988) confirmed the existence of a specific cannabinoid receptor. Subsequent cloning from rat brain (Matsuda *et al.*, 1990) led to the naming of the receptor CB_1 and to the confirmation of its membership of the G-protein coupled receptor superfamily. The CB_1 receptor has since been cloned from human and mouse brain, and human testis (Chakrabarti *et al.*, 1995; Gérard *et al.*, 1991). cDNA cloned encode proteins of 472 (human) and 473 (rat and mouse) amino acids. These three receptors possessed 97 to 99% amino acid sequence identity. A splice variant of the CB_1 receptor, CB_{1A}, has been found in the human lung (Shire *et al.*, 1995).

1.3.2. CB_1 receptor distribution

Detailed investigations into the distribution of CB_1 receptors within the CNS have been performed using techniques such as quantitative autoradiography, *in situ* hybridisation, and immunocytochemistry. In addition to the CNS, CB_1 receptors are widely expressed in the peripheral nervous system, both on sensory nerve fibres and in the autonomic nervous system, although detailed comparative anatomical studies have not been conducted on receptor expression. CB_1 receptors have also been found in moderate levels in the testis (Gérard *et al.*, 1991; Wenger *et al.*, 2001) and in some immune cells.

Autoradiography studies within the CNS, performed with [^{3}H]-CP 55,940 prior to the cloning of the receptor in several species including human, monkey, and rat, assisted in establishing the existence of a high-affinity cannabinoid receptor (Herkenham *et al.*, 1990; 1991; Glass *et al.*, 1997). Cannabinoid receptors were found at particularly high levels in the cerebral cortex, hippocampus, basal ganglia, and cerebellum, regions correlating well with the behavioural effects of cannabinoids. Lower levels were found in hypothalamus and spinal cord. The absence of receptor binding in respiratory centres of the brainstem showed consistency with the low toxicity of cannabis overdose (Robson, 2001). Quantitative estimates found expression levels of greater than 1 pmol/mg tissue, greater than those of most other G-protein-coupled receptors and comparable with levels found for common ionotropic receptors (Greenamyre *et al.*, 1984; Bowery *et al.*, 1987). With cloning, the *in situ* hybridisation identification of CB_1 receptor mRNA corroborated with autoradiography studies (Mailleux *et al.*, 1992; Matsuda *et al.*, 1993). As *in situ* hybridisation detected mRNA within cell bodies, analysis in conjunction with autoradiography studies suggested that CB_1 receptors are often found on axons and probably their terminals.

With the development of antibodies to the CB_1 receptor, immunocytochemical studies demonstrated similar distribution patterns as observed with autoradiography and *in situ* hybridisation studies (Tsou *et al.*, 1998; Egertová and Elphick, 2000).

1.3.3. CB_2 receptor

Evidence for a second cannabinoid receptor first came with the cloning of human CB_2 cDNA from HL-60 cells by Munro *et al.* (1993). It possesses a 360-amino acid sequence

that bears only 48% homology with the human CB_1 receptor between the transmembrane domains 1 and 7. Mouse and rat CB_2 genes have been cloned, with the mouse expressing only 82% homology in the amino acid sequence to the human receptor (Shire *et al.*, 1996; Griffin *et al.*, 2000). CB_2 receptors are primarily expressed by leukocytes with a rank order of B cells > natural killer [NK] cells >> monocytes/macrophages > neutrophils > $CD8^+$ T cells > $CD4^+$ T cells (Galiègue *et al.*, 1995). While many laboratories have reported the absence of CB_2 receptor expression in healthy brain (Carlisle *et al.*, 2002; Chakrabarti *et al.*, 1995; Derocq *et al.*, 1995; Galiègue *et al.*, 1995; Griffin *et al.*, 1999; Shatz *et al.*, 1997; Sugiura *et al.*, 2000), several publications have reported low levels of CB_2 receptors in specific brain structures, such as the brain stem and hippocampus (Gong *et al.*, 2006; Van Sickle *et al.*, 2005). In addition the expression of CB_2 receptors in cells in pathological conditions has been observed in activated microglial cells in mouse models of multiple sclerosis and Alzheimer's disease (Benito *et al.*, 2003). Recently expression of the CB_2 receptor in the rat myenteric plexus after exposure to LPS has been reported (Duncan *et al.*, 2005; 2006) and unpublished studies reviewed by Wright *et al.* (2008) suggested the presence of the CB_2 receptor in intestinal epithelial cells.

1.3.4. Signal transduction mechanisms of CB_1 and CB_2 receptors

Cannabinoid receptor activation has been associated with a number of signal transduction mechanisms, the majority of which are conveyed via the $G_{i/o}$-protein, these include modulation of ion channel opening, inhibition of adenylyl cyclase, up regulation of mitogen-activated protein (MAP) kinase, activation of phospholipase C, and mobilisation of arachidonic acid. A sizeable amount of evidence exists for these mechanisms and has

been well reviewed (Pertwee, 1997). Under certain conditions the CB_1 receptor has been shown to couple to the G_s-protein to activate adenylyl cyclase and reduce outward potassium current (Glass and Felder, 1997; Calandra *et al.,* 1999; Hampson *et al.*, 2000; Bonhaus *et al.*, 1998). An increasing number of alternative signalling mechanisms are emerging through which cannabinoid receptors may act. These include phosphatidylinositol-3-kinase (PI3K) activation, focal adhesion kinase (FAK) activation and ceramide synthesis.

1.3.4.1. G-protein coupling

The CB_1 and CB_2 receptors are members of the G-protein coupled receptor family (GPCR) and consists of 7 transmembrane domains interspaced by alternating extracellular and intracellular loops. These receptors belong to a subset of the GPCR family referred to as the rhodopsin-type or Class I subfamily, which consists of a large number of GPCR including the muscarinic, dopamine and opioid receptor families (Pierce *et al.*, 2002).

Ligand binding to the extracellular loops and N-terminal domain stabilises a conformation that allows the intracellular loops and C-terminal domain of the receptor to associate and activate G-proteins. The heterotrimeric G-protein consists of an α, a β and a γ subunit. The α subunit is responsible for GTP and GDP binding and GTP hydrolysis, while the β and γ subunits exist in a tightly bound dimer complex. In the absence of GPCR agonists the receptor exists in a bound state with the G-protein complex, which is bound to GDP. Binding of an agonist causes the release of GDP and replacement with GTP. This leads to a release of the G-protein complex from the receptor and dissociation

of the α and βγ complexes, which both activate several effectors. To date, 16 α, 5 β and 14 γ subunits have been cloned, with the CB_1 receptor binding to the $G\alpha_{i/o}$-protein subunit. The $G\alpha_{i/o}$-protein subunit has been shown to inhibit adenylyl cyclases (AC-II and AC-IV), while the βγ dimer has been shown to activate G-protein coupled inwardly rectifying potassium (GIRK) channels (KIR3.1-3.4) and inhibit voltage-gated calcium channels (VGCC) as detailed later within this chapter. The bacterial toxin, pertussis toxin, selectively inactivates $G_{i/o}$-proteins (Hescheler *et al.*, 1987).

The ability of the CB_1 receptor to activate G_i-proteins has been demonstrated through the analysis of activation of [^{35}S]-GTPγS in brain homogenates (Selley *et al.*, 1996; Breivogel *et al.*, 1997). A study by Glass and Northup demonstrated activation of GDP-GTP exchange through G_i and G_o-proteins dependent mechanisms in membranes derived from *Spodoptera frugiperda* cells transfected with the CB_1 receptor and with exogenously added purified G-protein subunits ($G\alpha_i$, $G\alpha_o$ and βγ subunits). In contrast, the CB_2 receptor induced activation through a G_i-protein but not a G_o-protein dependent mechanism (Glass and Northup, 1999).

1.3.4.2. Inhibition of adenylyl cyclase

Cannabinoid evoked inhibition of adenylyl cyclase through negative coupling of the $G_{i/o}$-protein is well established. First observed in 1984 by Howlett and Fleming, adenylyl cyclase was inhibited by micromolar concentrations of Δ^9-THC in N18TG2 neuroblastoma cells. This inhibition was shown to be PTX sensitive, suggesting $G_{i/o}$-protein involvement (Howlett *et al.*, 1986). Since, cannabinoid receptor inhibition of cyclic adenosine monophosphate (cAMP) production has been shown in a number of

cultured cell lines expressing CB_1 receptors and in transfected cell lines (Howlett, 1987; Vogel *et al.*, 1993; Hirst and Lambert, 1995; Matsuda *et al.*, 1990; Felder *et al.*, 1993). The rank order of potency correlates well with CB_1 receptor binding affinity (Felder *et al.*, 1992, 1995) and efficacy is stereoselective (Pacheco *et al.*, 1991, 1993; Howlett *et al.*, 1988, 1990; Matsuda *et al.*, 1990). The selective CB_1 receptor antagonist, SR141716 readily antagonised inhibition (Ho and Zhao, 1996; Bouaboula *et al.*, 1995; Felder *et al.*, 1995). Further substantiation is demonstrated by cannabinoids showing greatest efficacy in inhibiting adenylyl cyclase in areas of the brain possessing the highest concentration of CB_1 receptors (Bidaut-Russell *et al.*, 1990; Pacheco *et al.*, 1991; Childers *et al.*, 1994).

An increase in cAMP through coupling of the CB_1 receptor to G_s-proteins has been observed in CHO cells, cultured hippocampal neurones and striatal neurones in primary culture upon inhibition of $G_{i/o}$-proteins (Glass and Felder, 1997; Calandra *et al.,* 1999; Hampson *et al.*, 2000; Bonhaus *et al.*, 1998).

CB_2 receptors expressed in CHO and COS cells have been shown to mediate cannabinoid inhibition of adenylyl cyclase activity through a PTX sensitive mechanism (Bayewitch *et al.*, 1995; Slipetz *et al.*, 1995). However in contrast to CB_1 receptors, G_s-protein stimulation of cAMP accumulation was not observed with $G_{i/o}$-protein inhibition in CHO cells transfected with the CB_2 receptor (Glass and Felder, 1997; Calandra *et al.,* 1999).

Nine isoforms of adenylyl cyclase have been identified (Patel *et al.*, 2001). Coexpression of adenylyl cyclase isoforms 1, 3, 5, 6, or 8 with either the CB_1 or CB_2 receptors in COS-7 monkey kidney cells, showed cannabinoid inhibition of cAMP accumulation, however coexpression of either cannabinoid receptor type with adenylyl cyclase isoforms 2, 4, or 7 resulted in stimulation of cAMP accumulation (Rhee *et al.*, 1998).

1.3.5. Modulation of ion channel currents

Direct CB_1 receptor modulation of voltage-gated calcium and inward rectifying potassium channels through $G_{i/o}$-protein βγ-subunits is well established. Inhibition of A and D-type potassium channels have also been shown to occur through phosphorylation mediated by a cAMP-dependent protein kinase A (PKA) pathway. The CB_2 receptor is believed not to modulate ion channel function, with the lack of interaction observed solely in artificial models including AtT-20 cells, which express Q-type calcium channels and inward rectifying potassium channels, transfected with CB_2 receptors (Felder *et al.*, 1995) and *Xenopus* oocytes transfected with CB_2 and GIRK1/4 (McAllister *et al.*, 1999).

1.3.5.1. Activation of calcium channels

The voltage-gated calcium channel family comprises of ten members categorised into 5 distinct classes; L-type, N-type, P/Q-type, R-type and T-type. L-type calcium currents typically require a strong depolarisation for activation, are long-lasting, and are blocked by the organic L-type calcium channel antagonists, including dihydropyridines, phenylalkylamines, and benzothiazepines. They are the main calcium currents recorded in muscle and endocrine cells, where they initiate contraction and secretion. L-type currents activating at lower voltages also exist predominantly in neurones and cardiac pacemaker cells. N-type, P/Q-type, and R-type calcium currents also require strong depolarisation for activation. They are blocked by specific polypeptide toxins from snail and spider venoms, and are expressed primarily in neurones, where they initiate

neurotransmission at most fast synapses and mediate calcium entry into cell bodies and dendrites. N-type channels are highly prevalent in peripheral nerve terminals and are largely responsible for synaptic transmission in autonomic and sensory neurones. T-type calcium currents are activated by weak depolarisation and are transient. They are expressed in a wide variety of cell types, where they are involved in shaping the action potential and controlling patterns of repetitive firing (Catterall *et al.*, 2005; Dolphin, 2006). Dunlap and Fischbach first observed G-protein inhibition of calcium currents in 1981 in chick dorsal root ganglia neurones by noradrenaline and serotonin. The involvement of the $G_{\beta\gamma}$-subunits as opposed to the G_{α}-subunit was elucidated by both Ikeda in 1996 and Catterall and Hille in the same year through injection or overexpression of $G_{\beta\gamma}$-subunits (Ikeda, 1996; Herlitze *et al.*, 1996).

CB_1 receptor inhibition of N-type voltage-gated calcium channels (VGCC) in the NG108-15 neuroblastoma-glioma cell line by WIN 55,212-2 and CP 55,940 was first shown by Mackie and Hille (1992) using whole-cell patch clamp. Inhibition was shown to be blocked by prior treatment with pertussis toxin, demonstrating mediation by $G_{i/o}$-proteins but, as the response was not inhibited by the hydrolysis-resistant analogues of cAMP, dibutyryl-cAMP and 8-chlorophenylthio-cAMP, it was not dependent upon the cAMP pathway. The inactive enantiomer WIN 55,212-3 did not reduce calcium currents at high doses. As WIN 55,212-2 inhibition did not occur when applied in conjunction with ω-Conotoxin GVIA, the N-type VGCC inhibitor, but did occur in the presence of the L-type VGCC inhibitor nitrendipine, the majority of cannabinoid inhibition was hypothesised to occur through blockade of N-type VGCC (Mackie and Hille, 1992; Caulfield and Brown, 1992). Sugiura *et al.* (1997) demonstrated an inhibition of the rise

in intracellular calcium caused by voltage-activated calcium channel opening with the use of fura-2 imaging in differentiated NG108-15 cells. Anandamide inhibition of VGCC was demonstrated in N18 neuroblastoma cells (Mackie *et al.*, 1993; Felder *et al.*, 1993). Inclusion of guanosine-5'-O-(2-thiodiphosphate), a nonhydrolyzable analogue of GDP, in the intracellular patch pipette solution blocked cannabinoid inhibition in adult rat superior cervical ganglion neurones transiently expressing rat brain CB_1 receptors, confirming a G-protein dependent mechanism (Pan *et al.*, 1996), while SR141716 antagonism of WIN 55,212-2 inhibition substantiated the role of the CB_1 receptor (Pan *et al.*, 1998). WIN 55,212-2 inhibition of glutamatergic transmission at corticostriatal synapses was demonstrated in brain slice preparations to be blocked by SR141716, PTX and ω-Conotoxin GVIA, suggesting a CB_1 receptor, $G_{i/o}$-protein mediated inhibition of N-type VGCC (Huang *et al.*, 2001). Guo and Ikeda (2004) demonstrated blockade of N-type VGCC by the endocannabinoids 2-AG, anandamide and 2-arachidonylglycerol in adult rat superior cervical ganglion neurones transiently expressing rat brain CB_1 receptors.

Cannabinoids inhibited P/Q-type, but not L-type, calcium currents in AtT-20 pituitary cells transfected with CB_1 receptors. This response was blocked by pertussis toxin indicating $G_{i/o}$-protein dependence (Mackie *et al.*, 1995). Interestingly, CB_1 receptor mediated inhibition P/Q-type calcium currents and inwardly rectified K^+ currents in AtT-20 pituitary cells was shown to be inhibited by protein kinase C phosphorylation of the CB_1 receptor (Garcia *et al.*, 1998). The *N*-methyl-D-aspartate (NMDA)-induced influx of calcium via P/Q-type calcium channels (blocked by T-agatoxin-IVa) was inhibited by cannabinoids as determined by fura-2 fluorescence in rat cortical and cerebellar brain

slices (Hampson *et al.*, 1998). Inhibition was blocked by SR141716 and pertussis toxin, confirming the role of CB_1 receptors and $G_{i/o}$ proteins.

In cultured rat hippocampal neurones, WIN 55,212-2, CP 55,940 and anandamide reduced voltage-gated calcium currents through inhibition of N-type (ω-conotoxin-GVIA-sensitive) and P/Q-type (ω-conotoxin-MVIIC-sensitive) channels in an SR141716 and PTX sensitive manner (Twitchell *et al.*, 1997; Shen and Thayer, 1998). Intriguingly, at nanomolar doses of WIN 55,212-2 Shen and Thayer observed a saturating small degree of inhibition (17 ± 2% maximal inhibition), which was insensitive to the inactive stereoisomer WIN 55,212-3, and blocked by SR141716. However, higher doses (micromolar) induced further inhibition which was neither stereoselective nor antagonised by SR141716. This suggested CB_1 receptor mediated inhibition occurred at low agonist concentrations while inhibition at higher concentrations was dependent upon an alternate mechanism (Shen and Thayer, 1998).

Inhibition of low-voltage activated T-type calcium channels was observed by Chemin *et al.* (2001) in cells expressing endogenous T-type channels (NG108-15) and in recombinant cells (HEK 293, CHO and COS). Inhibition was not observed upon application of synthetic cannabinoids and the CB_1 antagonist SR141716 did not prevent inhibition. A lack of modulation of anandamide inhibition through the application of $G_{i/o}$-proteins, phospholipase pathways and phosphorylation pathways inhibitors coupled with inhibition of currents in excised inside-out patches in HEK 293 cells suggest direct inhibition the T-type channel. Acceleration of inactivation kinetics and a reduction in the degree of inhibition with lower holding potentials suggests inhibition is due to stabilization of the T-type channel in the inactive state (Chemin *et al.*, 2001).

Arterial smooth muscle cells from the cat brain, found to express cDNA for the CB_1 receptor, displayed SR141716 and pertussis toxin sensitive L-type calcium current inhibition evoked by cannabinoid agonists (Gebremedhin *et al.*, 1999). Inhibition of L-type calcium currents were observed in tiger salamander retinal bipolar cells and large single cone photoreceptors via an SR141716 sensitive mechanism (Straiker *et al.*, 1999; Straiker and Sullivan, 2003). Increased activation of L-type channels by WIN 55,212-2 was observed in rod photoreceptors through the CB_1 receptor and the cAMP/PKA-signalling pathway (Straiker and Sullivan, 2003).

1.3.5.2. Activation of potassium channels

Potassium-selective channels form the largest and most diverse group of ion channels with, in humans, the voltage-gated potassium channel family comprising of over 75 genes including Ca^{2+}-activated, inwardly-rectifying (K_{ir}) and two-pore families. The inwardly-rectifying potassium channel superfamily was first observed by Bernard Katz in 1949, and the G-protein regulated family observed with ligand-induced hyperpolarisation in the frog heart in 1955 (Del Castillo and Katz, 1955) although association with G-proteins was not elucidated until 1985 when work by Pfaffinger *et al.* reported the involvement of a pertussis toxin-sensitive G-protein in the muscarinic receptor induction of the K_{ACh} current in cardiac atrial myocytes (Pfaffinger *et al.*, 1985). Modulation by the $G_{\beta\gamma}$ subunit as opposed to the G_{α} subunit was first shown by Logothetis *et al.* (1987) through the application of subunits purified from bovine cerebral cortex to single-channel recordings from cardiac myocytes. Cannabinoid inhibition of GIRKs was first seen in 1995. Mackie *et al.*, (1995) found WIN 55,212-2 and anandamide to activate inwardly rectifying

potassium currents in CB_1 receptor transfected murine tumour AtT-20 cells. Activation was shown to be concentration dependent and stereoselective, suggesting mediation via the CB_1 receptor. In *Xenopus laevis* oocytes transfected with GIRK1 channels and CB_1 receptors, cannabinoid agonists increased the inwardly rectifying potassium current (Henry and Chavkin, 1995). Expression of CB_1/GIRK1/GIRK4 and different G-protein subunits revealed mediation by the βγ-subunit (Ho *et al.*, 1999). Transfection with GIRK1 and GIRK4 channels containing a mutated aspartate residue, shown to be critical for G-protein coupling in cannabinoid receptors, decreased the efficacy of cannabinoids in *Xenopus laevis* oocytes (McAllister *et al.*, 1999). HEK 293 cells transfected with the CB_1 receptor displayed WIN 55,212-2 and anandamide inhibition of endogenous inwardly rectifying K^+ currents through an AM251 sensitive mechanism (Vasquez *et al.*, 2003). Robbe *et al.* (2001) demonstrated a SR141716 sensitive CP 55,940 and WIN 55,212-2 inhibition of glutamatergic signalling in the mouse nucleus accumbens, which was blocked by Ba^{2+}, suggesting the involvement of inwardly rectifying K^+ channels. This cannabinoid inhibition was not altered by forskolin, implying an independence from the cAMP/PKA pathway. A role for the PKC pathway in governing CB_1 receptor mediated modulation of GIRKs was suggested with the observation that stimulation of PKC would inhibit cannabinoid modulation in rat CB_1 receptor transfected AtT-20 cells (Garcia *et al.*, 1998). Mutation of a single serine residue (S317) to an alanine in the CB_1 receptor blocked PKC inhibition suggesting G-protein activation to be dependent upon receptor phosphorylation.

Deadwyler *et al.* (1995) demonstrated, with cultured hippocampal neurones, cannabinoids evoked concentration dependent increases in voltage-dependent A-type

outward potassium currents through a pertussis toxin sensitive mechanism. Inhibition of the cAMP/PKA pathway mimicked cannabinoid effects whilst 8-Br-cAMP and forskolin, activators of the pathway, produced opposing effects suggesting cannabinoids act to inhibit phosphorylation of the channel and so increase channel activity (Hampson *et al.*, 1995; Mu *et al.*, 2000). Okadaic acid, an inhibitor of protein phosphatase 1 and 2A, blocked WIN 55,212-2 stimulation adding further weight to the hypothesis that increased channel activity occurs through a cannabinoid mediated transition into a dephosphorylated state (Mu *et al.*, 2000).

Hippocampal neurones have also demonstrated inhibition of D-type potassium currents with CB_1 receptor stimulation (Mu *et al.*, 1999). IP-20, an inhibitor of the cAMP/PKA pathway, inhibited D-type currents whilst 8-Br-cAMP increased currents suggesting different phosphorylation states govern activation of D-type compared to A-type currents (Mu *et al.*, 1999).

Cannabinoid inhibition of M-type potassium currents was observed in hippocampal CA1 neurones through an SR141716 sensitive mechanism (Schweitzer, 2000).

1.3.5.3. Inhibition of sodium channels

A cannabinoid-mediated inhibition of voltage-gated sodium currents has been reported. The mechanism of action has not been elucidated, although a CB_1/CB_2 receptor independent mechanism has been suggested.

Inhibition of voltage-gated inward sodium currents in a mouse neuroblastoma cell line with exposure to Δ^9-THC has been observed using the whole-cell voltage clamp technique. A change in reversal potential and the lack of inhibition of the outward sodium

current augmented the suggested modification of channel properties, however the principal metabolite of Δ^9-THC, 11-OH-Δ^9-tetrahydrocannabinol, depressed both inward and outward sodium currents and did not modify reversal potentials suggesting the presence of some degree of ligand specificity (Turkanis *et al.*, 1991a; 1991b). The cannabinoid agonists anandamide, AM404 and WIN 55,212-2 and the antagonist AM251 have been shown to inhibit veratridine, a voltage-gated sodium channel agonist, induced depolarisation and neurotransmitter release in a mouse brain synaptoneurosome preparation, as well as block tetrodotoxin (TTX)-sensitive sustained repetitive firing in cortical neurones (Nicholson *et al.*, 2003; Liao *et al.*, 2004). Kim *et al.* (2005) observed an anandamide mediated inhibition of both TTX-sensitive and TTX-resistant sodium currents in rat dorsal root ganglion neurones which was insensitive to the CB_1 and CB_2 receptor selective antagonists AM 251 and AM 630, and the TRPV1 antagonist capsazepine.

1.3.6. Regulation of Intracellular Ca^{2+} Transients

An increase of intracellular free calcium levels by cannabinoid agonists was first demonstrated by Sugiura and colleagues in undifferentiated N18TG2 neuroblastoma and NG108-15 neuroblastoma-glioma hybrid cells (Sugiura *et al.*, 1996; 1997). HU-210, CP 55,940, Δ^9-THC, anandamide, and R-(+)-methanandamide behaved as partial agonists compared with 2-arachidonoylglycerol or 1(3)-arachidonoylglycerol (Sugiura *et al.*, 1996; 1997; 1999). The role of the CB_1 receptor was confirmed through SR141716 blockade (Sugiura *et al.*, 1996; 1999). Pertussis toxin and a phospholipase C inhibitor blocked the 2-arachidonoylglycerol-evoked intracellular Ca^{2+} increase, suggesting

intracellular Ca^{2+} release may be governed by inositol-1,4,5-triphosphate (IP_3)/phospholipase Cβ and $G_{i/o}$ βγ subunits (Sugiura *et al.*, 1996; 1997). Support for this mechanism came from the observed interaction between CB_1 receptors and phospholipase C in augmenting the Ca^{2+} signal in response to NMDA receptor stimulation or K^+ depolarisation in cultured cerebellar granule neurones (Netzeband *et al.*, 1999). This response was antagonized by SR141716 and pertussis toxin, confirming an action through the CB_1 receptor, and by the phospholipase C inhibitor U-73122 and the inositol 1,4,5-trisphosphate (IP_3) receptor antagonist xestospongin C, suggesting release from an IP_3 receptor-sensitive Ca^{2+} store (Netzeband *et al.*, 1999). In primary cultures of striatal astrocytes, methanandamide depleted IP_3-sensitive Ca^{2+} stores, in a manner inhibited by PTX (Venance *et al.*, 1997). However this mechanism may not be active in all cells, as release of IP_3 or phosphatidic acid with exposure to anandamide or WIN 55,212 was not observed in CHO cells expressing recombinant CB_1 or CB_2 receptors (Felder *et al.*, 1992; 1995). A Δ^9-THC induced increase in intracellular calcium levels has been observed using fura-2 imaging in a hamster vas deferens smooth muscle cell line, DDT_1 MF-2 cells (Filipeanu *et al.*, 1997). This increase in cytosolic calcium was shown to comprise of release from both thapsigargin sensitive intracellular stores and capacitative calcium entry, and from calcium influx through a mechanism independent of calcium release from thapsigargin sensitive stores (Filipeanu *et al.*, 1997). Patch clamp recordings from the same cell line demonstrated a CB_1 receptor activated Ca^{2+}-dependent K^+ current that required both calcium influx and release from thapsigargin sensitive intracellular stores (Begg *et al.*, 2001). The thapsigargin sensitive store-independent

calcium entry component was shown to be mediated by a signalling pathway involving arachadoinic actid, phospholipase A2 and MAP kinase (DeMuth *et al.*, 2004).

Anandamide has been demonstrated to evoke a transient increase in intracellular calcium levels through the activation of CB_2 receptors in a calf pulmonary endothelial cell line. Blockade by a phospholipase C inhibitor and an IP_3 receptor antagonist suggested release from IP_3-sensitive Ca^{2+} stores while calcium imaging observed depletion of the endoplasmic reticulum and a transient elevation of mitochondrial Ca^{2+} (Zoratti *et al.*, 2003).

1.3.7. Regulation of Mitogen-Activated Protein Kinase and linking mechanisms

1.3.7.1. Mitogen-Activated Protein Kinase

The mitogen-activated protein kinase (MAPK) cascade is a family of serine/threonine kinases that are involved in the transduction of externally derived signals regulating cell growth, division, differentiation, and apoptosis, and are traditionally associated with the activation of the tyrosine kinase-linked receptor. The mammalian MAPK family consists of three subfamilies with multiple members; the extracellular signal-regulated kinases (ERK), the Jun amino-terminal kinases/stress-activated kinases (JUN/SAPK), and the p38 MAPKs. ERK has been shown to be involved in regulation of cell division and growth whilst JUN/SAPK and p38 MAPKs are activated by stress signals and inflammatory cytokines and are associated with cell death and immune disorders. Each cascade consists of a three member-protein kinase tandem in which the MAPK is activated by phosphorylation of both a tyr residue and a ser/thr residue by a dual MAPK

kinase (MEK), which in turn is activated by phosphorylation by a MAPK kinase kinase (MEKK).

CB_1 receptor mediated activation of the MAPK cascade was first observed in WI-38 fibroblasts, where anandamide promoted *tyr*-phosphorylation of ERKs and increased MAPK activity, and in human CB_1 receptor transfected CHO cells and cultured astrocytic cells, which showed activation through a $G_{i/o}$-protein dependent mechanism but did not involve the cAMP signal transduction pathway (Wartmann *et al.*, 1995; Bouaboula *et al.*, 1995). Δ^9-THC and HU-210 was shown to activate the ERK cascade using a SR141716 and pertussis toxin sensitive mechanism in C6 glioma and primary astrocyte cultures (Sánchez *et al.*, 1998; Guzmán and Sánchez, 1999). Δ^9-THC and methanandamide have been shown to promote Raf-1 translocation to the membrane of human prostate epithelial PC-3 cells and ERK kinase phosphorylation through CB_1 and CB_2 receptors (Sánchez *et al.*, 2003).

Inhibition of ERK activity has been observed in primary mouse splenocytes, where cannabinol inhibited AP-1 transcription factor binding and upregulation of the ERK cascade, and in PC-12 cells transfected with the CB_1 receptor, where anandamide inhibited NGF-induced sustained ERK activation (Faubert and Kaminski, 2000; Rueda *et al.*, 2002). This inhibition may result from the multiple roles possessed by cAMP in regulating Raf-1 isoforms, which regulate MEK activity.

Activation of stress-regulated MAP kinases alongside JNK and MAPK p38 has been observed in CB_1 receptor transfected CHO cells with the application of Δ^9-THC, anandamide and 2-AG (Cantley, 2002). Anandamide activated p38 kinase and JNK in

CB_1 receptor transfected ECV304 cells (Liu *et al.*, 2000), whilst in hippocampal slices Δ^9-THC and 2-AG activated p38 but not JNK (Derkinderen *et al.*, 2001).

Activation of the ERK cascade and increased expression and activation of the growth-related gene Krox-24 has been observed in CB_2 receptor transfected CHO cells. Activation was blocked by pertussis toxin suggesting $G_{i/o}$-protein dependence (Bouaboula *et al.*, 1996). In primary murine splenocytes and EL4.IL-2 T cells enhanced ERK activity was observed with exposure to cannabinol and suboptimal activation, however ERK activity after optimal activation was reduced by cannabinol (Jan and Kaminski, 2001). The ERK cascade as well as the MAPK-target gene protein c-Fos showed anandamide-induced enhanced activation in haemopoietic cells (Valk *et al.*, 2000). An increased phosphorylation of two isoforms of ERK was observed in HL-60 cells was observed with treatment with 2-AG (Derocq *et al.*, 2000; Kobayashi *et al.*, 2001).

Mechanisms for CB_1 receptor-mediated MAP kinase activation have not been fully elucidated. Several mechanisms have been proposed which include phosphatidylinositol-3-kinase (PI3K) activation, focal adhesion kinase (FAK) activation and ceramide synthesis.

1.3.7.2. Signal Transduction via phosphatidylinositol-3-kinase

Phosphatidylinositol-3-kinase (PI3K) comprises of a family of kinases that phosphorylate the inositol ring of phosphatidylinositol and other phosphoinostides, producing 3'-phosphoinostides. These enhance migration to the membrane and activation of proteins

containing pleckstrin homology domains that include protein kinase B, which is involved in regulation of apoptosis. In addition, the PI3K isoform I_H has been shown to be directly regulated by $G_{\beta\gamma}$ subunits suggesting the protein may possess independent kinase activity. In primary cultures of rat astrocytes the PI3K inhibitors wortmannin and LY 294002 were able to antagonize the Δ^9-THC-induced stimulation of glucose oxidation to CO_2, phospholipid synthesis and glycogen synthesis (Sanchez *et al.*, 1998b). Furthermore in human prostate epithelial PC-3 cells, CB_1 receptor activation induced a translocation of Raf-1 to the membrane and phosphorylation of ERK kinase, which was blocked by PI3K inhibitors (Sanchez *et al.*, 2003). Activation of protein kinase B was observed in CB_1 receptor transfected CHO cells and was inhibited by CB_1 receptor antagonists and PI3K inhibitors (Gómez del Pulgar *et al.*, 2000). Protein kinase B activation was also observed in the human astrocytoma cell line U373 MG, which expresses the CB_1 receptor, but not in the human promyelocytic cell line HL-60, which expresses the CB_2 receptor (Gómez del Pulgar *et al.*, 2000).

1.3.7.3. Signal Transduction via Focal Adhesion Kinase

Focal adhesion kinase (FAK) is a cytoplasmic tyrosine kinase that localises to regions of membrane attached to the extracellular matrix, where it acts as part of the intergrin signalling pathway transmitting signals controlling cell motility from the membrane to the cytoplasm. FAK has been shown to activate a number of biochemical pathways including the MAPK cascade.

Derkinderen *et al.* (1996) observed in hippocampal slices cannabinoid agonists stimulated *tyr*-phosphorylation of focal adhesion kinase (FAK) (pp125). This was

blocked by SR141716A and pertussis toxin suggesting mediation by the CB_1 receptor and the $G_{i/o}$-protein. *tyr*-phosphorylation was reversed by 8-Br-cAMP and mimicked by protein kinase A inhibitors, signifying stimulation was mediated through the $G_{i/o}$-protein inhibition of adenylyl cyclase (Derkinderen *et al.*, 1996).

1.3.7.4. Signal Transduction via ceramide synthesis

Ceramide is a ubiquitous sphingolipid second messenger that plays an important role in the control of cell survival through the regulation of various targets, for example the Raf-1/MEK/ERK cascade. The CB_1 cannabinoid receptor has been shown to increase generation of ceramide through upregulation of sphingomyelin hydrolysis and ceramide synthesis de novo. The coupling of receptors to sphingomyelinases is thought to involve different adaptor proteins. Coimmunoprecipitation experiments suggest the factor associated with neutral sphingomyelinase activation (FAN) may play a role in binding to the CB_1 receptor and a cytoplasmic nine-amino acid motif of the 55-kDa tumour necrosis factor (TNF) receptor, the so-called neutral sphingomyelinase-activating domain, thereby coupling the receptor to sphingomyelin breakdown (Sanchez *et al.*, 2001; for review see Velasco *et al.*, 2005). Prolonged (days) elevation of intracellular ceramide has been associated with events leading to decreased proliferation and apoptosis in glioma cells (see Guzmán *et al.*, 2001 for review). This response was initiated by chronic stimulation of both CB_1 and CB_2 receptors on a susceptible C6 glioma strain and involved increased ceramide synthesis via serine palmitoyltransferase, Raf-1 activation, and MAPK (p42/44) activation.

1.3.8. Regulation of nitric oxide production

Stimulation of nitric oxide (NO) production by cannabinoids has been observed in a number of tissues including human monocytes (Stefano *et al.*, 1996), rat median eminence fragments (Prevot *et al.*, 1998), human saphenous vein segments (Stefano *et al.*, 1998), cultured human arterial endothelial cells (Fimiani *et al.*, 1999; Mombouli *et al.*, 1999), cultured human umbilical vein endothelial cells (Maccarrone *et al.*, 2000), and in leech or muscle ganglia (Stefano *et al.*, 1997a,b). These responses were blocked by SR141716, suggesting a role for the CB_1 receptor and by N^G-nitro-L-arginine methyl ester (L-NAME), confirming regulation of nitric oxide synthase (NOS) (Prevot et al., 1998). Stimulation of Ca^{2+}-regulated constitutive NOS was implicated through the required presence of Ca^{2+} in the perfusate in saphenous vein endothelia, and the presence of a transient increase in intracellular Ca^{2+} concentration preceding NO generation in cultured human arterial endothelial cells (Stefano *et al.*, 1998; Fimiani *et al.*, 1999; Mombouli *et al.*, 1999). A cannabinoid induced, and SR141716 blocked, inhibition of lipopolysaccharide plus interferon-γ activated inducible NOS has been observed in saphenous vein endothelium (Stefano *et al.*, 1998), neonatal mouse astrocytes (Molina-Holgado *et al.*, 1997) and in rat microglial cells (Cabral *et al.*, 2001). Inducible NOS inhibition has been hypothesised to be due inhibition of cAMP production by NO generated as a result of stimulus of constitutive NOS (Stefano *et al.*, 1998).

In the macrophage line RAW 264.7, in which the CB_2 receptor and not the CB_1 receptor is expressed, Δ^9-THC markedly attenuated NO production and inducible NOS transcription evoked by lipopolysaccharide (Jeon *et al.*, 1996).

1.4. Other targets for cannabinoids

With the availability of CB_1 and CB_2 receptor knockout mice, evidence is now emerging for the existence of additional cannabinoid receptors and for the action of cannabinoids on established non-cannabinoid receptors.

1.4.1. The vanilloid type 1 (TRPV1) receptor

The vanilloid type 1 receptor (TRPV1) is a non-selective cation channel, activated not only by capsaicin but also by heat (>43°C), acid and various lipids (Caterina and Julius, 2001). As member of the TRP family of ion channels, characterized by a six transmembrane domain integral membrane protein, it shares structural similarity with Shaker-related voltage-gated K^+ channels (Caterina *et al.*, 1997). It is expressed in a subset of unmyelinated nociceptive neurones in dorsal root and trigeminal ganglia (Caterina and Julius, 2001), in visceral afferents (Tominaga *et al.*, 1998), in airway afferent nerve fibres (Kollarik and Undem, 2004), and in cells other than primary afferent neurones such as neurones intrinsic to the brain, epithelial cells of the bladder, and keratinocytes of the skin (Caterina, 2003). *In situ* hybridisation, immunohistochemistry and autoradiography have shown that several regions of the brain express small but possibly functionally active TRPV1 receptor populations, including: thalamic and hypothalamic nuclei, the locus coeruleus, periaqueductal grey and cerebellum, cortical and limbic structures (namely the hippocampus), the caudate putamen and the pars

compacta of the substantia nigra (Mezey *et al.*, 2000; Sanchez *et al.*, 2001; Cortright *et al.*, 2001; Roberts *et al.*, 2004).

The investigation into the action of anandamide at the TRPV1 originated with the realisation of the chemical similarity held between it and the TRPV1 agonist capsaicin (Di Marzo *et al.*, 1998). Experimentation in cultured cells transfected with rat or human TRPV1 demonstrated production by anandamide of membrane currents or increased intracellular calcium (Zygmunt *et al.*, 1999; Smart *et al.*, 2000; Ross *et al.*, 2001). Anandamide was also shown to act on naturally expressed vanilloid receptors in neonatal rat dorsal root ganglia to produce membrane currents (Tognetto *et al.*, 2001) and in rat or guinea-pig isolated arterial strips to produce release of calcitonin-gene-related peptide (CGRP) from perivascular sensory nerves and relaxation of precontracted tissues (Zygmunt *et al.*, 1999). Anandamide was shown to have a low affinity for the receptor, with a *Ki* of ~2 μM, similar to that of capsaicin (De Petrocellis *et al.*, 2001b; Ross *et al.*, 2001), whilst analyses of efficacy in TRPV1 currents in sensory neurones suggested anandamide to be a partial agonist (Zygmunt *et al.*, 1999; Roberts *et al.*, 2002). The endogenous cannabinoids 2-AG and palmitylethanolamide, and synthetic cannabinoids HU 210, WIN 55,212-2, CP 55,940 did not activate the TRPV1 channel (Zygmunt *et al.*, 1999).

In the guinea-pig ileum myenteric plexus-longitudinal muscle preparation anandamide increased basal [^{3}H]acetylcholine release and muscle tone in a capsazepine, a TRPV1 antagonist, sensitive manner but inhibited electrically evoked contractions in a capsazepine insensitive, SR141716 sensitive manner, suggesting activity at both TRPV1 and CB_1 receptors (Mang *et al.*, 2001). At high concentrations of anandamide, acting

through TRPV1 channels, the inhibition of electrically-evoked contractions by the GABA-releasing agent ethylenediamine was increased (Begg *et al.*, 2002).

1.4.2. The GPR55 receptor

GPR55 was first identified as an orphan GPCR in the brain (Sawzdargo *et al.*, 1999). It consists of a 319 amino acid protein located on chromosome 6 in humans. Northern blot analysis of human tissues, found GPR55 mRNA in caudate and putamen, but not in frontal cortex, hippocampus, thalamus, pons, cerebellum, or liver. Analysis of rat tissues showed mRNA in spleen, fetal tissues, and intestine. *In situ* hybridisation studies found GPR55 mRNA in rat hippocampus, thalamus, and midbrain (Sawzdargo *et al.*, 1999). Patent literature reported human GPR55 mRNA distribution with a rank order of adipose > testis > myometrium > adenoid = tonsil > spleen > ileum > brain = stomach (Brown and Wise, 2003).

A second patent application argued that the GPR55 receptor might constitute an additional cannabinoid receptor (Drmota *et al.*, 2004). It only shares 13.5% and 14.4% homology with CB_1 and CB_2, respectively. However, when expressed in HEK 293 cells, GPR55 bound CP 55,940 and SR141716, but not WIN 55,212-2. GTPγS binding was stimulated by wide range of cannabinoids, including Δ^9-THC, anandamide, 2-AG, virodhamine, and CP 55,940, all with EC_{50} values less than 20 nM. PEA, which possesses no binding affinity for CB_1 and CB_2 receptors stimulated GTPγS binding with an even lower nM potency. Pertussis toxin and cholera toxin did not alter GTPγS binding, suggesting, that in transfected HEK 293 cells, the GPR55 receptor does not activate $G_{i/o}$ or G_s proteins.

1.4.3. Putative neuronal cannabinoid receptors

1.4.3.1. A central TRPV1-like receptor

Hájos *et al*. (2001) examined cannabinoid actions on excitatory postsynaptic transmission in the hippocampus of wild type ($CB_1^{+/+}$) and CB_1 receptor knockout mice ($CB_1^{-/-}$). WIN 55,212-2, CP 55,940 and capsaicin inhibited excitatory transmission with equal efficacy in both wild type and $CB_1^{-/-}$ mice. Inhibition was blocked by capsazepine and SR141716 but not by the SR141716 analogue, AM251 (Hájos and Freund, 2002). The lack of expression of the CB_2 receptor in the brain (Munro *et al*., 1993) and the inactivity of WIN 55,212-2 and CP 55,940 at the TRPV1 receptor (Zygmunt *et al*., 1999) rule out a possible role for these mechanisms in modulating response, suggesting inhibition occurs through activation of a novel receptor. To further complement this data, desensitisation of this receptor by capsaicin was not observed although the classical TRPV1 receptor is readily desensitised by capsaicin (Hájos and Freund, 2002).

1.4.3.2. A central anandamide and WIN 55,212-2 sensitive, non-CB_1, non-CB_2, non-TRPV1 G-protein coupled receptor

Breivogel and colleagues examined whole brain membranes and homogenates prepared from $CB_1^{-/-}$ C57BL/6 and CD1 mice, and found that anandamide and WIN 55,212-2 stimulated ^{35}S-GTPγS binding (Di Marzo *et al*., 2000; Breivogel *et al*., 2001). CP 55,940, HU 210 and Δ^9-THC did not stimulate binding and SR141716 demonstrated only weak inhibition. Distribution of GTPγS binding only partially overlapped distribution of CB_1

receptors, accentuating a putative role for a novel receptor. It is unlikely that these compounds were acting at the TRPV1 receptor as WIN 55,212-2 shows low affinity and efficacy at the TRPV1 receptor, and the TRPV1 receptor is not coupled to G-proteins. Welch and colleagues found, when examining the analgesic efficacy of cannabinoids in spinal cord, the rank order potency of SR141716 in blocking analgesia produced by THC, anandamide, and CP 55,490 differed from that predicted for a CB_1 receptor-mediated response (Welch *et al.*, 1998; Houser *et al.*, 2000). To further complement this observation, differences in the analgesia synergistically produced by co-administration of morphine and THC compared with morphine and anandamide or CP 55,940, suggested the involvement of a novel receptor.

1.4.3.3. An intestinal SR141716-sensitive, non-CB_1, non-CB_2, non-TRPV1 receptor

Evidence for a novel SR141716-sensitive, non-CB_1, non-CB_2, non-TRPV1 receptor was obtained in nerve terminals of the myenteric plexus-longitudinal muscle preparation of the guinea-pig ileum (Mang *et al.*, 2001). Anandamide, but not CP 55,940, evoked an inhibition of electrically evoked release of acetylcholine, similar to that produced by the CB_1 receptor, which was insensitive to capsazepine. Blockade by SR141716 was observed, but at a potency far below that observed for the CB_1 receptor.

1.4.4. Putative cardiovascular cannabinoid receptors

Very strong evidence for novel cannabinoid receptors comes from a continuing series of investigations performed by several laboratories studying the effects of cannabinoids on

the vasculature. In summary, certain cannabinoids cause vasodilation and hypotension in the absence of CB_1, CB_2, or TRPV1 receptor activation. The best-characterised response is in mesenteric vessels, (Járai *et al.*, 1999) in which anandamide and methanandamide induce vasodilation, while the synthetic cannabinoids and THC do not, and are inhibited by high concentrations (>1 μM) of SR141716. Similar to studies performed by Hájos and colleagues, no blockade was produced by AM251. Vasodilation was sensitive to pertussis toxin, suggesting a mechanism dependent upon a GPCR and $G_{i/o}$-proteins. The cannabidiol analogue, abnormal cannabidiol (abn-CBD), which is inactive at CB_1 and CB_2 receptors, functioned as an agonist in some studies and was blocked by both cannabidiol and the synthetic cannabidiol analogue O-1918 (Offertáler *et al.*, 2003). Work by Begg *et al.* (2003) suggests this novel cannabinoid receptor is expressed by endothelial cells and that activation induces relaxation and vasodilation by the opening of potassium channels on vascular smooth muscle through a signalling pathway dependent upon the release of nitric oxide.

1.4.5. Putative cannabinoid receptors on immune cells

Palmitoylethanolamide (PEA, an analogue of anandamide that contains a 16:0 fatty acid moiety instead of 20:4 for AEA) has received considerable attention because of its anti-inflammatory properties (Lambert *et al.*, 2002). However, it shows little affinity for both CB_1 and CB_2 receptors (Lambert *et al.*, 1999; Griffin *et al.*, 2000). PEA was found to reduce the pain associated with an inflammatory response through a mechanism blocked by SR144528 (Calignano *et al.*, 1998; Jaggar *et al.*, 1998). It was hypothesised that PEA

might interact with a novel cannabinoid receptor that is antagonised by SR144528 or that PEA might stimulate a novel cannabinoid receptor that couples to phospholipases C and diacylglycerol lipase, increases 2-AG production, and thus indirectly activating CB_2 receptors.

1.4.6. A putative CB_2–like cannabinoid receptor

In the mouse abdominal stretch test and in the mouse formalin paw test both anandamide and PEA have been found to exhibit antinociceptive activity (Calignano *et* al., 1998; 2001). The synergistic interaction of the two cannabinoids and the antagonism of anandamide by SR141716 but not SR144528, and PEA by SR144528 but not SR141716 suggests activity through different mechanisms. The lack of observed activity of PEA at CB_2 and TRPV1 receptors suggested PEA may be acting through peripheral "CB_2-like" receptors which are sensitive to SR144528, but not to SR141716 and capsazepine.

1.4.7. Allosteric modulation of non-cannabinoid receptors

1.4.7.1. Voltage-gated calcium channels

Direct inhibition of voltage-gated calcium channels (VGCC) by cannabinoids has been suggested by a number of studies. The binding of dihydropyridine, phenylalkylamine and 1,5-benzothiazapine class L-type VGCC antagonists was demonstrated to be inhibited by anandamide in T-tubule membrane vesicles from rabbit skeletal muscle fibres (Shiamsue *et al.*, 1996). In similar tissue depolarisation-induced $^{45}Ca^{2+}$ fluxes mediated by the

activation of L-type VGCC were inhibited by anandamide and methanandamide through a mechanism insensitive to SR141716 or PTX treatments (Oz *et al.*, 2000). The synthetic cannabinoids CP 55,940 and WIN 55,212-2, and Δ^9-THC did not produce any inhibition. Arvanil, an anandamide-capsaicin hybrid compound with affinity for both CB_1 and TRPV1 receptors, inhibited L-type VGCC in the NG108-15 neuroblastoma cell line in the presence of a TRPV1 antagonist and PTX (Lo *et al.*, 2003).

Chemin and colleagues (2000) reported anandamide inhibition of T-type VGCC expressed on neuroblastoma NG108-15, CHO, COS, and HEK-293 cell lines and on *Xenopus* oocytes. Inhibition was not blocked by GDPβS, an inhibitor of G-protein activity, nor by the inhibitors of PLA2, PLC and PLD in HEK-293 cells. CP 55,490 and WIN 55,212-2 were ineffective and SR141716 alone produced a strong inhibition. Methanandamide produced equipotent inhibition indicating that the metabolic products of anandamide hydrolysis were not responsible for inhibition (Chemin *et al.*, 2000). Neuritogenesis of NG108-15 cells, which is dependent upon T-type VGCC, was shown to be inhibited by anandamide and methanandamide in the presence of SR141716 (Chemin *et al.*, 2002).

In superior cervical ganglion neurones that do not express endogenous cannabinoid receptors, N-type VGCC were inhibited by anandamide, but not by 2-AG. The effects were not blocked by SR141716 or PTX (Guo and Ikeda, 2004).

In rat cultured dorsal root ganglion neurones, anandamide induced 33% inhibition of high-voltage activated Ca^{2+} currents in a mechanism insensitive to SR141716 (Evans *et al.*, 2004). In trigeminal sensory neurones, WIN 55,212-2 and the inactive enantiomer WIN 55,212-3 inhibited the release of K^+-evoked calcitonin gene-related peptide

(CGRP), which is governed by the opening of Ca^{2+} channels, with similar efficacy (Price *et al.*, 2004).

1.4.7.2. Voltage-gated sodium channels

Nicholson and colleagues examined the susceptibility of voltage-sensitive sodium channels to cannabinoids in mouse cortical neurones and purified synaptosomes (Nicholson *et al.*, 2003). Anandamide, AM 404 and WIN 55,212-2 inhibited veratridine-dependent depolarisation of synaptoneurosomes and release of L-glutamic acid and GABA. The binding of [^{3}H]-batrachotoxinin A 20-alpha-benzoate to voltage-sensitive sodium channels was also inhibited by these cannabinoids. In addition, anandamide, AM 404 and WIN 55,212-2 blocked TTX-sensitive sustained repetitive firing in cortical neurones without altering primary spikes. None of the inhibition observed was blocked by AM 251. Na^+ currents in rat dorsal root ganglion neurones were inhibited by anandamide through increasing inactivation of channels. Inhibition was not reversed by AM 251, AM 630 or capsazepine, suggesting a mechanism involving either direct action at the channel or a novel receptor (Kim *et al.*, 2005)

1.4.7.3. Voltage-gated potassium channels

First evidence for the direct interaction of cannabinoids with voltage-gated K^+ channels was demonstrated on Shaker-related Kv1.2 K^+ channels expressed in the murine fibroblast B82 cell line (Poling *et al.*, 1996). Both anandamide and Δ^9-THC inhibited current with similar potency and showed no sensitivity to SR141716 and PTX. Internal

dialysis with anandamide in outside-out patch recordings demonstrated action upon the extracellular side of the membrane (Poling *et al.*, 1996).

In HEK 293 cells transfected with the large conductance Ca^{2+}-activated K^+ (BK) channel and in mouse aortic myocytes anandamide and methanandamide activated BK current, when measured using whole cell patch clamp techniques (Sade *et al.*, 2006). Potentiation of BK current was not modulated by AM251, modulators of G_s and $G_{i/o}$-protein activity (cholera and pertussis toxin) or by application of a selective CB_2 agonist (JWH133). Inhibition of calmodulin and MAP kinase dependent intracellular pathways also did not affect the potentiation. However, in excised inside-out patches methanandamide did not alter channel activity suggesting potentiation is mediated by intracellular factors (Sade *et al.*, 2006).

The delayed rectifier K^+ current in rat arterial myocytes was inhibited by anandamide and methanandamide through a mechanism insensitive to SR141716. These endocannabinoids were only active when applied externally but not internally (Van den Bossche and Vanheel, 2000).

The background (leak) K^+ (TASK-1) channel, transfected in COS cells, showed full inhibition upon exposure to anandamide and methanandamide with an IC_{50} of 700 nM (Maingret *et al.*, 2001). Blockade was not observed with pre-exposure to SR141716. High concentrations (10 μM) of WIN 55,212-2 and CP 55,940 produced inhibition, but 2-AG, HU210 and Δ^9-THC did not produce any inhibition. Following these findings, anandamide-induced depolarisations or inward currents due to the inhibition of TASK-1 channels have been demonstrated in several other preparations including turtle motor neurones (Perrier *et al.*, 2003), rat carotid body chemoreceptors (Fearon *et al.*, 2003), rat

mesenteric and pulmonary artery (Gardener *et al.*, 2004), rabbit pulmonary artery smooth muscle cells (Gurney *et al.*, 2003) and murine ventricular myocytes (Barbuti *et al.*, 2002). Oliver *et al.* (2004) demonstrated, using giant inside-out patches, complete inhibition by anandamide of delayed rectifier K^+ channels (Kv3.1) transfected in *Xenopus* oocytes. The rapidly inactivating A-type (Kv1.1+ Kvβ1.1) channel, which is converted into a non-inactivating, delayed rectifier channel with exposure to phosphatidyl inositol 4,5 bisphosphate (PIP_2; for a review, see Hilgemann *et al.*, 2001) was shown to revert back from the non-inactivating state to the rapidly inactivating state upon exposure to anandamide. Anandamide produced pronounced increase in inactivation in oriens-alveous interneurones of the hippocampus, which express mainly delayed rectifier K^+ channels (Kv3 subunits). The lack of expression of CB_1, CB_2 and TRPV1 receptors in *Xenopus* oocytes (Henry and Chavkin, 1995) suggest activation through a novel mechanism.

1.4.7.4. 5-HT_3 receptors

Cannabinoid inhibition of the 5-HT_3 ligand-gated cation channel was first reported by Fan *et al.* (1995) in nodose ganglion neurones, in which anandamide, CP 55,940 and WIN 55,212-2 produced inhibition. Addition of Sp-cAMP, the nonhydrolyzable analogue of cAMP, and GDP-β-S, the nonhydrolyzable analogue of GTP, did not affect inhibition by anandamide or WIN 55,212-12, suggesting that inhibition occurred through a G-protein independent mechanism.

Anandamide acted as a noncompetitive antagonist at the 5-HT_3 receptor transfected in *Xenopus* oocytes (Oz *et al.*, 2002). SR141716 and PTX did not affect the inhibition,

neither did preincubation with 8-Br-cAMP, a membrane-permeable analog of cAMP, or Sp-cAMPS, a membrane-permeable protein kinase A activator.

Barann *et al.* (2002) demonstrated, using excised outside-out patches from HEK 293 cells transfected with h5-HT_{3A} receptor cDNA, Δ^9-THC, WIN 55,212-2, anandamide, JWH-015 and CP 55,940 inhibited 5-HT induced currents. WIN 55,212-2-induced inhibition was not altered by SR141716 and WIN 55,212-3, and the CB_1 and CB_2 receptor inactive enantiomer of WIN55,212-2, did not affect the 5-HT-induced current. The lack of specific binding of [^{3}H]-SR141716 and [^{3}H]-CP 55,940 to parental HEK 293 cells suggested specific interaction with the $5HT_{3A}$ receptor, whilst a lack of competition with the binding of [^{3}H]-GR65630, a specific ligand for 5-HT_3 receptors, by WIN 55,212-2, CP 55,940, anandamide and SR141716 suggested noncompetitive antagonism (Barann *et al.*, 2002).

1.4.7.5. Nicotinic receptors

The nicotinic acetylcholine receptor is a ligand-gated, cation specific channel, which plays an essential role in fast synaptic excitation throughout both the peripheral and central nervous systems. Nicotinic receptors can be divided into two main families, muscle and neuronal nAChR. Functional neuronal nicotinic receptors are composed of five subunits comprising of different combinations of α and β subunits, of which there are eight α (α2- α9) and three β (β2-β4) subunits. The properties of different nicotinic receptor subtypes are determined by the specific subunit composition of the receptor (Colquhoun and Patrick, 1997; Luetje and Patrick, 1991).

Oz and colleagues have examined cannabinoid inhibition of nicotinic α7 homomeric receptors expressed in *Xenopus* oocytes. Initial work observed a noncompetitive inhibition of nicotine evoked currents which was shown to be G_s and $G_{i/o}$-protein independent through lack of modulation by PTX and 8-Br-cAMP (Oz *et al.*, 2002). CB_1 and CB_2 receptors, which are not expressed in *Xenopus* oocytes, were confirmed to not play a role through the lack of blockade of inhibition by SR141716 and SR144528. The lack of modulation of anandamide inhibition by the antagonists of anandamide metabolism, phenylmethylsulfonyl fluoride, superoxide dismutase, and indomethacin, or the anandamide transport inhibitor AM404, suggest inhibition is mediated by anandamide and not metabolites (Oz *et al.*, 2003). Further work demonstrated a lack of modulation by the synthetic cannabinoids WIN 55,212-2 and CP 55,940 and plant derived Δ^9-THC, whilst the anandamide metabolite arachadonic acid displayed inhibition, although with much lower potency than anandamide (Oz *et al.*, 2004). The endocannabinoid 2-AG was shown to possess similar inhibitory properties as anandamide (Oz *et al.*, 2004). Chimeric α7-nACh-5-HT_3 receptors comprised of the amino-terminal domain of the α7-nACh receptor and the transmembrane and carboxyl-terminal domains of the 5-HT_3 receptor suggested the site of action for anandamide is located in the transmembrane and carboxyl-terminal domains of the receptors (Oz *et al.*, 2005).

Using *in vitro* intracellular recording of myenteric S-type neurones, Lopez-Redondo *et al.* (1997) showed 46% and 37% inhibition of the fast e.p.s.ps amplitudes by WIN 55,212-2 (100 nM) and CP 55,940 (100 nM) respectively. Blockade by the CB_1 receptor antagonist SR141716 occurred in only 38% of neurones demonstrating WIN 55,212-2 inhibition and when tested on its own, SR141716 (1 μM) caused a 40-50% reduction in the amplitude of

fast e.p.s.ps. The (−)enantiomer of WIN 55,212-2, WIN 55,212-3 was inactive at a concentration of 100 nM. Ionophoretic application of acetylcholine induced depolarisations, which were inhibited by 63% by WIN 55,212-2 (100 nM) in 5 out of 11 neurones tested. Reversal of WIN 55,212-2 inhibition by SR141716 (1 μM) was observed in 5 out of 12 neurones tested (Lopez-Redondo *et al.*, 1997).

Preliminary findings in disassociated myenteric neurones showed both CP 55,940 and anandamide induced full inhibition of nicotine evoked currents (DeMuth *et al.*, 2004). Inhibition was not blocked by PTX and anandamide inhibition was not blocked by SR141716 (1 μM). When tested alone, SR141716 (300 nM) inhibited current. PEA, which does not show binding to CB_1 and CB_2 receptors, inhibited current at concentrations of 1 μM (DeMuth *et al.*, 2004).

1.4.7.6. Glycine receptor

The glycine receptor (GlyR) is an anionic member of the cys-loop superfamily of ligand-gated ion channels (Betz *et al.*, 1999; Lester *et al.*, 2004). Although best associated with mediating inhibitory neurotransmission in the spinal cord, recent work suggests it may also have other physiological roles in various brain regions including cerebral cortex, hippocampus, and ventral tegmental area (Legendre, 2001; Lynch, 2004). Local alignment of amino acid sequences of cannabinoid receptors and GlyR subunits revealed that GlyRs contain few fragments that display a high level of homology with regions suggested to be responsible for agonist binding within CB_1 and CB_2 receptors (Mahmoudian, 1997; Tao *et al.*, 1999; Shim *et al.*, 2003).

Both endocannabinoids, 2-AG and anandamide, were observed in isolated hippocampal pyramidal neurones at physiological concentrations (0.2–2 μM) to strongly inhibit peak amplitudes of postsynaptic current and accelerate rise time and desensitization (Lozovaya *et al.*, 2005). In contrast WIN 55,212-2 (1 μM) did not inhibit peak amplitude, but did accelerate rise time and desensitization. The effects of these cannabinoids were not inhibited by SR141716 or capsazepine and the G-protein inhibitor GDPβS. Seizure-like activity, induced by short bursts of high-frequency stimulation of inputs to the hippocampal CA1 region, which are inhibited by GlyR antagonists, was reduced in the presence of anandamide (Lozovaya *et al.*, 2005).

A potentiation of GlyR currents by anandamide and Δ^9-THC was reported in acutely isolated neurones from rat ventral tegmental area and in *Xenopus* oocytes expressing human homomeric (α1) and heteromeric (α1β1) subunits of GlyR (Sun *et al.*, 2005; Hejazi *et al.*, 2006). Persistence of potentiation in the presence of SR141716 and the lack of expression of CB_1 and CB_2 receptors in *Xenopus* oocytes suggest modulation through either direct effects or a novel receptor (Hejazi *et al.*, 2006).

1.4.7.7. Ionotropic glutamate receptor

Ionotropic glutamate receptors consist of a family of ligand-gated ion channels that include NMDA, kainate and AMPA receptors (Madden, 2002).

Potentiation of NMDA-induced Ca^{2+} flux by anandamide and methanandamide in the presence of SR141716 or PTX was reported in rat cortical, cerebellar, and hippocampal slices (Hampson *et al.*, 1998). Anandamide, but not THC, also augmented NMDA-stimulated currents in *Xenopus* oocytes expressing NR1 and NR2A genes and enhanced

the amplitudes of field potentials in hippocampal slices in a SR141716 insensitive manner (Hampson *et al.*, 1998).

1.5. Project aims and objectives

The overall aim of this study is to investigate the cannabinoid signalling mechanisms governing neurotransmission and their interaction with the mechanisms by which other neurologically active drugs act.

Although the action of cannabinoid on gastric motility has been examined for some time, work has been restricted to examining the modulation of electrically evoked contractions. Chapter 2 examines the role of cannabinoids in modulating contractions evoked through a mechanism which bares greater similarity to that found in *in vivo* conditions, the activation of the nicotinic acetylcholine receptor, and investigates the mechanisms by which cannabinoids modulate the role of the nicotinic acetylcholine receptor through the use of the guinea-pig ileum myenteric plexus-longitudinal muscle (MPLM) organ bath preparation and using the whole-cell patch clamp technique to study nicotine evoked currents in primary cultures of guinea-pig ileum myenteric AH neurones.

Furthermore, the mechanisms through which cannabinoids act in the gut have not been elucidated. To investigate this chapter 3 explores the effects of cannabinoid receptor ligands on Ca^{2+} currents in primary cultures of guinea-pig ileum myenteric AH neurones.

As opioids act through similar intracellular mechanisms to cannabinoids, chapter 4 examines the interaction between cannabinoid and opioid receptor ligands on electrically evoked contractions of the MPLM preparation and opioid-withdrawal evoked contractions of the whole ileum, and their action in both primary myenteric and NG108-15 neuronal cell cultures.

Drugs of abuse, for example cocaine, influence neural activity within the mesolimbic reward pathway. Cannabinoids have been shown to also modulate the function of this

pathway, although the mechanism by which this occurs has not been fully elucidated. Chapter 5 discusses initial work examining the interaction between cannabinoid and dopaminergic systems within the ventral tegmental area of brain slices through the use of whole-cell blind patch clamping.

Chapter 2 - The interaction between cannabinoids and the nACh receptor in the guinea-pig ileum myenteric plexus

2. Chapter 2 - The interaction between cannabinoids and the nACh receptor in the guinea-pig ileum myenteric plexus

2.1. Introduction

2.1.1. The guinea-pig ileum myenteric plexus

Modulation of contractions induced by electrical stimulus of the guinea-pig myenteric plexus-longitudinal muscle preparation (MPLM) has been used for some time as a measure of cannabinoid activity through the CB_1 receptor (Pertwee *et al.*, 1996). Contractions within the ileum are considered to be evoked through the stimulus of action potential firing within neurones, inducing the release of neurotransmitters, including acetylcholine, which act upon the longitudinal muscle to cause contraction. This preparation consists of a large variety of neurones responsible for conveying both excitatory and inhibitory stimulus. As a result of electrical stimulus, both inhibitory and excitatory neurotransmitters are released within the myenteric plexus and may interact independently with cannabinoids.

2.1.1.1.Structure of the guinea-pig ileum

The lumen of the guinea-pig ileum is lined by the mucosa and submucosal plexus, which are primarily responsible for secretion into the lumen. The submucosal plexus is surrounded by the circular muscle, myenteric plexus and longitudinal muscle, which

control gastric motility. Within the myenteric plexus, stimulus from the central nervous system, via parasympathetic and sympathetic neurones, and the lumen, via primary afferent neurones, is transferred to interneurones, before exciting longitudinal and circular muscle motor neurones and initiating peristalsis.

2.1.1.2.Classification of myenteric neurones

Enteric neurones are characterised on the basis of electrical, immunological and morphological properties.

Characterisation on the basis of electrical properties is derived from intracellular studies by Nishi and North (1973) and Hirst *et al.* (1974). Neurones were separated into three main groups, type 1, 2 and 3 by Nishi and North on the basis of their membrane properties and ability to fire action potentials in response to depolarising currents. Type 1 cells demonstrate low membrane potential, high input resistance and an ability to fire action potentials initiated by depolarising currents. Type 2 cells exhibited a more negative membrane potential, lower input resistance and only fired action potentials at the start of a depolarising current pulse. Type 3 cells displayed similar passive properties to type 2 cells but did not fire action potentials even with very large depolarisations.

Hurst divided neurones into AH neurones, which possess a long after-hyperpolarisation following action potentials, and S neurones demonstrating fast, cholinergic synaptic inputs and no after-hyperpolarisation. These classification schemes have since been amalgamated to form a scheme comprising of four classes; type 1/S, type 2/AH, type 3 and type 4 (Bornstein *et al.*, 1994). Type 3 neurones display S neuron-like excitatory input but are unable to generate action potentials in response to large depolarisations, and

type 4 neurones are unexcitable immediately after electrode impalement but develop type 2/AH properties if impalement is maintained.

Morphologically, enteric neurones were first categorised in a study published over 100 years ago (Dogiel, 1899). Dogiel type I neurones possess a single axon and short lamellar dendrites. Dogiel type II cells have multiple long processes arising from a smooth cell body. Other morphological types of cells have been identified by Dogiel and in other studies but less consensus exists for the use of this extended classification. Within the guinea-pig small intestine Dogiel type II cells possess the electrical characteristics of AH neurones and Dogiel type I cells possess the electrical characteristics of S neurones (Brookes *et al.*, 1995). Multiple-labelling immunohistochemistry has enabled classification on the basis of the presence of particular proteins or peptides either possessing a known or unknown functional role within the neurone (figure 2.1). For example, the presence of modulatory peptides, such as enkephalin, or proteins responsible for the production of neurotransmitters, such as choline acetyltransferase, within a nerve cell suggest these neurotransmitters are released and have action on other cells under some circumstances. Many of the markers used to distinguish enteric neurones have no known physiological role yet are very useful in classifying neurones.

2.1.1.3.Primary afferent neurones

By projecting in to the mucosa, primary afferent neurones transmit information regarding the nature and intensity of the stimulus to neurones within the myenteric and submucosal plexus. They all possess Dogiel type II morphology, comprising of multipolar cell bodies

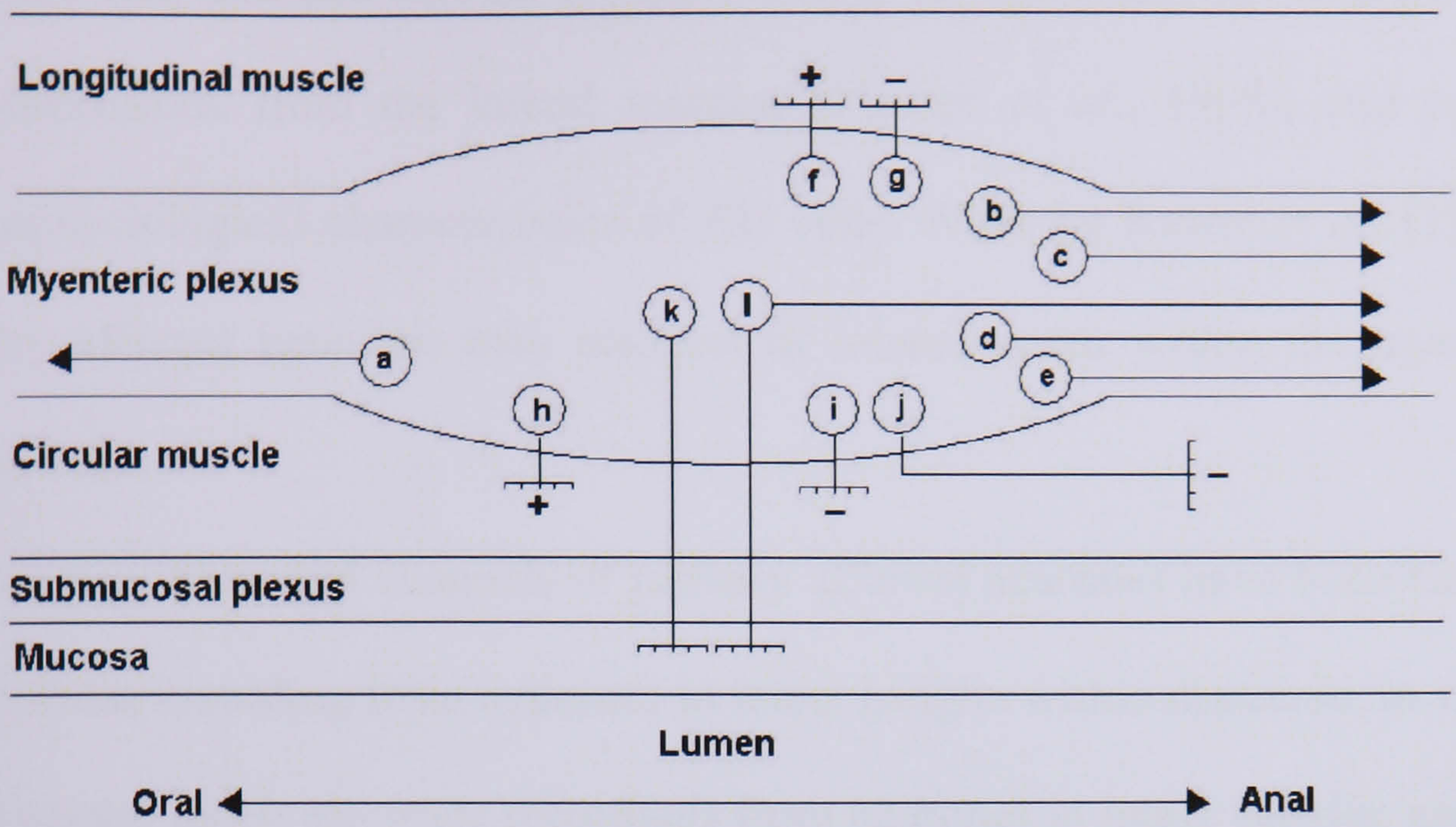

Figure 2.1 Schematic diagram showing morphological classes of enteric neurones and axon projections. Letters on the neurones to aid identification are detailed in table 2.1. (Adapted from Brookes *et al*., 1995).

Table 2.1 Summary of cell types listed in figure 2.1.

	Immunoreactivity	Morphology	Function
a	ChAT/Calret/ENK/NFP/SP	Dogiel type I/S	Ascending interneurone
b	ChAT/5-HT/NFP	Dogiel type I/S	Descending interneurone
c	ChAT/SOM	filamentous	Descending interneurone
d	ChAT/VIP/NPY/GRP	Dogiel type I/S	Descending interneurone
e	VIP/NOS/NFP/NPY/GRP/AP	Dogiel type I/S	Descending interneurone
f	ChAT/Calret/SP	Dogiel type I/S	Excitatory motor neurone, longitudinal muscle
g	VIP/NOS/NPY/GABA	Dogiel type I/S	Inhibitory motor neurone, longitudinal muscle
h	ChAT/SP/ENK/NFP/GABA/ AP	Dogiel type I/S	Excitatory motor neurone, circular muscle
i	VIP/NOS/ENK/GABA/AP	Dogiel type I/S	Short inhibitory motor neurone, circular muscle
j	VIP/NOS/NFP/GABA/AP	Dogiel type I/S	Long inhibitory motor neurone, circular muscle
k	ChAT/Calb/SP/NMU	Dogiel type II/AH	Primary afferent neurone
l	ChAT/Calb/SP/NMU	Dogiel type II/AH	Primary afferent neurone, long aboral axon

Abbreviations: 5-HT: 5-hydroxytryptamine, AP: endogenous alkaline phosphatase, Calb: calbindin, Calret: calretinin, ChAT: choline acetyltransferase, ENK: enkephalin, GABA: gamma amino butyric acid, GRP: gastrin-releasing peptide, NFP: neurofilament protein triplet, NMU: neuromedin U, NOS: nitric oxide synthase, NPY: neuropeptide Y, SOM: somatostatin, SP: substance P (or related tachykinins), VIP: vasoactive intestinal polypeptide.

that were flat, thin and smooth on upper and lower surfaces, with neuritis projecting in two dimensions from the lateral margins (Hanani *et al.*, 1998), and possessing the electrophysiological characteristics of AH cells. Work by Kunze *et al.* (1993) suggests primary afferent neurones may also act as interneurones within the myenteric plexus (figure 2.1).

Electrical currents and channels of primary afferent neurones have been examined using intracellular recording from neurones in intact ganglia within dissected, *in vitro* intestinal preparations, patch electrode recordings from neurones in intact ganglia, and using patch electrode recordings from dissociated neurones in primary culture. The mode of recording is considered to influence both resting and active current states. Lower input resistances have been observed with the use of intracellular electrodes compared with patch electrodes, and very often neurones are hyperpolarised for a considerably long time after impalement suggesting some membrane damage may occur allowing Ca^{2+} influx and activation of Ca^{2+}-activated K^+ channels (Hodgkiss and Lees, 1983; Baidan *et al.*, 1992; Rugiero *et al.*, 2002). This is complemented by the observation that input resistance increases and resting membrane potential decreases after an hour of recording. Conversely, wash-out may occur during patch recordings in which Ca^{2+} chelators (such as EGTA) may enter the cytoplasm of the neurones and inappropriately buffer intracellular Ca^{2+} levels. Furthermore, characteristics may change with dissociation and primary culture.

Under resting conditions, AH neurones possess a relatively higher membrane potential of approximately -60 mV and display a lower input resistance than S-type neurones. Rugiero *et al.* (2002; 2003) demonstrated that about 20% of the resting conductance was

controlled by a hyperpolarisation-activated cation current (I_H). This highly sensitive inward rectifier carried both Na^+ and K^+ currents and was blocked by Cs^+ but not Ba^+. RT-PCR, single-cell profiling, and immunostaining experiments indicated that $Na_v1.9$ transcripts and subunits were expressed by myenteric sensory neurones. The A-type K^+ current (I_A) may contribute to resting membrane potential as Starodub and Wood (2000) demonstrated an overlap of steady-state activation and inactivation curves at a potential close to the resting membrane potential (-55 mV). Resting Ca^{2+} conductance may also play a role due to the presence of Ca^{2+}-dependent K^+ and cation channels. However, the large conductance Ca^{2+}-activated K^+ channel (BK) and the intermediate conductance Ca^{2+}-activated K^+ channel (IK) showed little activity at rest, and resting membrane potential showed little variation in the presence of the channel blockers charybdotoxin and iberiotoxin (Kunze *et al.*, 2000; Vogalis *et al.*, 2002).

Unlike S-type neurones, AH neurones do not fire repetitively in the resting state and possess a long-duration hyperpolarising afterpotential that lasts for several seconds. The action potential in AH neurones possess a large amplitude of about 80-90 mV, when measured with intracellular electrodes, and a half-width of about 2.5 ms. This inward current comprises of a TTX-sensitive Na^+ current and a high voltage-activated Ca^{2+} current. Work by Zholos *et al.* (2002) showed, using whole-cell patch clamp of cultured myenteric AH neurones derived from adult guinea pigs, a Na^+ current activated between -50 and -40 mV that peaked at -10 mV. Steady-state inactivation curves were fit to the Boltzmann equation with a potential for half-inactivation of -55.6 mV and a slope factor of 6.4 mV. Inactivation was fast with the time constant ranging from a maximum of 161 $\pm$ 23 ms at -70 mV to a minimum of 2.3 $\pm$ 0.2 ms at -30 mV, and recovery was also rapid

with time constants ranging between 7.3 ± 1.1 ms and 21.5 ± 5.1 ms for -100 mV and -80 mV respectively. Fit of the Boltzmann equation led authors to suggest the presence of only one type of Na^+ channel, behaving in a "classical" voltage-gated TTX-sensitive fast channel manner. RT-PCR has shown expression of $Na_v1.2$, $Na_v1.3$, $Na_v1.6$, and $Na_v1.7$ mRNA in small and large intestinal preparations from guinea-pigs (Bartoo *et al.*, 2005). Immunohistochemical analysis demonstrated $Na_v1.2$ presence primarily within the soma of the majority of myenteric and submucosal neurones, although faint immunoreactivity was occasionally observed in ganglionic and internodal fibres. $Na_v1.3$ was observed in dendrites, soma, and axons in a small group of myenteric neurones, as well as in numerous myenteric internodal fibres; immunoreactivity was rarely observed in the submucosal plexus. The $Na_v1.6$ channel was primarily observed in the initial axonal segment of colonic myenteric neurones and the $Na_v1.7$ channel was observed in dorsal root ganglia neurones but not in the myenteric plexus of the small and large intestine (Bartoo *et al.*, 2005).

The high voltage-activated Ca^{2+} current, which is activated during the action potential of AH-neurones, has been shown to be mainly mediated by N-type channels (Hirst *et al.*, 1974; Rugiero *et al.*, 2002). Action potentials, elongated through the inhibition of the after-hyperpolarisation potassium current, were shown to be mostly inhibited by the highly specific N-type channel blockers ω-conotoxin GVIA (ω-CgTX GVIA) and ω-CgTX MVIIA. The residual current was not blocked by further addition of the P/Q- and N-type channel blocker ω-CgTX MVIIC, and the P/Q-type channel specific blocker ω-aga IVA had no effect on the prolonged action potential (Rugiero *et al.*, 2002). Exposure

to the L-type calcium channel blockers nicardipine and nifedipine is also established not to affect action potentials (North and Tokimasa, 1987; Kunze *et al.*, 1994).

The long after-hyperpolarisation (AH) that characterises these neurones is the result of the voltage-dependent influx of calcium opening of calcium-dependent potassium channels that render the soma refractory to further stimuli (Nishi and North, 1973; Hirst *et al.* 1974). Unlike in S neurones in which action potentials are completely blocked by TTX, this influx of calcium enables action potentials to be evoked in the presence of TTX.

2.1.1.4.Interneurones

Interneurones are grouped into networks of orally projecting ascending neurones and aborally projecting descending neurones.

Ascending interneurones consist entirely of a single class of neurones comprising of Dogiel type I neurones with S cell electrophysiological characteristics and express immunoreactivity for choline acetyltransferase and substance P (Brookes *et al.*, 1997). Ascending interneurones account for 5% of all myenteric neurones (Costa *et al.*, 1996)

Descending interneurones consist of at least five different types of neurones showing among them immunoreactivity for somatostatin, 5-hydroxytryptamine, vasoactive intestinal polypeptide and acetylcholine. They possess Dogiel type I and II morphology and, in the presence of somatostatin, numerous filamentous dendrites and a single axon.

Through the use of pharmacologically divided organ baths, the transmission between ascending interneurones, and between interneurones and excitatory motor neurones has been shown to be cholinergic, mediated through the nicotinic receptor. Descending

inhibition has been shown to be resistant to the nicotinic antagonist hexamethonium (Johnson *et al.*, 1996).

2.1.1.5.Motor Neurones

Motor neurones are responsible for the transfer of stimulus from interneurones to the longitudinal and circular muscle and consist of excitatory and inhibitory Dogiel type I neurones (uniaxonal with flattened laminar dendrites) with S cell electrophysiological characteristics.

Longitudinal muscle motor neurones make up approximately 24% of the neurones in the guinea-pig myenteric plexus (Brookes *et al.*, 1992). Almost all are immunoreactive for choline transferase, while approximately 3% are immunoreactive for VIP and NOS (Williamson *et al.*, 1996). This suggests, in the guinea-pig, neural stimulus is only capable of inducing contractions of the longitudinal muscle. Approximately half the neurones expressing choline transferase show immunoreactivity for tachykinins (Brookes *et al.*, 1991a).

Circular muscle motor neurones make up approximately 17% of the neurones in the guinea-pig myenteric plexus of which approximately 70% display immunoreactivity for choline transferase (Brookes *et al.*, 1991b).

2.1.2. Role of cannabinoids within the myenteric plexus

Cannabinoid inhibition of electrically evoked contractions of guinea-pig MPLM through the inhibition of ACh release is well accepted. Cannabinoids are considered to act at CB_1 receptors within the ileum due to agonists possessing a similar order of potency as that found in other preparations, stereospecificity (Pertwee, 2001), blockade by the CB_1 specific antagonist SR141716 (Pertwee *et al.*, 1996), inhibition by antagonists of $G_{i/o}$-protein signal transduction (Coutts and Pertwee, 1998), and finally by proof of the presence of CB_1 receptors through binding studies (Lynn and Herkenham, 1994), immunohistochemistry (Coutts *et al.*, 2002) and the detection of CB_1 receptor mRNA within the MPLM (Griffin *et al.*, 1997).

The CB_1 receptor is considered to be located upon excitatory motor neurones based on pharmacological and immunohistochemical evidence. Pharmacologicial evidence includes the cannabinoid induced reduction of release of acetylcholine from unstimulated and stimulated tissue (Coutts and Pertwee, 1997), the reduction in the amplitude of electrically evoked action potentials in S type myenteric neurones (Lopez-Redondo *et al.*, 1997), and the lack of inhibition of contractions evoked by exogenously applied ACh (Pertwee *et al.*, 1996). Coutts *et al.* (2002) recently showed, using dual labelling immunohistochemisty, the CB_1 receptor was expressed in virtually all neurones expressing choline acetyltransferase, an enzyme responsible for the production of ACh and so present in the majority of excitatory motor neurones. The CB_1 receptor was also shown to be present on cholinergic sensory and interneuronal neurones.

2.1.2.1.CB_1 receptor independent cannabinoid activity

Inhibition in the myenteric plexus may not be mediated exclusively by the CB_1 receptor. Mang *et al.* (2001) observed a vanilloid and tachykinin receptor independent inhibition of electrically-evoked contractions by anandamide that was antagonised by SR141716 with a potency much lower than expected for a CB_1 receptor mediated effect. Thus K_B values for the antagonism of anandamide by SR141716 for electrically-evoked acetylcholine release and contraction were 251 and 631 nM respectively, while corresponding values for the antagonism of CP 55,940, presumably acting on CB_1 receptors, were 4 and 1.3 nM.

Using intracellular recording of myenteric S-type neurones *in vitro*, Lopez-Redondo *et al.* (1997) showed blockade by the CB_1 receptor antagonist SR141716 occurred in only a proportion of cells demonstrating cannabinoid inhibition. Reversal of WIN 55,212-2 inhibition by SR141716 of fast e.p.s.ps was observed in only 38% of neurones and in only 42% of neurones when inhibiting ACh-induced depolarisations. When tested alone, they showed SR141716 induced a 40-50% reduction in the amplitude of fast e.p.s.ps.

The SR141716 evoked inhibition was also reported by DeMuth *et al.* (2004) who also observed a SR141716-independent cannabinoid inhibition of currents in disassociated myenteric neurones. In addition they observed an inhibition by PEA, which does not show binding to CB_1 and CB_2 receptors, and a lack of blockade of cannabinoid inhibition by pertussis toxin, which inhibits $G_{i/o}$-proteins thus rendering both CB_1 and CB_2 receptors inactive (Sones *et al.*, 2006).

In the rat isolated gastric fundus, the CB_2 receptor antagonist AM 630 was shown to reverse anandamide but not WIN 55,212-2 inhibition of electrically-evoked contractions (Storr *et al.*, 2002).

The presence of CB_2 receptor mRNA was initially shown by Griffin *et al.* (1997) to be present in the whole ileum, but not in the myenteric plexus-longitudinal muscle segments, suggesting the presence solely in immune tissue. However, recent work by Duncan *et al.* (2005; 2006) suggests, using quantitative RT-PCR and immunohistochemistry, a low level presence of the CB_2 receptor in the myenteric plexus-longitudinal muscle segments, which is increased with exposure to LPS. This proposition is reinforced by the observation of a CB_2 mediated inhibition of gastrointestinal transit after LPS enhancement, which was not present in the absence of LPS (Mathison *et al.*, 2004). Evaluation of the mode of action through the use of different antagonists suggest inhibition is mediated by the cyclooxygenase enzymes and is independent of inducible nitric oxide synthase (NOS) and platelet-activating factor.

2.1.2.2.Mechanism of cannabinoid inhibition of acetylcholine release

Although the exact mechanism through which cannabinoids act to inhibit acetylcholine release in the ileum has not been established, it is believed that they act in a similar manner to that established for the CB_1 receptor in the brain. Possible mechanisms include the inhibition of voltage-gated calcium channels which would reduce the rise in intracellular calcium that plays a role in the propagation of action potentials in AH neurones and is necessary for inducing exocytosis (Parsons *et al.*, 1993), hyperpolarisation of the neurone through GIRK channel opening thereby inhibiting action potential generation, and a protein kinase A mediated inhibition of release through phosphorylation of exocytosis machinery (Evans and Morgan, 2003).

2.1.2.3.Endocannabinoids within the ileum

The selective CB_1 antagonist SR141716 increases the amplitude of electrically evoked contractions when added alone to guinea-pig MPLM and circular smooth muscle preparations (Pertwee *et al.*, 1996; Izzo *et al.*, 1998), and increased electrically evoked ACh release from MPLM (Coutts and Pertwee, 1997). This suggests SR141716 may be inhibiting the action of released endocannabinoids on CB_1 receptors present on excitatory motor neurones. An alternative explanation is that SR141716 may be acting as an inverse agonist at the CB_1 receptor. This hypothesis assumes that the receptor exists in either a $G_{i/o}$–protein bound precoupled state, the extent to which is reduced by SR141716, or the G-protein to which the CB_1 receptor binds to may change. The existence of an endocannabinoid system is backed by the presence of the endocannabinoid 2-AG, isolated by Mechoulam *et al.* (1995) in the canine gut, and the anandamide and 2-AG metabolising enzyme FAAH in the rat intestine (Ueda and Yamamoto, 2000). Although the FAAH inhibitor phenylmethylsulphonyl potentiates the inhibition of anandamide on electrically evoked contractions within the guinea-pig MPLM, it does not induce any inhibition when administered alone (Pertwee *et al.*, 1995), suggesting the lack of existence of an endocannabinoid based signalling system.

2.1.3. Role of acetylcholine within the myenteric plexus

Within the enteric nervous system acetylcholine plays an important role in the transmission of stimulus between neurones, and between neurones and muscle. Work

carried out by Dale in 1914 distinguished two types of activity, from which the concept of muscarinic and nicotinic receptors evolved.

2.1.3.1.Nicotinic receptors

The nicotinic acetylcholine receptor is a ligand-gated, cation specific channel, which plays an essential role in fast synaptic excitation throughout both the peripheral and central nervous systems. Nicotinic receptors can be divided into two main families, muscle and neuronal nAChR. Functional neuronal nicotinic receptors are composed of five subunits comprising of different combinations of α and β subunits, of which there are eight α (α2- α9) and three β (β2-β4) subunits. The properties of different nicotinic receptor subtypes are determined by the specific subunit composition of the receptor (Colquhoun and Patrick, 1997; Luetje and Patrick, 1991).

Within the guinea-pig enteric nervous system, acetylcholine at nicotinic acetylcholine receptors predominantly mediates interneuronal excitatory transmission (Galligan and North, 2004). S-type motorneurones in the myenteric plexus, which innervate and induce contraction in smooth muscle, have been demonstrated to receive fast nicotinic excitatory input mediated via nAChRs located on somatodendritic regions of the neurone (Bornstein *et al.*, 1994; Nishi and North, 1973; Hirst *et al.*, 1974; Galligan and Bertrand, 1994). nAChRs have also been demonstrated to be present at the nerve endings of longitudinal muscle motor neurones (Galligan, 1999). Blockade of axonal conductance through the use of tetrodotoxin allowed the segregation of somatodendritic nicotinic receptors and those at the neuromuscular junction of motor neurones controlling the release of neurokinins. As the majority of neurokinin releasing neurones display immunoreactivity

for choline transferase (Brookes *et al.*, 1991a), this suggests acetylcholine release is also mediated by nicotinic receptors present at the neuromuscular junction. Further evidence for the existence of nicotine receptors at myenteric nerve endings was observed in an early neurochemical study (White, 1982) in which nicotine was shown to induce the release of ATP from synaptosomes derived from the guinea-pig ileum myenteric plexus (figure 2.2).

Immunohistochemical and pharmacological studies have revealed, in myenteric neurones maintained in cell culture, predominant expression of α3, α5, β2 and β4 nicotinic receptor subunits (Zhou *et al.*, 2002; Galligan and North, 2004). However, assembly of the subunits has not been established and so receptors may exist as either homologous populations or as multiple receptors of differing subunit composition. The presence of α7 nicotinic subunits is debatable. Zhou *et al.*, (2002) observed only a small proportion of cultured myenteric neurones showed staining on application of an α7 subunit selective antibody and, whilst under whole-cell patch-clamp, no inhibition of nicotinic receptors was observed with the α7 subunit specific blockers α-bungarotoxin and α-methyllycaconitine.

The nicotinic receptor has been shown to possess a number of allosteric binding sites through which endogenous non-competitive inhibitors, such as fatty acids including arachidonic acid a metabolite of anandamide, can act (Arias, 1998). Arachadonic acid has been shown to inhibit *Torpedo* and chick α7 nicotinic receptors, expressed in oocytes, possibly through a direct blocking effect on Ca^{2+}-modulatory sites on the nicotinic receptor (Nishizaki *et al.*, 1998). Unpublished studies investigating cannabinoid activity upon other nicotinic receptors have shown inhibition of human α4β2 nicotinic receptors

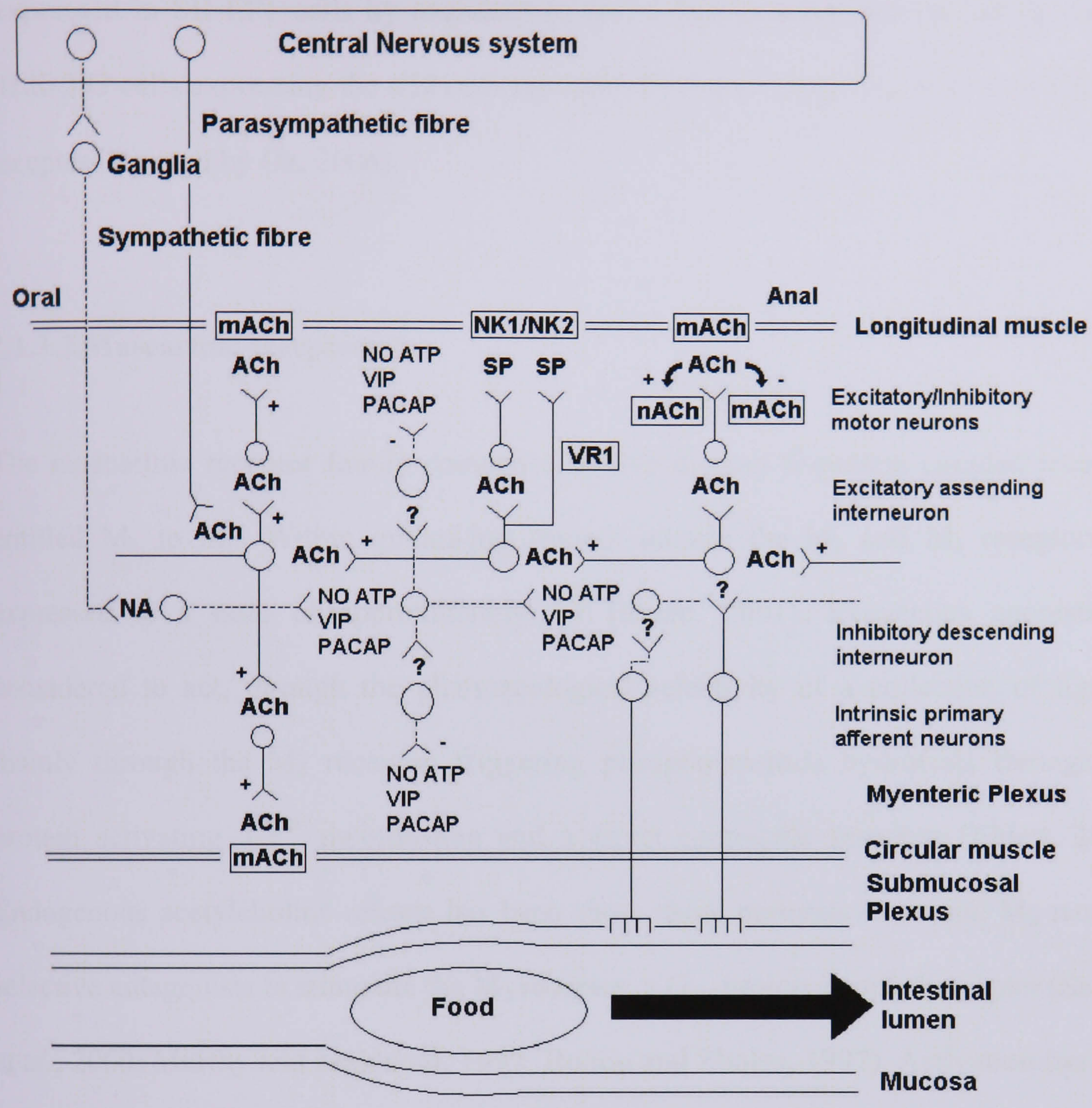

Figure 2.2 Physiology of the guinea-pig small intestine

expressed in SH-EP1 cells by anandamide and a lack of inhibition by anandamide in HEK-293 cells expressing the $\alpha 1\beta 1\varepsilon\gamma\delta$ subunits of mouse muscle nicotinic acetylcholine receptors (quoted by Oz, 2006).

2.1.3.2.Muscarinic receptors

The muscarinic receptor family comprises of five distinct G-protein coupled receptors entitled M_1 to M_5. Within guinea-pig smooth muscle the M_2 and M_3 receptors are expressed at a ratio of approximately 4:1 (Eglen, 2001). Exogenous agonists are considered to act, through the pharmacological selectivity of a collection of ligands, mainly through the M_3 receptor, triggering phosphoinositide hydrolysis through G_q-protein activating, Ca^{2+} mobilisation and a direct contractile response (Ehlert, 2003). Endogenous acetylcholine release has been show using pertussis toxin and M_2 receptor selective antagonists to stimulate the M_2 receptor, a $G_{i/o}$-protein coupled receptor (Sawyer *et al.*, 2000; Murthy and Makhlouf, 1997; Bolton and Zholos, 1997). Activation has been shown to decrease potassium channel opening times activated by sympathetic agonists, so attenuating relaxation (Kotlikoff *et al.*, 1999), and activate a non-selective cationic current (Bolton and Zholos, 1997). This current has been postulated to depolarise membrane potential to such an extent as to evoke opening of L-type Ca^{2+} channels and so inducing contraction (Eglen, 2001).

2.2. Method

2.2.1. Guinea-pig ileum myenteric plexus-longitudinal muscle preparation (MPLM)

2.2.1.1.Preparation of the MPLM

Male Dunkin Hartley or Heston-2 guinea-pigs (450–550 g; Harlan, UK) were killed by cervical dislocation. The abdomen was exposed and the ileum removed by gentle pulling whilst removing the mesentery at the same time. Tissues were immersed in Krebs solution (see *solutions* for composition) maintained at room temperature and supplied with 95% O_2 and 5% CO_2. A 5 cm section of ileum was stretched onto a 7 mm diameter glass pipette and the mesentery was lined up along the length of the pipette. The MPLM was dissected from the ileum by stroking tangentially away from it with a small cotton wool bud soaked in Krebs solution. This was repeated until a strip of longitudinal muscle, along with the myenteric plexus was separated from the underlying mucosal layers. The ileum and MPLM were kept moist with Krebs solution throughout the entire procedure.

2.2.1.2.Measurement of contraction

4 cm strips of MPLM were mounted in 30 ml organ baths, connected to an isometric transducer, and placed under an initial tension of 0.5 g (figure 2.3). Tissues were immersed in Krebs solution maintained at 37°C and supplied with 95% O_2 and 5% CO_2.

2.2.1.3.Experimental design

Nicotinic stimulus of contraction: Contractions were induced by nicotine, administered at 30 min intervals and washed twice upon achievement of maximum contraction to allow removal of nicotine and recovery from desensitisation. Before the addition of any subsequent compounds, tissue was allowed an hour to stabilise and three nicotine induced contractions were performed and averaged to establish a control response. Due to the adhesive nature of cannabinoids (Pertwee *et al.*, 1992) and the required washing upon addition of nicotine to recover from desensitisation, the response to only a single concentration of nicotine (100 μM) in the presence of a single concentration of cannabinoid was obtained per tissue. Upon establishment, cannabinoid agonists were applied 20 minutes prior to nicotine. To observe nerve terminal stimulation TTX was added after each wash to maintain a constant bath concentration. In competition studies the CB_1 receptor antagonist SR141716 was applied 30 minutes prior to and the competitive nicotinic receptor antagonist d-tubocurarine was applied 20 minutes prior to the addition of any subsequent compounds.

Electrical stimulus of contraction: Electrical field stimulation (110% of the voltage which produced a maximal contraction, 0.5 ms duration and 0.1 Hz frequency), applied through

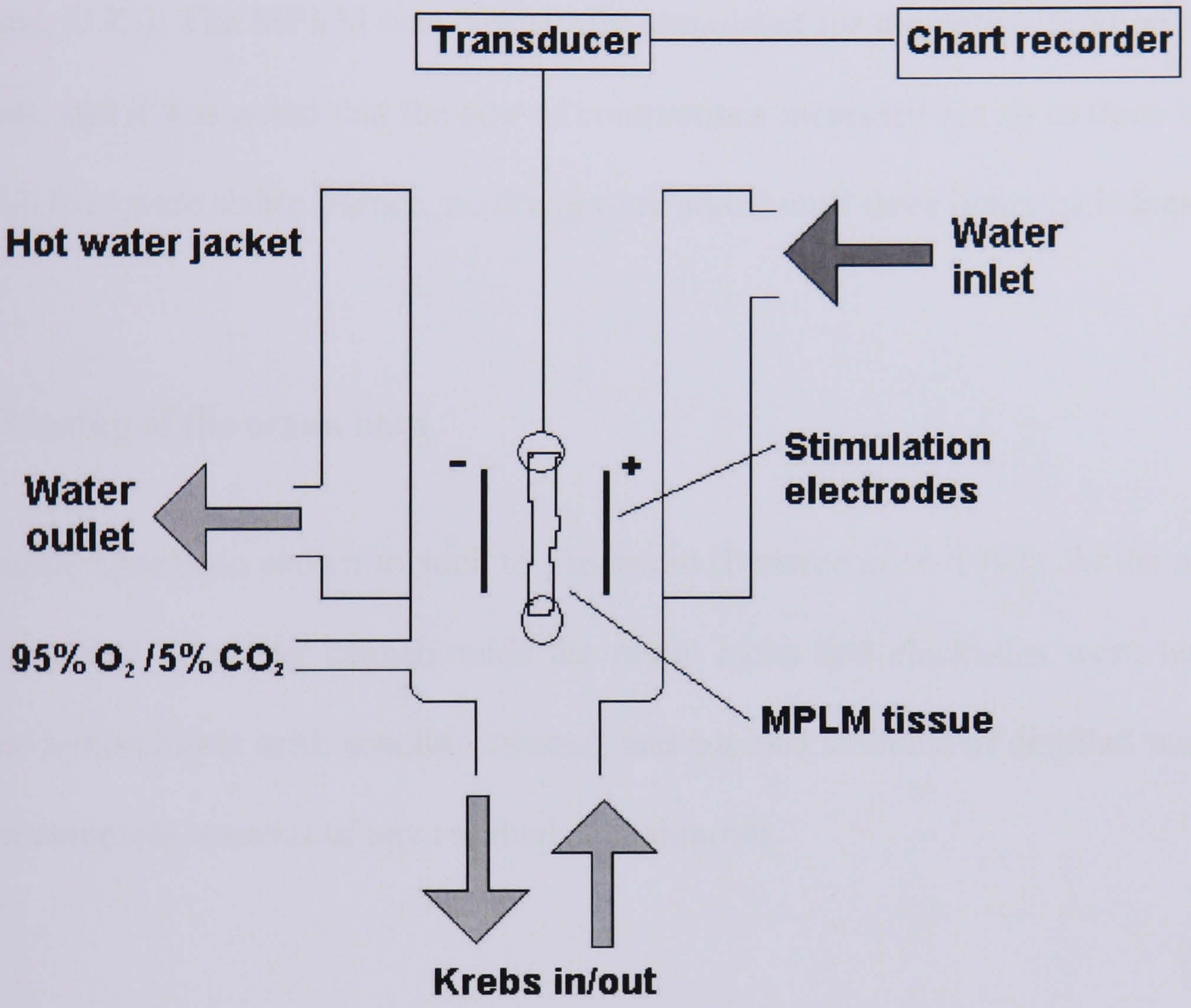

Figure 2.3 Organ bath containing the myenteric plexus-longitudinal muscle preparation.

two parallel platinum plate electrodes fixed at either side of the longitudinal strip, was generated using a Multistim D330 System stimulator (Digitimer, U.K.). Contractions of the MPLM were recorded by Dynamometer UF1 isometric transducers (Pioden Controls, U.K.), connected via a Conditioning Unit (Techman, U.K.) to a MX216 Chart Recorder (Lectromed, U.K.). The MPLM was electrically stimulated for the entire duration of the experiment, and it was noted that the size of contractions increased for up to three hours, after which they were stable. Hence, no drugs were added until three hours had elapsed.

2.2.1.4.Cleaning of the organ bath

Cannabinoids have been shown to stick to glassware (Pertwee *et al.* 1992). At the end of every experiment involving cannabinoids the organ baths and electrodes were washed with dilute hydrochloric acid, absolute ethanol, and copious amounts of distilled water to ensure the complete removal of any residual cannabinoids.

2.2.1.5.Analysis of data

Electrical stimulus: Each value is expressed as the mean ± standard error of mean (S.E.M.) of experiments on tissues obtained from at least four individual animals. The effects of cannabinoid receptor ligands are expressed as percentage inhibition of contraction. This was calculated by comparing the amplitude of the electrically evoked contraction immediately prior to adding any compound to the amplitude of the contraction at the maximal effect of the compound.

Nicotinic stimulus: Each value is expressed as the mean ± S.E.M. of experiments on tissues obtained from at least four individual animals. The effects of cannabinoid ligands are expressed as percentage inhibition of contraction. This was calculated by comparing the mean amplitude of the three nicotine evoked contraction prior to adding any compound to the amplitude of the nicotine-evoked contraction after addition of the compound.

GraphPAD Prism 4 statistical software (GraphPAD Software Inc, San Diego, CA., U.S.A.) was used to fit the concentration–response results to a sigmoidal function and generate 95% confidence intervals using the equation:

$$I = \frac{I_{max}}{1 + 10^{(\log_{IC_{50}} - \log_{drug}) \times \text{Hill slope}}},$$

Significant difference between mean values were calculated using Student's unpaired *t*-test, a *P* value of < 0.05 being taken as significant. Mean values of multiple data sets were compared using one way-ANOVA followed by either Dunnetts or Newman-Keuls multiple comparison *post hoc* tests.

2.2.2. Guinea-pig ileum preparation

2.2.2.1.Preparation of whole ileum

As described in section 2.2.1, male Dunkin Hartley or Heston-2 guinea-pigs (450–550 g; Harlan, UK) were killed by cervical dislocation and ileum removed. Tissues were

immersed in Krebs solution (see *solutions* for composition) maintained at room temperature and supplied with 95% O_2 and 5% CO_2.

2.2.2.2.Measurement of contraction

4 cm strips of whole ileum were mounted in 30 ml organ baths, connected to an isometric transducer, and placed under an initial tension of 1 g (figure 2.3). Tissues were immersed in Krebs solution maintained at 37°C and supplied with 95% O_2 and 5% CO_2.

2.2.2.3.Experimental design

Experiments were performed in accordance with details presented in section 2.2.1.3 and analysed in a similar manner.

2.2.3. Disassociated myenteric neurone patch-clamp preparation

2.2.3.1.Preparation of cultured myenteric neurones

A 4 cm strip of MPLM was prepared as in section 2.2.1 and cut into 0.5 cm sections. These sections were transferred into a sterile centrifuge tube containing 3 ml of papain solution and placed in a water bath for 10 minutes at 37°C. The papain solution was removed and replaced with 3 ml of collagenase solution, and returned to the water bath for 10 minutes. The tissue was titurated with a sterile, flame-polished tip pasteur pipette and returned to the water bath for a further 10 minutes. The tituration process was

repeated a further two times. Cells were centrifuged for 5 minutes at 600 rpm, supernatant discarded and resuspended in feeding medium. The centrifugation process was repeated and the media replaced. The suspension was transferred to P-60 dishes (Falcon, UK) containing collagen-coated glass slides and incubated at 37°C in an atmosphere of 95% CO_2/5% O_2. Feeding media was refreshed every three days.

2.2.3.2.Whole cell recordings

Single-cell patch clamping, first described by Neher and Sakmann (1976), comprises of a tight seal formed by suction between a blunt, low-resistance microelectrode and the surface of the cell membrane. These 'Gigaseals' form very high resistance, mechanically stable seals, allowing the patch of membrane within the tip of the pipette to be ruptured to form an electrical continuity between the conductive media within the pipette and the interior of the cell.

2.2.3.3.Micropipette preparation

Glass pipettes were pulled (P80 /PC; Stutter Instruments Co., USA) using borosilicate glass capillaries (GC150TF-10; Harvard Apparatus, UK). They were heat polished (MF-830; Narishige, Japan) and backfilled with intracellular solution (ICS; see *solutions* for composition) to give a typical resistance of 3-5 MΩ.

2.2.3.4.Whole-cell patch-clamp recordings

Glass slides with attached cells were placed upon the glass bottom of a 150 µl superfusion chamber (RC-26; Warner Instruments Inc., USA) and superfused under a gravity driven system with a physiological salt solution (ECS; extracellular salt solution; see *solutions* for composition) at a flow rate of 1.2 ml/min (see figure 2.4). Solutions were removed through a metal syringe needle located towards the rear of the bath using a vacuum fed mechanism. The superfusion chamber was maintained at room temperature. Cells were visualised using an inverted microscope (TMS; Nikon, Japan) under high power. Filled pipettes were mounted in the pipette holder, with the pipette filling fluid connected to the headstage input by a chloride coated silver wire. The pipette holder was attached to a tube allowing control over the pressure within the pipette. The headstage (CV-7A; Axon Instruments, USA) was mounted on a course manipulator (MC35A; Narishige, Japan) and fine movements controlled by using a hydraulic manipulator (MHW-3; Narishige, Japan). Cell voltage was amplified and filtered at 2 kHz (-3 dB) using a Multiclamp 700A (Axon Instruments, USA), and visualised and recorded using a digital interface (Digidata 1322A; Axon Instruments, USA) connected to a personal computer running pCLAMP 8 (Axon Instruments, USA).

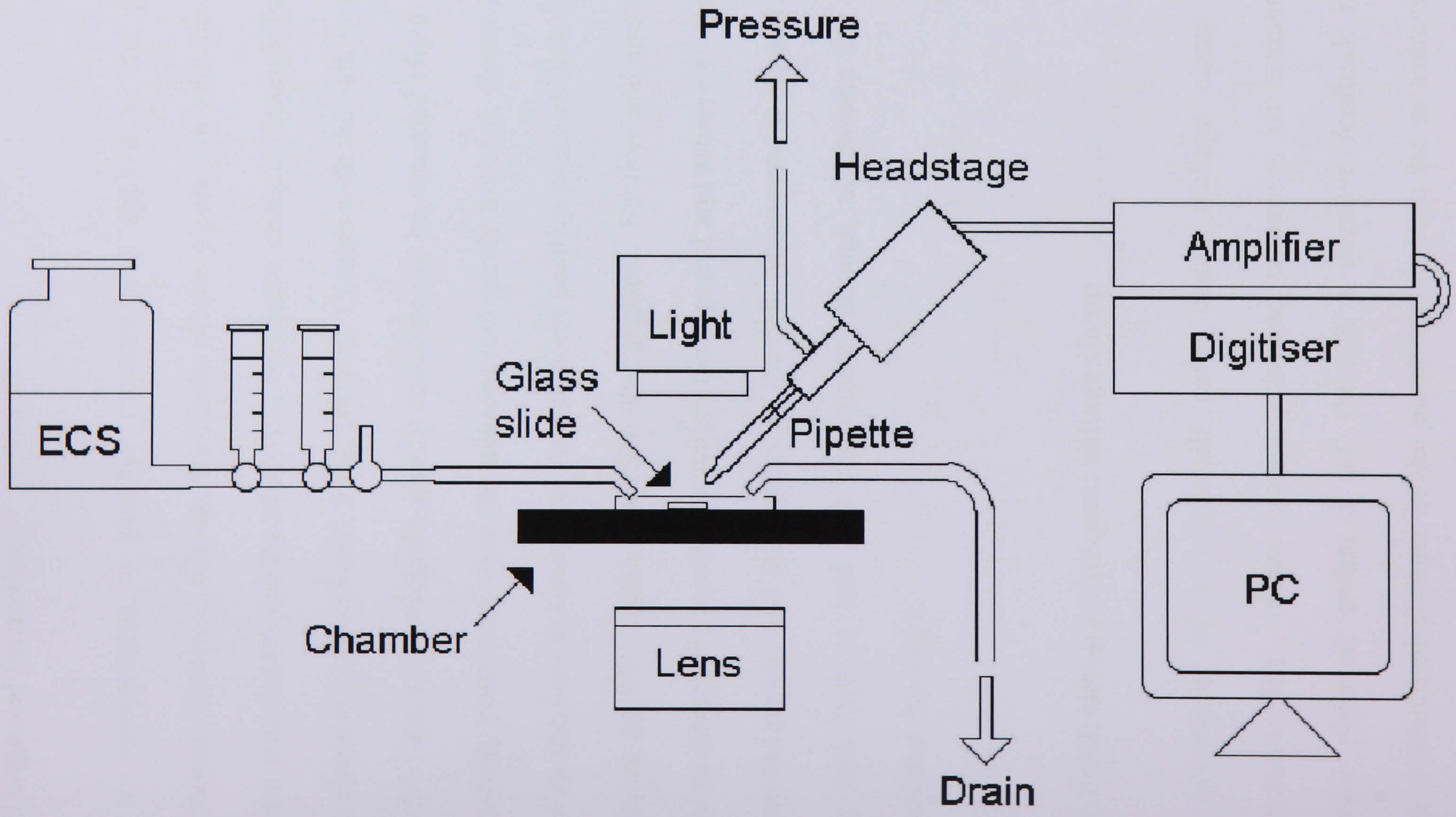

Figure 2.4Schematic diagram of the patch clamp apparatus

2.2.3.5.Gigaseal formation

Prior to commencing, a positive pressure was applied to the pipette to prevent contaminants blocking the tip. Blockade of the pipette tip and the approach towards neurones was monitored by observing resistance changes through the application of a square electrical pulse (5 mV, 5 ms, 100 Hz). Contact with the bathing fluid completes an electrical circuit allowing the pipette resistance to be recorded (figure 2.5). The pipette was visually positioned over the neurone and gently lowered. Contact with the neurone caused an increase in resistance. At this point positive pressure was removed and gentle continuous suction applied to form the gigaseal. Suction and electrical pulses were applied to disrupt the membrane within the gigaseal and achieve an electrical connection between the pipette and the interior of the cell. Measurement of, and compensation for, resting leak current and cell capacitance through adjustment of current flow was performed at this stage.

2.2.3.6.Patch clamp techniques: voltage clamp

Upon generation of a whole-cell patch clamp, voltage clamp techniques were implemented. The voltage clamp technique comprises of maintaining a constant membrane potential within a cell through a negative feedback mechanism whilst examining electrical changes in the membrane through the measurement of changes in current required to maintain membrane potential. As a result the injection of electrical current is recorded to produce a result proportional, but opposite in polarity, to the

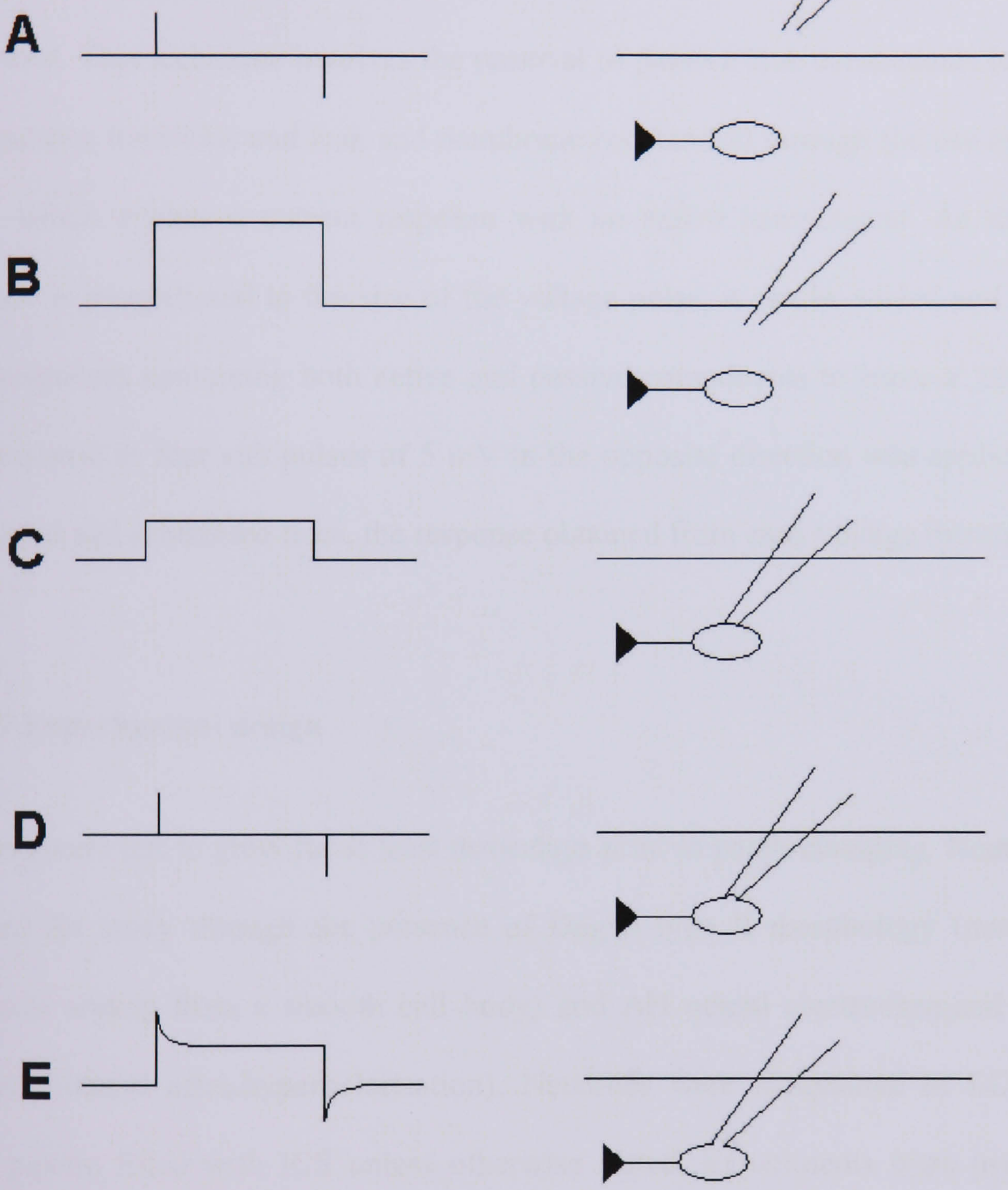

Figure 2.5 Current responses during gigaseal formation. No current flow is present when pipette is out of the bathing solution (A). Upon contact with the bathing solution the circuit completes and a current flow is observed when a 5 mV voltage step is placed upon the pipette (B). Neuronal contact results in an increase in pipette resistance, resulting in a decreased current flow (C), signifying the point in which suction is applied to the pipette, resulting in gigaseal formation (D). Further suction results in disruption of the cell membrane allowing whole cell recording (E). Spikes at the beginning and end of the voltage step describe the capacitive transient (RC current; figure adapted from Molleman, 2003).

membrane current of the patched cell. The voltage clamp technique allows control over the opening of ion channels. Whilst examining changes in current flow induced by controlled changes in membrane potential, positive/negative (P/N) leak subtraction was performed. This technique involves the removal of passive leak components (comprising of capacitive transients and leak and membrane resistances) through the use of a voltage pulse, which evokes a current response with no active components. As this passive response is proportional to the size of the voltage pulse, it can be scaled and subtracted from responses containing both active and passive components to leave a 'clean' trace. The response to four sub pulses of 5 mV in the opposite direction was applied prior to, and scaled and subtracted from, the response obtained from each voltage increment.

2.2.3.7.Experimental design

Cultures were left to grow for at least three days prior to patch-clamping. Neurones were selected for study through the presence of Dogiel type II morphology (multiple long processes arising from a smooth cell body) and AH neural electrochemical properties (action potential after-hyperpolarisation). Neurones were maintained in ECS and the patch pipette filled with ICS unless otherwise stated. Experiments were performed at room temperature with cells under voltage clamp at a holding potential of –70 mV. All drugs were administered in ECS, superfused at 1.2 ml/min.

2.2.3.8.Analysis of data

Data are transformed to account for cell size by dividing by cell capacitance and are expressed as either the mean ± S.E.M. of experiments. Significant difference between mean values were calculated using Student's unpaired *t*-test, a *P* value of < 0.05 being taken as significant. Mean values of multiple data sets were compared using own-way ANOVA followed by either Dunnetts or Newman-Keuls multiple comparison *post hoc* tests.

2.2.4. Drugs and solutions

2.2.4.1.Solutions

The Krebs solution contained (in mM): NaCl 118.3, KCl 4.7, $MgSO_4$ 1.2, KH_2PO_4 1.2, $NaHCO_3$ 25, glucose 11.1, $CaCl_2$ 2.5. Papain Solution (warmed to 37°C before use, pH balanced with 0.15 M $NaHCO_3$) comprised of Hank's Balanced Salt Solution (HBSS) containing 0.01 ml/ml papain and 0.4 mg/ml L-cysteine. Collagenase Solution (warmed to 37°C before use) comprised of HBSS containing 1 mg/ml collagenase Type 1 and 3.1 mg/ml dipase. Feeding Medium consisted of Dulbecco's modified Eagle's medium (DMEM) supplemented with 5% FBS, 1 mM L-glutamine, 8.3 mM glucose, 5 μM cytosine β-D-arabinofuranoside hydrochloride, 50 μM (+)-5-fluorodeoxyuridine, 2.5 μM uridine, 150 units/ml penicillin and 150 μg/ml streptomycin. ECS comprised of (mM): NaCl 125, KCl 6, $MgCl_2$ 2.5, NaH_2PO_4 1.2, Hepes 10, glucose 11, sucrose 67, $CaCl_2$ 1.2;

pH 7.35. Intracellular solution (ICS) contained (mM): NaCl 5, KCl 142, $MgCl_2$ 1.2, Hepes 20, glucose 11, K-ATP 5, Na-GTP 0.1, pH 7.2.

2.2.4.2.Drugs

CP 55,940 ((-)-cis-3-[2- hydroxy-4-(1,1-dimethylheptyl) phenyl]-trans-4-(3-hydroxypropyl) cyclohexanol) was a kind gift from Pfizer U.K. SR141716 (N-(piperidin-1-yl)-5-(4-chlorophenyl)-1-(2,4,-di-chlorophenyl)-4-methyl-1H-pyrazole-3-carboxamide hydrochloride) was a kind gift from Sanofi Recherche, France. All cannabinoid drugs were dissolved in ethanol, shielded from light and kept at -20°C. Atropine sulphate, carbachol, acetylcholine chloride and nicotine were obtained from Sigma. Tetrodotoxin citrate, WIN 55,212-2 and WIN 55,212-3 were obtained from Tocris Cookson, UK.

2.3. Results

2.3.1. Effects of nicotine on myenteric plexus-longitudinal muscle

Nicotine evoked rapidly developing contractions of the guinea-pig myenteric plexus-longitudinal muscle. The peak amplitude of contraction was concentration dependent (EC_{50} = 22.1 μM, 95% confidence limits of 9.67 to 50.7 μM, n = 5, figure 2.6a). A maximum peak amplitude of contraction of 2.52 ± 0.20 g (n = 10) was evoked by 1 mM nicotine. Contractions were fast in onset and transient, only lasting for a short duration in the continued presence of nicotine.

Application of 100 μM nicotine evoked a contraction with peak amplitude of 2.22 ± 0.12 g (n = 29). Repeat application of 100 μM nicotine, immediately after washing with Krebs, evoked a contraction with a smaller peak amplitude than previously evoked (0.52 ± 0.23, n = 3) suggesting some degree of desensitisation occurs. However, rest for 30 minutes after washing enabled repeat application of 100 μM nicotine to evoke a similar sized contraction (2.21 ± 0.12 g, n = 29, figure 2.6b).

2.3.2. Effects of cannabinoids on nicotine evoked contractions of the myenteric plexus-longitudinal muscle preparation and the whole ileum

Contractions of the myenteric plexus-longitudinal muscle preparation evoked by 100 μM nicotine were inhibited by the cannabinoid receptor agonist CP 55,940 in a concentration

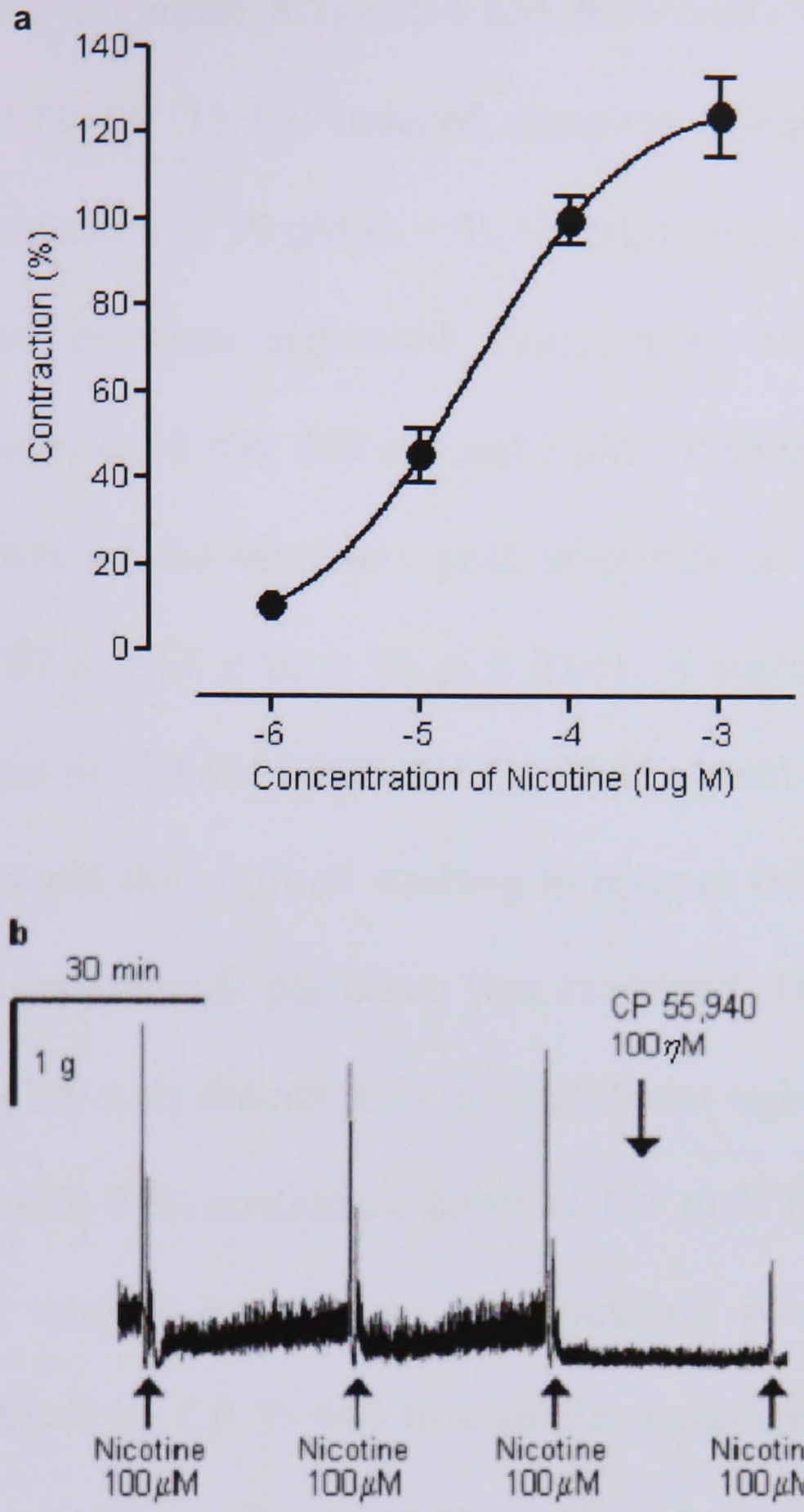

Figure 2.6 (a) Mean concentration-response curve for nicotine evoked contraction of the MPLM preparation. To ensure a stable, repeatable response to nicotine, tissue was exposed to three doses of 100 μM nicotine prior to exposure to varying nicotine concentrations. Each symbol represents the mean amplitude of peak contraction from multiple tissues, expressed as a percentage of the mean amplitude of peak contraction derived from prior tissue exposure to 100 μM nicotine (n = 10 different myenteric plexus-longitudinal muscle preparations); vertical lines indicate S.E.M. (b) Typical contractions of a strip of myenteric plexus-longitudinal muscle evoked by 100 μM nicotine prior to and post exposure to 100 nM CP 55,940.

dependent manner (peak amplitude IC_{50} = 215 nM, 95% confidence limits of 181 to 256 nM, n = 29, figure 2.7). CP 55,940 induced complete inhibition of nicotine evoked contractions at a concentration of 10 μM (n = 3). Nicotinic concentration-response curves showed a combination of some rightward displacement and decrease in maximal contraction upon exposure to 10 nM, 100 nM and 1 μM CP 55,940 (figure 2.8). 1 μM CP 55,940 significantly reduced the maximum peak amplitude of contraction from 2.52 ± 0.19 g (n = 10) to 1.97 ± 0.18 g (n = 10, $p < 0.05$). A significant shift in EC_{50} was observed in the presence of 100 nM CP 55,940 ($p < 0.05$, *f*-test). Because of the adhesive nature of cannabinoids and the required washing to recover from desensitisation only a single application of cannabinoids per tissue was examined. The specific CB_1 receptor antagonist SR141716 (300 nM) did not induce a significant rightward shift in CP 55,940 inhibition (IC_{50} = 181 nM, 95% confidence limits of 121 to 271 nM, n = 25, figure 2.7). However, electrically evoked contractions of myenteric plexus-longitudinal muscle preparation were inhibited by CP 55,940 in a similar concentration dependent manner (IC_{50} = 25 nM, 95% confidence limits of 23 to 27 nM, n = 14, figure 2.9) but this inhibition was significantly shifted to the right by SR141716 (300 nM, IC_{50} = 157 nM, 95% confidence limits of 118 to 218 nM, n = 5, $p < 0.001$, figure 2.9). Addition of SR141716 alone caused a slight but non-significant increase in size of contraction evoked by electrical stimulus.

To further examine activity at cannabinoid receptors, modulation by the cannabinoid receptor agonist WIN 55,212-2 was compared with that of the (-)-enantiomer WIN 55,212-3, which has been shown not to activate CB_1 and CB_2 receptors (Savinainen *et al.*, 2005), WIN 55,212-2 (300 nM) inhibited contraction by 73.0 ± 4.5% (n = 6) while

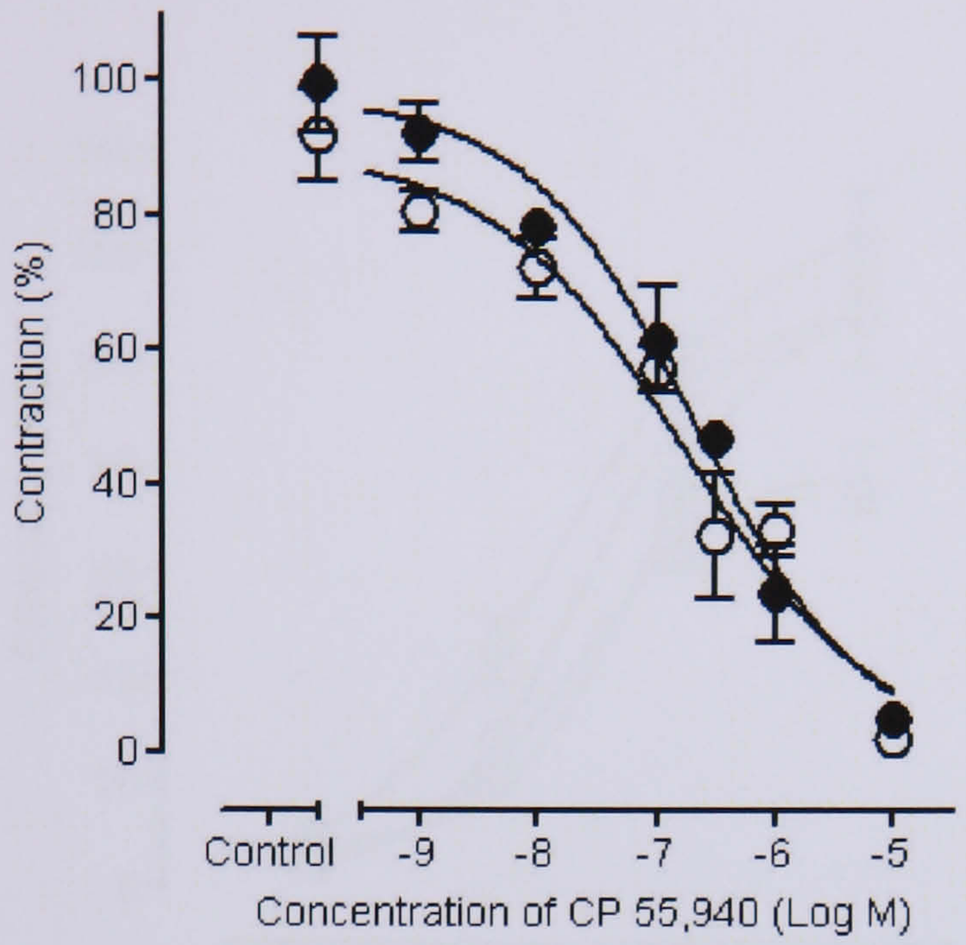

Figure 2.7 Mean concentration-response curves for the inhibition of contraction of the MPLM preparation evoked by 100 μM nicotine by CP 55,940 (●) and CP 55,940 in the presence of 300 nM SR141716 (○). Preparations were exposed to varying concentrations of cannabinoids for 20 mins prior to exposure to nicotine. Each symbol represents the mean amplitude of peak contraction expressed as a percentage of the amplitude of peak contraction derived prior to application of cannabinoid. Each symbol comprises of at least three different MPLM preparations. Vertical lines indicate S.E.M.

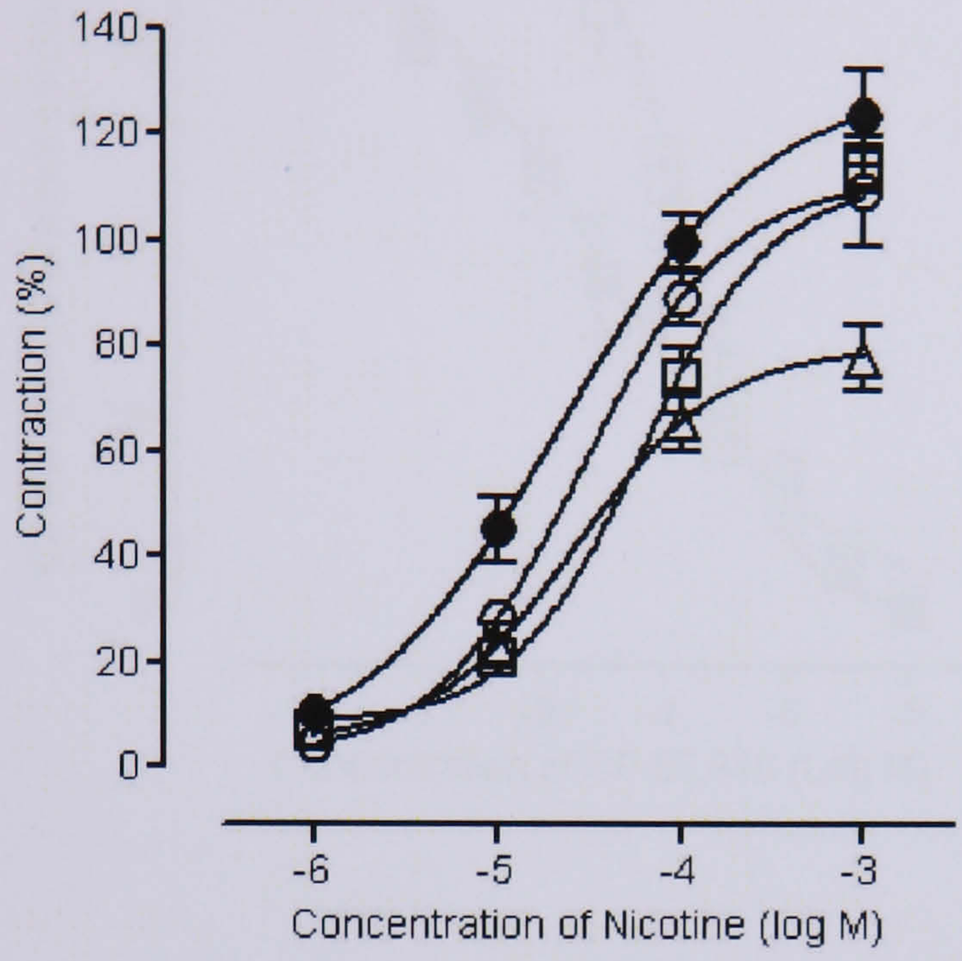

Figure 2.8 Inhibition by CP 55,940 of the mean concentration-response curve for contraction of the MPLM preparation evoked by nicotine. The concentration-response curve for nicotine (●) showed no significant shift in the presence of 10 nM CP 55,940 (○). A significant rightward shift in EC_{50} was observed in the presence of 100 nM CP 55,940 (□, $p < 0.05$, *f*-test) and a reduction in the size of maximal contraction to nicotine was observed in the presence of 1 μM CP 55,940 (△, $p < 0.05$). Preparations were exposed to varying concentrations of cannabinoids for 20 mins prior to exposure to nicotine. Each symbol represents the mean amplitude of peak contraction expressed as a percentage of the amplitude of peak contraction derived prior to application of cannabinoid. Each symbol comprises of at least three different MPLM preparations. Vertical lines indicate S.E.M.

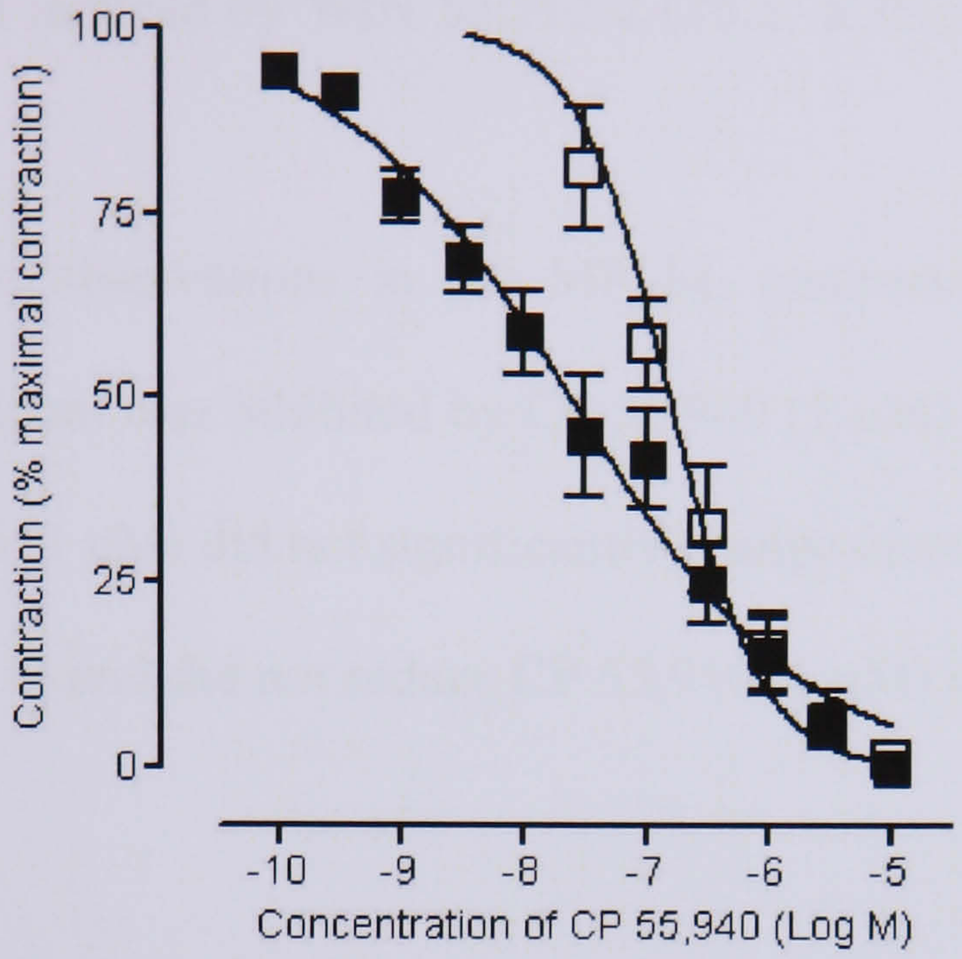

Figure 2.9 Mean concentration-response curves for the inhibition of electrically evoked contractions of the MPLM preparation by CP 55,940 (■, n = 14) and CP 55,940 in the presence of 300 nM SR141716 (□, n = 4). Each symbol represents the mean amplitude of peak contraction evoked by electrical stimulus from multiple tissues expressed as a percentage of the mean amplitude of peak contraction derived immediately prior to addition of cannabinoid. Vertical lines indicate S.E.M.

WIN 55,212-3 (300 nM) reduced the peak amplitude of contraction by a significantly lower amount than that induced by WIN 55,212-2 (35.5 6.3% (n = 4, $p < 0.001$, figure 2.10).

To further substantiate observations in the MPLM, contraction evoked by 100 μM nicotine in the whole ileum was inhibited by CP 55,940 (1 μM) by 38.9 ± 6.69% (n = 6, figure 2.11). SR141716 (1 μM) did not significantly change nicotine induced contractions when added alone (n = 6) and did not reduce CP 55,940 (1 μM) inhibition (40.5 ± 8.01%, n = 6).

2.3.3. Effects of cannabinoids on nicotine evoked contraction contractions of the myenteric plexus-longitudinal muscle preparation in the presence of tetrodotoxin

In an attempt to elucidate the location within a neurone in which cannabinoids act, activity in the presence of the voltage-gated sodium channel blocker tetrodotoxin (TTX) was investigated. TTX prevents action potential propagation, segregating the neuromuscular synapse from the remainder of the neurone. TTX (300 nM) reduced 100 μM nicotine evoked contraction by 68.9 ± 1.90% (n = 35, figure 2.12). Addition of CP 55,940 (300 nM, n = 6) produced a further reduction; lowering contraction to 84.6% of the untreated response to 100 μM nicotine evoked. CP 55,940 inhibition proved significant when compared with TTX alone ($p < 0.001$). SR141716 (300 nM, n = 6) also induced a further significant inhibition when applied in conjunction with TTX (84.6 ± 2.23%, n = 6, $p < 0.001$). With application of TTX (300 nM), CP 55,940 (300 nM) and SR141716 (300 nM) the peak amplitude of contraction evoked by 100 μM nicotine was

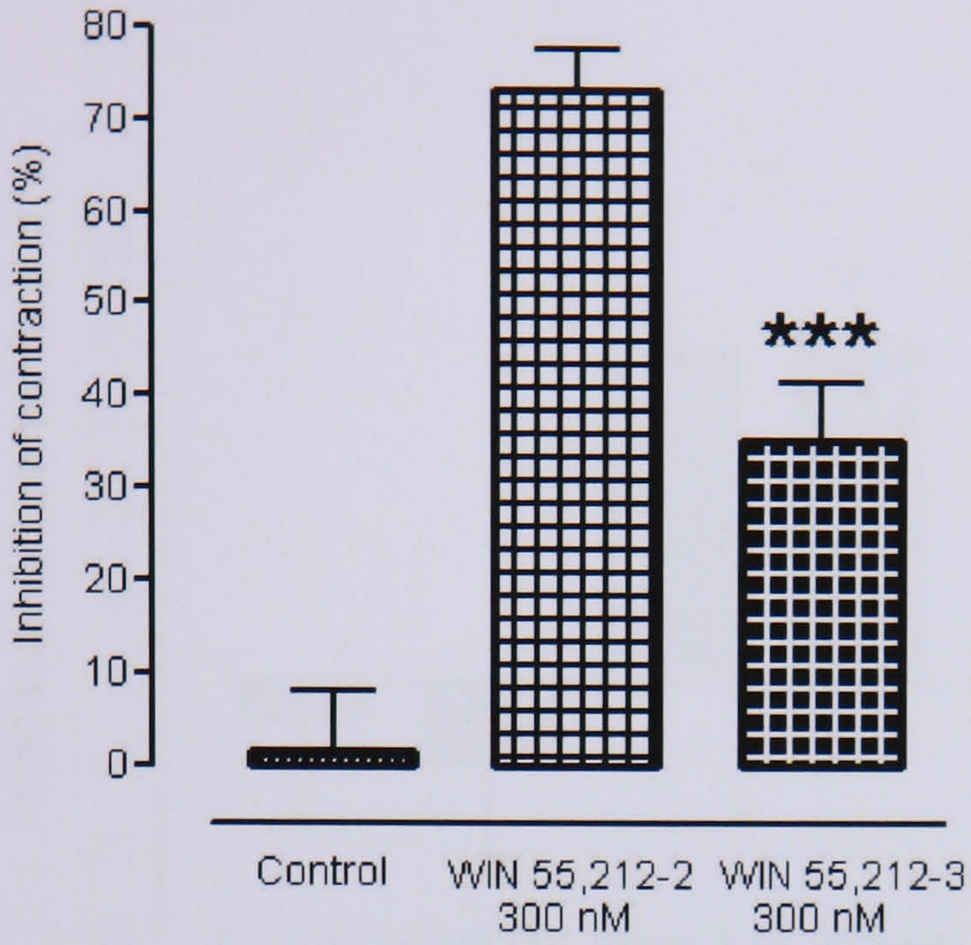

Figure 2.10 Effect of WIN 55,212-2 and the inactive (-)-enantiomer WIN 55,212-3 on contractions of the MPLM preparation evoked by nicotine (100 μM). Preparations were exposed to either WIN 55,212-2 (300 nM, n = 6) or WIN 55,212-3 (300 nM, n = 4) for 20 mins prior to exposure to nicotine. Each column represents the mean amplitude of peak contraction expressed as a percentage of the amplitude of peak contraction evoked prior to application of cannabinoid or vehicle. Vertical lines indicate S.E.M. The significance of the difference between columns representing WIN 55,212-2 and WIN 55,212-3 was calculated using ANOVA followed by Dunnett's test with *** indicating a significant difference of $p < 0.001$.

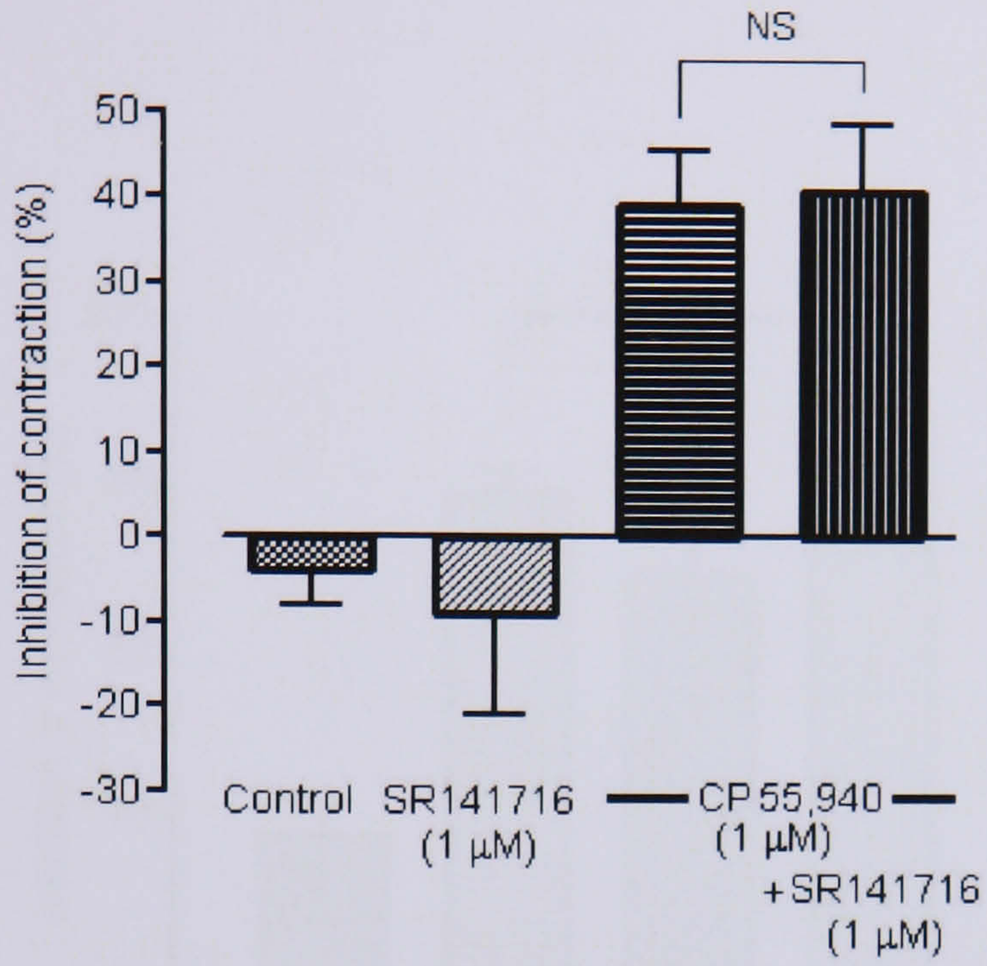

Figure 2.11 Effect of CP 55,940 and SR141716 on contractions of the whole ileum preparation evoked by nicotine (100 μM). Preparations were exposed to either CP 55,940 (1 μM, n = 6), SR141716 (1 μM, n = 6) or CP 55,940 (1 μM) and SR141716 (1 μM, n = 6) for 20 mins prior to exposure to nicotine. Each column represents the mean amplitude of peak contraction expressed as a percentage of the amplitude of peak contraction evoked prior to application of cannabinoid or vehicles. Vertical lines indicate S.E.M. The significance of the difference between columns representing CP 55,940 and CP 55,940 in conjunction with SR141716 was calculated using ANOVA followed by Dunnett's test with NS indicating no significant difference.

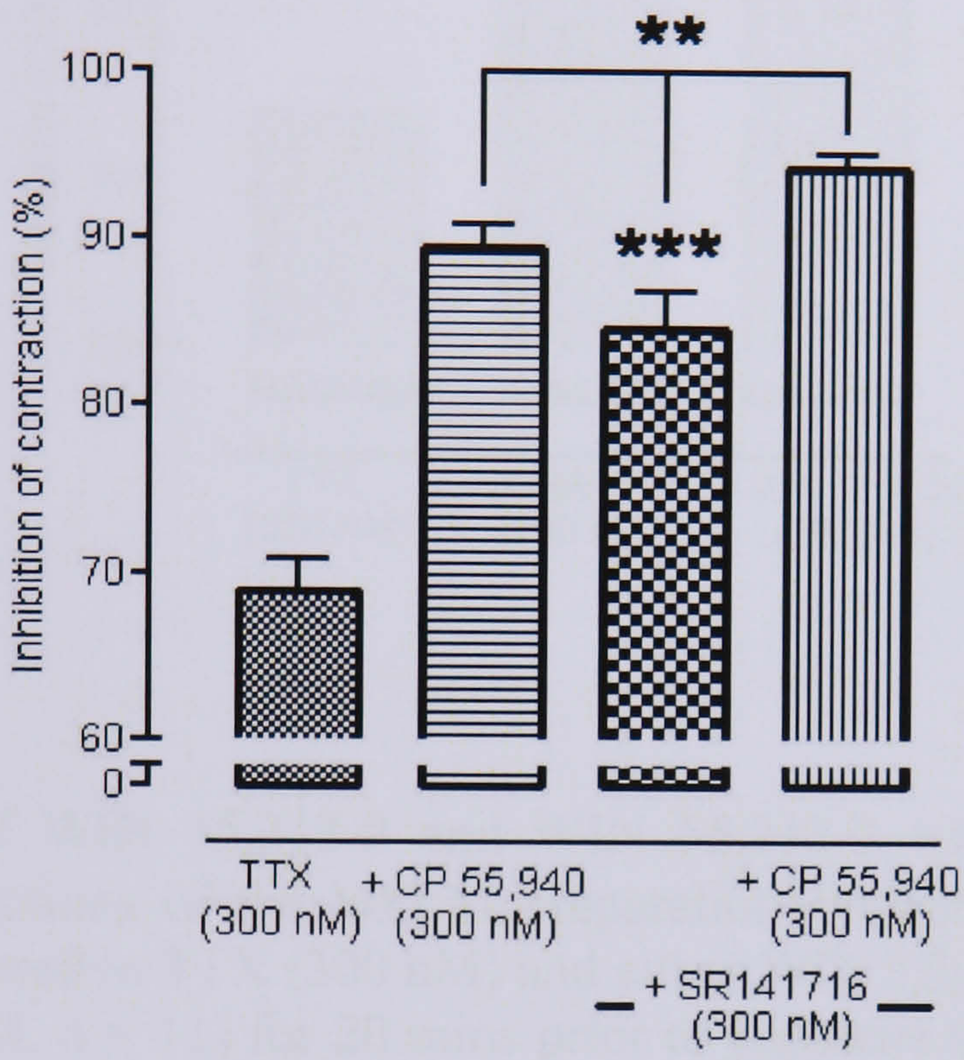

Figure 2.12 Effect of CP 55,940 and SR141716 whilst in the presence of tetrodotoxin on contractions of the MPLM preparation evoked by nicotine (100 μM). Preparations were exposed to TTX (300 nM) and either CP 55,940 (300 nM, n = 6), SR141716 (300 nM, n = 6) or CP 55,940 (300 nM) and SR141716 (300 nM, n = 5) for 20 mins prior to exposure to nicotine. Each column represents the mean amplitude of peak contraction expressed as a percentage of the amplitude of peak contraction evoked prior to application of cannabinoid or vehicle. Vertical lines indicate S.E.M. The significance of the difference between columns was calculated using ANOVA followed by Dunnett's test with ** indicating a significant difference of $p < 0.01$ existing between the column representing CP 55,940 in conjunction with SR141716 and the columns representing CP 55,940 and SR141716 independently. *** indicates a significant difference of $p < 0.001$ existing between the column representing SR141716 and that representing TTX alone.

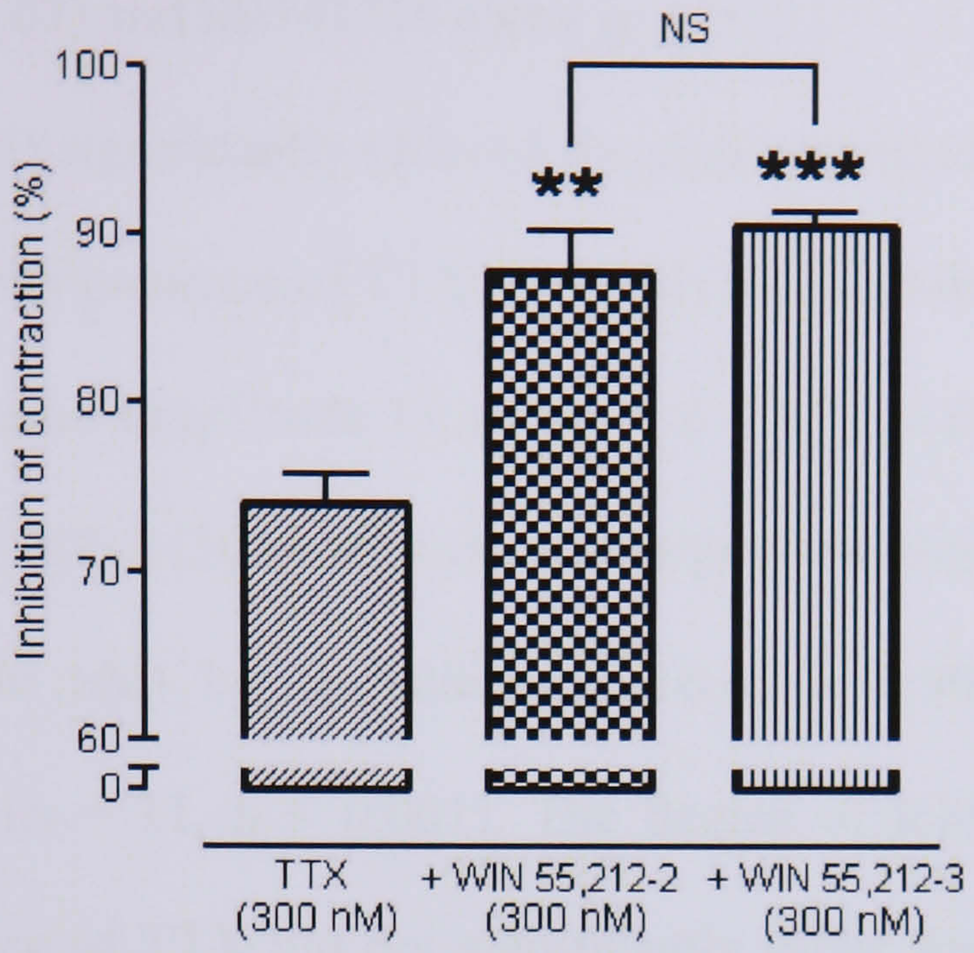

Figure 2.13 Effect of WIN 55,212-2 and WIN 55,212-3 whilst in the presence of tetrodotoxin on contractions of the MPLM preparation evoked by nicotine (100 μM). Preparations were exposed to TTX (300 nM) and either WIN 55,212-2 (300 nM, n = 6) or WIN 55,212-3 (300 nM, n = 11) for 20 mins prior to exposure to nicotine. Each column represents the mean amplitude of peak contraction expressed as a percentage of the amplitude of peak contraction evoked prior to application of cannabinoid or vehicle. Vertical lines indicate S.E.M. The significance of the difference between columns was calculated using ANOVA followed by Dunnett's test with ** indicating a significant difference of $p < 0.01$ and *** indicating a significant difference of $p < 0.001$ versus TTX alone. NS indicates no significant difference existing between the column representing WIN 55,212-2 and WIN 55,212-3.

reduced by 94.3 ± 0.78% (n = 5). Inhibition was significantly greater than that evoked by CP 55,940 alone ($p < 0.01$) and SR141716 alone ($p < 0.01$).

WIN 55,212-2 (300 nM) significantly reduced the peak amplitude of contraction evoked by 100 μM nicotine in the presence of TTX (300 nM) by an additional 13.75 ± 2.44 upon the untreated contraction amplitude (S.E.M. =, n = 6, $p < 0.05$, figure 2.13). The (-)-enantiomer WIN 55,212-3 (300 nM) reduced the peak amplitude of contraction in the presence of TTX (300 nM) by an additional 16.45 ± 0.90% upon the untreated contraction amplitude (n = 11, $p < 0.001$). The degree of inhibition evoked by WIN 55,212-3 in the presence of TTX did not significantly differ from that evoked by WIN 55,212-3 ($p > 0.05$).

2.3.4. Effects of cannabinoids on contraction evoked by lower concentrations of nicotine or in the presence of tubocurarine

Experimentation portrayed in figure 2.8 demonstrated 10 nM CP 55,940 inhibition of contraction evoked by 10 μM nicotine, however at 100 μM nicotine, inhibition produced by 10 nM CP 55,940 was diminished. To investigate this discrepancy further the potency of CP 55,940 in the presence of 10 μM nicotine was examined.

A reduced concentration (10 μM) of nicotine evoked a mean contraction of 0.79 ± 0.07 g (n = 8), smaller than that evoked by 100 μM nicotine (2.22 ± 0.12 g, n = 29). CP 55,940 inhibited contraction with an IC_{50} of 0.55 nM (95% confidence limits of 0.22 to 1.38 nM, figure 2.14). This proved to be significantly leftward shifted when compared with inhibition induced by CP 55,940 of contractions evoked by 100 μM nicotine (IC_{50} = 215

nM, 95% confidence limits of 181 to 256 nM, n = 29, $p < 0.01$). In the presence of SR141716 (100 nM), the concentration-response curve for CP 55,940 inhibition of contraction evoked by 10 μM nicotine was significantly shifted to the right (IC_{50} 19.5 nM, 95% confidence limits of 3.82 to 99.4 nM, n = 4, $p < 0.01$, figure 2.14).

One possible explanation for the increased potency of CP 55,940 at the lower concentration of nicotine was that the cannabinoid receptor agonist acts as a competitive antagonist of nicotine binding. The reduced exposure to nicotine would allow CP 55,940 greater access to the shared binding site thereby producing the observed greater potency. To investigate this we examined CP 55,940 inhibition of a nicotine evoked contraction reduced through the presence of the nACh receptor competitive antagonist tubocurarine. If CP 55,940 acts as a competitive antagonist, the presence of tubocurarine and a larger concentration of nicotine competing for binding to the same site would result in CP 55,940 demonstrating a lower potency.

Tubocurarine (10 μM) reduced the mean peak amplitude of contraction evoked by 100 μM nicotine from 1.76 ± 0.11 g (n = 6) to 0.95 ± 0.09 g (52.7% of the untreated amplitude). CP 55,940 inhibited peak amplitude of contraction evoked by nicotine in the presence of tubocurarine with an IC_{50} of 0.74 nM (95% confidence limits of 0.20 to 2.76 nM, n = 8). The IC_{50} for CP 55,940 was significantly shifted to the left when compared to concentration-response curves for CP 55,940 in the absence of tubocurarine (IC_{50} in absence of tubocurarine = 170 nM, 95% confidence limits of 108 to 270 nM, n = 6, $p < 0.0001$). A reduced concentration (10 μM) of nicotine evoked a smaller mean contraction of 0.79 ± 0.07 g (n = 8), comparable to that evoked by 100 μM nicotine in the presence of

10 μM tubocurarine. CP 55,940 inhibited contraction with an IC_{50} of 0.55 nM (95% confidence limits of 0.22 to 1.38 nM, figure 2.15). This proved to be significantly

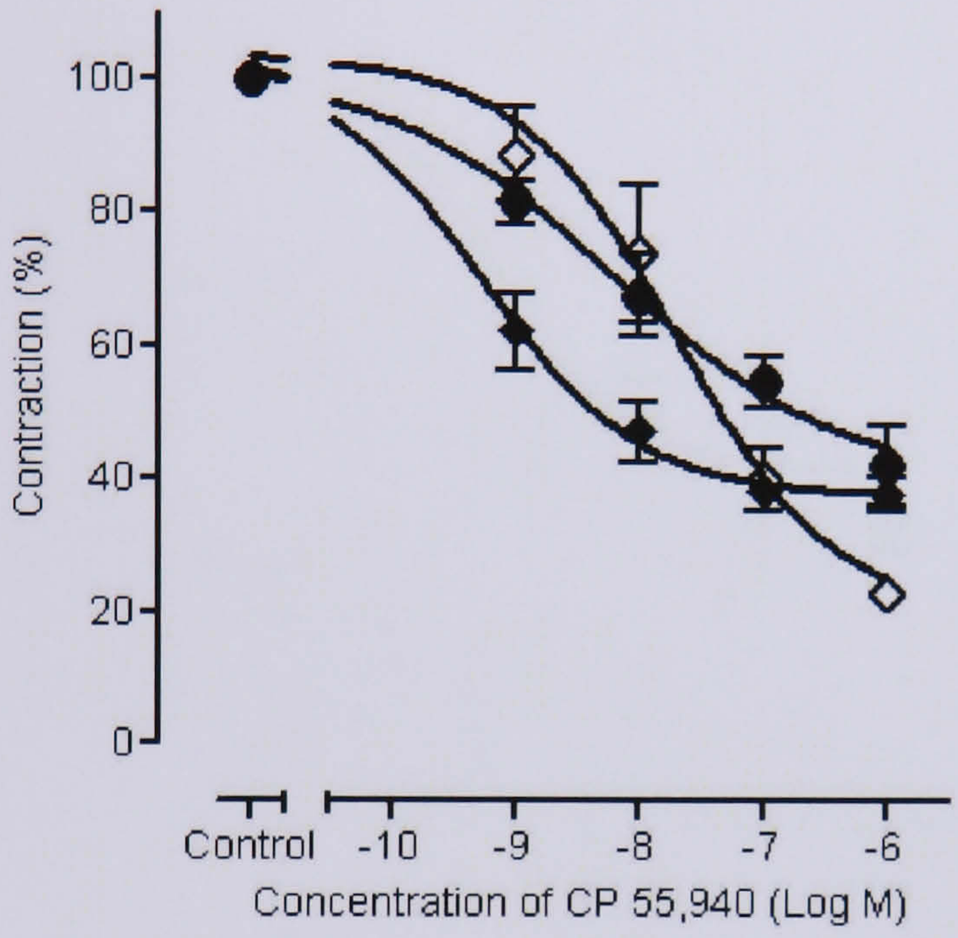

Figure 2.14 Mean concentration-response curves for the inhibition by CP 55,940 of contraction of the MPLM preparation evoked by 100 μM nicotine (●), and 10 μM nicotine in the absence (◆) and presence of 100 nM SR141716 (◇). Preparations were exposed to varying concentrations of cannabinoids for 20 mins prior to exposure to nicotine. Each symbol represents the mean amplitude of peak contraction expressed as a percentage of the amplitude of peak contraction derived prior to application of cannabinoid. Each symbol comprises of at least four different myenteric plexus-longitudinal muscle preparations. Vertical lines indicate S.E.M.

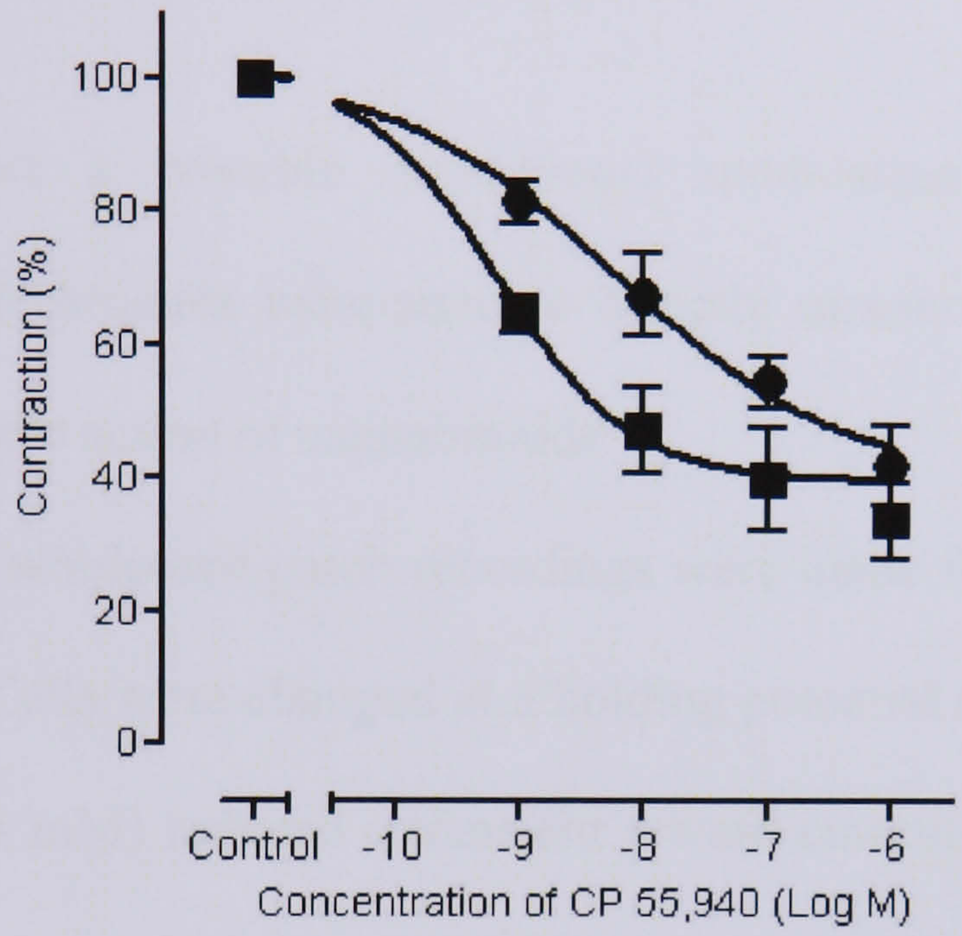

Figure 2.15 Mean concentration-response curves for the inhibition of contraction of the MPLM preparation evoked by 100 μM nicotine by CP 55,940 alone (●) and in the presence of 10 μM tubocurarine (■). Preparations were exposed to tubocurarine and varying concentrations of cannabinoids for 20 mins prior to exposure to nicotine. Each symbol represents the mean amplitude of peak contraction expressed as a percentage of the amplitude of peak contraction derived prior to application of cannabinoid. Each symbol comprises of at least four different myenteric plexus-longitudinal muscle preparations. Vertical lines indicate S.E.M.

leftward shifted when compared with inhibition induced by CP 55,940 of contractions evoked by 100 μM nicotine ($p < 0.01$ for shift in IC_{50}).

2.3.5. Effects of nicotine in cultured myenteric neurones

To further investigate a possible cannabinoid modulation of the nACh receptor electrophysiological techniques were used to directly measure nACh receptor channel properties and assess the action of cannabinoids.

Stable voltage-clamp whole-cell patch recordings were made from a total of 54 cultured myenteric neurones. Cells were clamped at a holding potential of -60 mV. Application of exogenous nicotine (1 mM) induced a transient inward current with a peak amplitude of 10.17 ± 1.54 pA.pF^{-1} (n = 18, figure 2.16). Reapplication of nicotine upon the same cell resulted in a transient inward current with a much smaller peak amplitude, probably due to channel desensitisation. To combat this, neurones were exposed to only a single application of nicotine.

2.3.6. CP 55,940 modulation of nicotine-evoked currents

Pre-treatment with the cannabinoid agonist CP 55,940, at concentrations of 300 nM and 3 μM, significantly depressed the maximum amplitude of current elicited by 1 mM nicotine in a concentration dependent manner, producing currents of 4.11 ± 0.22 pA.pF^{-1} (n = 3) and 1.22 ± 0.30 pA.pF^{-1} (n = 5, $p < 0.01$, figure 2.17) respectively.

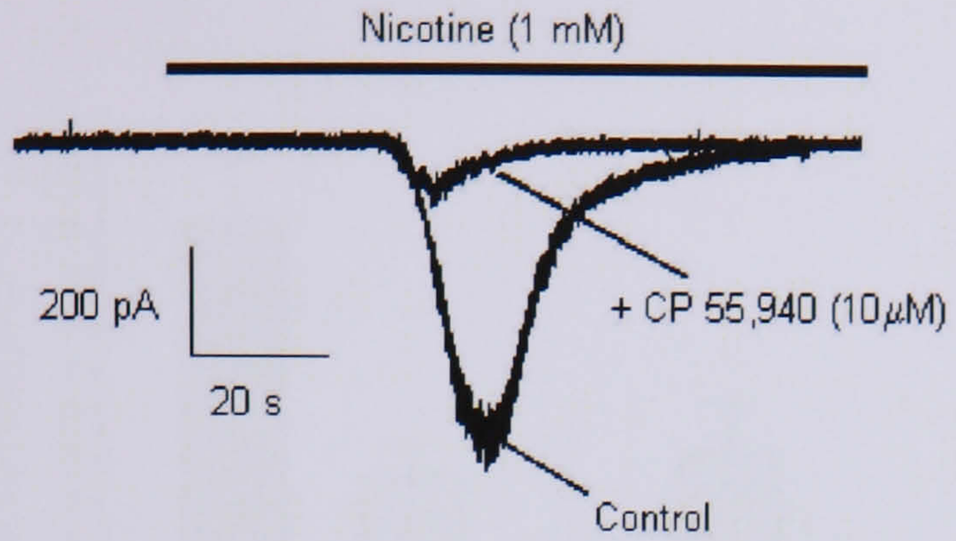

Figure 2.16 Superimposed currents in cultured myenteric neurones evoked through the application of 1 mM nicotine in the absence and presence of 10 μM CP 55,940. Holding potential -70 mV.

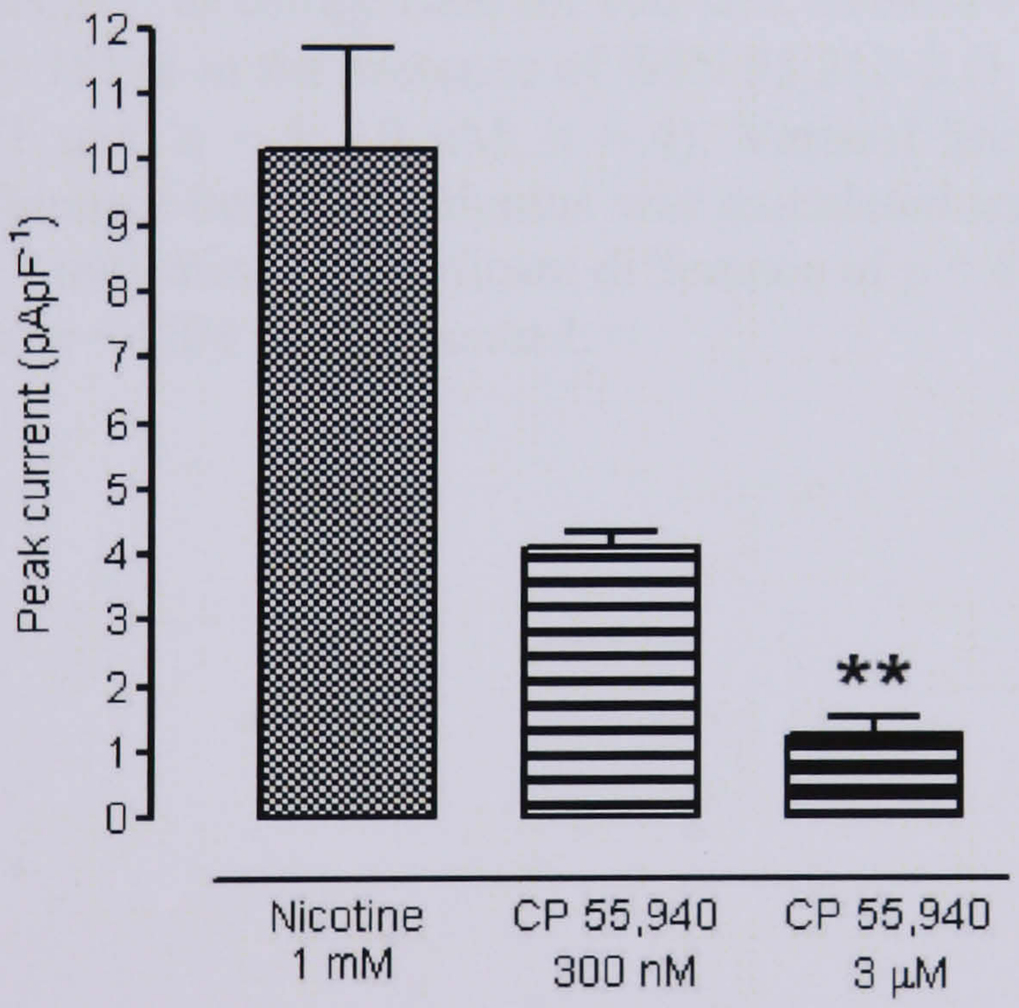

Figure 2.17 Effect of CP 55,940 on peak nicotinic current in cultured myenteric neurones. Each column represents the mean peak current, expressed as $pA.pF^{-1}$ to compensate for cell size, evoked by 1 mM nicotine in the absence of (control, n = 18) or in the presence of CP 55,940 (300 nM, n =3; 3 μM, n = 5). Vertical lines indicate S.E.M. The significance of the difference between columns was calculated using ANOVA followed by Dunnett's test with ** indicating a significant difference of $p < 0.01$ versus control.

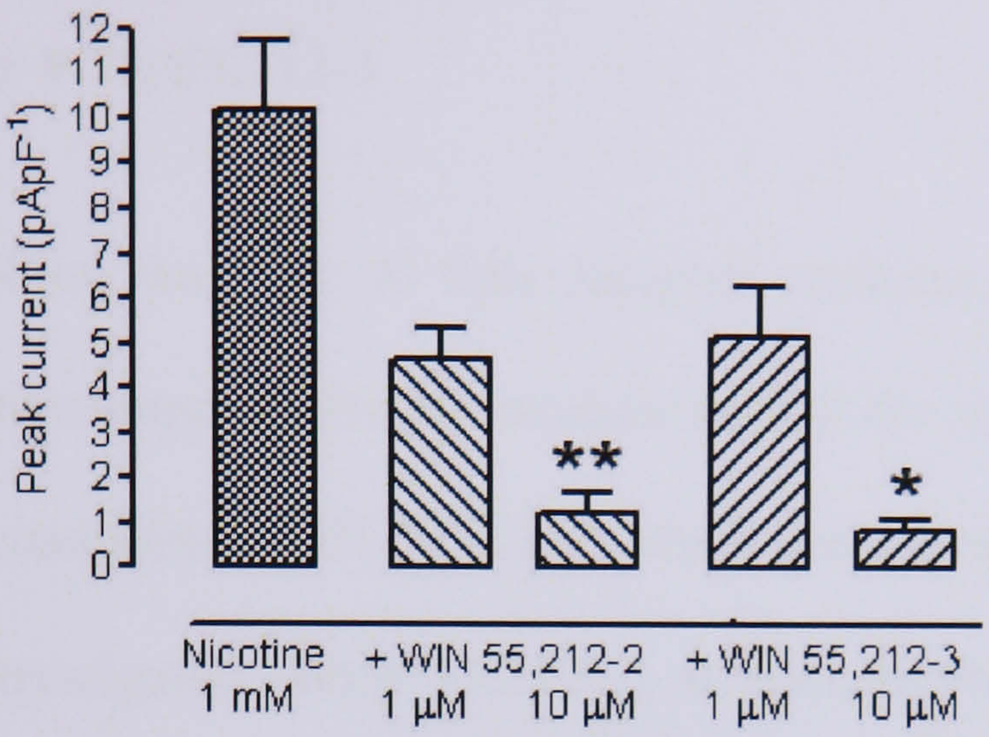

Figure 2.18 Effect of WIN 55,212-2 and the (-)-enantiomer WIN 55,212-3 on peak nicotinic current in cultured myenteric neurones. Each column represents the mean peak current, expressed as $pA.pF^{-1}$ to compensate for cell size, evoked by 1 mM nicotine in the absence of (control, n = 18) or in the presence of WIN 55,212-2 (1 µM, n = 3; 10 µM, n = 8) or WIN 55,212-3 (1 µM, n = 3; 10 µM, n = 4). Vertical lines indicate S.E.M. The significance of the difference between columns was calculated using ANOVA followed by Dunnett's test with * indicating a significant difference of $p < 0.05$ and ** indicating a significant difference of $p < 0.01$ versus control.

2.3.7. Modulation of nicotine-evoked currents by WIN 55,212-2 and CB_1 receptor inactive stereoisomer WIN 55,212-3

To examine if inhibition was due to CB_1 receptor stimulus, transmitted through an intracellular second messenger pathway, modulation by the cannabinoid agonist WIN 55,212-2 and the (-)-enantiomer WIN 55,212-3, which possesses a reduced efficacy at the CB_1 receptor was investigated. WIN 55,212-2, at concentrations 1 μM and 10 μM, significantly reduced the amplitude of nicotine (1 mM) evoked currents from 10.2 ± 1.54 $pA.pF^{-1}$ (n = 18) to 4.65 ± 4.65 $pA.pF^{-1}$ (n = 3) and 1.26 ± 0.46 $pA.pF^{-1}$ (n = 8, $p < 0.01$, figure 2.18) respectively. WIN 55,212-3 also significantly reduced the current amplitude. A concentration of 1 μM reduced amplitude to 5.16 ± 1.15 $pA.pF^{-1}$ (n = 3) and 10 μM reduced amplitude to 0.83 ± 0.30 $pA.pF^{-1}$ (n = 4, $p < 0.01$). Currents evoked in the presence of WIN 55,212-3 did not significantly differ from those evoked in the presence of WIN 55,212-2 ($p > 0.05$).

2.3.8. Cannabinoid modulation of nicotine-evoked currents in the presence of 8-Br-cAMP

To further examine the mechanism whereby cannabinoids modulated nicotine evoked currents, the effects of CP 55,940 were observed in the presence of 8-bromo-adenosine 3′,5′-cyclic monophosphate (8-Br-cAMP). Modulation of intracellular cAMP levels is a major mechanism through which numerous GPCRs, including CB_1 and CB_2 receptors,

act to evoke a response. The presence of the hydrolysis resistant cAMP analogue prevents GPCR modulation of cAMP-dependent pathways and so helps in determining whether cannabinoid inhibition is the result of direct action upon the nACh receptor or by the interaction with an intracellular pathway activated by some alternate receptor.

Application of 0.2 mM 8-Br-cAMP induced a non-significant increase in amplitude of current evoked by nicotine (1 mM) to 15.45 ± 3.00 $pA.pF^{-1}$ (n = 4) from a control response of 10.2 ± 1.54 $pA.pF^{-1}$ (n = 18, figure 2.19). Exposure to CP 55,940 (3 μM) in conjunction with 8-Br-cAMP resulted in a significant reduction in current when compared to control current (2.84 ± 1.83 $pA.pF^{-1}$, n = 5, $p < 0.05$). This current amplitude did not significantly differ from the current amplitude evoked by nicotine in the presence of 3 μM CP 55,940 alone (1.22 ± 0.30 $pA.pF^{-1}$, n = 5).

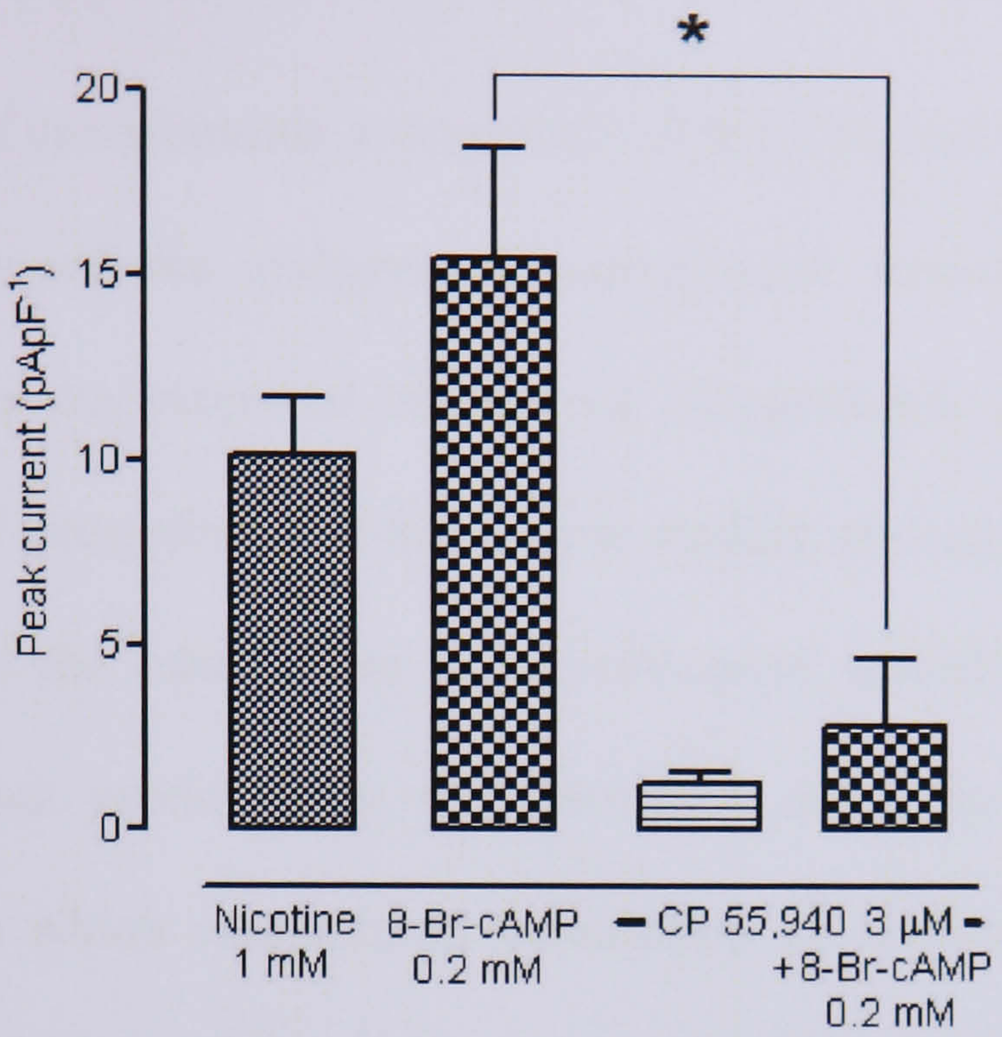

Figure 2.19 Effect of 8-bromoadenosine 3′,5′-cyclic monophosphate (8-Br-cAMP) on inhibition induced by CP 55,940 of peak nicotinic current in cultured myenteric neurones. Each column represents the mean peak current, expressed as $pA.pF^{-1}$ to compensate for cell size, evoked by 1 mM nicotine in the absence of (control, n = 18; 8-Br-cAMP 0.2 mM, n = 4) or in the presence of CP 55,940 alone (3 µM, n = 5) and in the presence of 8-Br-cAMP (n = 5). Vertical lines indicate S.E.M. The significance of the difference between columns was calculated using ANOVA followed by Dunnett's test with * indicating a significant difference of $p < 0.05$ between columns representing 8-Br-cAMP alone and CP 55,940 and 8-Br-cAMP.

2.4. Discussion and conclusion

Recently the concept of cannabinoids acting solely at the CB_1 and CB_2 receptors has been questioned. The action of the endogenous cannabinoid anandamide at the TRPV1 receptor, coupled with the proposed activity of cannabinoids at a number of novel receptors and allosteric sites, observed in multiple studies, strongly suggest cannabinoids play a diverse role in the modulation of physiological activity. This work supports electrophysiological data produced by our laboratory suggesting the existence of an additional site through which cannabinoid modulation of neuronal activity may occur. Data indicates an inhibition of nicotinic receptor activity by cannabinoids exists in myenteric neurones in the guinea-pig ileum that is dependent upon either a $G_{i/o}$-protein independent or an allosteric mechanism.

Interest first arose with the observation that inhibition by CP 55,940 of nicotine evoked contractions in the MPLM preparation was not blocked by SR141716. This was contrary to what would be expected from work published previously by Pertwee and colleagues, who observed a CB_1 receptor dependent inhibition of electrically evoked contraction, which was blocked by SR141716 (Pertwee *et al.*, 1996; Coutts and Pertwee, 1997). Coupled with the partial inhibition of contraction by the CB_1 receptor inactive enantiomer WIN 55,212-3, the data suggested an additional CB_1 receptor independent mechanism might exist through which cannabinoids act to inhibit the action of nicotine in myenteric neurones. The lack of antagonism by SR141716 suggests more than one inhibitory mechanism exists governing contraction evoked by nicotinic stimulus, but not with electrical stimulus, and the presence of some inhibition of contraction suggests a lack of stereoselectivity for WIN 55,212-2 over WIN 55,212-3.

To further examine this hypothesis, TTX was used to prevent voltage-dependent sodium influx and so the generation of action potentials, allowing the stimulation of longitudinal muscle contraction through solely nicotinic receptors located at the nerve terminal of the excitatory motor neurones (Galligan, 1999; Kirchgessner and Liu, 1998). This enabled the examination of cannabinoid modulation of nicotine evoked contractions independent of the action potential, which has been shown in chapter 3 to be modulated by cannabinoids through CB_1 and CB_2 receptor dependent voltage-dependent calcium channel inhibition in cultures of myenteric neurones. Under these conditions, both CP 55,940 and SR141716 independently inhibited nicotine evoked contractions, and both WIN 55,212-2 and the CB_1 receptor inactive enantiomer WIN 55,212-3 inhibited contraction with the same potency, suggesting action at a site other than the CB_1 receptor. It is unlikely that the concentration of TTX used was insufficient to block nerve-mediated responses as electrically evoked contractions of the guinea-pig MPLM preparation have been shown previously to be completely blocked by similar concentrations of TTX (see Yunker and Galligan, 1996 for example).

Examination of cannabinoid inhibition of contraction evoked with either a lower concentration of nicotine or in the presence of the competitive antagonist tubocurarine showed an intriguing leftward shift in CP 55,940 concentration-response curves, resulting in an IC_{50} in a range similar to that observed by Pertwee *et al.* (1996) with the inhibition of electrically-evoked currents in MPLM. The rightward shift in CP 55,940 concentration-response curve in the presence of SR141716, coupled with the increased potency of CP 55,940 strongly suggests inhibition of contraction evoked with this lower concentration of nicotine to be mediated by the CB_1 receptor. This decrease in sensitivity

to cannabinoids may resemble the decreased sensitivity to morphine observed with higher frequency electrically induced acetylcholine release in the MPLM (Cowie *et al.*, 1968). Higher concentrations of nicotine may result in a large depolarisation of the soma and so initiate the firing of multiple action potentials in a manner similar to that evoked by high frequency electrical stimulation, while lower concentrations of nicotine may result in the firing of a pattern of action potential similar to that evoked by low frequency electrical stimulation and so possess more susceptibility to a G-protein mediated inhibition. The more simple hypothesis that different potency of cannabinoids to inhibit contraction evoked by different neuronal firing frequencies is rebuked by the observation than cannabinoid inhibition of contraction evoked by higher nicotine concentrations is not blocked by the CB_1 receptor specific antagonist SR141716.

Ikeda and colleagues (Pan *et al.*, 1998) observed, in whole-cell patch clamping of rat superior cervical ganglion neurones expressing the CB_1 receptor, strongly depolarising neurones immediately prior to inducing activation of N-type calcium channels prevented CB_1 receptor mediated inhibition of these channels. This nicely corroborates the hypothesis that the multiple action potentials evoked by exposure to large quantities of nicotine may mimic the strong depolarisation and so inactivate the $G_{\beta\gamma}$-protein mediated pathway through which the CB_1 receptor acts (figure 2.20).

Whole-cell patch-clamp electrophysiology confirmed a cannabinoid dependent inhibition of the opening of the nicotinic ion channel in cultured myenteric neurones. In previous work, this inhibition displayed properties not anticipated of the CB_1 receptor; being inhibited by PEA and showing not only a lack of blockade by SR141716, but an inhibition by this CB_1 receptor selective antagonist. The current study demonstrated no

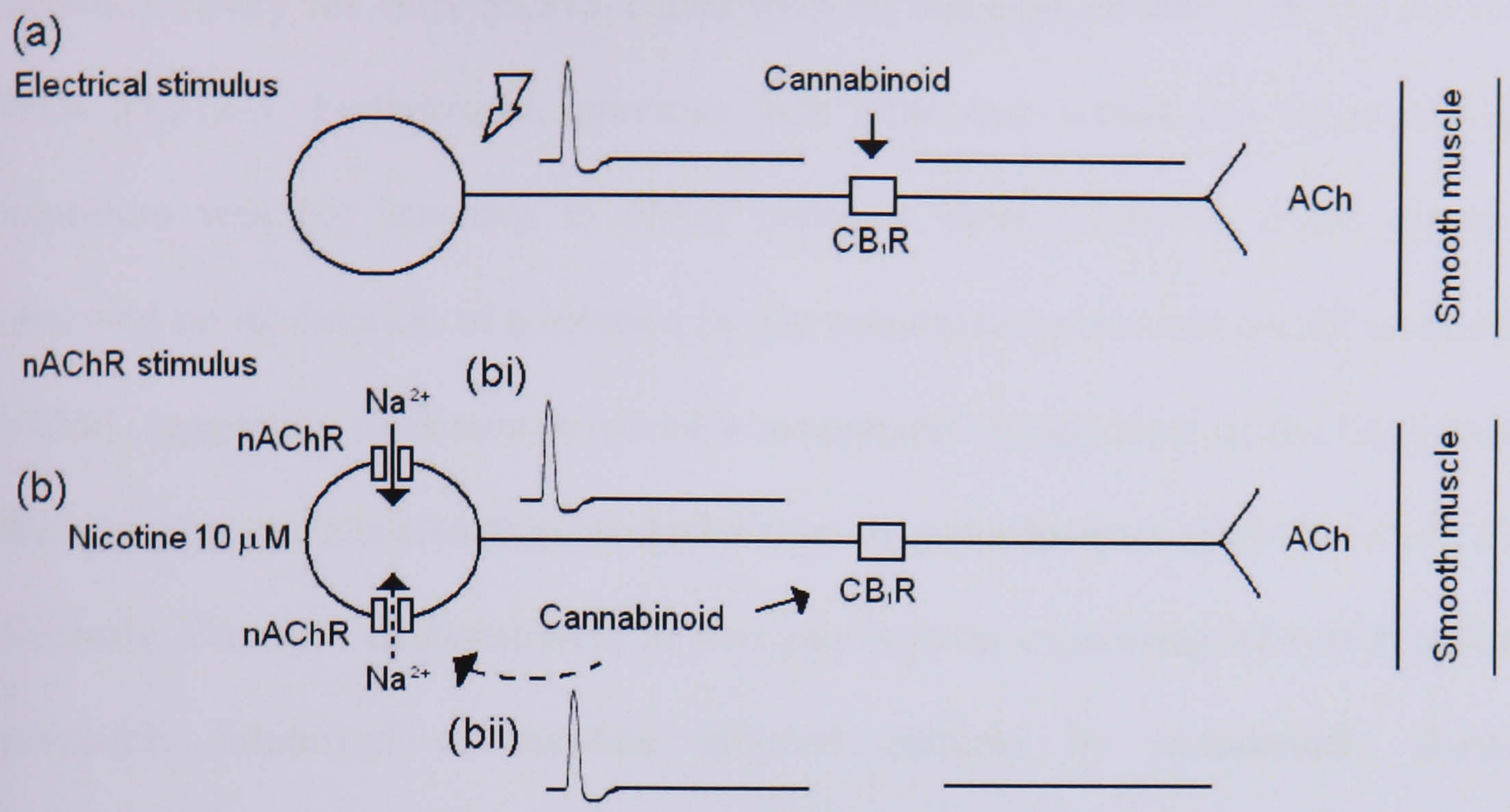

Figure 2.20 Hypothesised model through which cannabinoids act to inhibit nicotinic stimulation of contraction of the MPLM. (a) Low frequency electrical stimulus evokes an action potential by stimulating the axon. This can be blocked by CB_1 receptor activation. (b) Low concentrations of nicotine cause a moderate degree of depolarisation within the soma (bi) evoking a single action potential. (bii) Cannabinoids act at both the CB_1 receptor and the nicotinic receptor to inhibit action potentials. However, as cannabinoids show greater potency at the CB_1 receptor, inhibition of the nicotinic receptor is masked. (c) High concentrations of nicotine induce a marked depolarisation within the soma (ci) evoking the firing of multiple action potentials. (cii) Cannabinoids act at the CB_1 receptor to inhibit initial action potentials, but the continued presence of high frequency action potentials in the axon desensitise the CB_1 receptor and/or related pathways allowing action potentials to propagate and evoke ACh release. This unmasks an alternative mechanism through which cannabinoids act to inhibit contraction, through blockade of the nicotinic receptor.

stereoselectivity for WIN 55,212-2 over the CB_1 and CB_2 receptor inactive stereoisomer WIN 55,212-3. Furthermore, previous data generated within our laboratory showed inhibition was not sensitive to either pertussis toxin treatment while current work observed no modulation of inhibition by the membrane-permeable cAMP analogue 8-Br cAMP, suggesting inhibition involved a mechanism independent of the $G_{i/o}$-protein and the adenylate cyclase/cAMP intracellular signalling mechanisms (DeMuth *et al.*, 2005). Recently, Oz *et al.* demonstrated, in *Xenopus* oocytes expressing α7-nACh receptors, a reversible inhibition of nicotine induced currents by anandamide, 2-AG and methanandamide (Oz *et al.*, 2003; 2004). Inhibition was not reduced by the selective CB_1 and selective CB_2 receptor antagonists SR141716 and SR144528, and was insensitive to both pertussis toxin or to 8-Br-cAMP treatment. However, in contrast to what was observed in current and previous studies, the synthetic cannabinoids WIN 55,212-2, CP 55,940 and Δ^9-THC did not alter α7-nACh receptor function. This dissimilarity may be the result of cannabinoids acting at different receptors, both inducing inhibition of the nicotinic channel but expressing differing sensitivity to the cannabinoids or, if cannabinoid inhibition is the result of an allosteric interaction with the nicotinic receptor, the dissimilarity may be due to a differing subunit composition of the nicotinic receptors expressed by cultured myenteric neurones compared to the homologous transfection of α7 subunits in oocytes. The properties of different nicotinic receptor subtypes are determined by the specific subunit composition of the receptor (Colquhoun and Patrick, 1997; Luetje and Patrick, 1991). Functional neuronal nicotinic receptors are composed of five subunits comprising of different combinations of α and β subunits, of which there are eight α (α2-α9) and three β (β2-β4) subunits. Immunohistochemical and pharmacological

studies have revealed, in myenteric neurones maintained in cell culture, predominant expression of α3, α5, β2 and β4 nicotinic receptor subunits (Zhou *et al.*, 2002; Galligan and North, 2004). However, assembly of the subunits has not been established and so receptors may exist as either homologous populations or as multiple receptors of differing subunit composition. The presence of α7 nicotinic subunits is debatable. Zhou *et al.*, (2002) reported only a small proportion of cultured myenteric neurones showed staining on application of an α7 subunit selective antibody and, whilst under whole-cell patch-clamp, no inhibition of nicotinic receptors was observed with the α7 subunit specific blockers α-bungarotoxin and α-methyllycaconitine, similar to what we previously observed (DeMuth *et al.*, 2005). Unpublished studies investigating cannabinoid activity upon other nicotinic receptors have shown inhibition of human α4β2 nicotinic receptors expressed in SH-EP1 cells by anandamide and a lack of inhibition by anandamide in HEK-293 cells expressing the α1β1εγδ subunits of mouse muscle nicotinic acetylcholine receptors (quoted in Oz, 2006).

One possible manner in which cannabinoids may act is through a mechanism similar to that which arachadonic acid, a metabolite of anandamide, acts to inhibit nicotinic receptors. Arachadonic acid has been shown to inhibit *Torpedo* and chick α7 nicotinic receptors, expressed in oocytes, possibly through a direct blocking effect on Ca^{2+}-modulatory sites on the nicotinic receptor (Nishizaki *et al.*, 1998). This suggests the existence of an allosteric cannabinoid binding site on the nicotinic receptor. However, data so far does not rule out the possibility of binding and activation of an alternate receptor, leading to activation of intracellular signalling pathways and so an inhibition of the nicotinic receptor.

In summary, on the basis of cannabinoids expressing pharmacological properties in modulating contraction of the MPLM preparation and currents in myenteric neurones evoked by nicotinic receptor stimulus not consistent with that anticipated as a result of activation of the CB_1 receptor, data suggests an alternative mechanism may exist through which cannabinoids modulate neural activity as a result of nicotinic receptor stimulation.

Chapter 3 - Cannabinoid modulation of calcium channel activity in guinea-pig myenteric AH neurones

3. Chapter 3 - Cannabinoid modulation of calcium channel activity in guinea-pig myenteric AH neurones

3.1. Introduction

Modulation of contractions induced by electrical stimulation of the guinea-pig ileum myenteric plexus-longitudinal muscle preparation (MPLM) has been used for some time as a measure of cannabinoid activity through the CB_1 receptor (for review see Pertwee, 2001). Electrically evoked contractions of the MPLM are considered to result from excitation of enteric neurones inducing the release of neurotransmitters, including acetylcholine, which act upon the longitudinal smooth muscle to cause contraction. Cannabinoids are believed to act through the inhibition of acetylcholine release, but as the MPLM preparation consists of a large variety of neurones responsible for conveying both excitatory and inhibitory stimuli, electrical stimulation would be expected to result in the release of a mixture of both inhibitory and excitatory neurotransmitters, which opens the possibility of a more complex role for cannabinoids within the gastrointestinal tract.

Morphologically, enteric neurones were first categorised in a study published over 100 years ago (Dogiel, 1899). Dogiel type I neurones possess a single axon and short lamellar dendrites while Dogiel type II cells have multiple long processes arising from a smooth cell body. Hirst *et al.* (1974) divided enteric neurones according to their electrical characteristics into AH neurones, which show a long after-hyperpolarisation following action potentials, and S neurones demonstrating fast, cholinergic synaptic inputs and no after-hyperpolarisation. The distinct after-hyperpolarisation is the result of a voltage-dependent influx of Ca^{2+}, opening Ca^{2+} dependent K^+ channels that

render the soma refractory to further stimuli (Nishi and North, 1973; Hirst *et al.* 1974). Unlike in S neurones in which action potentials are completely blocked by TTX, in AH neurones the influx of calcium induces membrane potential changes enabling (slow) action potentials to be evoked.

This high voltage-activated Ca^{2+} current has been shown pharmacologically to be mainly mediated by N-type channels because of the inhibitory effects of the highly specific N-type channel blocker ω-conotoxin GVIA, and the lack of effect of the P/Q-type channel specific blocker ω-aga IVA and the L-type calcium channel blockers, nicardipine and nifedipine (Rugiero *et al.*, 2002; North and Tokimasa, 1987; Kunze *et al.*, 1994). The existence of a low-voltage activated T-type channel has been hypothesised by Starodub and Wood (1999) based upon the continued presence of a low-voltage activated calcium current after application of the duel N-type and P/Q-type channel blocker ω-conotoxin MVIIC. Within the guinea-pig small intestine, Dogiel type II cells possess the electrical characteristics of AH neurones while the majority of Dogiel type I cells possess the electrical characteristics of S neurones (Brookes *et al.*, 1995). Motor neurones, responsible for the transfer of stimulus directly to the longitudinal muscle, consist of excitatory and inhibitory Dogiel type I neurones with S cell electrophysiological characteristics, while primary afferent neurones, which project to the mucosa transmitting information regarding the nature and intensity of the stimulus to neurones within the myenteric and submucosal plexus, all possess Dogiel type II morphology and possess the electrophysiological characteristics of AH cells.

CB_1 receptor agonist inhibition of N-type voltage-gated calcium channels (VGCC) was first shown by Mackie and Hille (1992) using the whole-cell patch clamp technique in the NG108-15 neuroblastoma-glioma cell line. Inhibition was shown,

through pertussis toxin blockade, to be mediated by the CB_1 receptor acting via $G_{\beta\gamma}$-protein subunits (Mackie and Hille, 1992; Caulfield and Brown, 1992).

Within the ileum, there is evidence that cannabinoids act at CB_1 receptors. The potency of cannabinoid agonists in the inhibition of electrically evoked contractions correlates well with that of their psychotropic potencies and of their affinities for specific CB_1 receptor binding sites in brain tissue (Nye *et al.*, 1985; Pertwee *et al.*, 1996). The inhibition shows ligand stereospecificity, is reduced by CB_1 receptor specific antagonists, and attenuated by inhibitors of $G_{i/o}$-protein signal transduction (Roth, 1978; Pertwee *et al.*, 1992; 1996; Coutts and Pertwee, 1997; 1998). Binding studies, immunohistochemistry, and the detection of CB_1 receptor mRNA within the MPLM, confirm their presence (Lynn and Herkenham, 1994; Coutts *et al.*, 2002; Griffin *et al.*, 1997). Using intracellular recordings, López-Redondo *et al.* (1997) demonstrated in S type neurones an inhibition of the amplitude of action potentials elicited by presynaptic electrical stimulus and through the application of acetylcholine (ACh) in approximately two thirds of neurones treated with the cannabinoids WIN 55,212-2 and CP 55,940. The CB_1 receptor specific antagonist, SR141716 (1 μM), inhibited only a small proportion of the neurones it was tested on (3 out of 8 electrically stimulated neurones and 5 out of 12 stimulated with ACh), suggesting cannabinoid activity at more than just the CB_1 receptor.

The presence of the CB_2 receptor in the MPLM is equivocal. Griffin *et al.* (1997) demonstrated the presence of CB_2-like mRNA in guinea-pig whole ileum, but not in MPLM, and found the CB_1 receptor specific antagonist SR141716 completely reversed the inhibition of electrically evoked contractions produced by a non-specific cannabinoid receptor agonist in the MPLM. Binding assays in the MPLM showed displacement of [^{3}H]-CP 55,940 by the CB_2 receptor specific antagonist SR144528

with a K_i of 0.36 μM (Ross *et al.*, 1998). However, in CHO cells expressing the hCB_2 receptor and in rat spleen, SR144528 gave K_i values of 0.30 and 5.6 nM respectively, while K_i values of 0.31 and >10 μM were observed in rat brain and CHO cells expressing the hCB_1 receptor (Rinaldi-Carmona *et al.*, 1998; Ross *et al.*, 1999). This suggested an absence of CB_2 receptors in the MPLM. No modulation of action potential amplitude or area above the amplitude-versus-time curve was observed through intracellular recordings in AH neurones upon exposure to WIN 55,212-2 (López-Redondo *et al.*, 1997). In contrast, other studies have suggested the presence of the CB_2 receptor in the gut. In the rat fundus, Storr *et al.* (2002) observed increased nerve stimulation-elicited relaxation in response to a CB_2 receptor antagonist and were able to isolate CB_2 receptor mRNA. Gastrointestinal transit in the rat is inhibited by a CB_1 receptor mediated mechanism. Lipopolysaccharide (LPS) treatment increased transit and prevented a CB_1 receptor mediated inhibition. However, application of a CB_2 receptor agonist, which did not affect transit in animals not treated with LPS, reduced transit to control levels, suggesting a possible role for the CB_2 receptor in pathophysiological conditions (Mathison *et al.*, 2004). More recently, immunohistochemical studies have detected the CB_2 receptor co-localised with neuronal markers in the myenteric plexus and, using quantitative real time-PCR, have shown an increase in CB_2 receptor mRNA in tissue derived from LPS treated rats (Duncan *et al.*, 2005; 2006). However, in contrast, mice experiencing croton oil induced diarrhoea showed WIN 55,212-2 inhibition of intestinal transit that was blocked by SR141716 but not by SR144528 (Izzo *et al.*, 2000b).

Several studies have suggested the presence of non-CB_1 and CB_2 receptors in the intestinal tract. Izzo and colleagues observed decreased intestinal transit in mice with exposure to palmitoylethanolamide (PEA), a cannabinoid that has been shown not to

act at CB_1 and CB_2 receptors, but at a putative "CB_2-like" receptor (Lambert and Di Marzo, 1999; Calignano *et al.*, 1998; 2001; Izzo *et al.*, 2001). However, as the CB_2-like receptor displayed sensitivity to SR144528 (Calignano *et al.*, 2001), the lack of inhibition observed by Izzo *et al.* (2001) by both SR141716 and SR144528 suggests an alternative mechanism may be responsible. A CB_1, CB_2 and TRPV1 receptor independent inhibition was reported by Mang *et al.* who showed anandamide inhibition of guinea-pig MPLM motility and acetylcholine release that possessed lower sensitivity to SR141716 than CP 55,940, while TRPV1 activation was ruled out by insensitivity to capsazepine (Mang *et al.*, 2001).

With CB_1 receptor activation established to inhibit I_{Ca} in other neuronal preparations, this chapter investigates whether cannabinoid receptors act to inhibit I_{Ca} in AH neurones isolated from the guinea-pig ileum myenteric plexus.

3.2. Methods

3.2.1. Preparation of ileum

Methods for preparation of MPLM tissue are detailed in Section 2.4.1. Briefly, Heston-2 guinea-pigs (300-500 g) of either sex were killed by cervical dislocation and strips of myenteric plexus-longitudinal muscle derived from segments of small intestine were prepared using the method of Paton and Zar (1968). Tissues were immersed in Krebs solution, maintained at 37°C and supplied with 95% O_2 and 5% CO_2.

3.2.2. Preparation of cultured myenteric neurones

Methods for disassociation of myenteric neurones are detailed in Section 2.3.2.1. Briefly, sections of myenteric plexus-longitudinal muscle were first digested in HBSS containing 0.01 ml/ml papain. This was followed by tituration whilst digesting in 1 mg/ml collagenase Type 1 and 3.1 mg/ml dispase. Cells were incubated in Dulbecco's modified Eagle's medium (DMEM) supplemented with 5% FBS, 1 mM L-glutamine, 8.3 mM glucose, 5 μM cytosine β-D-arabinofuranoside hydrochloride, 50 μM (+)-5-fluorodeoxyuridine, 2.5 μM uridine, 150 units/ml penicillin and 150 μg/ml streptomycin, plated on to collage-coated glass slides and incubated at 37°C in an atmosphere of 95% CO_2 and 5% O_2.

3.2.3. Patch clamp

Methods for patch clamping of myenteric neurones are detailed in Section 2.3.2. Briefly, glass pipettes were pulled from borosilicate glass capillaries (Clark (UK) GC150TF-10) using a P-87 Flaming-Brown micropipette puller, fire polished on a microforge (Narishige, Japan) and backfilled with an intracellular solution (see solutions) to give a typical resistance of 3–7 MΩ. Chloride-coated silver wire connected the pipette filling fluid to the probe input. The probe of the patch clamp amplifier (Multiclamp 700A, Axon Instruments, USA) was mounted on a course manipulator (MC35A, Narishige, Japan) and directed to the cells by means of a hydraulic micromanipulator (MHW-3, Narishige, Japan). Data acquisition was performed at 10 kHz sampling rate using a digital interface (Digidata 1322A, Axon Instruments, USA) connected to a personal computer using the software Clampex 8.2 (Axon Instruments, USA). Clampfit 8.2 (Axon Instruments, USA) was used for offline data analysis. Whole cell patch clamp measurements under voltage clamp were performed after gigaseal formation (Hamill *et al.*, 1981), followed by disruption of the membrane under the pipette by a suction pulse. The process was monitored by applying a test pulse (10 mV, 5 ms, 100 Hz) to the cell, which allowed the analysis of a resting leak current and enabled optimal capacitive transient cancellation. Leakage current was accounted for using P/N leak subtraction. Whole-cell currents were low-pass filtered at 2 kHz with the four-pole Bessel filter of the clamp amplifier.

3.2.4. Experimental design

All experiments were performed at room temperature (22°C). Neurones were selected for study through the presence of Dogiel type II morphology (multiple long processes

arising from a smooth cell body) and AH neural electrochemical properties (action potential after-hyperpolarisation). Voltage-gated calcium currents were measured through the addition of tetrodotoxin (300 nM) to the extracellular solution to inhibit voltage-gated Na^+ currents and the presence of CsCl and tetraethylamonium-Cl in the intracellular medium to inhibit K^+ currents. Amplification of calcium currents was obtained through the use of a high calcium extracellular solution (see section 3.3.6). To account for Cl^- currents only data generated at the Cl^- reversal potential was examined. Cells were clamped at a holding potential of -70 mV and stepped to varying potentials for 100 ms every 10 s. To compensate for cell size, data are expressed as $pA.pF^{-1}$ membrane capacitance.

3.2.5. Drugs

All drugs were obtained from SigmaAldrich, UK, unless stated otherwise. O-2050 and AM 251 were obtained from Tocris, UK. SR144528 was a kind gift from Sanofi Recherche, France. Penicillin and streptomycin were obtained from Gibco, UK. All stock solutions of cannabinoid drugs were dissolved in ethanol, shielded from light and kept at -20°C.

3.2.6. Solutions

Dulbecco's modified Eagle's medium and HBSS were obtained from SigmaAldrich, UK. Electrophysiological measurements were performed in high calcium extracellular solution (high Ca^{2+}-ECS) containing (mM): NaCl 125, KCl 6, $MgCl_2$ 2.5, NaH_2PO_4 1.2, HEPES 10, glucose 11, sucrose 67, $CaCl_2$ 2.4, pH 7.35. Intracellular solution

contained (mM): NaCl 10, CsCl 132, $MgCl_2$ 1.2, HEPES 20, glucose 11, Na-ATP 5, Na-GTP 0.1, tetraethylamonium chloride 10, EGTA 0.1, pH 7.2. All drugs were administered in the ECS, superfused at a rate of 2 ml min^{-1} with the exception of pertussis toxin, which was added to the cell culture medium 18 hr before recording to allow entry into the cell. After each experiment the apparatus was thoroughly washed with dilute hydrochloric acid, ethanol and distilled water to remove any adhering cannabinoid.

3.2.7. Analysis of data

Each value is expressed as the mean ± standard error of the mean (S.E.M.) of at least four experiments. Concentration–response curves were calculated using non-linear regression to fit data to a standard sigmoidal dose-response curve. The concentration which produced 50% of the maximum response (IC_{50}), and the maximal level of inhibition were calculated for certain experiments using the GraphPAD Prism statistical software (GraphPAD Software, CA, USA). Mean values of two sets of data were compared using Student's unpaired *t*-test, a P value < 0.05 being taken as significant. Mean values of multiple data sets were compared using ANOVA followed by either Dunnetts or Newman-Keuls Multiple Comparison Test. Gaussian distribution of data was examined using the Kolmogorov-Smirnov test.

3.3. Results

Stable patch-clamp recordings were made from a total of 164 neurones derived from 30 independent preparations of myenteric neurones. AH neurones, chosen for the presence of Ca^{2+} currents, were identified on the basis of morphological and electrophysiological characteristics upon suppression of K^+ and Na^+ currents. Seals remained stable for at least 10 minutes, after which degradation would occur. To ensure loss of seal did not occur during the recording of results, cells were exposed to cannabinoids for at least 5 minutes prior to patching.

An inward Ca^{2+} current of 892 ± 79 pA (28.9 ± 2.1 $pA.pF^{-1}$) was elicited in 30 neurones (derived from 30 guinea pigs) by a 100 ms depolarising pulse to 0 mV from a holding potential of -70 mV. The current consisted of a sharp transient increase followed by a slowly decreasing component (figure 3.1). The maximum inward current evoked by this depolarisation possessed a distribution between neurones not significantly different from a Gaussian distribution ($P > 0.05$, Kolmogorov-Smirnov normality test) suggesting all AH neurones possess Ca^{2+} channels with similar characteristics. Inward current initiated upon a depolarising pulse to -30 mV and achieved a peak inward current between -10 to 0 mV (figure 3.2b). An outward current was observed at positive potentials greater than 50 mV (figure 3.3b). The majority of inward current elicited by a depolarising pulse to 0 mV was inhibited by the specific N-type Ca^{2+} channel blocker ω-conotoxin GVIA (100 nM reduced current to 10.0 ± 2.4 $pA.pF^{-1}$, reducing by 65.6% of control; n = 3) whilst the L-type Ca^{2+} channel blocker nifedipine (10 μM) did not induce any significant reduction in current (a current of 34.2 ± 1.6 $pA.pF^{-1}$ was observed, n = 4).

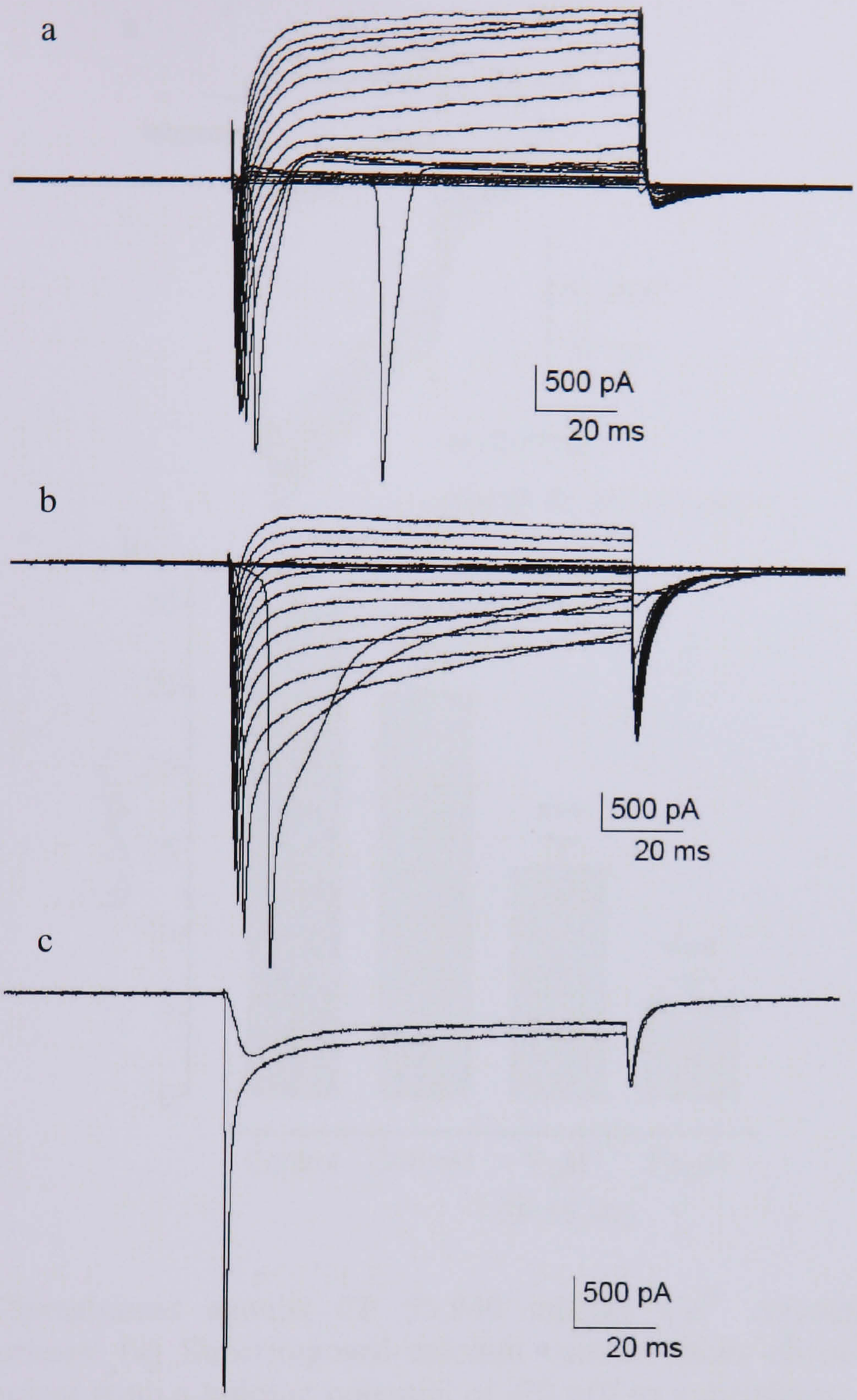

Figure 3.1 Superimposed traces derived from cultured myenteric neurones held under voltage clamp. (a) Depicts current flow evoked by 100 ms, 10 mV steps in membrane potential ranging from –80 to 90 mV. (b) Depicts current flow evoked voltage steps in the presence of TEA and CsCl. (c) Depicts current flow evoked by a voltage step to 0 mV in the absence and presence of TTX.

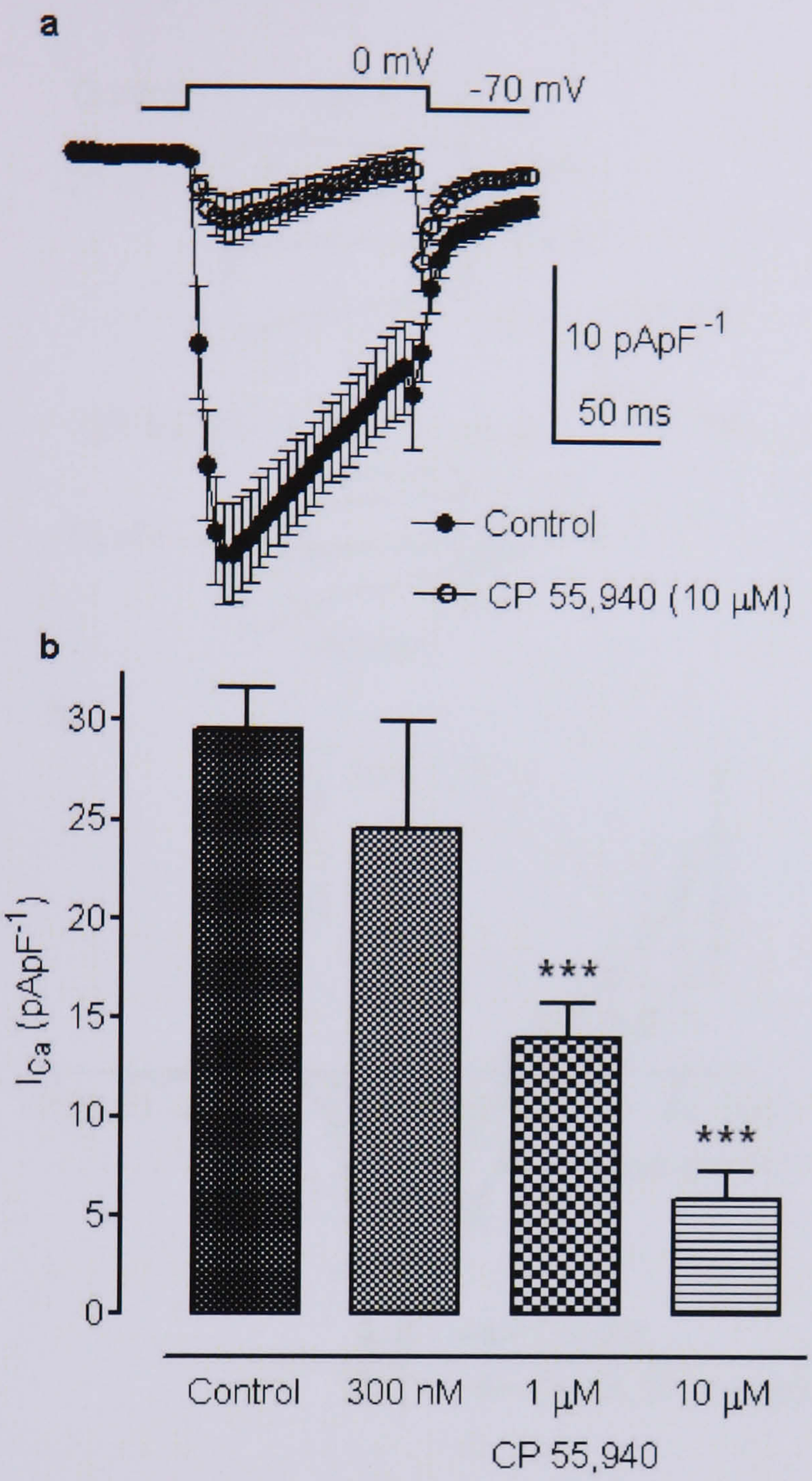

Figure 3.2 Cannabinoid agonist CP 55,940 inhibits Ca^{2+} currents in cultured myenteric neurones. (a) Superimposed calcium current traces elicited by 100 ms depolarising pulses from a holding potential of -70 mV to a membrane potential of 0 mV in the absence and pre-treated presence of CP 55,940 (1 μM). Each point represents the mean current, expressed as $pApF^{-1}$ membrane capacitance to compensate for cell size, over a 5 ms period required to maintain membrane potential and consists of at least 7 neurones. (b) CP 55,940 significantly inhibited (***, $P <$ 0.001, ANOVA followed by Newman-Keuls) peak Ca^{2+} current elicited by a 0 mV depolarising pulse. Columns show the mean current, expressed as $pApF^{-1}$ membrane capacitance, in the absence and pre-treated presence of CP 55,940 at concentrations of 300 nM, 1 μM and 10 μM. Bars show S.E.M. Non-linear regression to a sigmoidal concentration-response curve presented an IC_{50} and maximal blockade for CP 55,940 of 0.54 μM and 80.0% respectively.

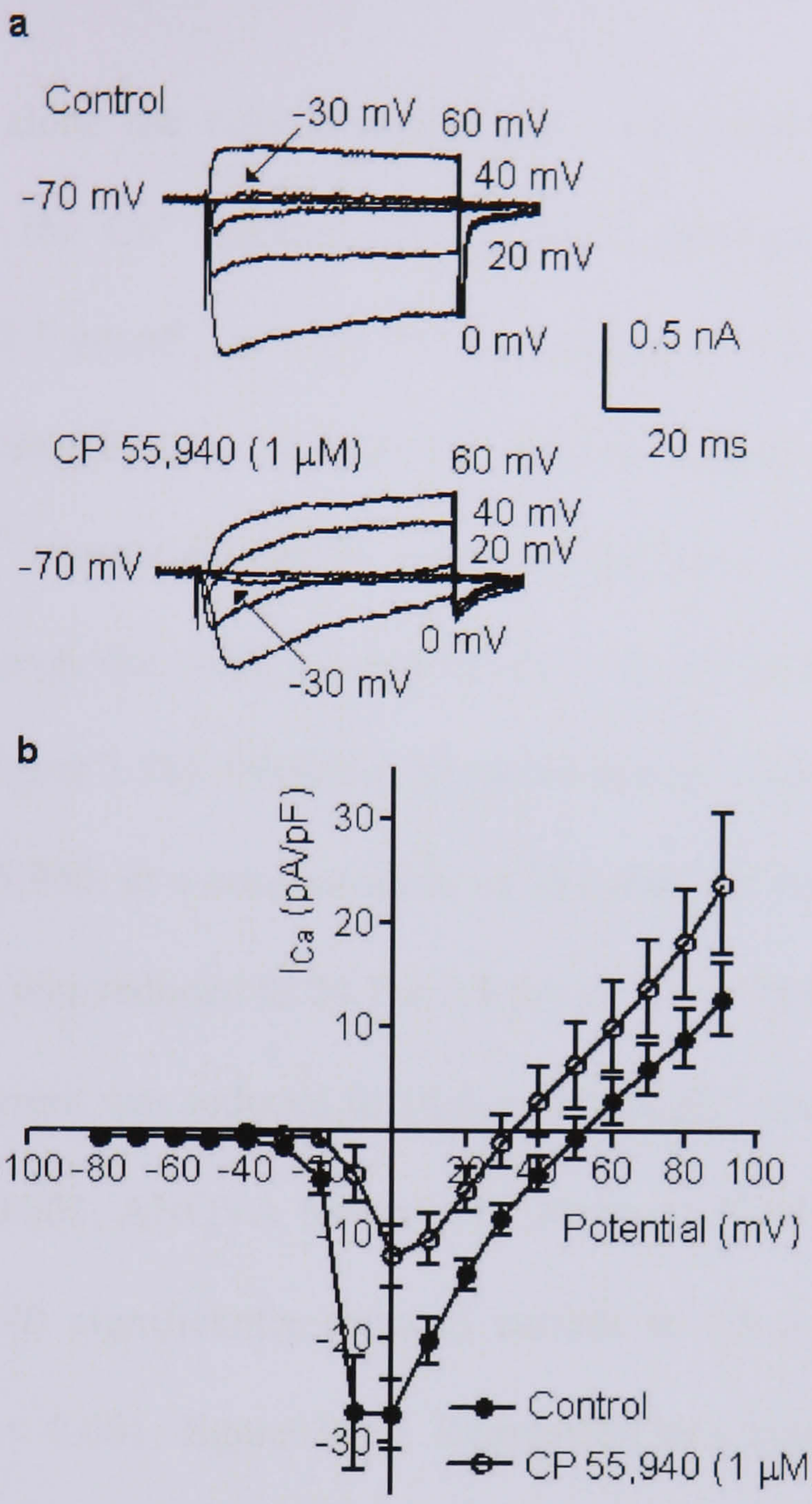

Figure 3.3 (a) Calcium current traces in cultured myenteric neurones under control conditions and after exposure to CP 55,940 (1 µM) prior to patching. Currents were activated by 100 ms voltage steps in 10 mV increments from a holding potential of -70 mV to potentials ranging from -80 mV to 90 mV. (b) Superimposed I-V curves of peak I_{Ca}, expressed as $pApF^{-1}$ membrane capacitance, in myenteric neurones in the absence of (●) and presence of CP 55,940 (1 µM, ○). Each point represents the mean ± S.E.M. of at least 5 neurones.

3.3.1. Cannabinoid inhibition of Ca^{2+} currents

When administered alone the vehicle ethanol, at a concentration of 0.1%, did not significantly reduce the Ca^{2+} current elicited by a depolarising pulse to 0 mV (reduction to 23.8 ± 2.1 $pA.pF^{-1}$, n = 10, $P > 0.05$, unpaired *t*-test). Pre-treatment with the non-selective cannabinoid agonist CP 55,940 significantly depressed the amplitude of the Ca^{2+} current elicited by a depolarising pulse to 0 mV, with maximal inhibition occurring over the voltage range of -10 to 0 mV or at the peak of the I-V relationship (n = 5, figure 3.3b). Inhibition occurred over a concentration range of 300 nM to 10 μM. CP 55,940, at a concentration of 300 nM, did not significantly inhibit Ca^{2+} current (current was reduced to 24.7 ± 5.3 $pA.pF^{-1}$, n = 7), but at a concentration of 1 μM the Ca^{2+} current was reduced to 14.0 ± 1.8 $pA.pF^{-1}$ (current was reduced by 51.5%, n = 11, $P < 0.001$, ANOVA followed by Newman-Keuls). At a concentration of 10 μM, CP 55,940 significantly reduced current to 5.9 ± 1.4 $pA.pF^{-1}$ (79.7% inhibition, n = 7, $P < 0.001$, figure 3.2b). Regression to a sigmoidal dose-response curve yielded an IC_{50} for CP 55,940 of 0.54 μM and a maximum reduction of current of 80.0%.

Another non-selective cannabinoid agonist, WIN 55,212-2, at a concentration of 10 μM, significantly inhibited the Ca^{2+} current elicited by a depolarising pulse to 0 mV. Current was reduced to 7.3 ± 1.8 $pA.pF^{-1}$ (74.7% inhibition, n = 5, $P < 0.001$, figure 3.4).

To examine whether inhibition was the result of CB_1 or CB_2 receptor stimulation, the (-)-enantiomer, WIN 55,212-3 (10 μM), which does not activate CB_1 or CB_2 receptors was applied. This also significantly inhibited the Ca^{2+} current, reducing it to 16.5 ± 2.7 $pA.pF^{-1}$ (43.1% inhibition, n = 5, $P < 0.05$). However, the

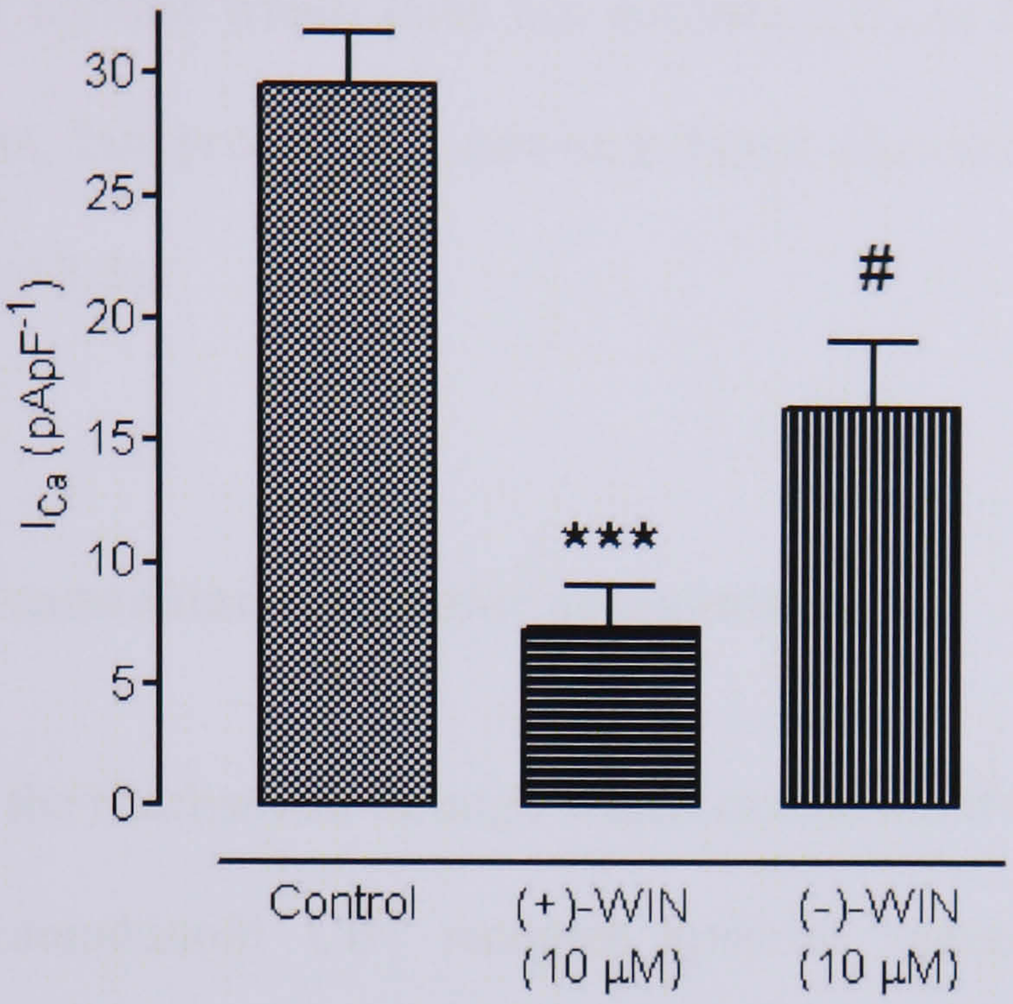

Figure 3.4 Stereoselectivity of the cannabinoid agonist WIN 55,212-2. The active enantiomer WIN 55,212-2 ((+)-WIN, 10 μM) significantly reduced (***, $P < 0.001$) mean current, evoked by depolarisation to 0 mV. WIN 55,212-3 ((-)-WIN, 10 μM), the inactive enantiomer, produced significantly less inhibition (#, $P < 0.05$) of mean current when compared with WIN 55,212-2. Each column represents the mean ± S.E.M. of at least 5 neurones.

degree of inhibition evoked by the (-)-enantiomer was significantly less than that evoked by WIN 55,212-2 ($P < 0.05$, unpaired t test).

This was confirmed by the observation that palmitoylethanolamide (PEA), a putative "CB_2-like" receptor agonist which does not activate CB_1 or CB_2 receptors, did not inhibit Ca^{2+} currents, but produced a non-significant increase in size of 4.8 ± 5.1 $pA.pF^{-1}$ (n = 3, figure 3.5).

3.3.2. Effects of cannabinoid receptor antagonists

To further examine the mechanism through which cannabinoid inhibition was evoked, the role of the cannabinoid CB_1 receptor specific antagonist SR141716 was investigated. When applied alone at a concentration of 1 μM a non-significant decrease in amplitude of the inward current elicited by a depolarising pulse to 0 mV was observed (current was reduced to 21.3 ± 1.7 $pA.pF^{-1}$, n = 6). At a concentration of 10 μM a significant decrease in amplitude to 13.6 ± 3.7 $pA.pF^{-1}$ was observed (n = 5, $P < 0.01$, figure 3.6a). In the combined presence of 1 μM CP 55,940 and 1 μM SR141716 the depolarising pulse elicited a current of 13.3 ± 3.5 $pA.pF^{-1}$ (n = 6). This current did not significantly differ from the current evoked by depolarisation in the presence of 1 μM CP 55,940 alone ($P > 0.05$, figure 3.6b). The combined presence of 1 μM CP 55,940 and 10 μM SR141716, when compared with 1 μM CP 55,940 alone, significantly reduced the amplitude of inward current from 14.0 ± 1.8 $pA.pF^{-1}$ to 3.0 ± 0.5 $pA.pF^{-1}$ (n = 4, $P < 0.05$, figure 3.6c).

AM 251, another CB_1 receptor specific antagonist that possesses a similar chemical structure to SR141716, at a concentration of 1 μM did not induce a significant inhibition of evoked current. A current of 30.1 ± 5.6 $pA.pF^{-1}$ (n = 7, $P > 0.05$) was

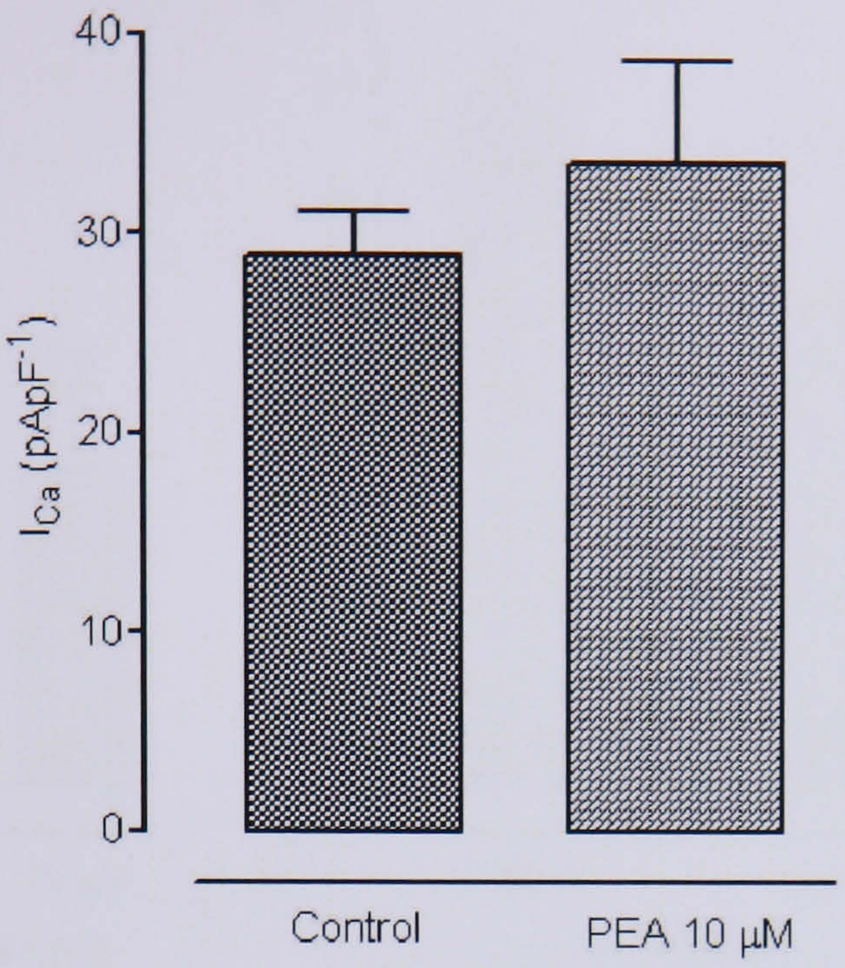

Figure 3.5 PEA does not inhibit current. PEA, a cannabinoid that has been shown not to act at CB_1 or CB_2 receptors, at a concentration of 10 μM did not inhibit current evoked by depolarisation to 0 mV. Each column represents the mean ± S.E.M. of at least 3 neurones.

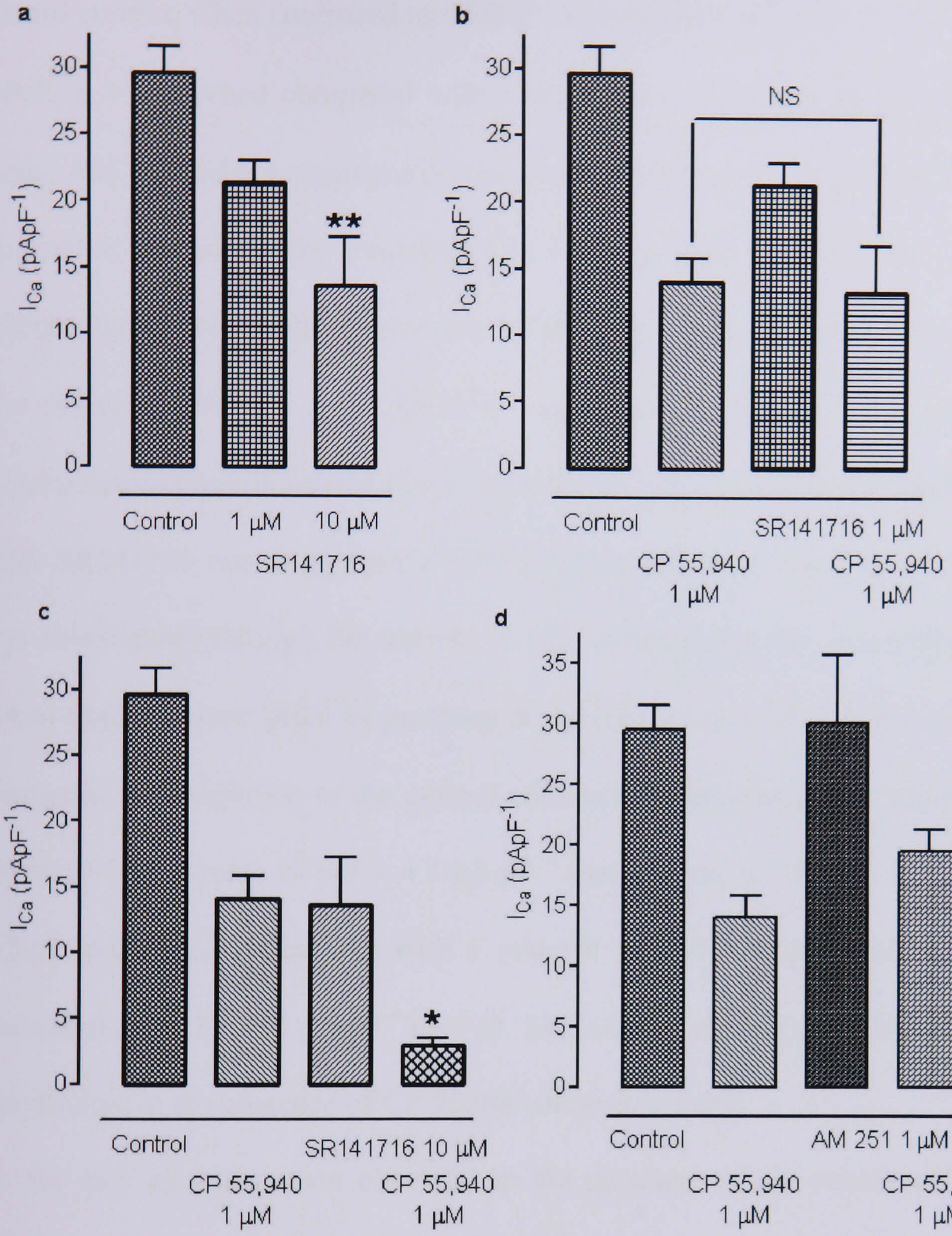

Figure 3.6 Modulation of cannabinoid agonist activity by the CB_1 receptor antagonists SR141716 and AM 251. (a) Myenteric neurones exposed prior to patching to SR141716 (10 μM) displayed a significant reduction in the amplitude of peak current evoked by a depolarising step to 0 mV (**, $P < 0.01$). 1 μM SR141716 did not significantly reduce amplitude. (b) In the presence of SR141716 (1 μM), the decrease in amplitude of peak current induced by CP 55,940 (1 μM) did not significant differ from that induced by CP 55,940 (1 μM) alone (NS, $P > 0.05$). (c) In the presence of SR141716 (10 μM), the decrease in amplitude of peak current induced by CP 55,940 (1 μM) was significant greater than that induced by CP 55,940 (1 μM) alone (*, $P < 0.05$). (d) AM 251 (1 μM) did not significantly change the amplitude of peak current when compared to control currents ($P > 0.05$). The reduction in amplitude induced by CP 55,940 (1 μM) was not significantly decreased in the presence of AM 251 (1 μM). Each column represents the mean ± S.E.M. of at least 4 neurones.

recorded. Combined application of 10 μM AM 251 and 1 μM CP 55,940 inhibited the inward current, when compared to control, reducing current to 19.6 ± 1.7 pA.pF^{-1} ($P <$ 0.001, n = 7). When compared with the inhibition produced by 1 μM CP 55,940 alone, AM 251 did not significantly reduce this inhibition ($P > 0.05$, figure 3.6d).

To further investigate the inhibition observed by SR141716, O-2050, a novel CB_1 receptor ligand that possesses putative 'silent antagonist' properties, was applied. At a concentration of 10 μM, O-2050 significantly reduced the amplitude of depolarisation-elicited current to 5.1 ± 1.4 pA.pF^{-1} ($P < 0.001$, n = 4, figure 3.7).

With SR141716 not antagonising CP 55,940 inhibition, a role for the CB_2 receptor was investigated through the use of the CB_2 receptor specific antagonist SR144528. When applied alone prior to patching at a concentration of 0.1 μM, no significant change in the amplitude of the current elicited by a depolarising pulse to 0 mV was observed (an increase of 0.3 ± 4.7 pA.pF^{-1} was present, n = 4, $P > 0.05$, figure 3.8). When applied in conjunction with 1 μM CP 55,940, the amplitude of the current decreased to 21.2 ± 1.2 pA.pF^{-1} (n = 5). This current did not significantly differ from that elicited in the presence of CP 55,940 alone ($P > 0.05$).

As the lack of antagonism observed in the presence of the selective CB_1 receptor antagonist and CB_2 receptor antagonists does not rule out the possible presence of either receptor, when expressed in conjunction with the other, the activity of CP 55,940 in the presence of both selective antagonists was investigated. Combined pre-treatment with both CB_1 and CB_2 receptor antagonists, SR141716 (1 μM) and SR144528 (0.1 μM) produced a non-significant reduction in the amplitude of depolarisation-elicited current, reducing size of current to 25.2 ± 3.3 pA.pF^{-1} (n = 7, $P > 0.05$, figure 3.9). When applied in combination with 1 μM CP 55,940, the amplitude of current evoked by depolarisation (24.9 ± 3.8 pA.pF^{-1}, n = 5) was significantly

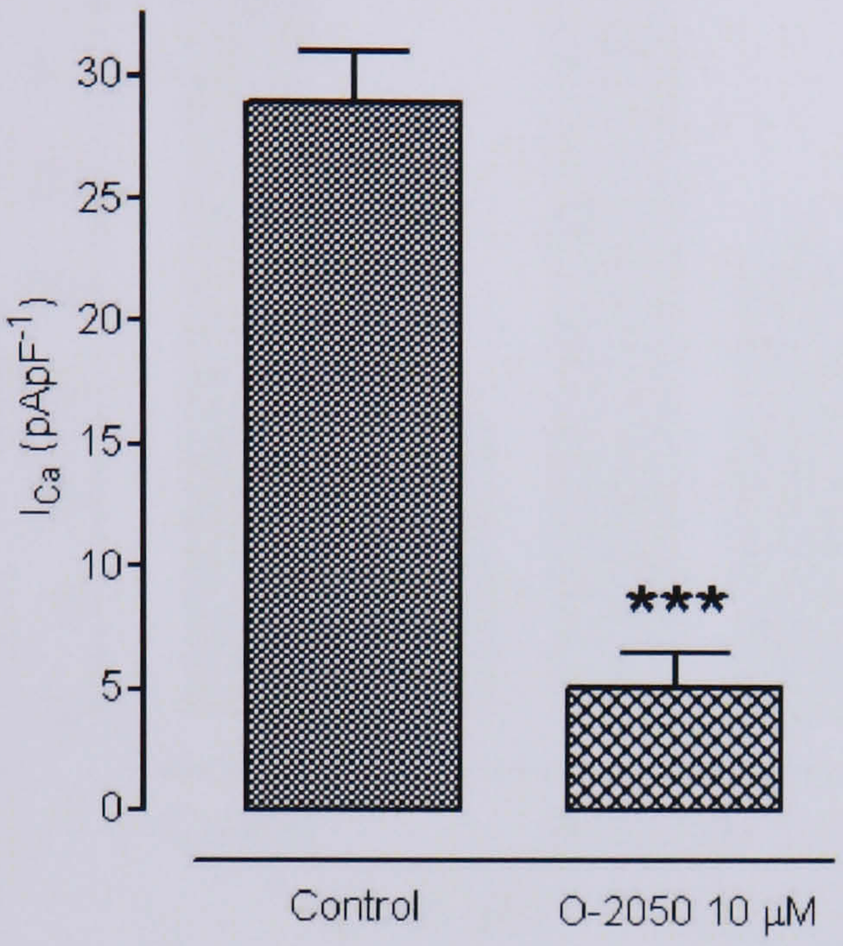

Figure 3.7 The 'silent' antagonist O-2050 inhibits current. O-2050 (10 μM) significantly reduced (***, $P < 0.001$) mean current, evoked by depolarisation to 0 mV. Each column represents the mean ± S.E.M. of at least 4 neurones.

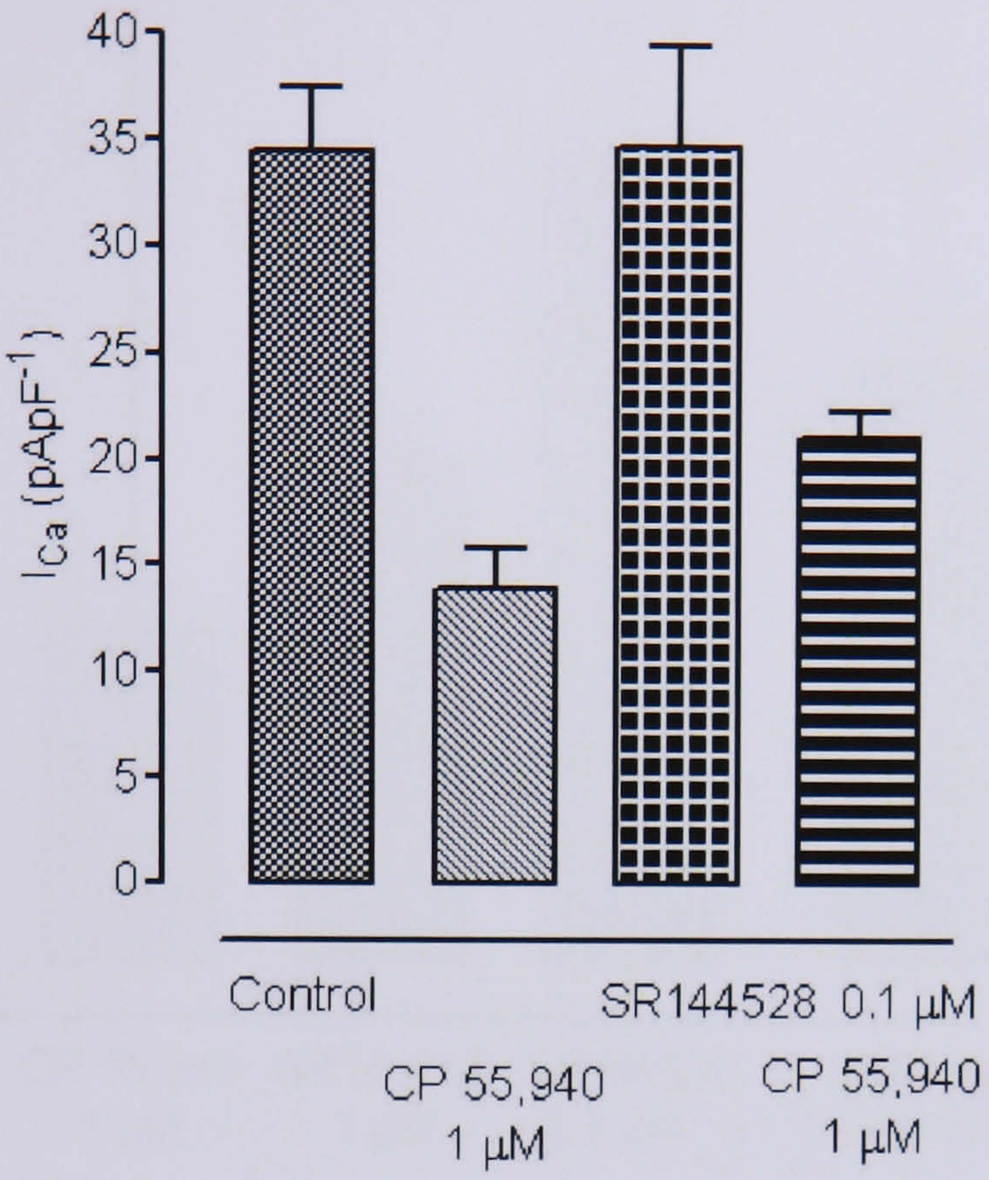

Figure 3.8 Modulation of CP 55,940 inhibition by the CB_2 receptor antagonist SR144528. Myenteric neurones exposed prior to patching to SR144528 (0.1 μM) did not significantly reduce the amplitude of peak current ($P > 0.05$). The amplitude of peak current evoked in the presence of CP 55,940 (1 μM) and SR144528 (0.1 μM) did not significantly differ from that evoked in the presence of CP 55,940 (1 μM) alone ($P > 0.05$). Each column represents mean ± S.E.M. of at least 5 neurones.

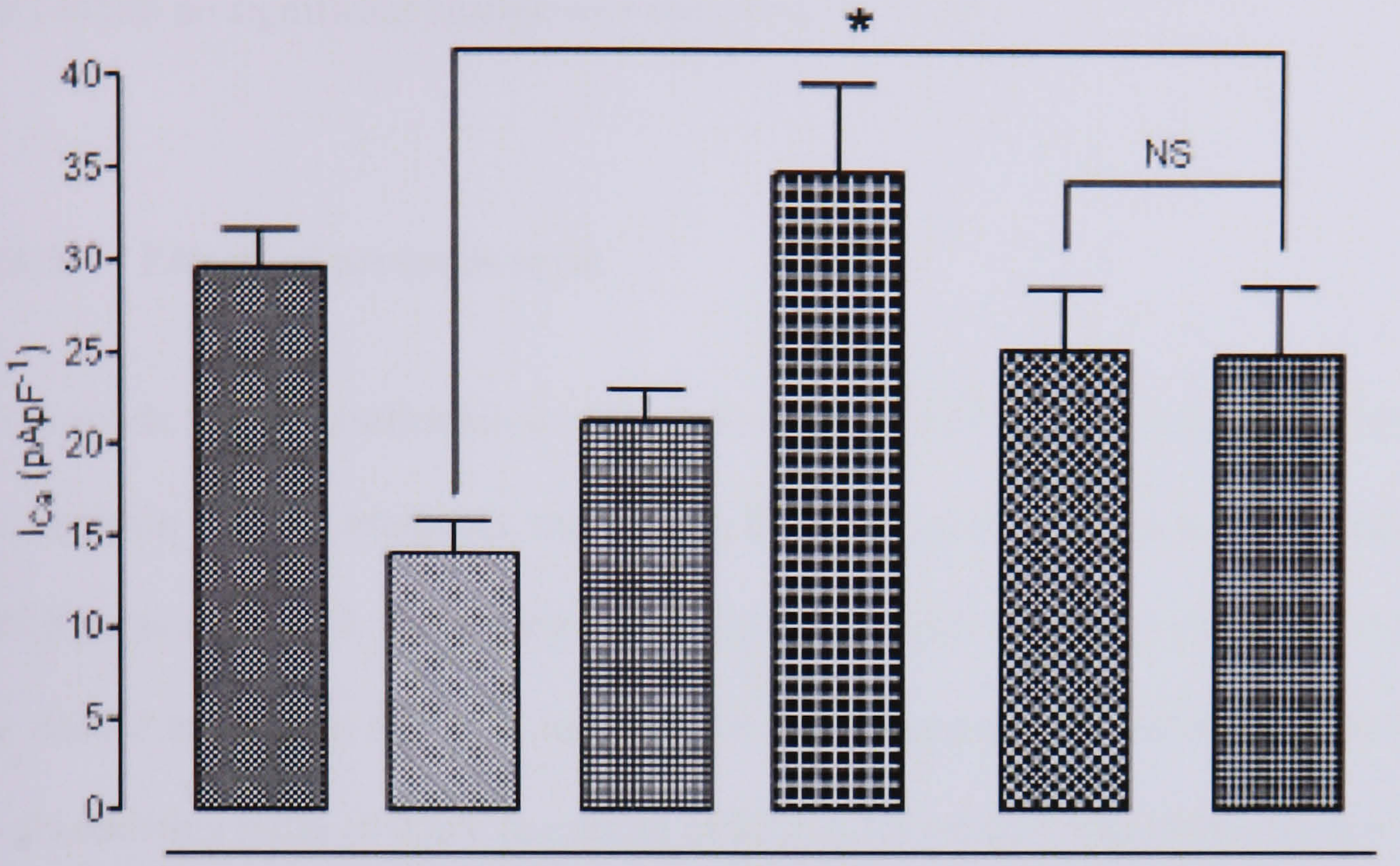

Figure 3.9 Modulation of CP 55,940 inhibition by the combined presence of the CB_1 receptor antagonist SR141716 and the CB_2 receptor antagonist SR144528. Exposure of myenteric neurones prior to patching to both SR141716 (1 μM) and SR144528 (0.1 μM) did not significantly reduce the amplitude of peak current ($P > 0.05$). The amplitude of peak current evoked in the presence of CP 55,940 (1 μM), SR141716 (1 μM) and SR144528 (0.1 μM) was significantly greater than that evoked in the presence of CP 55,940 alone (*, $P < 0.05$) and did not significantly differ from that evoked in the presence of the antagonists alone ($P > 0.05$). Each column represents mean ± S.E.M. of at least 5 neurones.

greater than that evoked in the presence of 1 μM CP 55,940 alone ($P < 0.05$). When compared with the amplitude of the current evoked in the presence of SR141716 and SR144528 no significant change was observed ($P > 0.05$).

3.3.3. Effects of pertussis toxin

To provide further confirmation of the role of CB_1 and CB_2 receptors, which are both $G_{i/o}$-protein coupled receptors, modulation by the $G_{i/o}$-protein inhibitor pertussis toxin (PTX) was examined. Incubation with PTX (100 ng/ml) for 18 hrs prior to patching, to ensure entry into the cell, induced no significant change in current elicited by a depolarising pulse to 0 mV (a current of 23.1 ± 3.6 $pA.pF^{-1}$ was observed, n = 7, $P > 0.05$, figure 3.10). PTX significantly reduced the degree of inhibition evoked by addition of 10 μM CP 55,940, increasing the amplitude of current evoked by a depolarising pulse from 5.9 ± 2.1 $pA.pF^{-1}$ to 19.0 ± 5.8 $pA.pF^{-1}$ (n = 5, $P < 0.05$). The blockade of CP 55,940 inhibition by PTX was further confirmed by the observation of a lack of significant difference between current evoked in the presence of PTX alone and that evoked in the presence of PTX and CP 55,940 ($P > 0.05$).

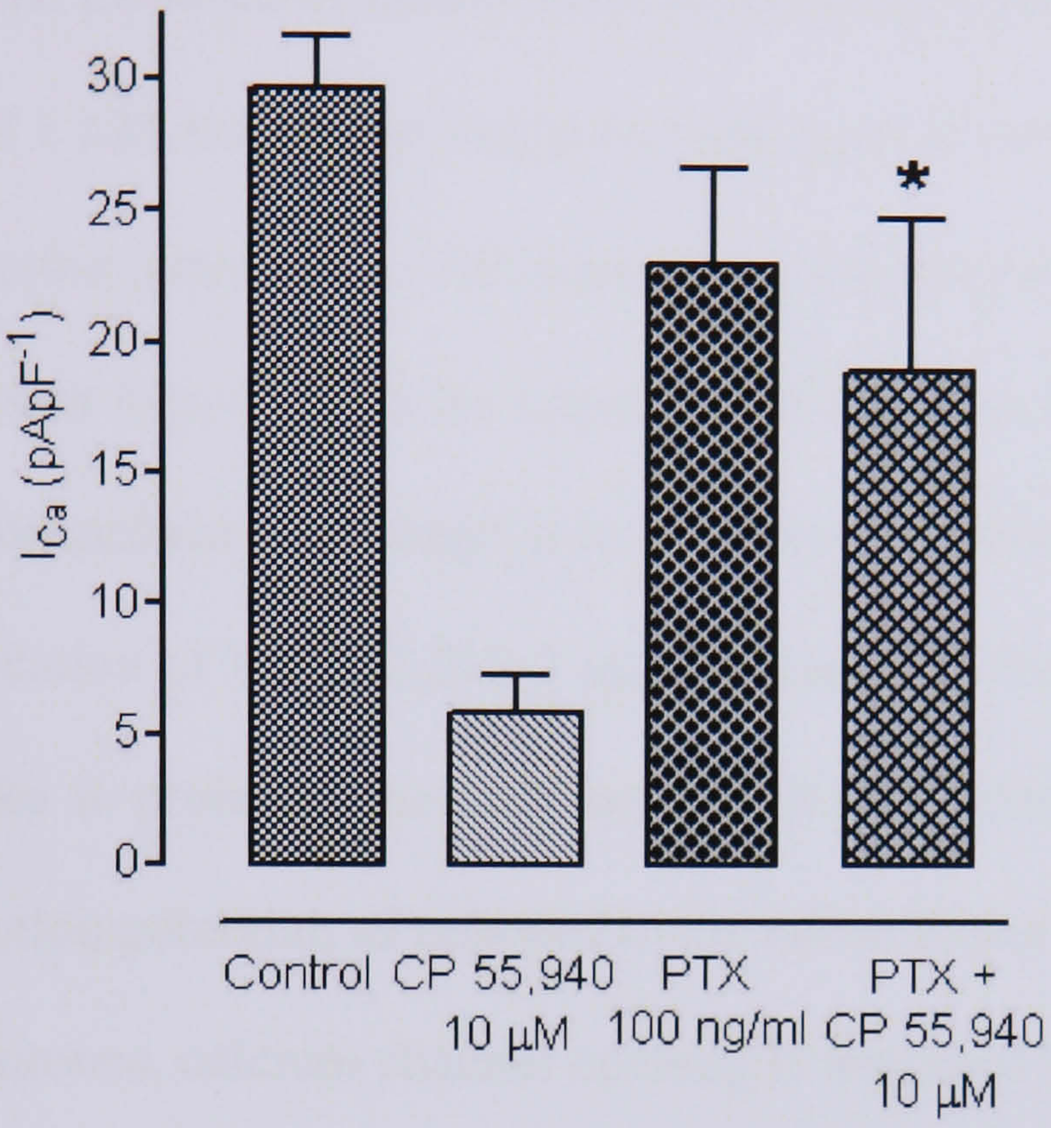

Figure 3.10 Blockade of CP 55,940 inhibition by pertussis toxin (PTX). Myenteric neurones incubated with the $G_{i/o}$-protein inhibitor PTX (100 ng/ml) for 18 hrs prior to patching induced a non-significant reduction in the amplitude of current elicited by a depolarising pulse to 0 mV ($P > 0.05$). PTX significantly reduced the degree of inhibition evoked by addition of 10 μM CP 55,940 (*, $P < 0.05$). Each column represents mean ± S.E.M. of at least 5 neurones.

3.4. Discussion and conclusion

The results from this investigation pose an intriguing story. The reduction of calcium entry coupled with the presence of inhibition in all neurones exposed to cannabinoids at a concentration of 1 μM and greater suggests cannabinoids can play a major role in the modulation of action potentials in AH neurones within the myenteric plexus. This is contrary to what was hypothesised by López-Redondo and colleagues (1997) who detected, through intracellular recordings, a lack of any alteration of action potentials in response to application of WIN 55,212-2 in AH neurones. The dissimilarity of the results of our studies is probably the consequence of our measurement of a single component of the action potential, as opposed to the entire action potential within AH neurones. In AH neurones, calcium channel opening is triggered by the depolarisation within an action potential. Action potential amplitude is mainly governed by sodium influx and potassium efflux, calcium entry produces a prominent 'shoulder' upon the repolarisation phase as well as extending the duration of the action potential. The modulation of action potentials by calcium does however markedly differ in shape and duration within the same neurone, and so Bornstein *et al.* (1994) recommend the measurement of the slow after-hyperpolarisation as a more robust measure of calcium entry. This slow after-hyperpolarisation, lasting at least 4 s, occurs in all AH neurones 50-70 ms after an action potential as a result of calcium-dependent potassium channel opening. By measuring solely changes in the action potential, and not examining the slow after-hyperpolarisation, it is possible that the change in calcium entry observed with application of cannabinoids may have been masked from López-Redondo *et al.* by the variability it possesses when measured as a component of the action potential.

The outward current at positive potentials greater than 50 mV in figure 3.3b has been observed by other laboratories (Baidan *et al.*, 1992). With the blockade of Na^+ and K^+ channels it probably results from the influx of Cl^- anions. Under conditions in this study, the Cl^- reversal potential (E_{Cl}) is approximately 0 mV, so by restricting data analysed to that evoked by a step to 0 mV, the passage of Cl^- anions should not induce a sizeable change in total current.

The high cannabinoid agonist concentrations required to produce inhibition in this study may be due to a reduced agonist efficacy often found with endogenous systems in cell cultures as a possible result of reduced receptor expression.

Modulation of calcium channel activity through the activation of TRPV1 channels is also unlikely to have occurred as the TRPV1 channel was reported by Zygmunt *et al.* (1999) to possess, on exposure to anandamide, pronounced outward rectification characteristics with a reversal potential of approximately 0 mV. If the TPRV1 channel were to be activated by the applied cannabinoids, then only a small influx of calcium would occur, which would not be expected to produce much, if any, change to the voltage dependent calcium influx.

The stereoselectivity indicated by the significantly reduced inhibition observed with application of WIN 55,212-3, the (-)-enantiomer of WIN 55,212-2 which has been shown not to activate CB_1 and CB_2 receptors (Savinainen *et al.*, 2005), strongly suggests the decrease in calcium entry on depolarisation is mediated by cannabinoid receptors. However, the inhibition that is evoked by WIN 55,212-3 may be the result of non-specific inhibition due to the high concentrations (10 μM) used. The lack of inhibition observed with palmitoylethanolamide suggest inhibition is not due to activation of a putative "CB_2-like" receptor.

Blockade by pertussis toxin implies that cannabinoids act via a $G_{i/o}$-protein mediated mechanism to inhibit calcium currents in myenteric neurones.

The inhibition of depolarisation induced calcium currents by the antagonist/inverse agonist SR141716 and the silent antagonist O-2050 when applied alone at a concentration of 10 μM is similar to that observed by López-Redondo *et al.* in which SR141716 reduced the amplitude of fast synaptic excitatory synaptic potentials in S type myenteric neurones. Pan *et al.* (1998) reported a SR141716 evoked increase in calcium current in transfected rat superior cervical ganglion neurones and major pelvic ganglion neurones with an EC_{50} of 32 nM. The most probable explanation for this observation is a loss of specificity at the high concentration used, but the lack of any inhibition evoked by AM 251, which possesses a very similar chemical structure to SR141716, does induce an element of doubt.

The complete reversal of CP 55,940 inhibition we observed in the presence of both the CB_1 and CB_2 antagonists, SR141716 and SR144528, coupled with the partial antagonism induced by SR144528 alone and the lack of antagonism displayed by SR141716 and another CB_1 receptor antagonist, AM 251, strongly suggest both the CB_1 and CB_2 receptors play a role in governing calcium influx in acutely disassociated myenteric AH neurones. This is contrary to the pharmacological and binding studies that found SR144528 to play no role in reducing cannabinoid inhibition of contraction or displacement of $[H^3]$-CP 55,940 in guinea-pig MPLM (Pertwee *et al.*, 1996; Ross *et al.*, 1998). One possible explanation for the presence of the CB_2 receptor may be derived from recent studies that detected a greater role for the CB_2 receptor in the rat intestinal tract upon exposure to LPS through the measurement of intestinal transit, immunohistochemistry and mRNA expression (Mathison *et al.*, 2004; Duncan *et al.*, 2005; 2006). An upregulation of the CB_2

receptor may have resulted from the damage induced by the enzymic and mechanical dissociation required in the production of these primary cultures.

The inhibition by both CB_1 and CB_2 receptor antagonists when applied in conjunction and not independently however does not rule out the possibility of the cannabinoid ligands acting at a non-CB_1, CB_2 $G_{i/o}$-protein coupled receptor, in which the two antagonists display low potency in the inhibition of response when applied independently, but act synergistically when applied together. One possible reason could be the presence of two binding sites, each of which activates the receptor to inhibit calcium currents, but one sensitive to only SR141716 and the other to only SR144528. Further conjecture would suggest that SR141716 might be acting as a weak partial agonist rather than an antagonist. Action through a novel receptor would explain the low potency of CP 55,940 and WIN 55,212-2, and the inhibition by WIN 55,212-3. *In vivo* and *in vitro* studies by Izzo *et al.* (2001) and Mang *et al.* (2001) have proposed the presence of non-CB_1 and CB_2 receptors in the ileum suggesting the existence of a non-CB_1, CB_2 $G_{i/o}$-protein coupled receptor may not be implausible (figure 3.11).

In summary cannabinoids play a prominent role in governing the electrical properties of myenteric AH neurones in the guinea-pig ileum. Data suggests this is mediated through the activation of $G_{\beta\gamma}$-protein subunits by either both CB_1 and CB_2 receptors or by a non-CB_1, CB_2 $G_{i/o}$-protein coupled receptor.

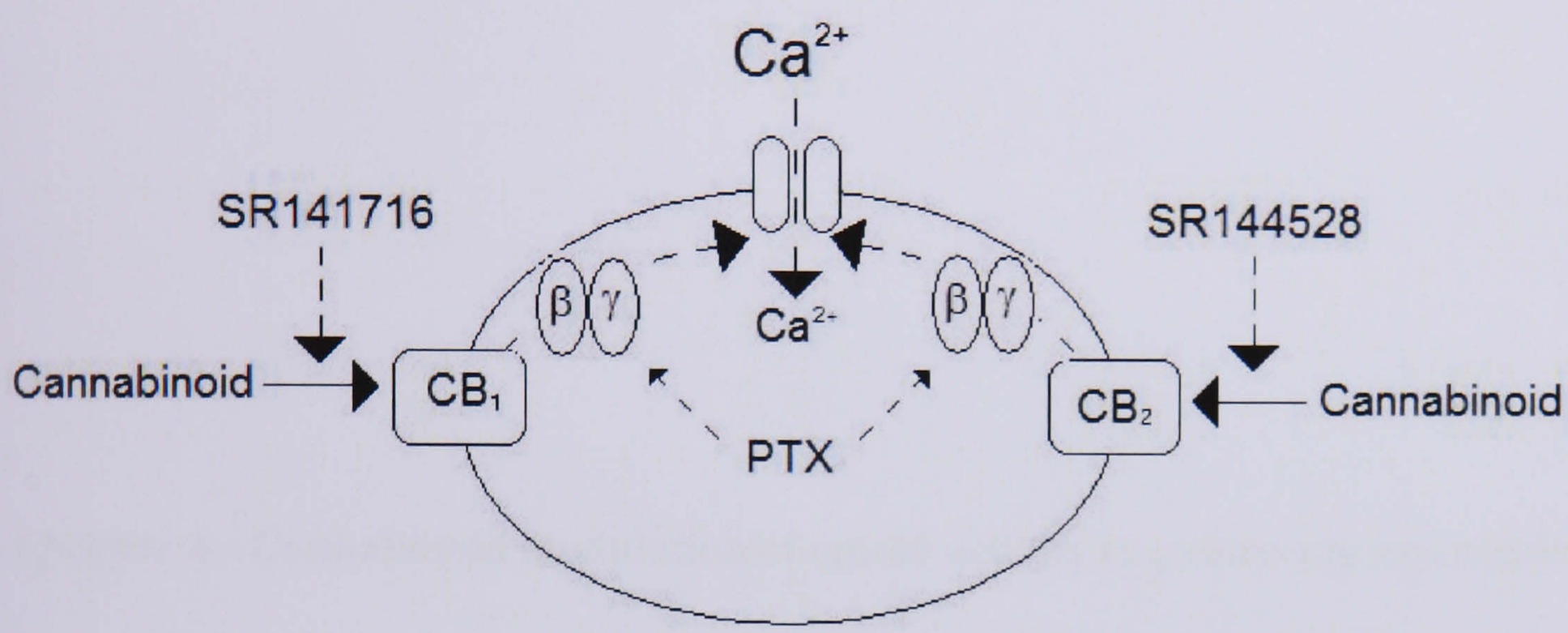

Figure 3.11 Hypothesised inhibition of calcium channels in guinea-pig myenteric neurones. Continuous lines represent activation of while segmented line represent inhibition of hypothesised pathways.

Chapter 4 - Cannabinoid modulation of opioid activity in guinea-pig myenteric neurones and NG108-15 neurones

4. Chapter 4 - Cannabinoid modulation of opioid activity in guinea-pig myenteric neurones and NG108-15 neurones

4.1 Introduction

4.1.1 Opioid ligands and receptors

The analgesic and euphoric properties of extracts of the opium poppy have been known for centuries, but it was not until the 20th century when an understanding of how opiates produced their powerful and selective effects on the body was established. Opioid interaction with a specific receptor was proposed in the 1950s with the observed structural and stereochemical requirements essential for activity. Evidence for multiple receptors arose in the 1960s and 1970s when Martin and colleagues demonstrated that a series of opioids displayed different profiles of pharmacological activity *in vivo* (Martin, 1979). They proposed the existence of three different types of receptor μ, κ and σ. With the discovery of the endogenous opioid ligands [Met]- and [Leu]-enkephalin (Hughes *et al.*, 1975), the existence of a fourth receptor, δ, was proposed with the observation of a pattern of agonist activity which differed to that possessed by the opium derived ligands (Lord *et al.*, 1977). In the 1990s, MOR-1, DOR-1, and KOR-1 genes, encoding the μ-, δ- and κ- receptors respectively, were cloned and the 'orphan' receptor, ORL_1, identified on the basis of high homology (>60%) with the classical opioid receptors (for review see Henderson and McKnight, 1997). The σ-receptor ceased to be classified as an opioid receptor as it does not display similar responses to opioid antagonists nor the stereoselective characteristic of other opioid receptors. The existence of subtypes of μ-, δ- and κ- and ORL_1-receptors

has been proposed largely on the basis of radioligand binding studies. Little evidence for different genes encoding these subtypes has been published but in some cases receptor heterodimerisation and splice variants have been proposed as possible explanations. All four opioid receptors are thought to form homomeric and hetromeric complexes, not only with other opioid receptors, but also nonopioid receptors (for example, μ and α_{2A}-adrenoceptors; for review see Devi, 2001; Milligan, 2004).

4.1.2 Endogenous opioids

Hughes and colleagues (1979) identified the first endogenous opioids, the pentapeptide enkephalins, from pig brain. Soon after this discovery, it was noted that a fragment of the pituitary hormone β-lipotropin contained the sequence of [Met]-enkephalin at its amino-terminus. This 31 amino acid fragment was shown to be a potent opioid agonist and was subsequently called β-endorphin. Three more families of opioid peptides, proenkephalin, pro-opiomelanocortin and prodynorphin, were rapidly discovered, all containing the sequence of either [Met]-enkephalin or [Leu]-enkephalin as the first five amino acids. All possessed no affinity for ORL_1-receptors (Corbett *et al.*, 1993). An endogenous ligand specific for the ORL_1-receptor, nociceptin/orphanin-FQ, was discovered in 1973 (for review see Henderson and McKnight, 1997), whilst the endomorphins, which possess high affinity and selectivity for the μ-receptor but bare little semblance to the enkephalins, were discovered by Zadina *et al.* (1997).

4.1.3 Intracellular signalling of opioid receptors

All opioid receptors mediate many of their cellular effects via activation of the PTX sensitive $G_{i/o}$-proteins. The μ-, δ- and κ- receptors have been shown to interact with the pertussis toxin-insensitive G_z and G_{16}-proteins (Connor and Christie, 1999). The most common second messenger pathways activated include inhibition of adenylyl cyclase, activation of a potassium conductance, inhibition of calcium conductance, and an inhibition of transmitter release. More recent observations have extended the actions of opioids to include the activation of protein kinase C (PKC), the release of calcium from extracellular stores, the activation of the mitogen-activated protein kinase (MAPK) cascade (for review see Williams *et al.*, 2001).

Two effects have been associated with the inhibition of adenylyl cyclase by opioids. A modulation of a voltage-dependent nonselective cation current, which is activated at hyperpolarised potentials to cause an inward current that depolarizes the membrane potential, has been identified. As voltage dependence of this current is regulated by cAMP, the decrease in intracellular cAMP by opioid receptor activation shifts the voltage dependence to more negative potentials (Ingram and Williams, 1994). The second consequence of the inhibition of adenylyl cyclase was an inhibition of transmitter release that was dependent on the activation of cAMP-dependent protein kinase (PKA) (for review see Williams *et al.*, 2001).

Opioids have been shown to activate at least three separate potassium conductances including the G protein-activated inwardly rectifying conductance (GIRK), which is activated by $G_{\beta\gamma}$-subunits (Jan and Jan, 1997). Activation of a voltage-dependent potassium conductance, suggested on the basis of the blockade of opioid inhibition of transmitter release and activation of the BK calcium sensitive potassium conductance,

which has been associated with the release of Ca^{2+} from internal stores, has been observed (for review see Williams *et al.*, 2001).

The inhibition of calcium currents by activation of all opioid receptor subtypes has been observed in many studies (for review see Williams *et al.*, 2001). Inhibition possessed similar properties to other $G_{i/o}$-protein coupled receptors, acting through the βγ-subunit which directly couples to the calcium channel (see section 1.6.3).

Inhibition of neurotransmitter release has been observed at numerous sites both in the CNS and periphery. Inhibition is thought to be mediated through mainly increased potassium conductance and inhibition of voltage-activated calcium currents. However, inhibition of adenylyl cyclase has been shown to be responsible for some of the decrease in transmitter release, whilst direct inhibition of the release machinery, independent of potassium and calcium conductances, has also been reported (Capogna *et al.*, 1993; for review see Williams *et al.*, 2001).

4.1.4 Opioids and cannabinoids

Although cannabinoids and opioids possess very dissimilar structures, both share similar pharmacological profiles, inducing analgesia, catalepsy, hypothermia, motor depression, hypotension, immunosuppression, sedation and reward effects (Manzanares *et al.*, 1999; Massi *et al.*, 2001; Varvel *et al.*, 2004). Both cannabinoid and opioid receptors are coupled to $G_{i/o}$-proteins and activate similar intracellular signalling pathways. Within the central nervous system a similar distribution of CB_1 and μ- receptors in the dorsal horn of the spinal cord has been reported (Hohmann *et al.*, 1999; Salio *et al.*, 2001), while areas such as the caudate putamen, dorsal hippocampus, and substantia nigra express high levels of both cannabinoid and opioid

receptors (Mansour *et al.*, 1988; Herkenham *et al.*, 1991; Mailleux and Vanderhaeghen, 1992; Rodriguez *et al.*, 2001).

An interaction between cannabinoids and opioids have been observed in studies examining antinociceptive properties. A synergistic interaction between cannabinoid and opioid agonists has been reported in various models of acute pain (for review see Cichewicz, 2004). A growing body of literature attests to the interaction between opioids and cannabinoids with respect to reward processes. Self-administration studies have provided the most direct evidence for interaction in addiction, for example SR141716 reduced self-administration of heroin in rats and mice (Chaperon *et al.*, 1998; Braida *et al.*, 2001; Mas-Nieto *et al.*, 2001; Navarro *et al.*, 2001; De Vries *et al.*, 2003) whilst the opioid antagonists naloxone and naltrexone reduced self-administration of Δ^9-THC in squirrel monkeys (Tanda *et al.*, 2000; Justinova *et al.*, 2003; 2004; for review see Tanda and Goldberg, 2003). Results from CB_1 receptor knock-out mice suggest interactions between reward pathways do exist. Ledent *et al.* (1999) reported CB_1 receptor knock-out mice do not appear to self-administer morphine. However, contradictory results in different lines of CB_1 receptor knock-out mice suggest that different compensative adaptations to the lack of CB_1 receptors occurred in the different lines (for reviews see Viganò *et al.*, 2005; Tanda and Goldberg, 2003).

4.1.5 Opioids in myenteric plexus

The first observation of a specific opioid effect in vitro was made in the guinea pig ileum by Trendelenburg (1917) who showed that morphine inhibited the peristaltic reflex. Both the preparatory phase, comprising a contraction of the longitudinal

muscle, and the emptying phase, comprising contractions of the circular muscle, were shown to be inhibited by opioids (Kosterlitz and Robinson, 1957). Inhibition was shown to be due to an action upon neurones, rather than directly on the muscle layers themselves as contractions evoked by acetylcholine acting at muscarinic receptors on the muscle was not affected by morphine (Kosterlitz and Robinson, 1958), whereas cholinergic contractions evoked indirectly by nicotine (Kosterlitz and Robinson, 1958; Gaddum and Picarelli, 1957; Schaumann, 1955), 5-HT (Kosterlitz and Robinson, 1958; Gaddum and Picarelli, 1957), and neurotensin (Huidobro-Toro *et al.*, 1984) were inhibited.

Immunohistochemical studies have reported the presence of μ-, δ- and κ-receptors in enteric neurones of rat, guinea-pig and porcine gastrointestinal tract. In the rat, μ- and κ-receptors have been localised to myenteric and submucosal neurones, fibres distributed in the muscle layer, mucosa, blood vessels and lymphatic nodes, and to putative interstitial cells of Cajal (ICC) in the myenteric plexus and deep muscular plexus (Bagnol *et al.*, 1997). In contrast, μ-receptor immunoreactivity in the guinea-pig distal ileum has been localised predominantly to myenteric neurones and dense neuropil in the muscle layer and deep muscular plexus (Sternini *et al.*, 1995; 1996; Ho *et al.*, 2003). δ-receptors have been located in both myenteric and submucosal plexuses where it is predominantly found in varicose fibres in the plexuses, muscle and mucosa (Sternini *et al.*, 2004). κ-receptor immunoreactivity appears to be confined to the myenteric plexus and to bundles of fibres in the muscle (Sternini *et al.*, 2004). In porcine ileum, δ-receptors have been localised to both submucosal and myenteric neurones and to fibres in the muscle and mucosa, whereas κ-receptors are found only in the myenteric plexus (Poonyachoti *et al.*, 2002).

Inhibition by opioids of electrically evoked contractions of myenteric plexus-longitudinal muscle segments was demonstrated to be due to depression of the release of acetylcholine from the myenteric plexus (Paton, 1957; Schaumann, 1957; Cox and Weinstock, 1966; Paton and Zar, 1968; Szerb, 1982; Vizi *et al.*, 1984). Opioids have also been shown to decrease the release of acetylcholine evoked by agents that elicit action potentials in myenteric neurones, such as substance P (Vizi and Bartho, 1985; Yau *et al.*, 1986), PGE_1 (Jaques, 1969; Yagasaki *et al.*, 1981), neurotensin (Yau *et al.*, 1983a), and caerulein (Yau *et al.*, 1983b). The release of and contractions mediated by Substance P, which is released from myenteric neurones by high frequency electrical stimulus (Franco *et al.*, 1979), has been shown to be depressed by opioids (Holzer, 1984; Gintzler and Scalisi, 1982; Bartho *et al.*, 1982).

In acutely isolated longitudinal-muscle myenteric-plexus preparations from the guinea-pig intestine, opioids have been shown to inhibit action-potential firing of myenteric neurones through the use of extracellular recording techniques (Ehrenpreis *et al.*, 1976; North and Williams, 1977; Karras and North, 1981). The use of receptor selective agonists suggested that single neurones from guinea-pig ileum myenteric plexus coexpressed both μ- and δ-receptors and that activation of either receptor inhibited neuronal firing (Egan and North, 1981). Intracellular recording demonstrated, through the use of selective agonists, that μ-receptors were present on both S- and AH-type neurones and that morphine induced activation of a potassium channel mainly through an action on μ-receptors (Galligan and North, 1991; North and Tonini, 1977). Application of opioids by iontophoresis was shown to induce potassium channel activation when applied to the surface of the ganglion and not soma, suggesting opioid receptors are not expressed on the soma (North *et al.*, 1979). Intriguingly, intracellular recordings from AH-neurones have suggested μ- and κ-

opioid receptors play different roles in governing inhibition. μ-receptors have been shown to prolong the calcium-dependent after-hyperpolarisation without altering peak amplitude, whilst, in contrast, κ-receptor receptor activation reduces the duration of calcium spikes through inhibition of N-type neurones (Cherubini and North, 1985; Kojima *et al.*, 1994). A reduced calcium entry would be expected to reduce activation of the calcium-dependent potassium channels which after-hyperpolarisation is dependent on. However, an inhibition of calcium entry would also be expected to reduce the calcium-dependent transmitter release, suggesting multiple mechanisms are involved in the inhibition of transmitter release by opioids.

4.1.6 Opioids and cannabinoids in myenteric plexus

Few studies have been performed examining the interaction between acute administration of cannabinoids and opioids in the ileum. Coutts and Pertwee (1997) reported, with a supermaximal dose of WIN 55,212-2 (1.2 μM), a 35.6% inhibition of maximal electrically evoked acetylcholine release. Additional application of normorphine (400 nM), which expresses greater affinity for μ-receptors than other opioid receptors, decreased release to 65.6% of maximal release (Coutts and Pertwee, 1997).

Withdrawal contraction, resulting from the antagonism of chronic opioid receptor stimulus, has been shown to be inhibited by cannabinoids. Hine *et al.* (1975) showed inhibition by Δ^9-THC, but not cannabidiol, of the naloxone induced heightened gastric activity in morphine dependent rats. Frederickson *et al.* (1976) demonstrated 100 nM Δ^9-THC induced a stereospecific, 100 fold inhibitory shift in naloxone induced withdrawal contracture in the MPLM preparation derived from guinea-pigs treated *in*

vivo 25 hours before with morphine. More recent work found 50 nM WIN 55,212-2 completely blocked withdrawal contracture induced by 10 μM naloxone in guinea-pig MPLM exposed for 5 hours to 100 nM morphine (Basilico *et al.*, 1999), suggesting the existence of some form of interaction. Cross-tolerance between morphine and WIN 55,212-2 was also reported. A 5 hour incubation with either morphine or WIN 55,212-2 reduced the inhibitory effects of the other drug (Basilico *et al.*, 1999).

4.1.7 The NG108-15 neuronal cell line

The NG108-15 neuronal cell line is a hybrid cell line derived from the fusion of mouse neuroblastoma N18TG-2 and rat glioma C6BU-1 (Klee and Nirenberg, 1974). These cells display a wide range of membrane currents (for review see Hamprecht, 1977) including TTX-sensitive sodium currents (Bodewei *et al.*, 1985) and M-type potassium currents (Brown and Higashida, 1988). The low voltage activated T-type and Q-type calcium currents, and the high voltage activated (HVA) L-type current have been reported to be present in undifferentiated cells whilst the HVA N-type calcium current has been reported after differentiation (Lukyanetz, 1998).

4.1.8 Opioids and cannabinoids in the NG108-15 neuronal cell line

Expression of opioid receptors in this cell line was first observed by Klee and Nirenberg (1974) in binding assays, with sole expression of the δ-subtype established pharmacologically by Chang *et al.* (1978). Opioid inhibition of HVA calcium currents in NG108-15 cells was first reported by Tsunoo *et al.* (1986) through the use of the

whole-cell patch clamp technique and shown to be $G_{i/o}$-protein mediated (McFadzean and Docherty, 1989).

The presence of a cannabinoid receptor in NG108-15 cells was demonstrated by Δ^9-THC and da-*l*-nan inhibition of cAMP accumulation through a PTX sensitive mechanism (Devane *et al.*, 1986, Law *et al.*, 1982, Howlett *et al.*, 1986). Using the whole-cell patch clamp technique, Mackie and Hille (1992) reported inhibition of N-type voltage-gated calcium channels by WIN 55,212-2 and CP 55,940. Inhibition was shown to be blocked by prior treatment with pertussis toxin, and no inhibition was observed with exposure to the inactive enantiomer WIN 55,212-3 (Mackie and Hille, 1992; Caulfield and Brown, 1992). Sugiura *et al.* (1997) demonstrated an inhibition of the rise in intracellular calcium caused by voltage-activated calcium channel opening with the use of fura-2 imaging in differentiated NG108-15 cells through a SR141716 sensitive mechanism.

Interaction of cannabinoid and opioid agonists have been reported in both the NG108-15 cell line and the parental N18TG-2 cell line. Long-term exposure has been reported to induce desensitization of the ability of alternative agonists to inhibit cAMP production in N18TG-2 and NG108-15 cells (Dill and Howlett, 1988; Law *et al.*, 1982, Di Toro *et al.*, 1998), and reduce receptor binding and increase mRNA production in NG108-15 cells (Di Toro *et al.*, 1998). The modulation of opioid receptor properties, induced by long-term exposure to Δ^9-THC were both SR141716 and PTX sensitive suggesting CB_1 receptor modulation. In N18TG-2 cells, Shapira *et al.* (1998, 2000) demonstrated, through the use of [^{35}S]GTPγS binding, that interaction between the opioid agonist etorphine and the cannabinoid agonist desacetyl-levonantradol (DALN) was solely additive, suggesting responses were evoked through independent mechanisms. Partial ablation of the G-protein reservoir

with a low concentration of PTX did not modify this additive interaction, indicating that opioid and cannabinoid receptors activated different pools of G-proteins in these cells, comprising of either different subtypes of $G_{i/o}$-proteins or the same protein compartmentalized in separate segments within the cell (Shapira *et al.*, 1998). In contrast, COS cells transfected with opioid and cannabinoid receptors showed inhibitory interaction with maximal inhibition of [^{35}S]GTPγS binding by one receptor type blocking inhibition evoked by the other receptor type (Shapira *et al.*, 2000).

4.2 Methods

4.2.1 Guinea-pig ileum myenteric plexus-longitudinal muscle preparation (MPLM)

Methods for preparation of the MPLM preparation are detailed in Section 2.3.1.1. Briefly, Heston-2 guinea-pigs (300-500 g) of either sex were killed by cervical dislocation and strips of myenteric plexus-longitudinal muscle derived from segments of small intestine were prepared using the method of Paton and Zar (1968). Tissues were immersed in Krebs solution, maintained at 37°C and supplied with 95% O_2 and 5% CO_2.

4.2.2 Disassociated myenteric neurone patch-clamp preparation

Methods for disassociation of myenteric neurones are detailed in Section 2.3.2.1. Briefly, sections of myenteric plexus-longitudinal muscle were first digested in HBSS containing 0.01 ml/ml papain. This was followed by tituration whilst digesting in 1 mg/ml collagenase Type 1 and 3.1 mg/ml dispase. Cells were incubated in Dulbecco's modified Eagle's medium (DMEM) supplemented with 5% FBS, 1 mM L-glutamine, 8.3 mM glucose, 5 μM cytosine β-D-arabinofuranoside hydrochloride, 50 μM (+)-5-fluorodeoxyuridine, 2.5 μM uridine, 150 units/ml penicillin and 150 μg/ml streptomycin, plated on to collage-coated glass slides and incubated at 37°C in an atmosphere of 95% CO_2 and 5% O_2.

4.2.3 NG108-15 patch-clamp preparation

4.2.3.1 Cell culture

The NG108-15 cell line was a gift from Professor Graeme Henderson from the University of Bristol. Cell monolayers were cultured continuously in 25 cm^3 vented tissue culture flasks at 37°C in growth media consisting of Dulbecco's Modified Eagle's Medium (DMEM), supplemented with 10% foetal calf serum, hypoxanthine (0.1 mM), aminopterin (0.4 μM), thymidine (160 μM), penicillin (50 μg/ml), streptomycin (50 μg/ml) and L-glutamine (2 mM) in 95% CO_2 and 5% O_2. Every three days, upon reaching confluency, cells were harvested by means of a plastic scraper and transferred to a 15 ml Falcon tube. Cells were pelleted by means of centrifugation and resuspended in 5 ml fresh growth media. A 1:5 dilution was made by transferring 1 ml of this solution into a fresh 25 cm^3 culture flask and adding 4 ml fresh growth media. Vials of cells (passage 20) in DMSO were kept frozen in liquid nitrogen until required. New batches of cells were grown when passage number reached over 30 as expression of calcium channels diminished.

To induce differentiation for patch clamping, cells were plated onto glass cover slips in 9.6 cm^3 6-well plates, resuspended in differentiation media, consisting of growth media with the addition of prostaglandin E_1 (10 μM) and isobutyl-1-methylxanthine (50 μM), and incubated for three days at 37°C in 95% CO_2/5% O_2. All culture media and supplements were obtained form Gibco, UK with the exception of isobutyl-1-methylxanthine, which was obtained from SigmaAldrich, UK.

4.2.3.2 NG108-15 neurone patch-clamp preparation

Techniques similar to those detailed in Section 2.4.3 were applied to obtain gigaseal and patch formation.

4.2.3.3 Patch clamp techniques: current clamp

To observe changes in membrane potential a fixed current, determined by the current required to maintain a holding potential of -70 mV, was passed into the cell to account for leakage via the patch.

4.2.3.4 Patch clamp techniques: voltage clamp

Voltage clamp and recording of calcium currents were performed using similar techniques detailed in section 3.4.1. In recording of G-protein activated inward rectifier potassium currents, changes in current characteristics were examined prior to and post ligand application in response to a 100 ms step in membrane potential to voltages ranging from -120 mV to -50 mV. After each step, membrane potential returned to holding potential and positive/negative (P/N) leak subtraction was performed. Voltages were increased cumulatively in 10 mV increments. Recording was performed in both extracellular solution and 50 mM potassium extracellular solution (detailed in section 4.3.5).

4.2.4 Analysis of data

Electrical stimulus: Each value is expressed as the mean ± standard error of mean (S.E.M.) of experiments on tissues obtained from at least three individual animals. The effects of cannabinoid receptor ligands are expressed as percentage inhibition of contraction. This was calculated by comparing the amplitude of the electrically evoked contraction immediately prior to adding any compound to the amplitude of the contraction at the maximal effect of the compound.

GraphPAD Prism 4 statistical software (GraphPAD Software Inc, San Diego, CA., U.S.A.) was used to fit the concentration–response results to a sigmoidal function and generate 95% confidence intervals using the equation:

$$I = \frac{I_{max}}{1 + 10^{(\log_{[illegible]} - \log_{drug}) \times \text{Hill slope}}},$$

Significant difference between mean values were calculated using Student's unpaired *t*-test, a *P* value of < 0.05 being taken as significant. Mean values of multiple data sets were compared using either one way or two way-ANOVA followed by either Dunnetts or Newman-Keuls multiple comparison *post hoc* tests. Comparison of fitted concentration-response curves was performed using the *f*-test.

4.2.5 Drugs

Morphine and carbachol were obtained from SigmaAldrich, UK. Other drugs used are detailed in previous chapters.

4.2.6 Solutions

Krebs, extracellular and intracellular solutions have been detailed in section 2.4.4. 50 mM potassium extracellular solution comprised of (mM): NaCl 81, KCl 50, $MgCl_2$ 2.5, NaH_2PO_4 1.2, Hepes 10, glucose 11, sucrose 67, $CaCl_2$ 1.2; pH 7.35.

4.3 Results

4.3.1 Effects of morphine on electrically evoked contractions of the myenteric plexus-longitudinal muscle preparation

Supermaximal electrical stimulus of the MPLM preparation at a frequency of 0.1 Hz evoked a contraction of 0.44 ± 0.03 g (n = 53). The opioid receptor agonist morphine inhibited electrically evoked contractions in a concentration-dependent manner (EC_{50} = 17 nM, 95% confidence limits of 16 and 18 nM, n = 9, figure 4.1). 1 μM morphine evoked maximal inhibition, reducing contraction by 40.0 ± 5.8% (n = 9) of untreated contraction. Inhibition developed rapidly and remained for the duration of the experiment. Inhibition was reversed by washing with Krebs.

4.3.2 Interaction of cannabinoids with morphine inhibition of electrically evoked contractions in the myenteric plexus-longitudinal muscle preparation

To investigate the possibility of interaction between opioid and cannabinoid inhibitory mechanisms, concentration-response curves for morphine inhibition of electrically-evoked contraction of the guinea-pig MPLM, in the presence of varying levels of CP 55,940, were examined.

CP 55,940 (0.1 nM) administered alone did not reduce the size of electrically evoked contraction (n = 3, figure 4.2). In the presence of 0.1 nM CP 55,940, the morphine concentration-response curve did not differ from that evoked in the absence of CP

a

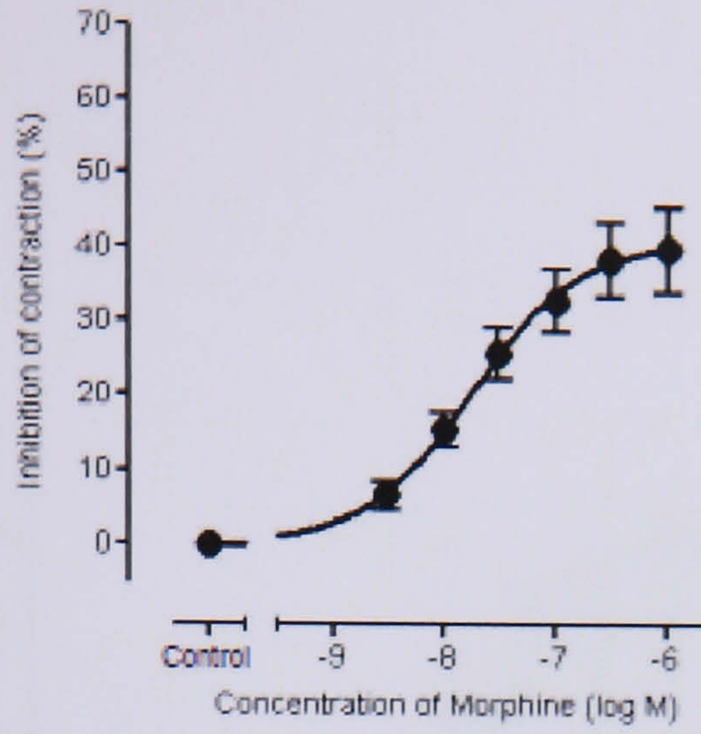

b

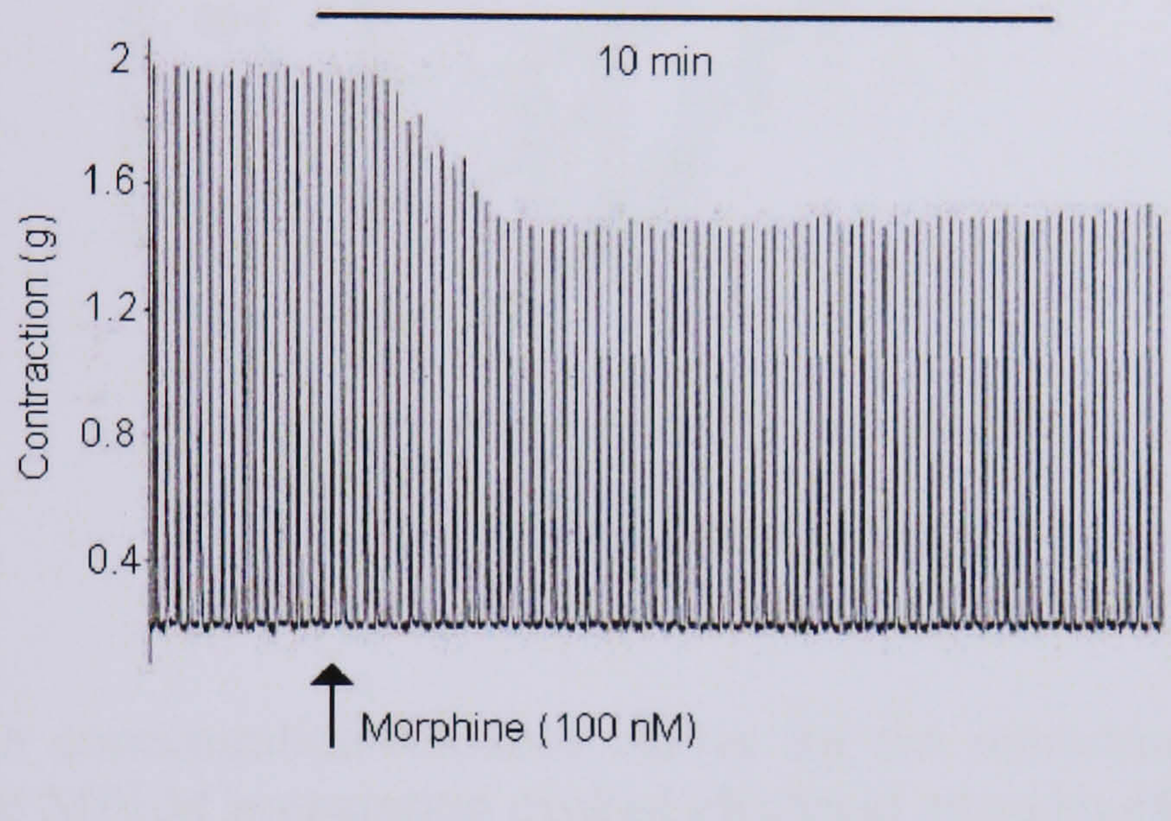

Figure 4.1 (a) Mean concentration-response curves for the inhibition by morphine of contraction of the MPLM preparation evoked electrical stimulus (●). Data is expressed as a percentage of contraction evoked in the absence of morphine. Preparations were exposed for five minutes to ascending concentrations of morphine. Each symbol represents the mean amplitude of peak contraction expressed as a percentage of the amplitude of peak contraction derived prior to application of morphine. Each symbol comprises of at least nine different MPLM preparations. Vertical lines indicate S.E.M. (b) Sample trace demonstrating inhibition of electrically evoked contraction by morphine (100 nM) in the MPLM preparation.

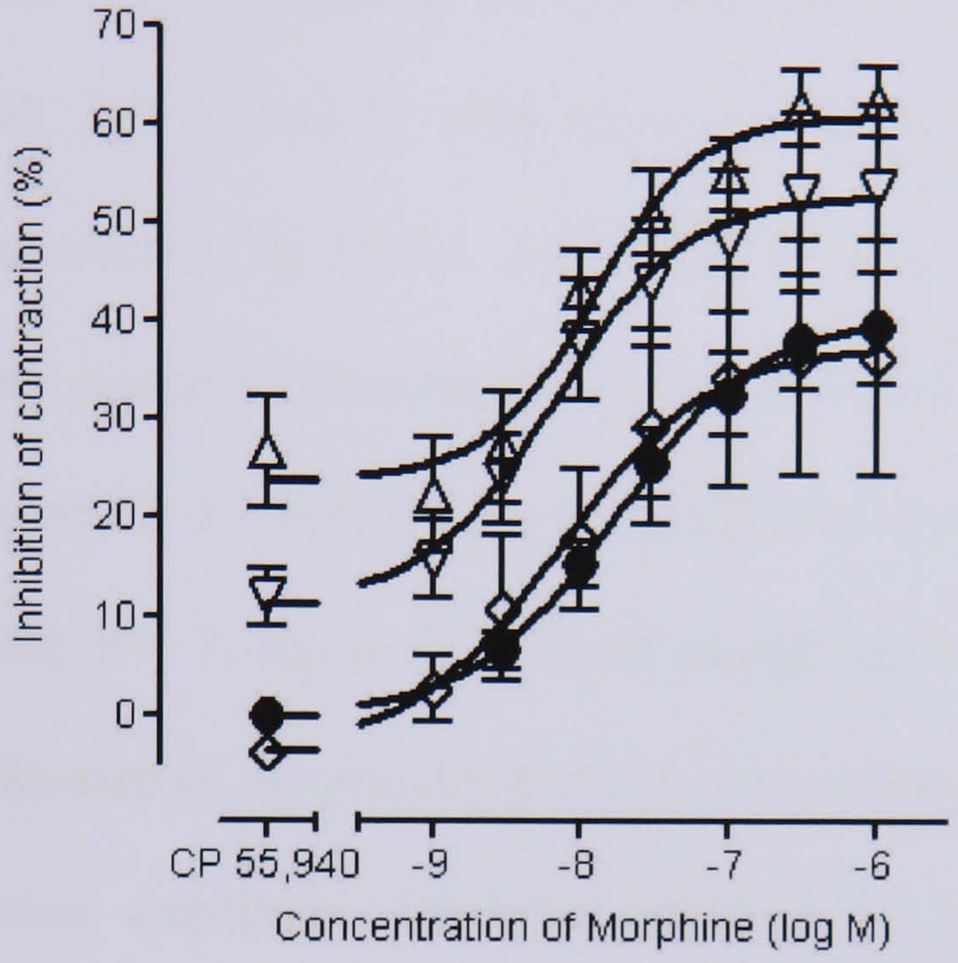

Figure 4.2 Mean concentration-response curves for the inhibition by morphine of contraction of the MPLM preparation evoked electrical stimulus (●) in the presence of 0.1 nM (◇), 1 nM (▽) and 10 nM (△) CP 55,940. Data is expressed as a percentage of contraction evoked in the absence of morphine and CP 55,940. Preparations were exposed to CP 55,940 for 20 minutes prior to ascending concentrations of morphine for five minutes. Each symbol represents the mean amplitude of peak contraction expressed as a percentage of the amplitude of peak contraction derived prior to application of morphine. Each symbol comprises of at least three different MPLM preparations. Vertical lines indicate S.E.M.

55,940 (EC_{50} = 7.3 nM, 95% confidence limits of 1.1 to 48.9 nM compared with 17 nM, 95% confidence limits of 16 to 18 nM). 1 μM morphine, in the presence of 0.1 nM CP 55,940, reduced the size of electrically evoked contraction by 36.5 ± 12.0% (n = 3) of untreated contraction amplitude. Inhibition evoked by 1 μM morphine in the presence of 0.1 nM CP 55,940 did not significantly differ from that evoked in the absence of CP 55,940. CP 55,940 (1 nM) administered alone reduced the size of electrically evoked contraction by 12.0 ± 2.9% (n = 7). In the presence of 1 nM CP 55,940, the morphine concentration-response curve remained parallel with that evoked in the absence of CP 55,940 (EC_{50} = 6.4 nM, 95% confidence limits of 5.8 to 7.1 nM, $p > 0.05$, *f*-test, n = 7, figure 4.2). 1 μM morphine, in the presence of 1 nM CP 55,940, reduced the size of electrically evoked contraction by 53.9 ± 8.4% (n = 7) of untreated contraction amplitude. Inhibition evoked by 1 μM morphine in the presence of 1 nM CP 55,940 did not significantly differ from that evoked in the absence of CP 55,940.

CP 55,940 (10 nM) alone reduced the size of electrically evoked contraction by 26.8 ± 5.6% (n = 11). The morphine concentration-response curve remained parallel with that evoked in the absence of CP 55,940 (EC_{50} = 10.5 nM, 95% confidence limits of 9.3 to 11.9 nM, $p > 0.05$, *f*-test, n = 8, figure 4.2). 1 μM morphine, in the presence of 10 nM CP 55,940, reduced the size of electrically evoked contraction by 62.7 ± 3.4% (n = 11) of untreated contraction amplitude. Inhibition evoked by 1 μM morphine in the presence of 10 nM CP 55,940 significantly differed from that evoked in the absence of CP 55,940 ($p < 0.01$, figure 4.2). Analysis of morphine inhibition, through the expression of inhibition evoked by morphine in the presence of 10 nM CP 55,940 as a percentage of that evoked by 10 nM CP 55,940 alone, demonstrated no difference when compared to the control (figure 4.3).

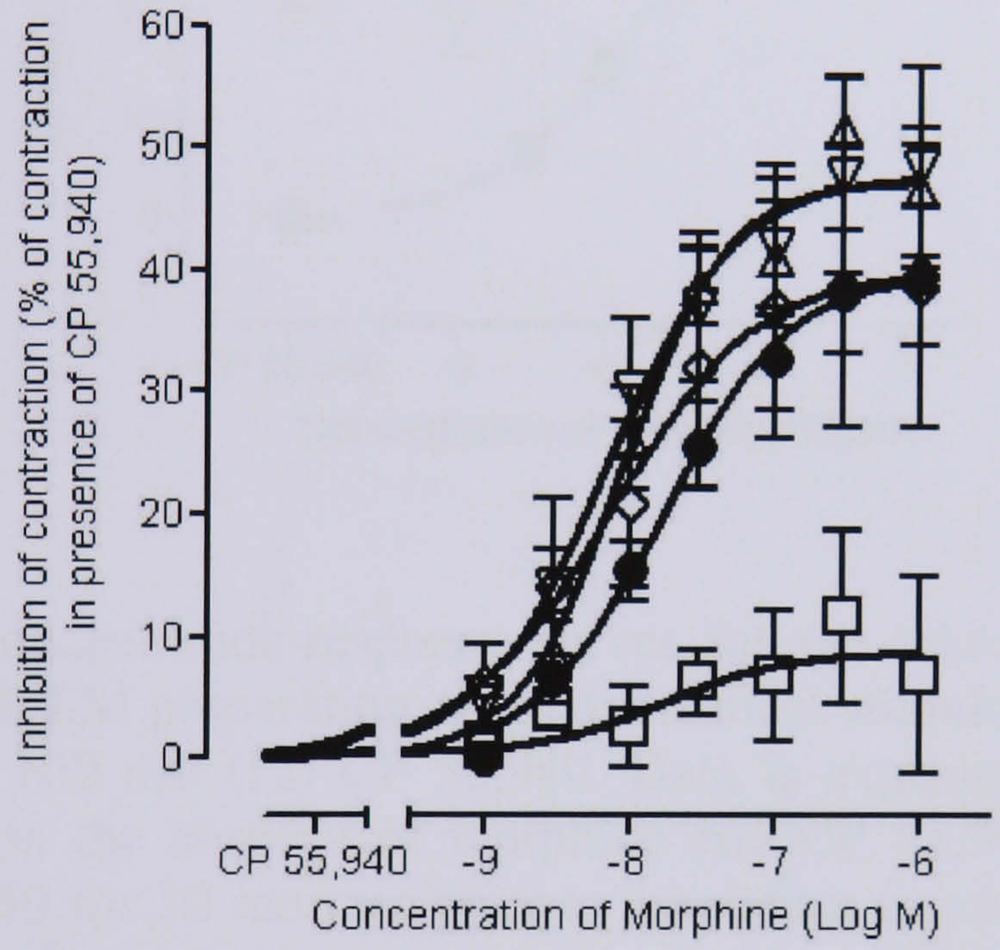

Figure 4.3 Mean concentration-response curves for the inhibition by morphine of contraction of the MPLM preparation evoked electrical stimulus (●) in the presence of 0.1 nM (◇), 1 nM (▽), 10 nM (△) and 100 nM (□) CP 55,940. Data is expressed as a percentage of contraction evoked in the presence of CP 55,940. Preparations were exposed to CP 55,940 for 20 minutes prior to ascending concentrations of morphine for five minutes. Each symbol represents the mean amplitude of peak contraction expressed as a percentage of the amplitude of peak contraction derived prior to application of morphine. Each symbol comprises of at least three different MPLM preparations. Vertical lines indicate S.E.M.

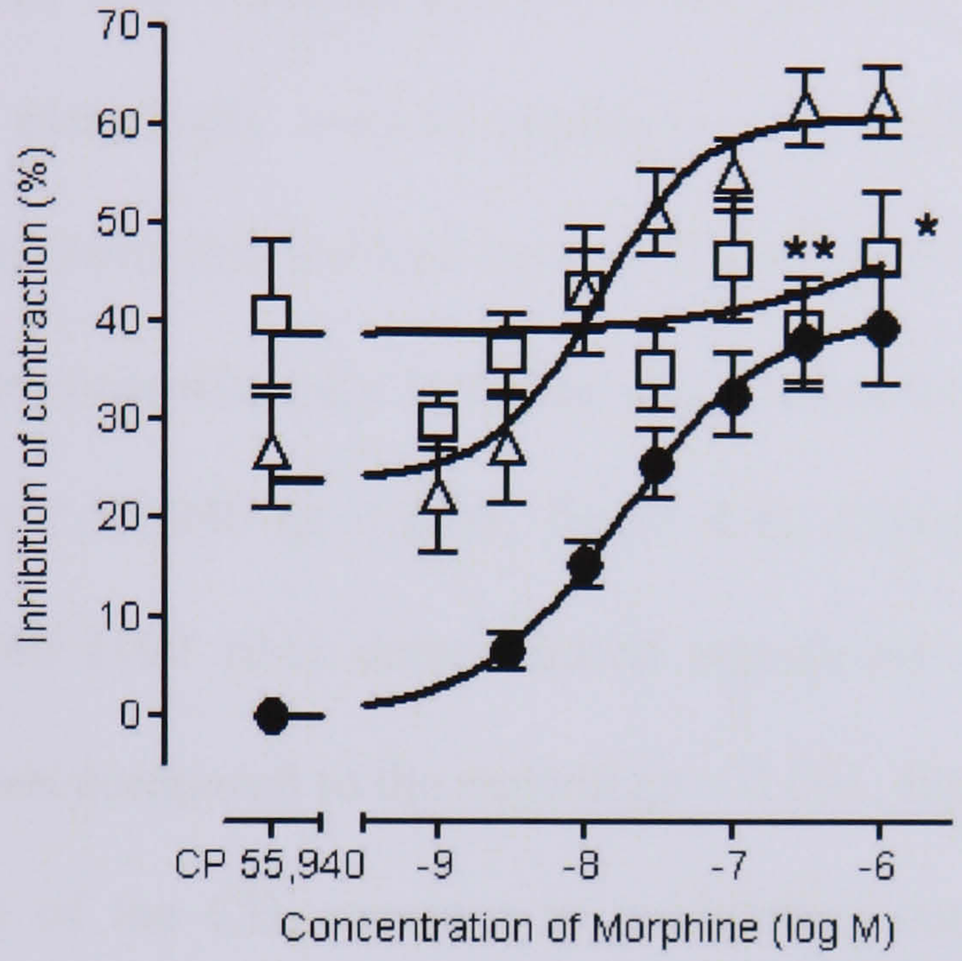

Figure 4.4 Mean concentration-response curves for the inhibition by morphine of contraction of the MPLM preparation evoked electrical stimulus (●) in the presence of 10 nM (△) and 100 nM (□) CP 55,940. Data is expressed as a percentage of contraction evoked in the absence of morphine and CP 55,940. Preparations were exposed to CP 55,940 for 20 minutes prior to ascending concentrations of morphine for five minutes. Each symbol represents the mean amplitude of peak contraction expressed as a percentage of the amplitude of peak contraction derived prior to application of morphine. Each symbol comprises of at least eight different MPLM preparations. Vertical lines indicate S.E.M. * indicates a significant difference of $p < 0.05$ and ** indicates a significant difference of $p < 0.01$ for inhibition of electrically-evoked contraction by morphine in the presence of 100 nM CP 55,940 compared with that observed in the presence of 10 nM CP 55,940.

100 nM CP 55,940 pre-treatment alone reduced the size of electrically evoked contraction by 40.8 ± 7.5% (n = 9, figure 4.4). In the presence of 100 nM CP 55,940, the morphine concentration-response curve EC_{50} remained significantly similar to that generated in the absence of CP 55,940 (EC_{50} = 9.8 nM, 95% confidence limits of 3.0 to 30 nM, n = 8, figure 4.4). 1 μM morphine, in the presence of 100 nM CP 55,940, reduced the size of electrically evoked contraction by 46.8 ± 6.8% (n = 9), not significantly different from that evoked by CP 55,940 in the absence of morphine. However inhibition was significantly less than that evoked by 1 μM morphine in the presence of 10 nM CP 55,940 ($p < 0.05$, figure 4.4). Compensation for inhibition evoked by CP 55,940 (100 nM) demonstrated significant reduction in morphine evoked inhibition when compared to the control ($p < 0.001$, figure 4.3).

To examine the role of the CB_1 receptor in modulating contraction, inhibition by morphine in the presence of the CB_1 receptor specific antagonist SR141716 was explored. SR141716 (100 nM) induced an increase in the size of electrically evoked contractions of the guinea-pig ileum MPLM by 80.3 ± 26.6% (n = 7, figure 4.5). The concentration-response curve EC_{50} for morphine in the presence of SR141716 remained statistically indistinguishable from that of morphine alone (EC_{50} = 10.5 nM, 95% confidence limits of 9.9 to 11.3 nM, n = 7). 1 μM morphine, in the presence of 100 nM SR141716, reduced the size of electrically evoked contraction to 49.0 ± 6.6% (n = 7) of the untreated electrically evoked contraction, which did not significantly differ from that induced by 1 μM morphine alone (figure 4.5a). Compensation for increased size of contraction evoked by SR141716 demonstrated significant increase in morphine evoked inhibition when compared to the control ($p < 0.01$, figure 4.5b).

a

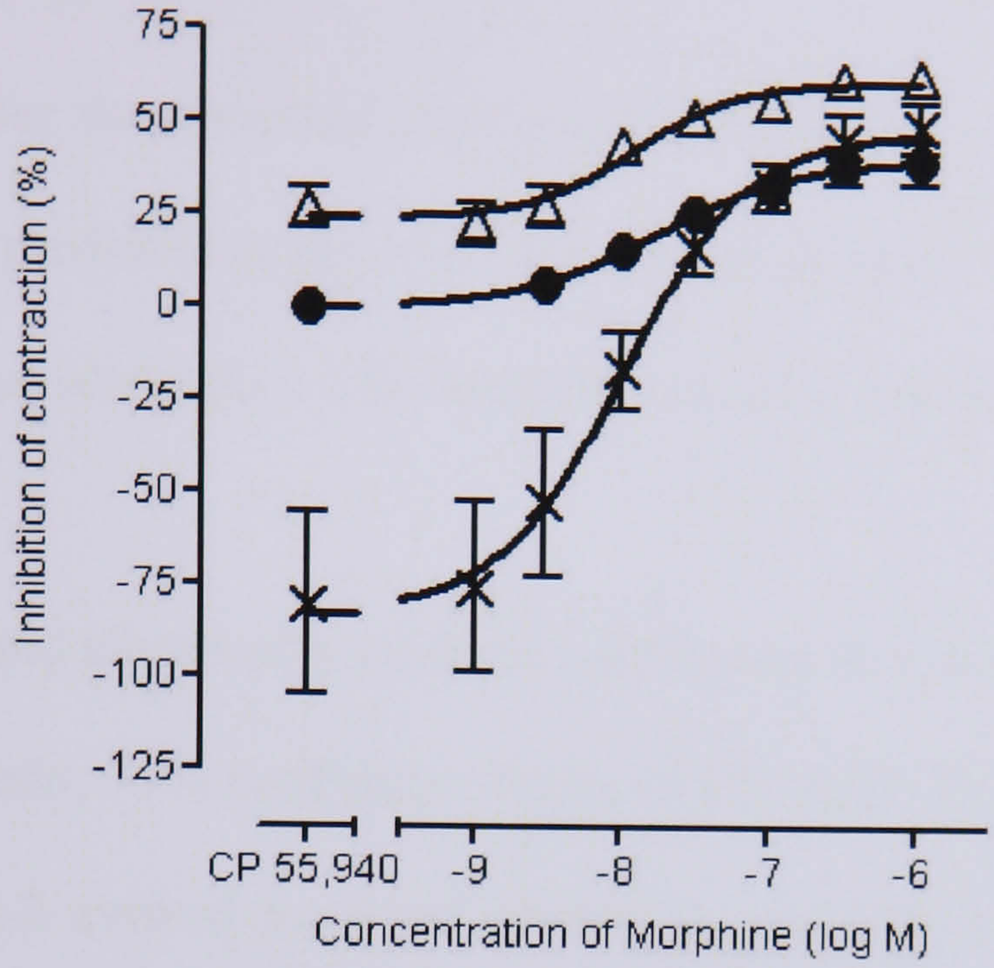

b

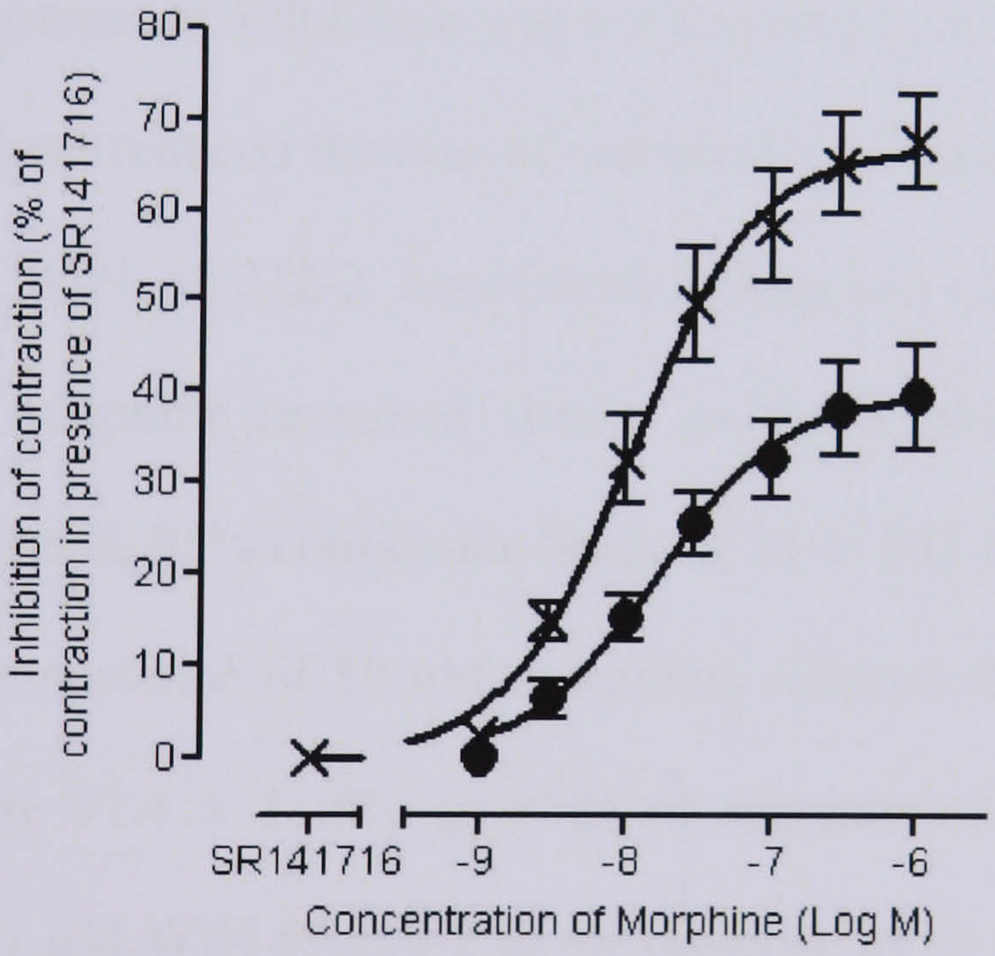

Figure 4.5 Mean concentration-response curves for the inhibition by morphine of contraction of the MPLM preparation evoked electrical stimulus (●) in the presence of 100 nM (×) SR141716 and 10 nM (△) CP 55,940. (a) Data is expressed as a percentage of contraction evoked in the absence of and (b) in the presence of SR141716. Preparations were exposed to SR141716 for 20 minutes prior to ascending concentrations of morphine for five minutes. Each symbol represents the mean amplitude of peak contraction expressed as a percentage of the amplitude of peak contraction derived prior to application of morphine. Each symbol comprises of at least seven different MPLM preparations. Vertical lines indicate S.E.M.

4.3.3 Interaction of morphine with WIN 55,212-2 inhibition of electrically evoked contractions of the myenteric plexus-longitudinal muscle preparation

To investigate whether the observed interaction of CP 55,940 with morphine was a CB_1 or CB_2 receptor mediated event, or a cannabinoid receptor independent event, the interaction between an alternative CB_1 and CB_2 receptor agonist, WIN 55,212-2 was examined.

WIN 55,212-2 inhibited electrically evoked contractions in a concentration-dependent manner (EC_{50} = 206 nM, 95% confidence limits of 121 and 353 nM, n = 3, figure 4.6). 10 μM WIN 55,212-2 evoked maximal inhibition, reducing contraction by 73.7 ± 4.3% (n = 3) of untreated contraction. Inhibition developed rapidly and remained for the duration of the experiment. Inhibition was not reversed by washing with Krebs.

Morphine (10 nM) alone reduced the size of electrically evoked contraction by 7.9 ± 3.3% (n = 7). The WIN 55,212-2 concentration-response curve obtained in the presence of 10 nM morphine remained similar to that evoked in the absence of morphine (EC_{50} = 269 nM, 95% confidence limits of 84 to 857 nM, figure 4.6). 1 μM WIN 55,212-2, in the presence of 10 nM morphine, reduced the size of electrically evoked contraction by 71.4 ± 11.9% (n = 2) of untreated contraction amplitude. Inhibition evoked by 1 μM WIN 55,212-2 in the presence of 10 nM morphine did not significantly differ from that evoked in the absence of morphine.

Morphine (100 nM) alone reduced the size of electrically evoked contraction by 30.3 ± 5.8% (n = 8). The WIN 55,212-2 concentration-response curve significantly differed from that evoked in the absence of morphine, with WIN 55,212-2 inducing less inhibition of contraction (EC_{50} = 8.2 nM, 95% confidence limits of 0.013 to 5235 nM, $p < 0.001$, 2-way ANOVA, figure 4.6). 1 μM WIN 55,212-2, in the presence of

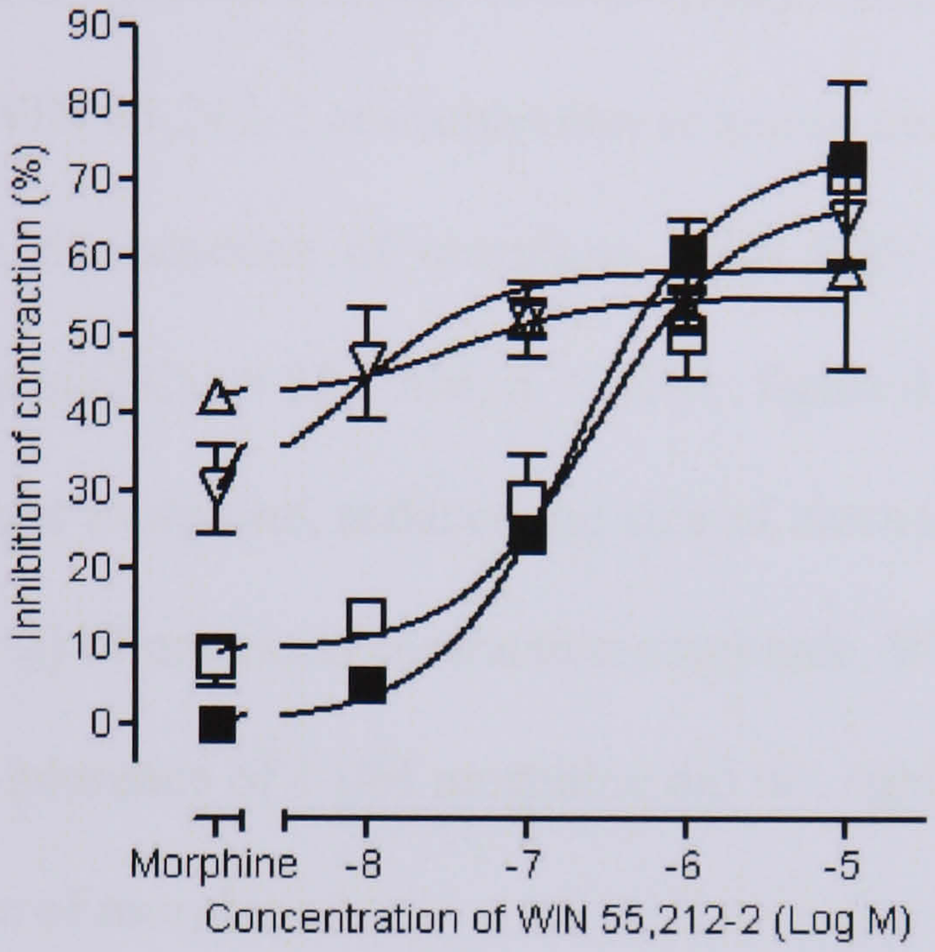

Figure 4.6 Mean concentration-response curves for the inhibition by WIN 55,212-2 of contraction of the MPLM preparation evoked electrical stimulus (■) in the presence of 10 nM (□), 100 nM (▽) and 1 μM (△) morphine. Data is expressed as a percentage of contraction evoked in the absence of morphine. Preparations were exposed to morphine for five minutes prior to ascending concentrations of WIN 55,212-2 for 20 minutes. Each symbol represents the mean amplitude of peak contraction expressed as a percentage of the amplitude of peak contraction derived prior to application of morphine. Each symbol comprises of at least two different MPLM preparations. Vertical lines indicate S.E.M.

100 nM morphine, reduced the size of electrically evoked contraction by 65.8 ± 5.5% (n = 6) of untreated contraction amplitude. Inhibition evoked by 1 μM WIN 55.212-2 in the presence of 100 nM morphine did not significantly differ from that evoked in the absence of morphine.

Morphine (1 μM) alone reduced the size of electrically evoked contraction by 42.4 ± 1.5% (n = 13). The WIN 55,212-2 concentration-response curve significantly differed from that evoked in the absence of morphine, with WIN 55,212-2 inducing less inhibition of contraction (EC_{50} = 35.7 nM, $p < 0.001$, figure 4.6). 1 μM WIN 55,212-2, in the presence of 1 μM morphine, reduced the size of electrically evoked contraction by 58.8 ± 12.8% (n = 2) of untreated contraction amplitude. Inhibition evoked by 1 μM WIN 55,212-2 in the presence of 1 μM morphine did not significantly differ from that evoked in the absence of morphine.

4.3.4 Interaction of cannabinoids with morphine withdrawal evoked contractions of the whole ileum

Both opioids and cannabinoids have been demonstrated to produce contraction upon abrupt withdrawal, after prolonged exposure, in whole ileum, and so a possible interaction in the production of this contraction was explored.

Opioid withdrawal, induced by the opioid receptor antagonist naloxone (10 μM) after three hour incubation with morphine (1 μM), evoked a rapid contraction of whole ileum of 1.77 ± 0.43 g (n = 10, figure 4.7). Contraction was rapidly followed by relaxation to basal levels of contraction. Re-application of naloxone after washing did not induce a contraction. Tissue incubated in a similar manner contracted by 3.56 ± 0.37 g (n = 12) upon exposure to Carbachol (1 μM).

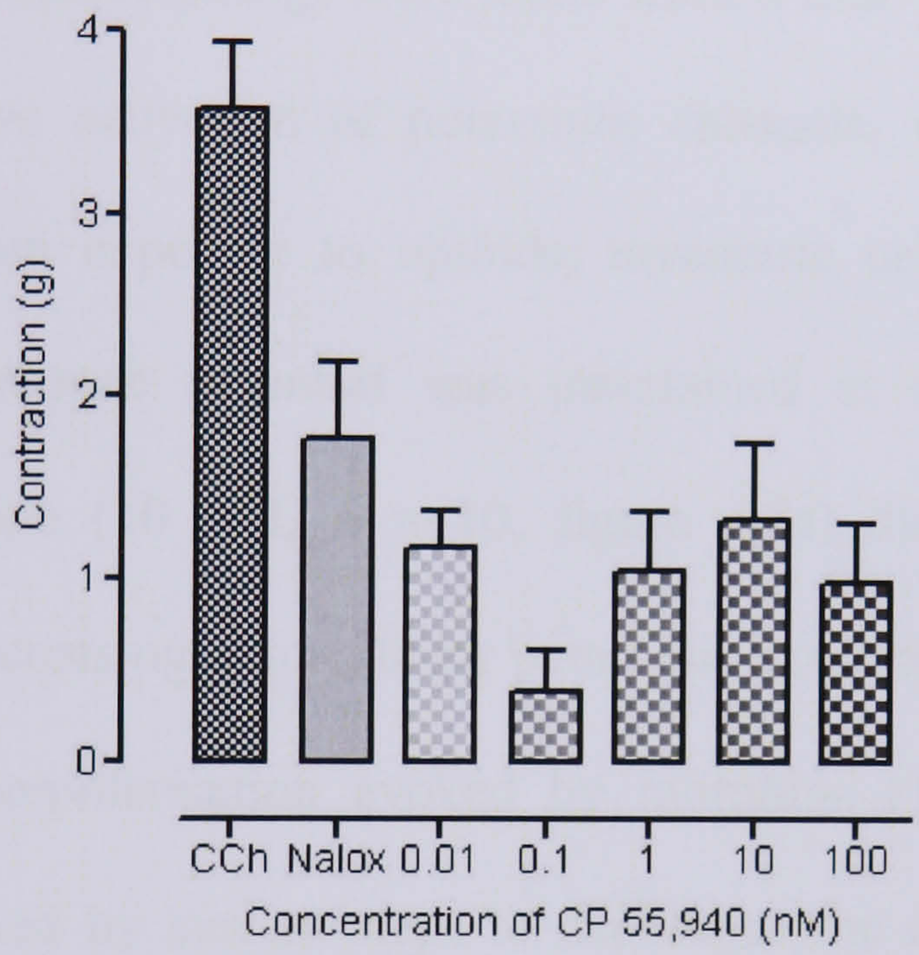

Figure 4.7 Effect of CP 55,940 on contractions of the whole ileum induced by abrupt withdrawal from 3 hr exposure to 1 μM morphine by the application of 10 μM naloxone. Each column represents the mean amplitude of peak contraction evoked by application of naloxone (10 μM) after exposure to CP 55,940 for 20 minutes. CCh represents control exposure to 1 μM carbachol. Nalox represents control exposure to naloxone in the absence of CP 55,940. Each comprises of at least 3 different MPLM preparations. Vertical lines indicate S.E.M.

CP 55,940, when applied 20 minutes prior to naloxone at doses ranging from 0.1 nM to 100 nM, did not induce significant changes in contraction (at least three different MPLM preparations were used for each concentration, $p > 0.05$, ANOVA, figure 4.7)

4.3.5 Effects of opioids on membrane hyperpolarisation in cultured myenteric neurones

Stable whole-cell patch recordings were made from a total of 30 cultured myenteric neurones. To observe activation of potassium channels, and therefore membrane hyperpolarisation with exposure to opioids, myenteric neurones were held under current clamp, membrane potential was maintained at approximately –80 mV. Exposure to morphine (10 μM, n = 10, figure 4.8a) did not induce membrane hyperpolarisation. Increasing extracellular potassium concentration to 50 mM did not change lack of hyperpolarisation evoked by morphine (10 μM, n = 5). Action potentials were evoked by current steps to depolarise the membrane (n = 3, figure 4.8b). Only single action potentials were evoked with each current step, probably as a result of after-hyperpolarisation observed after action potentials in myenteric AH-neurones.

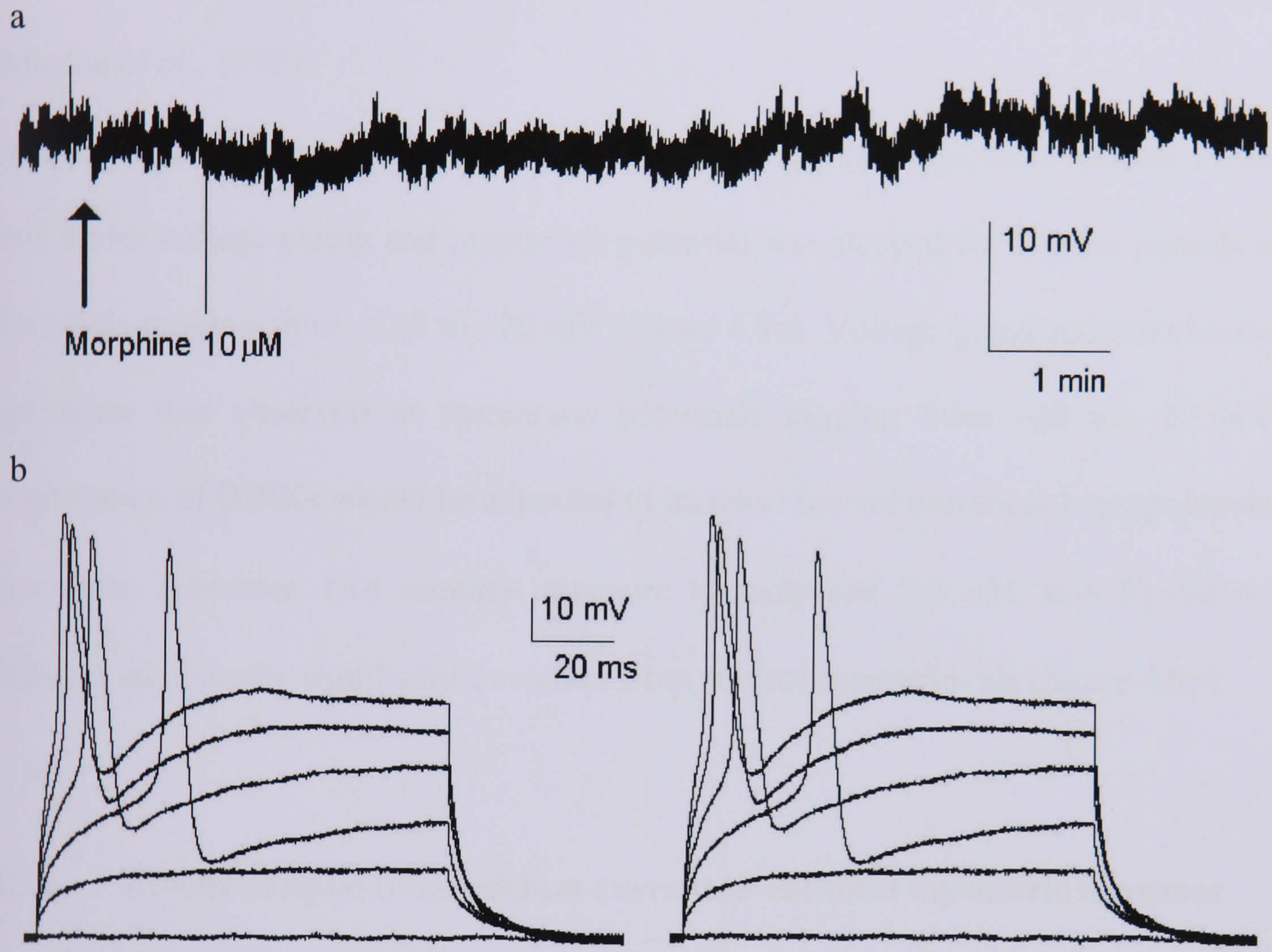

Figure 4.8 Sample traces derived from myenteric neurones held under current clamp. (a) Trace depicts changes in membrane potential evoked by morphine (10 μM) in a single cell in which an initial membrane potential of approximately –80 mV was achieved through application of a sustained current. (b) Superimposed traces depict action potentials evoked by 100 ms current steps, each producing a rise in membrane potential of approximately 20 mV.

4.3.6 Effects of opioids on G-protein coupled inwardly rectifying potassium current in cultured myenteric neurones

The G-protein coupled inwardly rectifying potassium current (GIRK) has been shown to be potentiated by both opioids (Galligan and North, 1991) and cannabinoids (Mackie *et al.,* 1995).

To observe potentiation of GIRKs with exposure to opioids, myenteric neurones were held under voltage clamp and membrane potential was stepped for 100 ms periods to potentials ranging from –120 to –20 mV (figure 4.9a). Voltage-gated sodium channel activation was observed at membrane potentials ranging from –40 to –20 mV. Potentiation of GIRKs would be expected to increase inward current at hyperpolarised potentials. However, five minutes exposure to morphine (10 μM, n = 8) did not induce a statistically significant deviation from control current levels (figure 4.9b).

4.3.7 Effects of opioids on calcium current in cultured myenteric neurones

Inhibition of voltage-gated calcium currents (I_{Ca}) by opioids have been demonstrated in many studies (Williams *et al.*, 2001). To isolate I_{Ca} in cultured myenteric neurones, sodium and potassium currents were inhibited through the application of TTX in

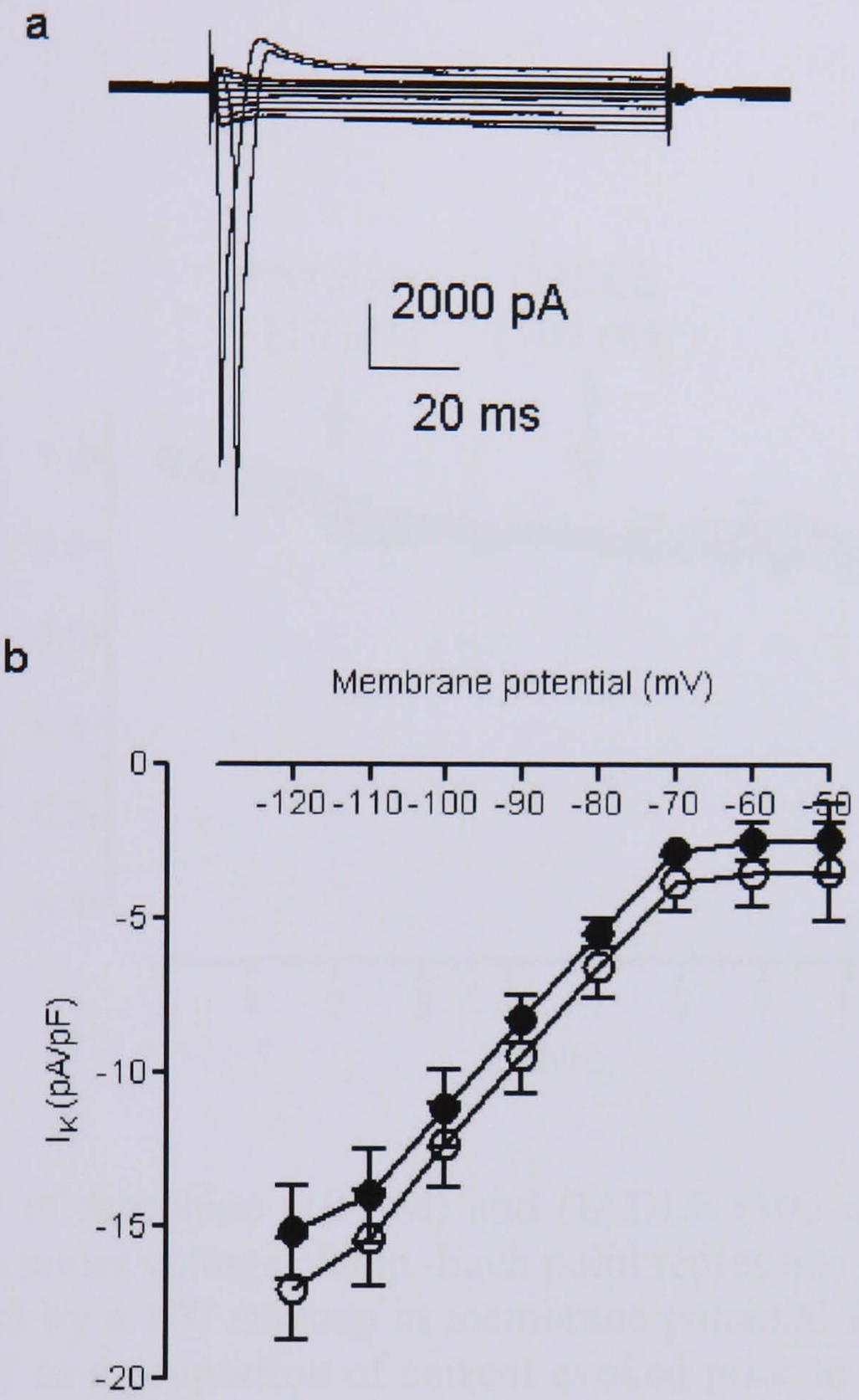

Figure 4.9 (a) Superimposed traces derived from cultured myenteric neurones held under voltage clamp. Traces depicts changes in current flow across the membrane evoked by 100 ms, 10 mV steps in membrane potential ranging from –120 to –20 mV. (b) Mean current-voltage relationship of 8 neurones prior to (●) and post five minutes exposure to morphine (10 μM, ○).

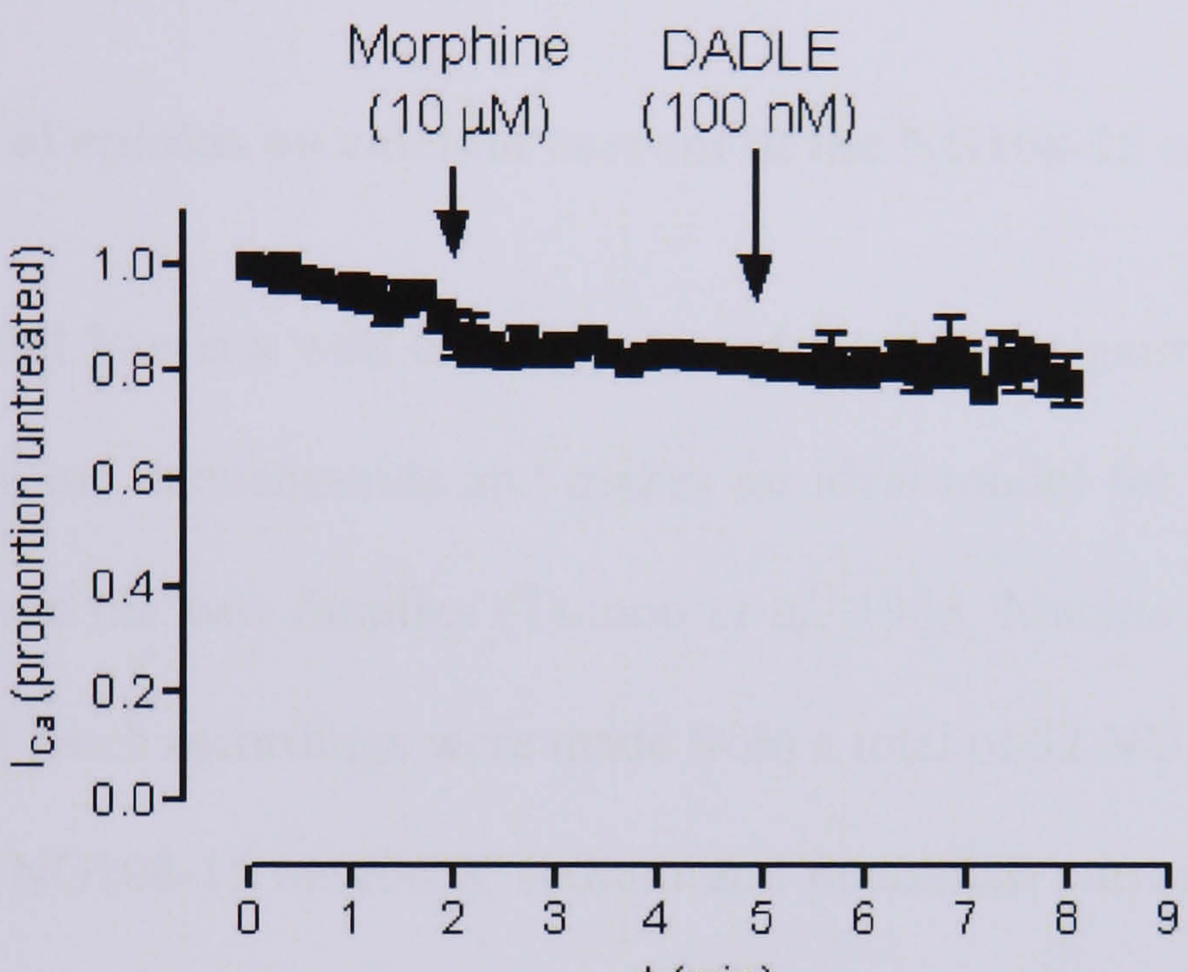

Figure 4.10 Effect of morphine (10 μM) and DADLE (100 nM) on I_{Ca} in cultured myenteric neurones under voltage clamp. Each point represents the mean amplitude of peak current evoked by a 100 ms step in membrane potential from a holding current of –70 mV to 0 mV as a proportion of current evoked prior to application of opioids (n = 4). Vertical lines indicate S.E.M.

extracellular solutions, to block sodium currents, and TEA and Cs^{2+} in intracellular solutions, to block potassium currents. Application of both morphine (10 μM) and the δ-receptor specific agonist, DADLE, (100 nM, n = 4, figure 4.10) did not significantly inhibit the current.

4.3.8 Effects of opioids on calcium current in the NG108-15 cell line

The NG108-15 cell line is a well established model for investigating the modulation of I_{Ca} by opioids and cannabinoids and makes an ideal model for investigating any interaction between the two families (Tsunoo *et al.* 1986, Mackie and Hille, 1992). Stable whole-cell patch recordings were made from a total of 32 NG108-15 neurones. To isolate I_{Ca} in NG108-15 neurones, sodium and potassium currents were inhibited through the application of TTX in extracellular solutions, to block sodium currents, and TEA and Cs^{2+} in intracellular solutions, to block potassium currents (figure 4.11). An inward Ca^{2+} current of 316 ± 32 pA (6.6 ± 1.0 $pA.pF^{-1}$) was elicited in 17 neurones by a 100 ms depolarising pulse to 0 mV from a holding potential of -70 mV. The current consisted of a sharp transient increase followed by a slowly decreasing component (figure 4.11c). Inward current initiated upon a depolarising pulse to -40 mV and achieved a peak inward current at 0 mV (figure 4.12a and b).

Treatment with the δ-opioid receptor selective agonist DADLE depressed the amplitude of the Ca^{2+} current elicited by a depolarising pulse to 0 mV, with maximal inhibition occurring at 0 mV, at the peak of the I-V relationship (n = 6, figure 4.12b and d). Inhibition occurred over a concentration range of 10 pM to 100 nM (figure 4.12c). Regression to a sigmoidal dose-response curve ascertained an IC_{50} for

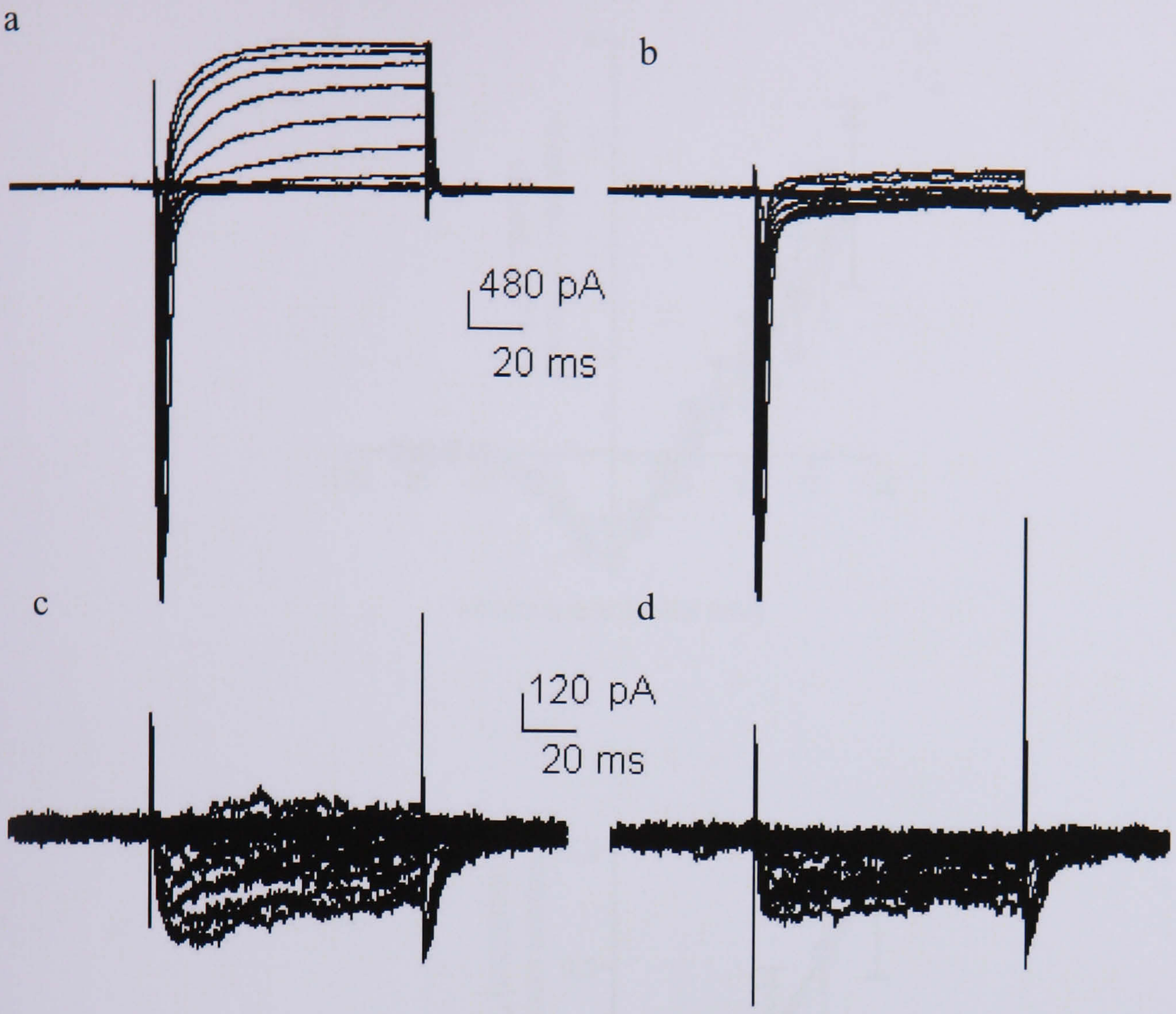

Figure 4.11 Sample traces derived from a single NG108-15 neurone held under voltage clamp. Traces depicts changes in current flow across the membrane evoked by 100 ms, 5 mV steps in membrane potential ranging from –80 to 90 mV. (a) Depicts current prior to blockade whilst (b) depicts current post I_K blockade and (c) depicts I_{Ca} upon blockade of I_{Na}. (d) Demonstrates inhibition of I_{Ca} upon application of CP 55,940 (10 μM). (e) NG108-15 under 500x magnification.

a

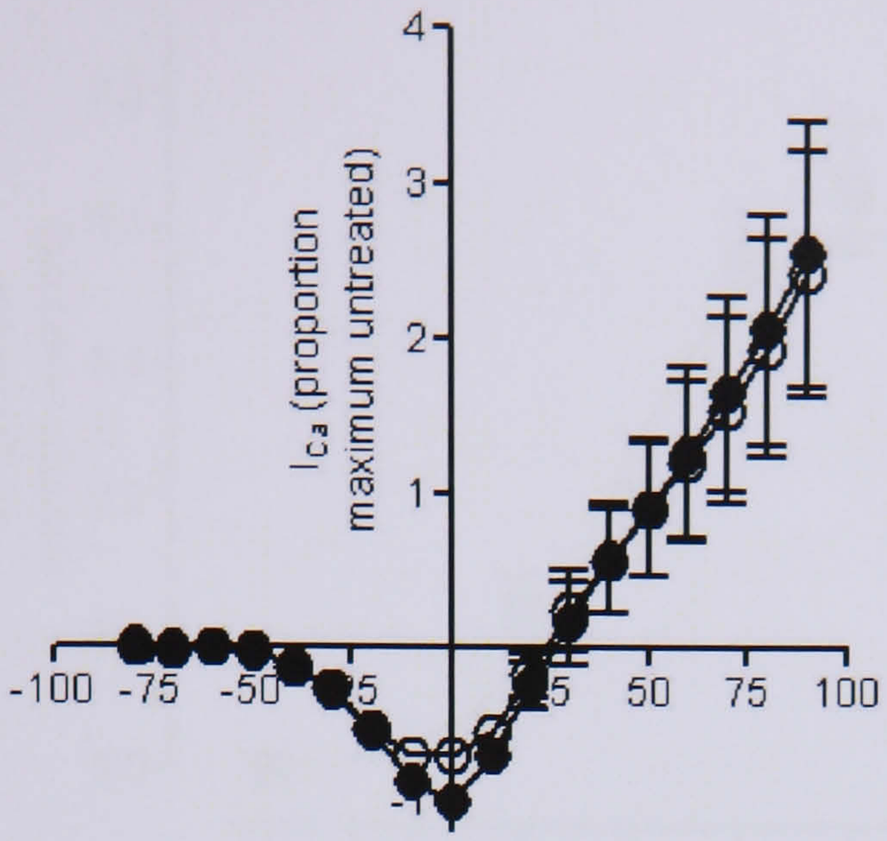
4
3
2
1
-1
I_{Ca} (proportion maximum untreated)
-100 -75 -50
50 75 100
Membrane potential (mV)

b

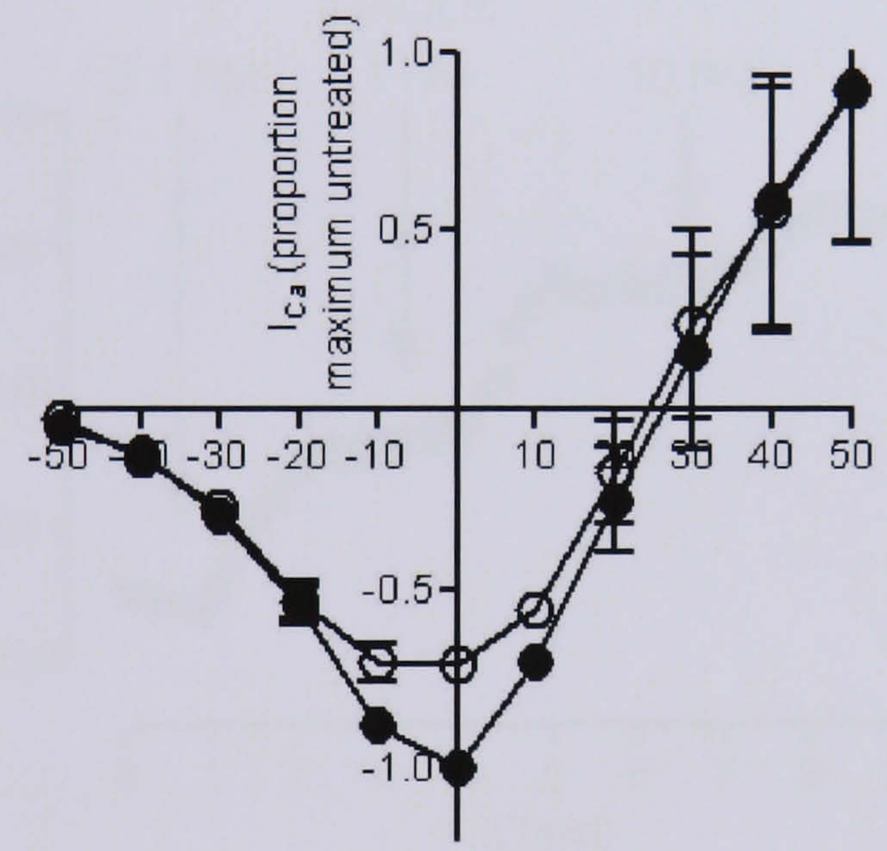
1.0
0.5
-0.5
-1.0
I_{Ca} (proportion maximum untreated)
-50 -30 -20 -10
10 40 50
Membrane potential (mV)

c

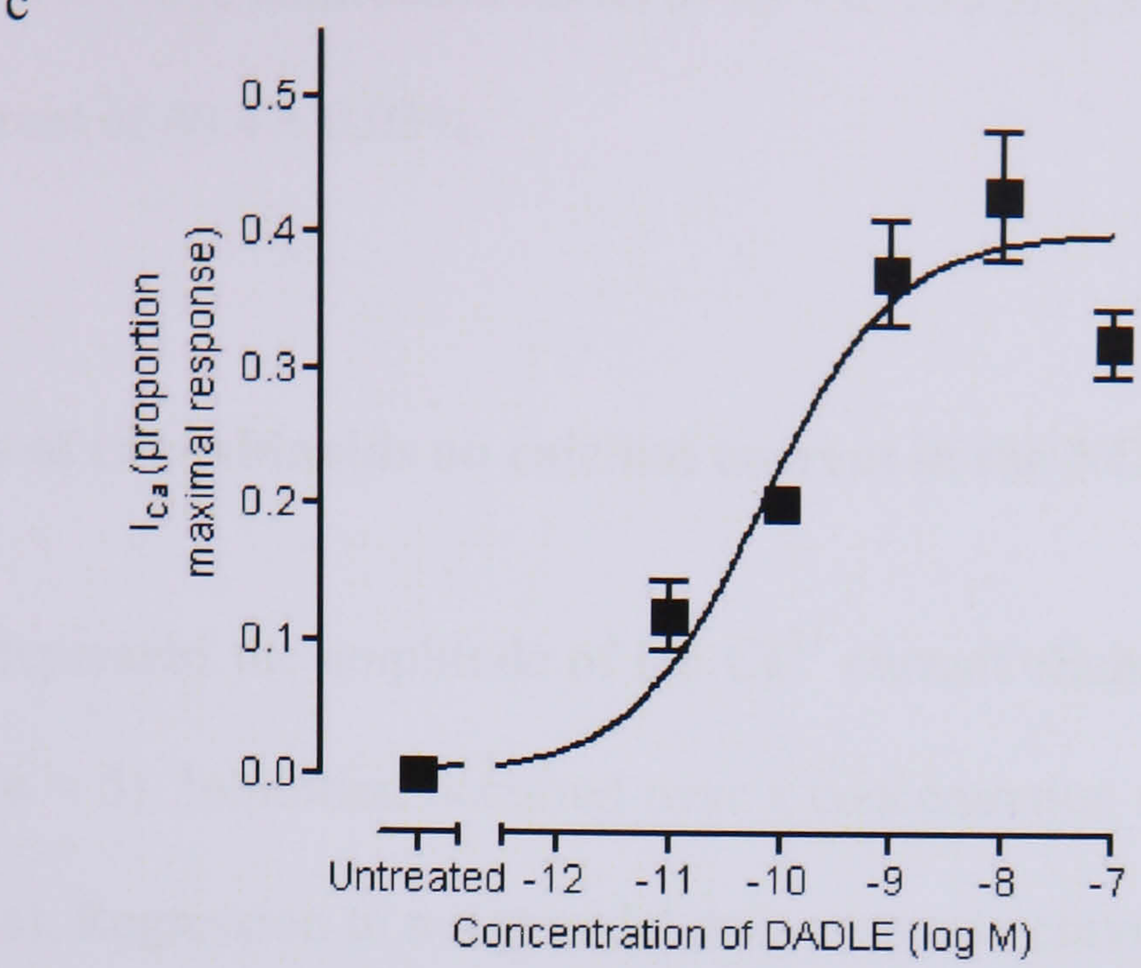

d

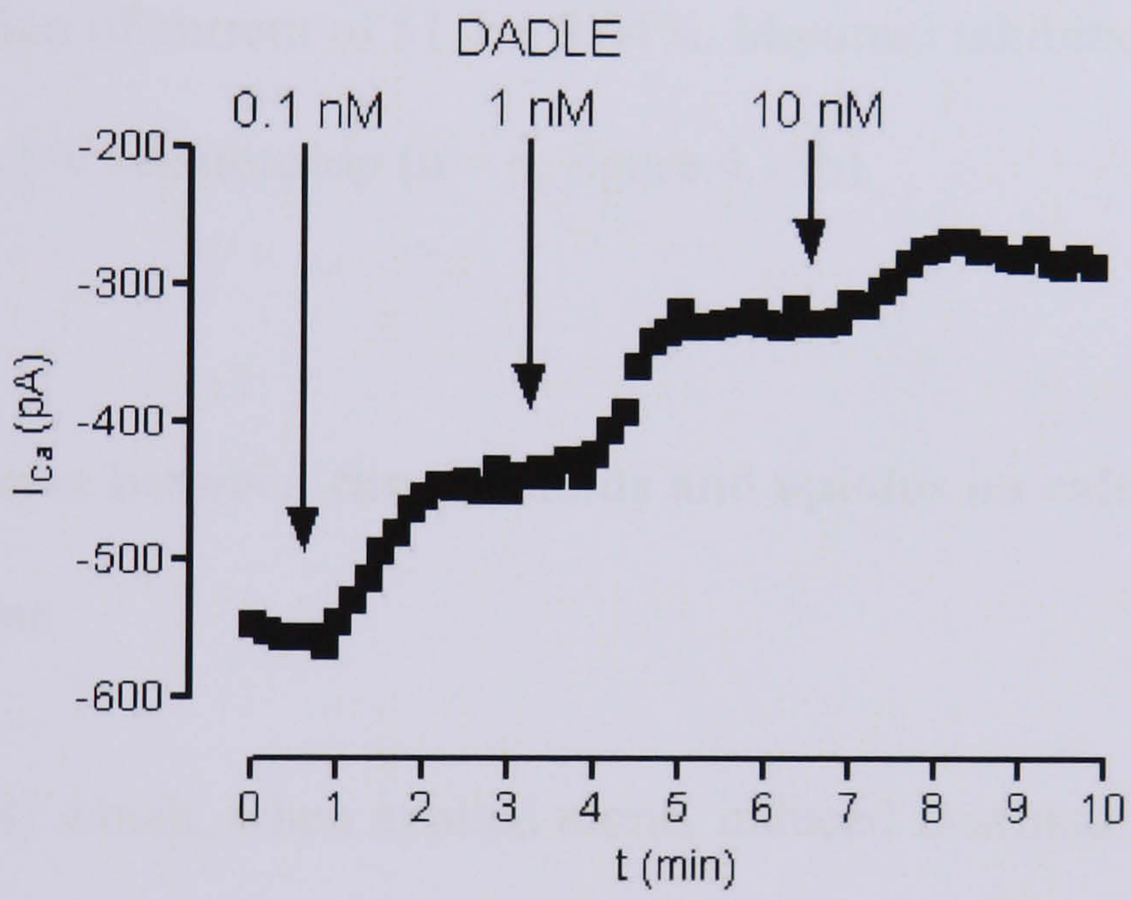

Figure 4.12 Modulation of calcium currents in NG108-15 neurones on exposure to DADLE. (a) Superimposed I-V curves of peak I_{Ca}, expressed as a proportion of inward current evoked by a 100 ms voltage step to 0 mV in the absence of (●) and presence of DADLE (100 nM, ○). Each point represents the mean ± S.E.M. of at least five neurones. (b) magnification of figure 4.12a, amplifying inhibition evoked by DADLE. (c) DADLE inhibited peak Ca^{2+} current elicited by a 0 mV depolarising pulse. Points show the mean current, expressed as a proportion of inward current evoked by a 100 ms voltage step to 0 mV in the absence of DADLE, evoked in the presence of DADLE at concentrations ranging from 10 pM to 100 nM. Bars show S.E.M. Non-linear regression to a sigmoidal concentration-response curve presented an IC_{50} and maximal blockade for DADLE of 67.3 pM and 40.4% respectively. (d) Sample trace derived from a single NG108-15 neurone held under voltage clamp. Trace depicts changes in current flow across the membrane evoked by a 100 ms voltage step to 0 mV on application of 0.1, 1 and 10 nM DADLE.

DADLE of 67.3 pM (95% confidence limits of 23.4 to 193 pM) and a maximum reduction of current of 40.4 ± 0.03%.

4.3.9 Effects of cannabinoids on calcium current in the NG108-15 cell line

WIN 55,212-2 depressed the amplitude of the Ca^{2+} current elicited by a depolarising pulse to 0 mV (n = 5). Inhibition occurred over a concentration range of 1 nM to 10 μM (figure 4.13a). Regression to a sigmoidal dose-response curve ascertained an IC_{50} for WIN 55,212-2 of 58.3 nM (95% confidence limits of 35.6 to 93.4 pM) and a maximum reduction of current of 51.7 ± 0.04%. Maximal inhibition occurred at 0 mV, at the peak of the I-V relationship (n = 6, figure 4.13b).

4.3.10 Interaction between cannabinoids and opioids on calcium current in the NG108-15 cell line

DADLE (100 nM) which, when applied alone, induced maximal inhibition, reducing inward current, evoked by a voltage step to 0 mV, by 32.2 ± 2.4% (n = 3). WIN 55,212-2 (10 μM) applied alone also induced maximal inhibition, reducing current by 26.6 ± 3.0% (n = 3). With prior exposure to WIN 55,212-2 (10 μM), addition of DADLE (100 nM) induced a further inhibition of inward current of 10.3 ± 1.0% (figure 4.14, n = 3). Inhibition was significantly smaller than that evoked by DADLE (100 nM) in the absence of WIN 55,212-2 ($p < 0.01$).

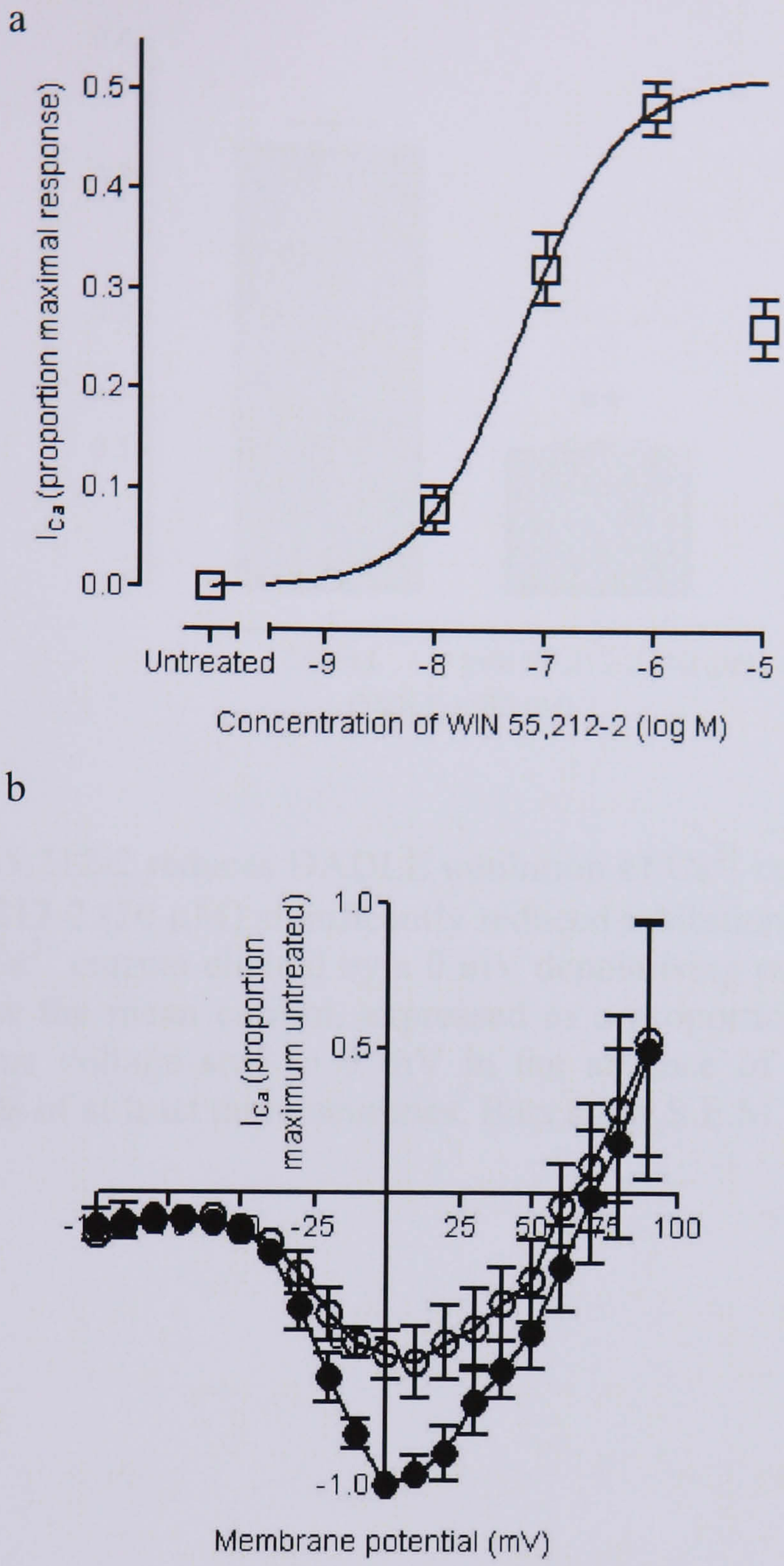

Figure 4.13 Modulation of calcium currents in NG108-15 neurones on exposure to WIN 55,212-2. (a) WIN 55,212-2 inhibited peak Ca^{2+} current elicited by a 0 mV depolarising pulse. Points show the mean peak current, expressed as a proportion of inward current evoked by a 100 ms voltage step to 0 mV in the absence of WIN 55,212-2, evoked in the presence of WIN 55,212-2 at concentrations ranging from 1 nM to 10 μM. Bars show S.E.M. Non-linear regression to a sigmoidal concentration-response curve presented an IC_{50} and maximal blockade for WIN 55,212-2 of 58.3 nM and 51.7% respectively. (b) Superimposed I-V curves of peak I_{Ca}, expressed as a proportion of inward current evoked by a 100 ms voltage step to 0 mV in the absence of (●) and presence of WIN 55,212-2 (1 μM, ○). Each point represents the mean ± S.E.M. of at least six neurones.

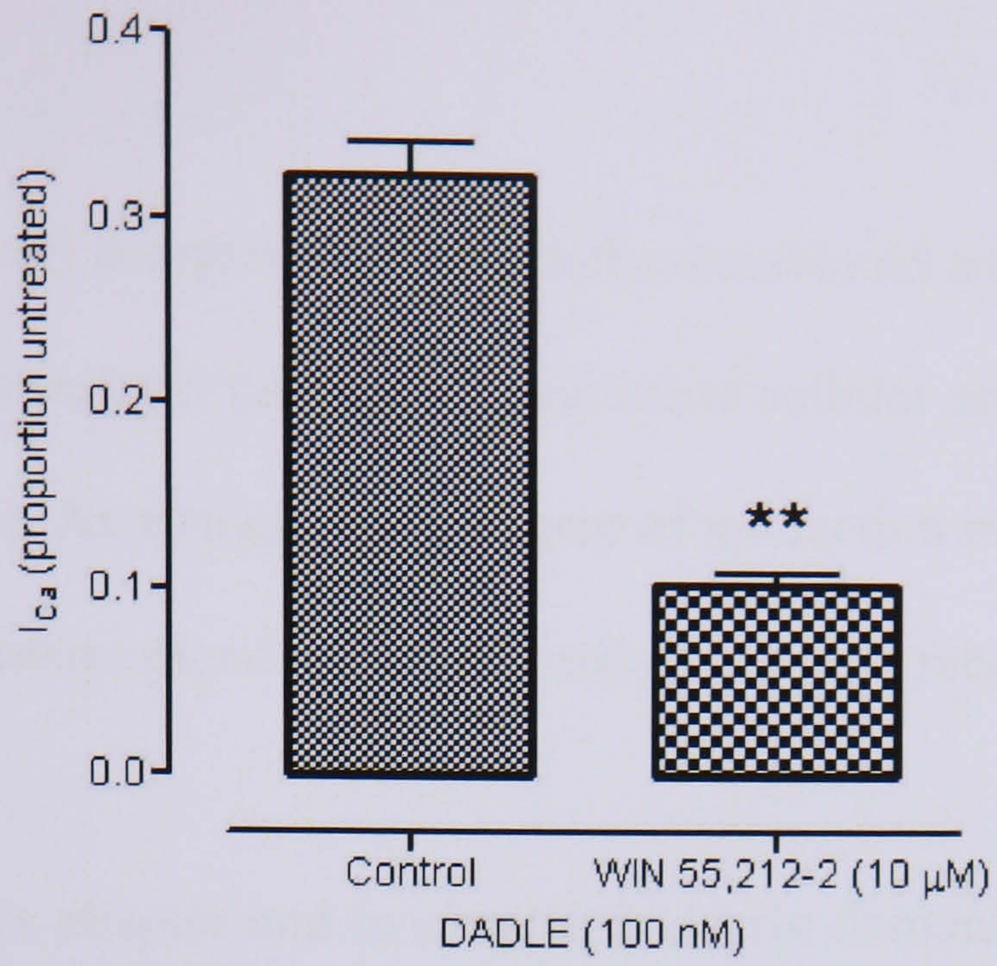

Figure 4.14 WIN 55,212-2 reduces DADLE inhibition of Ca^{2+} currents in NG108-15 neurones. WIN 55,212-2 (10 μM) significantly reduced inhibition evoked by DADLE (100 nM) of peak Ca^{2+} current elicited by a 0 mV depolarising pulse (**, $p < 0.01$, *t*-test). Columns show the mean current, expressed as a proportion of inward current evoked by a 100 ms voltage step to 0 mV in the absence of WIN 55,212-2 and DADLE and consists of at least three neurones. Bars show S.E.M.

4.4 Discussion

It is now generally well accepted now that both cannabinoid and opioid receptors act through $G_{i/o}$-protein mediated pathways to modulate cellular activity (Pertwee, 1997; Williams *et al.*, 2001). As a result, some degree of interaction may be hypothesised to exist within the myenteric plexus given the major role both receptors families play in governing motility.

Data presented in this chapter and in chapter 2 clearly demonstrate both CP 55,940 and morphine inhibit electrically evoked contraction of the guinea-pig MPLM preparation in a concentration-dependent manner, with CP 55,940 showing SR141716 sensitivity similar to that observed by Paton (1957) and Pertwee *et al.* (1996).

This study showed with morphine producing identical concentration-response curves, that inhibition produced by CP 55,940 at concentrations of 10 nM and below is evoked independently to that produced by morphine. While exposure to 100 nM CP 55,940 prevented all morphine-evoked inhibition. The presence of this blockade of morphine evoked inhibition by 100 nM CP 55,940, and its absence at lower concentrations, suggests either the exhaustion of a shared intracellular messenger or the activation by 100 nM CP 55,940 of an additional receptor or cannabinoid receptor mediated intracellular mechanism to interact with the opioid signalling mechanisms (figure 4.15). However, the possibility of the exhaustion of a shared intracellular messenger is ruled out by the observation that inhibition evoked by 1 μM morphine and 100 nM CP 55,940 was smaller than that evoked by 1 μM morphine and 10 nM CP 55,940. Should inhibition be dependent upon a shared intracellular messenger, inhibition produced by morphine in the presence of CP 55,940 would be expected to be limited, but not reduced in the presence of high CP 55,940 concentrations. This

interaction between cannabinoids and opioids is supported by the reduced potency displayed by WIN 55,212-2 in inhibiting contraction in the presence of 100 nM and 1 μM morphine.

If it is assumed that inhibition of endogenous tonically active cannabinoids are responsible for the increased amplitude of contractions evoked by SR141716, and these endogenous cannabinoids possess similar pharmacological properties to CP 55,940, then morphine would be expected to display the same additive interaction in the presence of SR141716 as displayed with low levels of CP 55,940. The observation of increased inhibition by morphine in the presence of SR141716 suggests the increase in the amplitude of contractions evoked by SR141716 is not due to inhibition of tonically active endogenous cannabinoids.

The lack of any significant modulation of opioid withdrawal evoked contractions by CP 55,940 is intriguing as Basilico *et al.* (1999) demonstrated cross-inhibition in the guinea-pig MPLM preparation. One possible explanation for the lack of inhibition observed may lie in the high variability of the data. Some reduction of the mean contraction size is apparent, but with the large variability this is not significant.

The lack of opioid inhibition of both potassium and calcium currents in myenteric neurones was anticipated in retrospect. Intracellular recording by North *et al.* (1979) observed potassium channel activation when opioids were applied by iontophoresis to the surface of the ganglion and not soma, inferring that opioid receptors are not expressed on the soma. In generating primary cultures of myenteric neurones mechanical force is applied through tituration of enzymatically digested tissue. It is probable that this mechanical force would split the soma and ganglia and so prevent patch clamping, which is performed upon the soma, from detecting opioid activity.

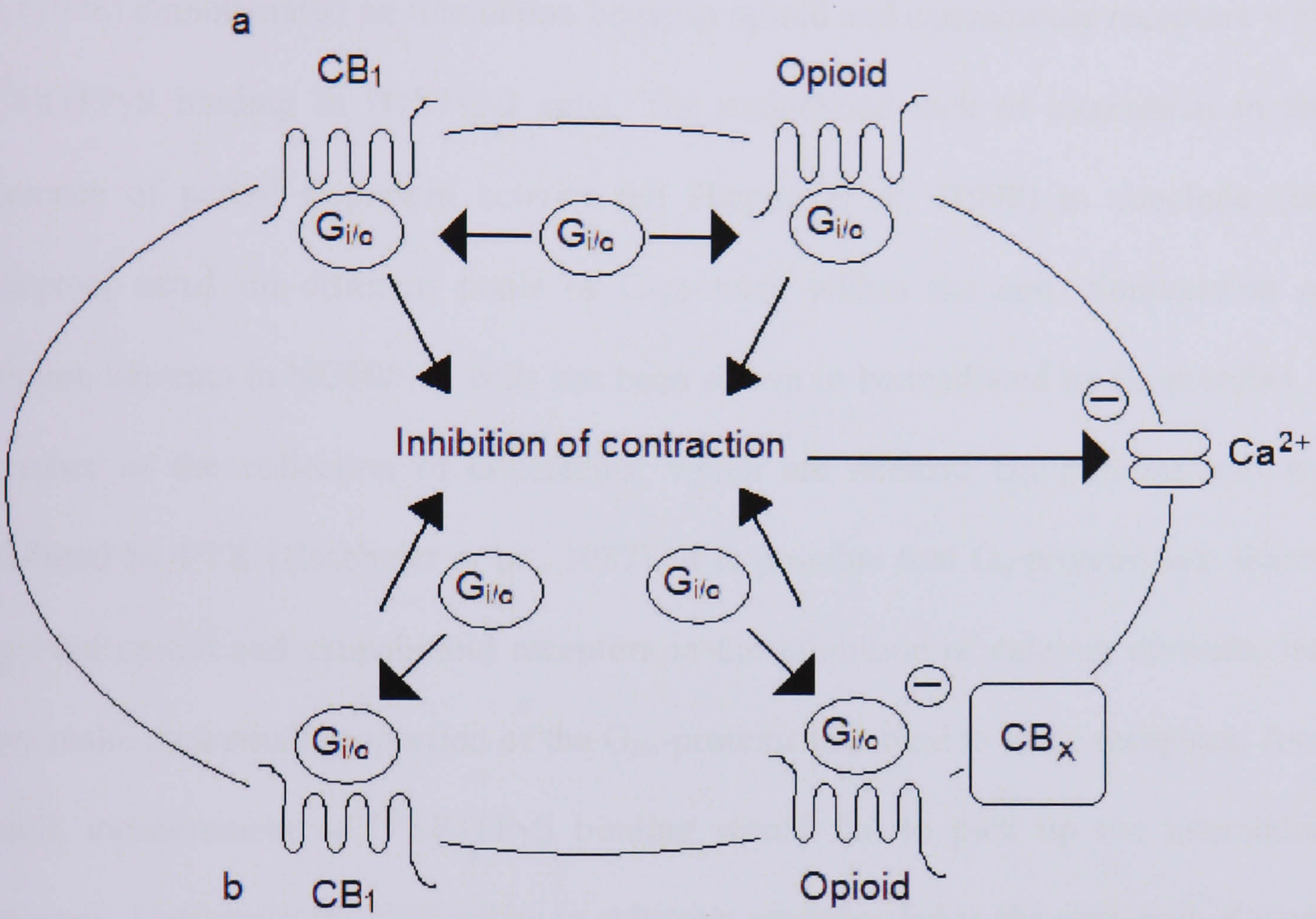

Figure 4.15: Hypothesised intracellular interaction between cannabinoids and opioids. (a) A shared intracellular messenger may be responsible for conveying signalling within a cell. Depletion of this shared messenger through activation of one receptor pathway will prevent stimulation of the other pathway from acting. (b) Both CB_1 and opioid receptors may possess independent mechanisms by which each evoke inhibition. The interaction observed may not be the result of greater CB_1 receptor stimulus and an increased role of already active intracellular mechanisms, but may be due to activation of an alternate mechanism (CB_X) to interact with the opioid receptor or associated mechanisms.

The observation that DADLE, at a concentration which produces maximal inhibition of Ca^{2+} currents, producing a reduced inhibition in the presence of WIN 55,212-2, also at a concentration which produces maximal inhibition, is interesting as Shapira *et al.* (1998) demonstrated no interaction between opioid and cannabinoid receptors with [^{35}S]GTPγS binding in N18TG-2 cells. The maintained lack of interaction in the presence of partial G-protein activity led Shapira *et al.* (1998) to conclude that receptors acted on different pools of G-proteins within the cell. Suppression of calcium currents in NG108-15 cells has been shown to be mediated by G_o-proteins, a member of the collection of G-proteins, which are deemed $G_{i/o}$-proteins and are inhibited by PTX (Hescheler *et al.*, 1987). It is possible that G_o-proteins are shared between opioid and cannabinoid receptors in the inhibition of calcium currents, but they make up a small proportion of the $G_{i/o}$-proteins that bind to these receptors. As a result, measurement of [^{35}S]GTPγS binding would fail to pick up the interaction observed. Unfortunately, difficulties in culturing neurones led to the cessation of work in this area as further examination of this interaction would prove interesting.

Chapter 5 - Modulation of the rat mesolimbic dopaminergic reward pathway by cannabinoids

5. Chapter 5 - Modulation of the rat mesolimbic dopaminergic reward pathway by cannabinoids

5.1. Introduction

Dopamine was recognised as a neurotransmitter in the late 1950s through the demonstration of its non-uniform distribution in the brain, which suggested a specific functional role for dopamine. Realisation of its role in certain brain diseases, for example Parkinson's disease and schizophrenia, led to a large increase in research.

5.1.1. Dopaminergic receptors and ligands

The dopamine receptor family consists of at least five different receptors, grouped into subfamilies termed D_1-like (D_1 and D_5) and D_2-like (D_2, D_3 and D_4). Both D_1-like and D_2-like receptors are G-protein coupled receptors consisting of a single amino acid chain comprising of seven transmembrane domains interspaced by intracellular and extracellular loops. D_1-like receptors are G_s-protein coupled while D_2-like receptors are $G_{i/o}$-protein coupled (Vallone *et al.*, 2000).

D_1-like receptors have been shown to increase intracellular cAMP levels, resulting in the activation of protein kinase A, and increasing and inhibiting differing calcium and potassium currents. D_1-like receptors also inhibit arachidonic acid synthesis (Vallone *et al.*, 2000). D_2-like receptors induce a wide variety of responses including inhibition of adenylate cyclase, modulation of outward potassium current, and direct G-protein inhibition of voltage operated calcium channels (Vallone *et al.*, 2000).

Within the rat brain the D_1 receptor is mainly expressed in the caudate-putamen, nucleus accumbens (NAcc), olfactory tubercle, cerebral cortex and amygdala. In addition, D_1 receptors have been detected at lower levels in the island of Calleja, in the subthalamic nucleus and in the substantia nigra pars reticulate (Jackson and Westlind-Danielsson, 1994). D_5 receptor expression is more restricted, having only been detected in the hippocampus, lateral mammillary nucleus, and in the parafascicular nucleus of the thalamus. The D_2 receptor is predominantly expressed in the caudate-putamen, NAcc and olfactory tubercle. This receptor is also expressed in the substantia nigra pars compacta and in the ventral tegmental area (VTA). D_3 receptor mRNA is restricted to a few regions including the islands of Calleja, septal nuclei, hypothalamus, and distinct regions of the thalamus and cerebellum. The D_4 receptor is highly expressed in the frontal cortex, amygdala, the olfactory bulb, hippocampus, hypothalamus and mesenchephalon (Jackson and Westlind-Danielsson, 1994). D_1–like receptors are thought to be exclusively postsynaptic while D_2–like receptors may have presynaptic locations (Civelli *et al.*, 1991).

5.1.2. Dopaminergic signalling physiology and psychostimulants

Dopamine, a catecholamine comprising of a catechol group and a ethylamine side chain, is produced from tyrosine by tyrosine hydroxylase and aromatic l-amino acid decarboxylase and stored in secretory vesicles, from which dopamine is directly released into the synapse. After signalling, dopamine is taken up from the synapse by the dopamine transporter into the presynaptic terminal and transported into vesicles by the vesicular monoamine transporter 2 (Gainetdinov *et al.*, 2002). Cocaine blocks the dopamine transporter causing an accumulation of dopamine within the synapse.

Amphetamine enters the presynaptic terminal and vesicle, via the dopamine transporter and the vesicular monoamine transporter 2, causing a disruption in vescular pH gradient and redistribution of dopamine into the cytoplasm. Amphetamine induces a reversal of the dopamine transporter causing a massive outflow of dopamine into the synapse. In addition, amphetamine blocks monoamine oxidase thereby decreasing intracellular metabolism of dopamine (Gainetdinov *et al.*, 2002).

5.1.3. The rat mesocorticolimbic reward pathway

The mesocorticolimbic pathway is considered to play an important role in mediating reward within the brain and is therefore an interesting location to examine the interaction between cannabinoids and other drugs of abuse. The role of psychostimulants is well characterised in the reward pathway, producing an ideal location for investigating interactions with cannabinoids.

5.1.3.1. Neuroanatomy and physiology

The mesocorticolimbic pathway originates as a diffuse collection of soma, located within the anterior ventral limbic forebrain bundle, converging through myelinated moderately fast-conducting pathways to synapse on dopaminergic neurones in the VTA (figure 5.1). Primary excitatory and inhibitory input occurs via glutamatergic (from prefrontal cortex, the pedunculopontine nucleus and the bed nucleus of the stria terminalis) and GABAergic (mainly from the NAcc but also from the ventral pallidum) neurones. Additional modulation has been observed through the actions of

catecholamines, amino acids, neuropeptides and endocannabinoids (Mathon *et al.*, 2003). Within the VTA the principle neurones have been shown to be dopaminergic neurones (Johnson and North, 1992), while secondary neurones are considered to be GABAergic interneurones and projection neurones (Steffensen *et al.*, 1998; Carr and Sesack, 2000). In the brain, dopaminergic neurones are divided into cell groups, ranging from A8 to A17, on the basis of locations originating from and projecting to. The A8-A10 cell groups innervate the substantia nigra, the adjacent retrorubral field and the VTA, with A8 projecting from the retrorubral field to the locus ceruleus and leteral parabrachial nucleus, A9 projecting from the substantia nigra pars compacta to the prefrontal cortex, and A10 projecting from the VTA to the NAcc.

The NAcc forms part of the striatum (Bolam *et al.*, 2000), and comprises mainly (about 90-95% of the neuronal population) of medium-sized spiny neurones (MSNs), a class of GABAergic cells. In the NAcc, MSNs receive extensive glutamatergic input from different limbic areas such as prefrontal cortex, thalamus, hippocampus, and basolateral amygdala, as well as dopaminergic input. Dopaminergic input is mediated by both D_1-like and D_2-like receptors within the NAcc (Spanagel and Weiss, 1999). MSNs project their output to downstream areas of the mesocorticolimbic system like the ventral pallidum, the lateral hypothalamus, and mesencephalic dopaminergic areas (Chang and Kitai, 1985; Groenewegen and Russchen, 1984; Nauta *et al.*, 1978), as well as branching within the NAcc (Pennartz *et al.*, 1991) and projecting to the VTA to provide feedback tonic inhibition (Gardner and Vorel, 1998).

5.1.3.2. Addiction

Within the mesolimbic system addiction is considered to occur through the increased release of dopamine in the NAcc. Cocaine and amphetamine have been shown to act in the NAcc by inhibiting presynaptic dopamine transporters and inducing the release of vesicular monoamines from vesicles to the cytoplasm (Gainetdinov *et al.*, 2002), while opioids are considered to act through the inhibition of GABAergic inhibitory neurones innervating the VTA (Spanagel and Weiss, 1999).

5.1.3.3. Role of cannabinoids within the mesocorticolimbic pathway

Extracellular recordings of spontaneous firings within the VTA in anaesthetised rats were shown to increase in the presence of systemically administered Δ^9-THC and WIN 55,212-2, but not in the presence of the inactive enantiomer WIN 55,212-3 (French *et al.*, 1997a). Further experiments carried out by French (1997b), using single-cell recording techniques, showed systemic exposure to SR141716 not only blocked cannabinoid induced increases in firing rate, but produced a decrease, suggesting tonic activation by endocannabinoids. However, this decrease was not replicated by other *in vivo* studies (Cheer *et al.*, 2003; Gessa *et al.*, 1998). The opioid receptor antagonist naloxone did not affect the cannabinoid response, suggesting that cannabinoids were not acting through GABAergic neurones (French, 1997). Microinjection of Δ^9-THC into the VTA did not increase dopamine release in the NAcc, but increased levels in the VTA. Infusion of the cannabinoid directly into the NAcc increased levels in this dopaminergic terminal area (Chen *et al.*, 1993), suggesting cannabinoid modulation of dopamine release and not firing. Szabo *et al.* (2002) demonstrated, using rat coronal midbrain slices, a SR141716-sensitive, WIN

55,212-2-dependent inhibition of GABA release in the VTA, measured via $GABA_A$ receptor mediated inhibitory postsynaptic currents within dopaminergic neurones. This suggests the presence of CB_1 receptors on GABAergic neurones in the VTA.

A sizeable body of evidence exists demonstrating a cannabinoid dependent increase in dopamine release in the NAcc. *In vivo* studies showed systemic Δ^9-THC increased extracellular concentrations of dopamine in the NAcc in Lewis rats (Chen *et al.*, 1990, 1991). Sprague Dawley rats displayed a reduced increase while no increase was found in Fisher and Long Evans rats (Castaneda *et al.*, 1991). Rodriguez de Fonseca *et al.* (1992) and Navarro *et al.* (1993) showed conflicting levels of dopamine in the NAcc results when examining response to systemic application of cannabinoids *ex vivo*. The differing release of dopamine in response to cannabinoids within the NAcc may be due to increased release being only apparent in sections of the NAcc. Microdialysis experiments showed a SR141716-sensitive cannabinoid dependent increase in extracellular dopamine in the shell, but not the core, of the NAcc, in a manner similar to that induced by heroin (Tanda *et al.*, 1997). μ receptor antagonists inhibited both Δ^9-THC and heroin, which led the authors to suggest a common opioid receptor mediated mechanism governing release, conflicting with the opioid independence observed by French in the VTA. Szabo *et al.* (1999) showed, through the use of fast cyclic voltammetry recordings, cannabinoids did not increase electrically evoked dopamine release in brain slices. This ruled out a presynaptic modulation of dopamine release. Cannabinoids have been shown to act presynaptically to inhibit glutamatergic transmission in the NAcc and so affecting firing of MSNs (Pistis *et al.*, 2002; Robbe *et al.*, 2001, 2002), which feedback to the VTA and so may modulate dopaminergic firing.

Herkenham *et al.* (1991) showed through *in vitro* autoradiography studies a lack of CB_1 receptors in the VTA and intermediate levels in the NAcc. This was substantiated by studies demonstrating the lack of expression of CB_1 receptor mRNA within the VTA (Matsuda *et al.*, 1993) and the presence of CB_1 receptor immunoreactive fibres in the NAcc, but not in the VTA (Tsou *et al.*, 1998; Patel and Hillard, 2003).

In summary, cannabinoids have been shown to reduce GABA release and increased spontaneous firing in dopaminergic neurones within the VTA through electrophysiological studies, but the CB_1 receptor has been shown not to be present in the VTA. Cannabinoids have been shown to inhibit dopamine release in particular segments of the NAcc that are innervated by the mesocorticolimbic pathway and inhibit glutamatergic input into the NAcc.

Evidence for an influence of cannabinoids on spontaneous action potential activity in neurones in the VTA was sought in rat midbrain slices using the blind whole-cell patch-clamp technique.

5.2. Methods

5.2.1. Preparation of rat brain slice

Eighteen to twenty four-day-old Wistar female rats were sacrificed by cervical dislocation and decapitated. The brains were rapidly removed and placed in ice-cold artificial cerebrospinal fluid (ACSF; see section 5.4.3 for composition) gassed with 95% O_2 and 5% CO_2. 300-400 μm thick coronal midbrain slices containing the ventral tegmental area were cut (at 0°C) using a vibratome (1000plus; Vibratome, USA). Slices were stored in a Gibbs chamber (see figure 5.1) containing ACSF. In order to support the recovery of neurones, slices were kept at 35°C for one hour and subsequently stored at room temperature.

5.2.2. Blind whole-cell patch-clamp recordings

Brain slice extracellular recording allows the measurement of small field potentials, which arise from the flow of ionic current through extracellular fluid triggered by neural firing. These are measured by the insertion of a pipette filled with a conducting media (usually 3 M KCl) into the brain or brain slices. To achieve this, the brain slice must be kept in a bath mimicking, as closely as possible, the environment the tissue is exposed to *in vivo* whilst the recording pipette is coarsely positioned. Blind patch-clamp recording in brain slices is a combination of extracellular and whole-cell patch clamping techniques, but instead of the high-magnification visual guidance that is

required for approaching the cell in single-cell patch clamping, proximity to a cell is determined solely through a change in resistance at the pipette tip.

Slices were attached to the glass bottom of a 150 µl superfusion chamber (RC-26; Warner Instruments Inc., USA) with a nylon grid on a stainless steel frame and superfused with ACSF at a flow rate of 1.2 ml/min. The superfusion chamber was maintained at 35°C using a TC324B single channel automatic heater controller (Warner Instruments Inc., USA). Brain segments were observed using a Meiji EMT-2PB stereo microscope (Meiji Techno Co., Japan). The pipette was visually positioned over the VTA and gently lowered into the slice. Contact with surrounding support cells caused a slight increase in resistance. Upon contact with a neurone there would be a further and larger increase in resistance. Techniques for gigaseal and patch formation are detailed in section 2.4.2.

5.2.2.1. Patch clamp techniques: current clamp

To observe spontaneous action potentials, membrane potential was allowed to fluctuate at will although a fixed current, determined by the current required to maintain a holding potential of -70 mV, was passed into the cell to account for leakage via the patch.

5.2.3. Analysis of data

Significant difference between mean values were calculated using the Friedman test, a non-parametric repeat measures test, followed by a Dunn multiple comparison *post hoc* test, with a P value of < 0.05 being taken as significant.

5.2.4. Solutions

Brain slices were maintained in artificial cerebral-spinal fluid (ACSF), which contained (mM): NaCl 126, KCl 2.5, $MgCl_2$ 1.2, NaH_2PO_4 1.2, $NaHCO_3$ 21.4, glucose 11.1, $CaCl_2$ 2.4, ascorbic acid 0.1. All drugs were administered in ACSF, superfused at a rate of 1.2 ml/min.

5.2.5. Drugs

Dopamine (SigmaAldrich, UK) was dissolved in 0.1 M citric acid and kept on ice. Fresh solution were prepared daily. Other drugs used are detailed in previous chapters.

5.3. Results

Electrical recordings were obtained from 15 slices obtained from 12 animals. On patching a spontaneous action potential was observed displaying a transient depolarisation, followed by a hyperpolarisation (figure 5.2). Action potentials fired at a mean rate of 4.4 ± 0.8 Hz (n = 10).

5.3.1. Effects of dopamine on spontaneous firing frequency

Application of 1 μM dopamine significantly decreased mean firing rate to 3.2 ± 1.0 Hz and 3.2 ± 1.0 Hz after 1.5 and 2.5 minutes respectively (n = 6, $P < 0.01$, Friedman's test, figure 5.3a and b). *Post hoc* comparison with control reported a P value of < 0.05 for both 1.5 and 2.5 minutes (Dunn's test). 10 μM dopamine significantly decreased mean firing rate to 2.5 ± 1.2 Hz and 2.3 ± 1.2 Hz after 1.5 and 2.5 minutes respectively (n = 6, $P < 0.05$, Friedman's test). *Post hoc* comparison with control showed significance at 2.5 minutes ($P < 0.05$, Dunn's test)

5.3.2. Effects of CP 55,940 on spontaneous firing frequency

Application of 10 μM CP 55,940 induced no change in firing rate, producing a mean firing rate after 1.5 and 2.5 minutes of 4.3 ± 1.4 Hz and 4.5 ± 1.3 Hz respectively (n = 5, figure 5.3).

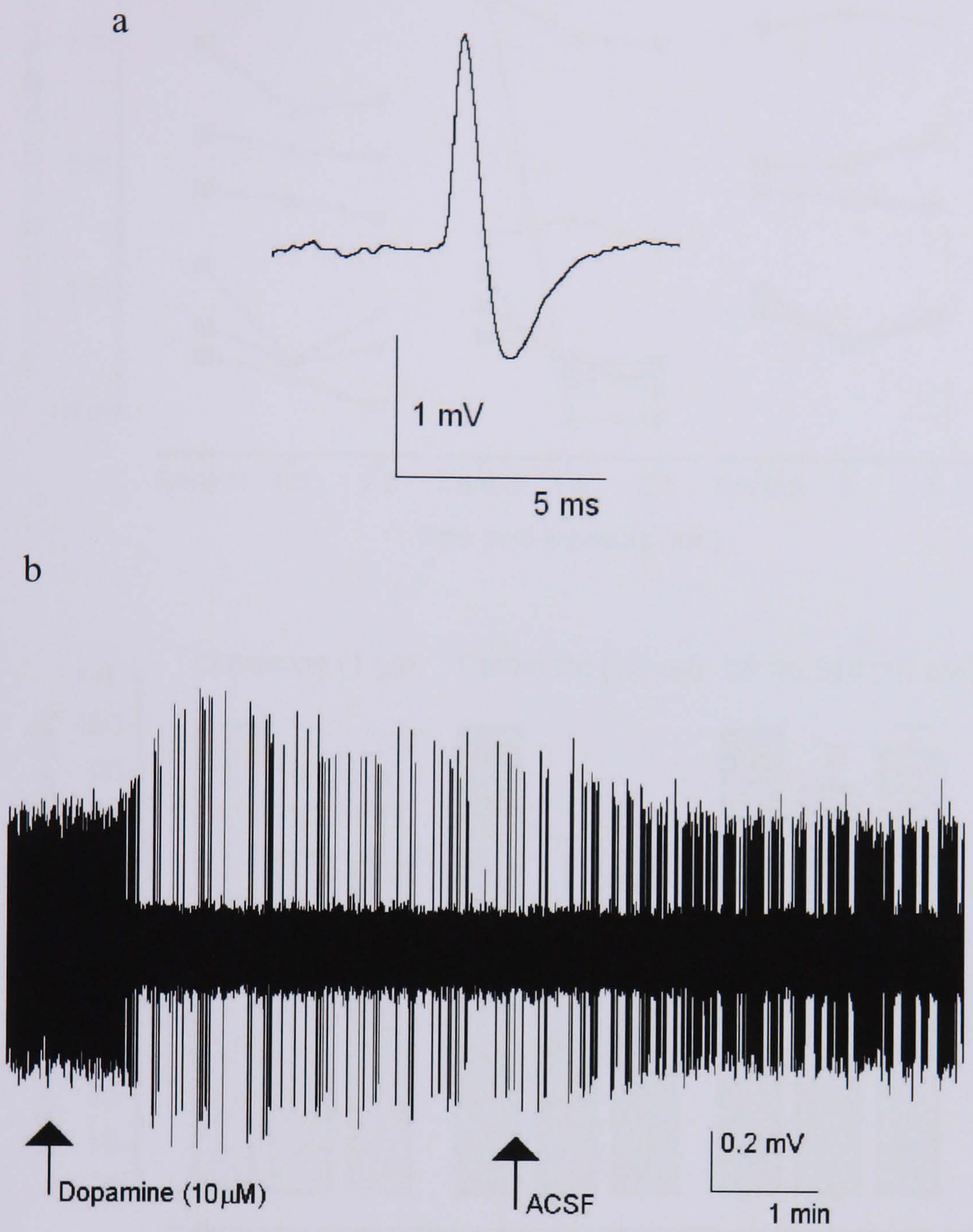

Figure 5.2 (a) Sample spontaneous action potential recorded from a neurone within the VTA of a rat brain slice through the use of blind patch clamping. (b) Sample recording from a neurone within the VTA demonstrating the reduction in firing frequency induced by application of dopamine.

a

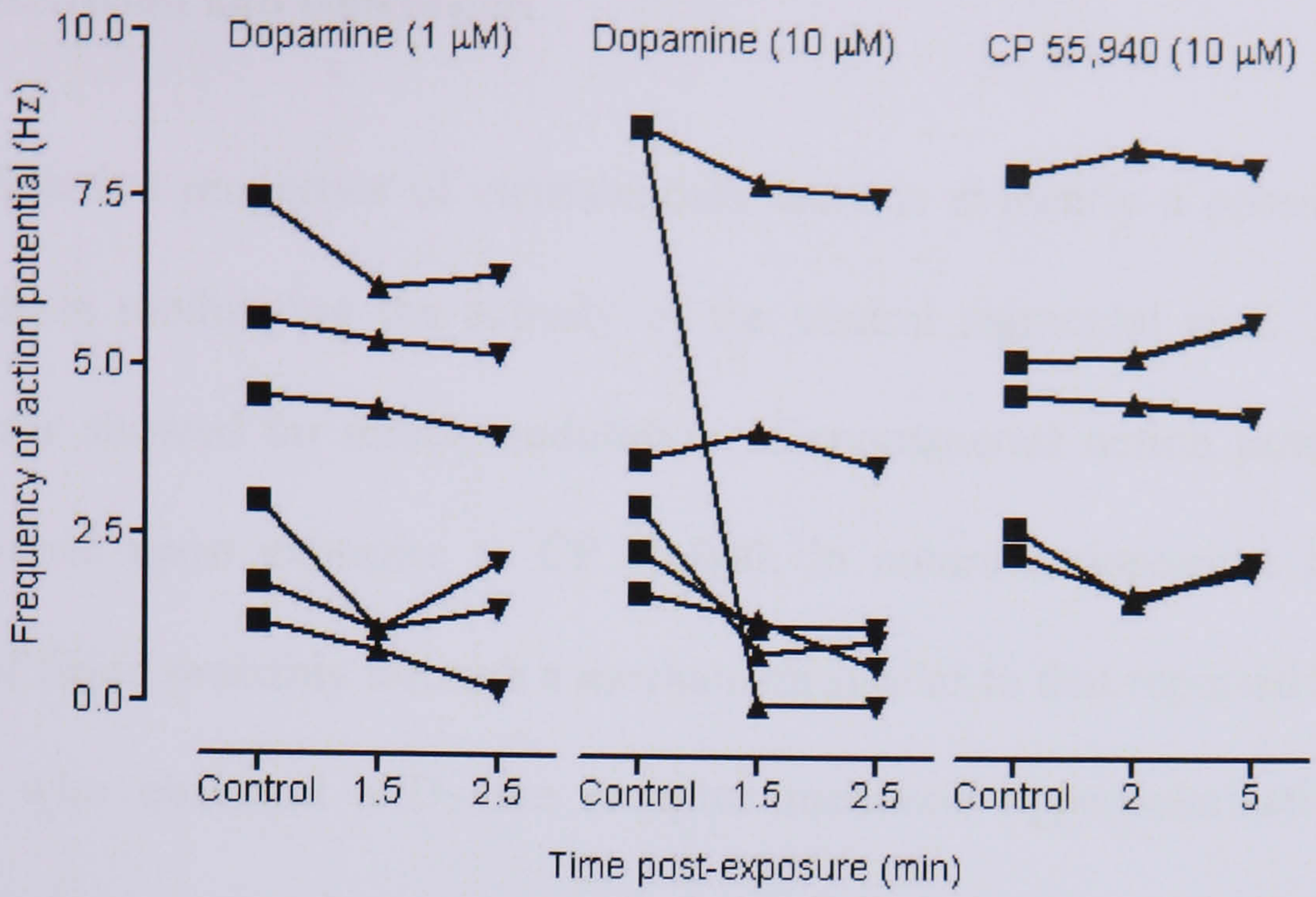

b

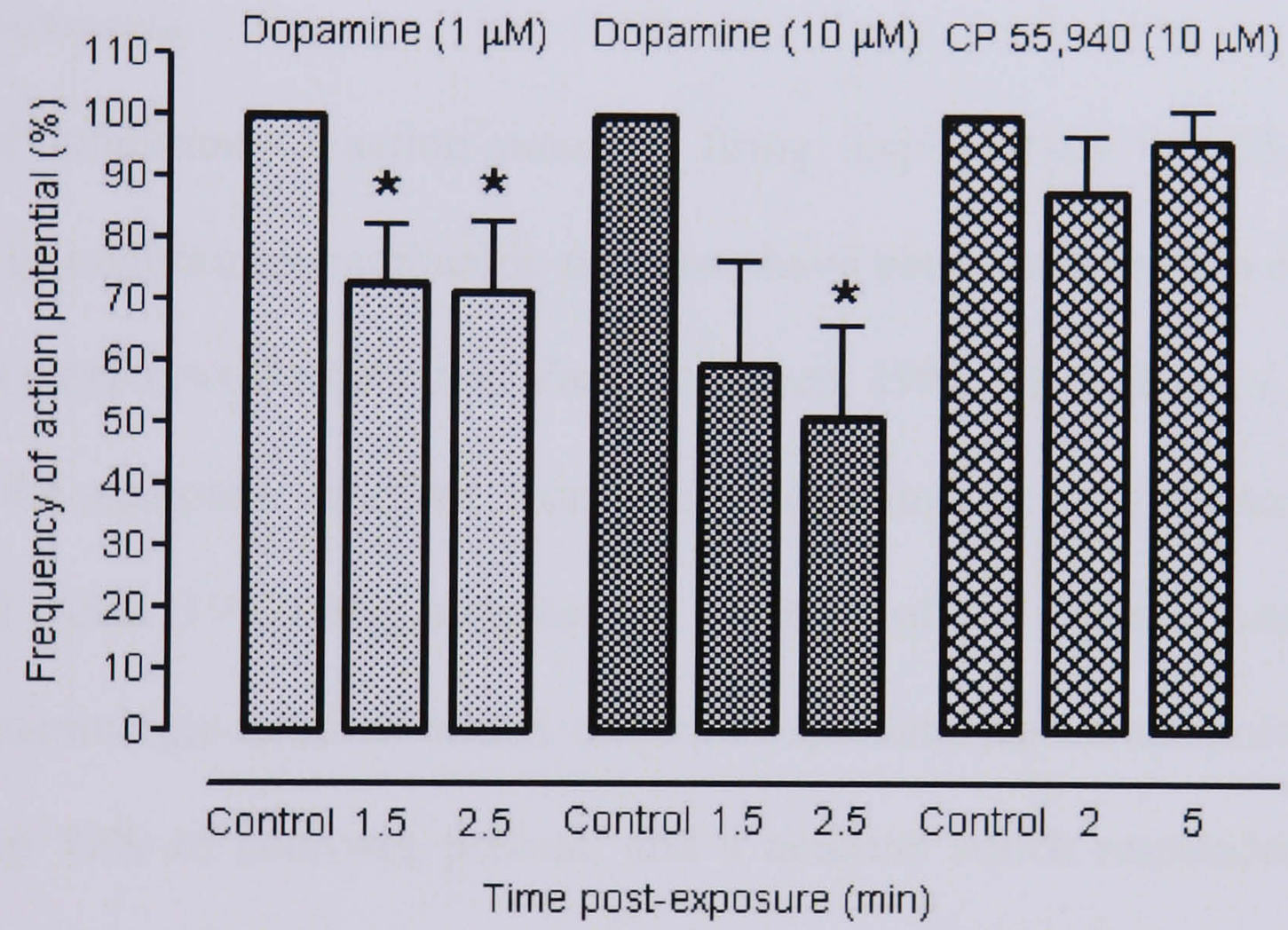

Figure 5.3 Modulation of spontaneous firing frequency in neurones within the VTA by dopamine and CP 55,940. (a) Each line represents the firing frequency of a single cell over a period of time prior to and post application of dopamine (1 and 10 μM) and CP 55,940 (10 μM). (b) Each column represents the mean firing frequency, expressed as a percentage of untreated firing frequency at differing time points prior to and post application of dopamine (1 μM, n = 6 and 10 μM, n = 6) and CP 55,940 (10 μM, n = 5). Vertical lines indicate S.E.M. The significance of the difference between columns was calculated using Friedman's test followed by Dunn's test with * indicating a significant difference of $p < 0.05$ versus control.

5.4. Discussion and conclusion

With the addictive properties of cannabinoids there is evidently a possible role for cannabinoids in modulating the activity of the ventral tegmental area. The present data, however showed no direct modulation of spontaneous action potential firing within neurones upon exposure to CP 55,940. In contrast, dopamine reduced the frequency of firing probably through a mechanism similar to that reported by Lacey *et al.* (1987), who observed a D_2-like receptor mediated hyperpolarisation through increasing potassium conductance in A9 dopaminergic neurones in the substantia nigra zona compacta.

The lack of inhibition of action potential firing displayed by CP 55,940 is not unexpected as midbrain dopaminergic neurones have been shown not to express CB_1 cannabinoid receptors (Mailleux and Vanderhaeghen, 1992; Matsuda *et al.*, 1993).

Proof that the neurones recorded from were dopaminergic was demonstrated by Johnson and North (1992) who observed the presence of two types of neurone in the VTA, a dopaminergic neurone which displayed spontaneous action potential firing and made up 77% of neurones present, and a neurone which responded to opioid agonists and did not show spontaneous firing.

Within the VTA in rat brain slices, Szabo and colleagues reported WIN 55,212-2 to elicit inhibition of electrically induced GABA release from adjoining neurones onto dopaminergic neurones. Direct action at $GABA_A$ receptors on dopaminergic neurones was excluded through the observation that WIN 55,212-2 did not alter miniature IPSP, a measure of spontaneous opening of $GABA_A$ channels (Szabo *et al.*, 2002). In support of this study, extracellular recordings of VTA neural firing in rat brain slices was shown to be increased by the synthetic cannabinoid agonist HU210 (Cheer *et al.*,

2000). Bicuculline also increased the firing rate of VTA neurones and occluded the effect of the synthetic cannabinoid HU210 (Cheer *et al.*, 2000).

In conclusion, data derived in this and other studies suggest cannabinoids do not directly modulate the firing of VTA dopaminergic neurones, but may act to suppress inhibitory regulation of these neurones by GABAergic neurones within the VTA.

The aim of this chapter was to investigate the interaction between cannabinoids and psychostimulants in the VTA. Unfortunately, difficulties in preparing viable slices led to the prevention of further work in this area. A brief sabbatical to the laboratory of Prof. Henderson in Bristol confirmed the quality of techniques and equipment employed in the preparation of slices, but unfortunately did not improve the quality of slices derived. One possible cause for this difficulty may have been the distance between rooms in which sacrifice occurred and recording performed. Shaking during transport may have caused physical damage to tissue, while lack of oxygenation may have resulted in oxygen starvation.

General Conclusion

6. General Conclusion

With the recent discovery of cannabinoid receptors and endogenous ligands for these receptors and the rising illegitimate use of cannabis the necessity for further research into the role cannabinoids play in the body has become apparent. This has been further emphasised by the growing use of cannabinoid ligands in the treatment of pathological conditions, examples of which include the use of Sativex for the treatment of neuropathic pain in multiple sclerosis sufferers and Marinol for the treatment of anorexia associated with weight loss in AIDS patients.

Although cannabinoid inhibition, through a SR141716 sensitive pathway, of gastrointestinal motility and electrically evoked contraction of the MPLM was first observed over ten years ago (Pertwee *et al.*, 1996; Izzo *et al.*, 1999), few studies have been performed to try to establish the mechanisms by which inhibition occurs. The presence of the CB_1 receptor was confirmed with binding and immunohistochemical studies (Lynn & Herkenham, 1994; Coutts *et al.*, 2002), and by the detection of CB_1 receptor mRNA within the MPLM (Griffin *et al.*, 1997). Debate as to whether the CB_1 receptor was the only mechanism through which cannabinoid ligands act in the intestinal tract was sparked by the observation by Mang *et al.* (2001) of a mechanism through which cannabinoid agonists act that requires higher SR141716 concentrations than expected for action at the CB_1 receptor. Intracellular recording of action potentials in myenteric S-type neurones *in vitro* by Lopez-Redondo *et al.* (1997) suggested CB_1 receptor independent cannabinoid activity through SR141716 alone producing inhibition, while DeMuth *et al.* (2004) observed a SR141716-independent

cannabinoid inhibition of nicotinic currents through a $G_{i/o}$-protein independent mechanism.

6.1. The interaction between cannabinoids and the nACh receptor in the guinea-pig ileum myenteric plexus

Within the enteric nervous system, the nicotinic acetylcholine receptor predominantly mediates interneuronal excitatory transmission (Galligan & North, 2004). Oz and colleagues reported cannabinoid inhibition of nicotinic α7 homomeric receptors, expressed in *Xenopus* oocytes, through a CB_1 and CB_2 receptor independent mechanism, suggesting cannabinoids may act through this mechanism to inhibit intestinal motility (Oz *et al.*, 2003; 2004). Through the use of nicotine evoked contraction of the MPLM preparation, this study observed cannabinoid inhibition occurring through both a CB_1 receptor dependent and an independent mechanism. These mechanisms demonstrated some degree of selectivity dependent upon the level of stimulus evoked by nicotine, with contraction evoked by 100 μM nicotine demonstrating CB_1 receptor independence whilst contraction evoked by 10 μM nicotine showed SR141716 sensitivity. This decrease in sensitivity to cannabinoids may resemble the decreased sensitivity to morphine observed with higher frequency electrically induced acetylcholine release in the MPLM (Cowie *et al.*, 1968). Higher concentrations of nicotine may result in a large depolarisation of the soma and so initiate the firing of multiple action potentials, in a manner similar to that evoked by high frequency electrical stimulation, while lower concentrations of nicotine may result in a single firing of or provoke a low frequency firing of action potential similar to that evoked by low frequency electrical stimulation and so possess more

susceptibility to a G-protein mediated inhibition. This would suggest that the CB_1 receptor acts to inhibit an action potential, but in doing so induces some form of desensitisation allowing high frequency trains of action potentials to overcome inhibition. This work also suggests, with the suppression of the CB_1 receptor, a CB_1 receptor independent mechanism also exists through which cannabinoids, at higher concentrations, act to inhibit nicotine evoked contraction.

Cannabinoid inhibition of nicotinic receptors in cultured myenteric neurones was confirmed using the whole cell patch clamp technique. Similar levels of inhibition of nicotine evoked current by both active and inactive WIN 55,212 stereoisomers suggested activity through a CB_1 and CB_2 receptor independent mechanism. Previous work observed inhibition by PEA, an endogenous cannabinoid shown to be inactive at CB_1 and CB_2 receptors, and showed not only a lack of blockade by SR141716, but an inhibition by this CB_1 receptor selective antagonist (DeMuth *et al.*, 2004). Furthermore, previous data showed inhibition was not sensitive to either pertussis toxin treatment, while current work observed no modulation of inhibition by the membrane-permeable cAMP analogue 8-Br-cAMP, suggesting inhibition involved a mechanism independent of the $G_{i/o}$-protein and the adenylate cyclase/cAMP intracellular signalling mechanisms. Although it is possible that inhibition may be occurring through an unknown receptor and second messenger mediated pathway, the lack of effect of PTX and 8-Br-cAMP, coupled with the work of Oz and colleagues (Oz, 2006), suggests that a direct cannabinoid action on the nicotinic receptor may be occurring.

Arachadonic acid, a metabolite of anandamide, has been reported to inhibit *Torpedo* and chick α7 nicotinic receptors, expressed in oocytes, through a blockade of the Ca^{2+}-modulatory sites (Nishizaki *et al.*, 1998). Further work examining whether the

cannabinoid inhibition observed occurred through this mechanism would be intriguing.

6.2. Cannabinoid modulation of calcium channel activity in guinea-pig myenteric AH neurones

CB_1 receptor inhibition of N-type voltage-gated calcium channels was first observed in 1992 (Mackie & Hille, 1992; Caulfield & Brown, 1992). In the enteric nervous system the N-type voltage-gated calcium channel has been shown to play a major role in governing the action potential in AH-neurones (Hirst *et al.*, 1974; Rugiero *et al.*, 2002). Using the whole cell patch clamp technique, the cannabinoid CB_1 and CB_2 receptor agonists CP 55,940 and WIN 55,212-2 were shown to inhibit voltage-gated calcium currents in cultured myenteric neurones. However, the CB_1 receptor specific antagonists SR141716 and AM251, and the CB_2 receptor specific antagonist SR144528 did not prevent CP 55,940 inhibition, but when both CB_1 and CB_2 receptor antagonists were applied, blockade of CP 55,940 action was observed. Inhibition was both pertussis toxin sensitive and showed some stereospecificity suggesting action through a $G_{i/o}$-protein coupled receptor. Intriguingly, at 10 μM SR141716 and the "silent" CB_1 receptor antagonist O2050 induced inhibition of voltage-gated calcium currents. These findings led us to hypothesise that either cultured myenteric neurones express both CB_1 and CB_2 receptors and SR141716, at 10 μM acts non-specifically to produce inhibition, or that a novel non-CB_1, CB_2 $G_{i/o}$-protein coupled receptor may exist possessing multiple binding sites for cannabinoids presenting sensitivity to either CB_1 or CB_2 receptor antagonists. The likelihood of the CB_2 receptor being present is strengthened by the work of Mathison *et al.* (2004) and Duncan *et al.* (2005; 2006)

who reported the presence of the CB_2 receptor in rat ileum after LPS treatment. This opens up the possibility that the act of culturing myenteric neurones may be evoking expression of the CB_2 receptor. Alternatively, the presence of a novel cannabinoid receptor is supported by the reported blockade by SR141716 of cannabinoid inhibition at higher concentrations than expected for action at the CB_1 receptor (Mang *et al.*, 2001). In this study, the high concentration of cannabinoid agonists may have masked the reduced inhibition produced by SR141716, resulting in the lack of inhibition observed. Further investigation into the presence of the CB_2 receptor, through the use of CB_2 receptor selective agonists and using immunohistochemical or binding studies, would prove interesting, distinguishing which proposed mechanism governed observed effects.

6.3. Cannabinoid modulation of opioid activity in guinea-pig myenteric neurones and NG108-15 neurones

A growing body of literature suggests an interaction between cannabinoids and opioids may exist in the CNS, while within the gut, studies have shown the existence of some interaction in governing agonist withdrawal (Basilico *et al.*, 1999). In this study, examination of cannabinoids and opioids in the inhibition of electrically evoked contraction of the MPLM preparation suggests an interaction occurs between cannabinoid and opioid signalling pathways at high concentrations of agonist in which an inhibition of response is observed. The observation that maximal opioid inhibition of electrically evoked contraction in the presence of 100 nM CP 55,940 was smaller than that produced in the presence of 10 nM CP 55,940 suggests depletion of a shared pool of intracellular messenger is not responsible for this blockade, as a

similar level of inhibition would be expected with 10 and 100 nM CP 55,940 should a shared second messenger be depleted. As a result this suggests that CP 55,940 acts upon the ileum through multiple pathways, one independent of, and another interacting with opioid pathways.

The increased morphine inhibition in the presence of SR141716 poses an interesting story. Should the increase in size of contraction observed with exposure to SR141716 be due to the blockade of endogenous cannabinoid inhibition, and should these endogenous cannabinoids act in a similar manner to low concentrations of CP 55,940, then morphine would be expected to produce an inhibition similar to that produced in the absence of cannabinoids. However, the observed increased opioid inhibition disputes this hypothesis suggesting the effects produced by SR141716 may be due to inverse agonism or action at an alternate site.

Unfortunately, a lack of opioid activity in cultured myenteric neurones led to the examination of interaction in NG108-15 neurones. However, difficulties in maintenance of cultures resulted in the cessation of this avenue of research, but preliminary data did suggest that some degree of reduction in morphine inhibition of calcium currents by WIN 55,212-2 was present, supporting the premise of cannabinoid and opioid interaction. Further work into the intracellular mechanisms through which this interaction occurs would provide interesting support to the findings and may provide help in the treatment of opioid withdrawal and open up greater opportunities for the medicinal use of opioids.

6.4. Modulation of the rat mesolimbic dopaminergic reward pathway by cannabinoids

With the growing use of cannabis as a drug of abuse, further work into elucidating the mechanism by which addiction occurs is necessary. The mesolimbic pathway plays a major role in governing reward, with addiction occurring as a result of increased release of dopamine in the NAcc. Using the blind whole cell patch clamp technique, CP 55,940 was shown not to modulate spontaneous action potential firing in dopaminergic neurones within the rat ventral tegmental area. This was expected as midbrain dopaminergic neurones have been shown not to express CB_1 cannabinoid receptors (Mailleux & Vanderhaeghen, 1992; Matsuda *et al.*, 1993). However, work by Szabo *et al.* (2002) reported cannabinoid inhibition of GABAergic neurones within the VTA, suggesting cannabinoids may act in a manner similar to opioids. Unfortunately, difficulties in deriving and maintaining viable slices made work in this area unfeasible, even though a possible interaction between cannabinoids and opioids on GABAergic neurones within the VTA would prove very interesting.

In summary, a growing wealth of evidence is developing suggesting the presence of more sites of action for cannabinoids than the accepted CB_1 and CB_2 receptors. This is certainly true within the intestinal tract where data suggests multiple sites of action for cannabinoids exist.

Chapter 7- References

7. Chapter 7- References

Abood, M.E. and Martin, B.R. (1996). Molecular neurobiology of the cannabinoid receptor. *Int. Rev. Neurobiol.*, **39**, 197-221.

Arias, H.R. (1998). Noncompetitive inhibition of nicotinic acetylcholine receptors by endogenous molecules. *J. Neurosci. Res.*, **52**, 369-379.

Baidan, L.V., Zholos, A.V., Shuba, M.F. and Wood, J.D. (1992). Patch-clamp recording in myenteric neurons of guinea pig small intestine. *Am. J. Physiol. (Lond.),* **262**, G1074-G1078.

Bagnol, D., Mansour, A., Akil, H. and Watson, S.J. (1997). Cellular localization and distribution of the cloned mu and kappa opioid receptors in rat gastrointestinal tract. *Neuroscience*, **81**, 579–591.

Barann, M., Molderings, G., Bruss, M., Bonisch, H., Urban, B.W. and Gothert, M. (2002). Direct inhibition by cannabinoids of human 5-HT_{3A} receptors: probable involvement of an allosteric modulatory site. *Br. J. Pharmacol.*, **137**, 589-596.

Barbuti, A., Ishii, S., Shimizu, T., Robinson, R. B. and Feinmark, S. J. (2002). Block of the background $K(^{+})$ channel TASK-1 contributes to arrhythmogenic effects of platelet-activating factor. *Am. J. Physiol. (Lond.),* **282**, H024–H030.

Bartho, L., Sebok, B. and Szolcsanyi, J. (1982). Indirect evidence for the inhibition of enteric substance P neurones by opiate agonists but not by capsaicin. *Eur. J. Pharmacol.*, **77**, 273-279.

Bartoo, A.C., Sprunger, L.K. and Schneider, D.A. (2005). Expression and distribution of TTX-sensitive sodium channel alpha subunits in the enteric nervous system. *J. Comp. Neurol.*, **486**, 117-131.

Basilico, L., Parolaro, D., Colleoni, M., Costa, B. and Giagnoni, G. (1999). Cross-tolerance and convergent dependence between morphine and cannabimimetic agent WIN 55,212-2 in the guinea-pig ileum myenteric plexus. *Eur. J. Pharmacol.*, **376**(3), 265-271.

Bass, C.E., Griffin, G., Grier, M., Mahadevan, A., Razdan, R.K. and Martin, B.R. (2002). SR-141716A-induced stimulation of locomotor activity. A structure-activity relationship study. *Pharmacol. Biochem. Behav.*, **74**, 31-40.

Bayewitch, M., Avidor-Reiss, T., Levy, R., Barg, J., Mechoulam, R. and Vogel, Z. (1995). The peripheral cannabinoid receptor: adenylate cyclase inhibition and G protein coupling. *FEBS Lett.*, **375**, 143–147.

Bayewitch, M., Rhee, M.H., Avidor-Reiss, T., Breuer, A., Mechoulam, R. and Vogel, Z. (1996). (-)-Δ^9-tetrahydrocannabinol antagonizes the peripheral cannabinoid receptor-mediated inhibition of adenylyl cyclase. *J. Biol. Chem.*, **271**, 9902-9905.

Bell, M.R., D'Ambra, T.E., Kumar, V., Eissenstat, M.A., Herrmann, J.L., Wetzel, J.R., Rosi, D., Philion, R.E., Daum, S.J., Hlasta, D.J., Kullnig, R.K., Ackerman, J.H., Haubrich, D.R., Luttinger, D.A., Baizman, E.R., Miller, M.S. and Ward, S.J. (1991) Antinociceptive (aminoalkyl)indoles. *J. Med. Chem.*, **34**, 1099–1110.

Begg, M., Baydoun, A., Parsons, M.E. and Molleman, A. (2001). Signal transduction of cannabinoid CB_1 receptors in a smooth muscle cell line. *J. Physiol. (Lond.),* **531**, 95–104.

Begg, M., Mo, F.M., Offertaler, L., Batkai, S., Pacher, P., Razdan, R.K., Lovinger, D.M. and Kunos, G. (2003). G protein-coupled endothelial receptor for atypical cannabinoid ligands modulates a Ca^{2+}-dependent K^+ current. *J. Biol. Chem.*, **278**, 46188-46194.

Begg, M., Molleman, A. and Parsons, M. (2002). Modulation of the release of endogenous gamma-aminobutyric acid by cannabinoids in the guinea pig ileum. *Eur. J. Pharmacol.*, **434**, 87-94.

Ben-Shabat, S., Fride, E., Sheskin, T., Tamiri, T., Rhee, M.-H., Vogel, Z., Bisogno, T., De Petrocellis, L., Di Marzo, V. and Mechoulam, R. (1998). An entourage effect: inactive endogenous fatty acid glycerol esters enhance 2-arachidonoyl-glycerol cannabinoid activity. *Eur. J. Pharmacol.*, **353**, 23–31.

Benito, C., Nunez, E., Tolon, R.M., Carrier, E.J., Rabano, A., Hillard, C.J. and Romero, J. (2003). Cannabinoid CB_2 receptors and fatty acid amide hydrolase are

selectively overexpressed in neuritic plaque-associated glia in Alzheimer's disease brains. *J. Neurosci.*, **23**, 11136-11141.

Betz, H., Kuhse, J., Schmieden, V., Laube, B., Kirsch, J. and Harvey, R. J. (1999). Structure and functions of inhibitory and excitatory glycine receptors. *Ann. N. Y. Acad. Sci.*, **868**, 667–676.

Bidaut-Russell, M., Devane, W.A. and Howlett, A.C. (1990). Cannabinoid receptors and modulation of cyclic AMP accumulation in the rat brain. *J. Neurochem.*, **55**, 21-26.

Bisogno, T., Melck, D., Bobrov, M.Yu., Gretskaya, N.M., Bezuglov, V.V., De Petrocellis, L. and Di Marzo, V. (2000). N-acyl-dopamines: novel synthetic CB_1 cannabinoid-receptor ligands and inhibitors of anandamide inactivation with cannabimimetic activity in vitro and in vivo. *Biochem. J.*, **351**, 817-824.

Bodewei, R., Hering, S., Schubert, B. and Wollenberger A. (1985). Sodium and calcium currents in neuroblastoma x glioma hybrid cells before and after morphological differentiation by dibutyryl cyclic AMP. *Gen. Physiol. Biophys.*, **4**, 113-127.

Bolam, J.P., Hanley, J.J., Booth, P.A. and Bevan, M.D. (2000). Synaptic organisation of the basal ganglia. *J. Anat.*, **196**, 527-542.

Bolton, T.B. and Zholos, A.V. (1997). Activation of M_2 muscarinic receptors in guinea-pig ileum opens cationic channels modulated by M_3 muscarinic receptors. *Life Sci.*, **60**, 1121-1128.

Bonhaus, D.W., Chang, L.K., Kwan, J. and Martin, G.R. (1998). Dual activation and inhibition of adenylyl cyclase by cannabinoid receptor agonists: evidence for agonist-specific trafficking of intracellular responses. *J. Pharmacol. Exp. Ther.*, **287**, 884-888.

Bornstein, J.C., Furness, J.B. and Kunze, W.A.A. (1994). Electrophysiological characterization of myenteric neurons: how do classification schemes relate? *J. Auton. Nerv. Syst.*, **48**, 1-15.

Bouaboula, M., Perrachon, S., Milligan, L., Canat, X., Rinaldi-Carmona, M., Portier, M., Barth, F., Calandra, B., Pecceu, F., Lupker, J., Maffrand, J.-P., Le Fur, G. and Casellas, P. (1997). A selective inverse agonist for central cannabinoid receptor inhibits mitogen-activated protein kinase activation stimulated by insulin or insulin-like growth factor 1. Evidence for a new model of receptor/ligand interactions. *J. Biol. Chem.*, **272**, 22330–22339.

Bouaboula, M., Poinot-Chazel, C., Marchand, J., Canat, X., Bourrie, B., Rinaldi-Carmona, M., Calandra, B., Le Fur, G. and Casellas, P. (1996). Signalling pathway associated with stimulation of CB_2 peripheral cannabinoid receptor. Involvement of both mitogen-activated protein kinase and induction of Krox-24 expression. *FEBS Lett.*, **237**, 704–711.

Bouaboula, M., Poinot-Chazel, C., Bourrie, B., Canat, X., Calandra, B., Rinaldi-Carmona, M., Le Fur, G. and Casellas, P. (1995). Activation of mitogen-activated protein kinases by stimulation of the central cannabinoid receptor CB_1. *Biochem. J.*, **312**, 637-641.

Bowery, N.G., Hudson, A.L. and Price, G.W. (1987). $GABA_A$ and $GABA_B$ receptor site distribution in the rat central nervous system. *Neuroscience*, **20**, 365–383.

Braida, D., Pozzi, M., Parolaro, D. and Sala, M. (2001). Intracerebral self-administration of the cannabinoid receptor agonist CP 55,940 in the rat: interaction with the opioid system. *Eur. J. Pharmacol.*, **413**, 227–234.

Breivogel, C.S., Griffin, G., Di Marzo, V. and Martin, B.R. (2001). Evidence for a new G protein-coupled cannabinoid receptor in mouse brain. *Mol. Pharmacol.*, **60**(1), 155-163.

Breivogel, C.S., Selley, D.E. and Childers, S.R. (1998). Cannabinoid receptor agonist efficacy for stimulating [^{35}S]GTPγS binding to rat cerebellar membranes correlates with agonist-induced decreases in GDP affinity. *J. Biol. Chem.*, **273**, 16865-16873.

Breivogel, C.S., Sim, L.J. and Childers, S.R. (1997). Regional differences in cannabinoid receptor/G-protein coupling in rat brain. *J. Pharmacol. Exp. Ther.*, **282**, 1632–1642.

Brookes, S.J., Meedeniya, A.C., Jobling, P. and Costa, M. (1997). Orally projecting interneurones in the guinea-pig small intestine. *J. Physiol. (Lond.),* **505**, 473-491.

Brookes, S.J., Song, Z.M., Steele, P.A. and Costa, M. (1992). Identification of motor neurons to the longitudinal muscle of the guinea pig ileum. *Gastroenterology*, **103**, 961-973.

Brookes, S.J.H., Song, Z.M., Ramsay, G.A. and Costa, M. (1995). Long aboral projections of Dogiel type II, AH neurons within the myenteric plexus of the guinea pig small intestine. *J. Neurosci.*, **15**, 4013–4022.

Brookes, S.J., Steele, P.A. and Costa, M. (1991a). Calretinin immunoreactivity in cholinergic motor neurones, interneurones and vasomotor neurones in the guinea-pig small intestine. *Cell. Tissue Res.*, **263**, 471-481.

Brookes, S.J., Steele, P.A. and Costa, M. (1991b). Identification and immunohistochemistry of cholinergic and non-cholinergic circular muscle motor neurons in the guinea-pig small intestine. *Neuroscience*, **42**, 863-878.

Brown, A. and Wise, A. (2003). GlaxoSmithKline, assignee. Identification of modulators of GPR55 activity. US patent 0 113 814.

Brown, D.A. and Higashida, H. (1988). Voltage- and calcium-activated potassium currents in mouse neuroblastoma x rat glioma hybrid cells. *J. Physiol.*, **397**, 149-165.

Cabral, G.A. (2001). Marijuana and cannabinoids: effects on infections, immunity and AIDS. *J. Cannabis Ther.*, **1**, 61–85.

Calandra, B., Portier, M., Kerneis, A., Delpech, M., Carillon, C., Le Fur, G., Ferrara, P. and Shire, D. (1999). Dual intracellular signaling pathways mediated by the human cannabinoid CB_1 receptor. *Eur. J. Pharmacol.*, **374**, 445-455.

Calignano, A., La Rana, G., Giuffrida, A. and Piomelli, D. (1998). Control of pain initiation by endogenous cannabinoids. *Nature*, **394**, 277–281.

Calignano, A., La Rana, G. and Piomelli, D. (2001). Antinociceptive activity of the endogenous fatty acid amide, palmitylethanolamide. *Eur. J. Pharmacol.*, **419**, 191-198.

Cantley, L.C. (2002). The phosphoinositide 3-kinase pathway. *Science*, **296**, 1655-1657.

Capasso, R., Izzo, A.A., Fezza, F., Pinto, A., Capasso, F., Mascolo, N. and Di Marzo, V. (2001). Inhibitory effect of palmitoylethanolamide on gastrointestinal motility in mice. *Br. J. Pharmacol.*, **134**, 945-950.

Capogna, M., Gahwiler, B.H. and Thompson, S.M. (1993). Mechanism of μ-opioid receptor-mediated presynaptic inhibition in the rat hippocampus in vitro. *J. Physiol. (Lond.)*, **470**, 539-558.

Carlisle, S.J., Marciano-Cabral, F., Staab, A., Ludwick, C. and Cabral, G.A. (2002). Differential expression of the CB_2 cannabinoid receptor by rodent macrophages and macrophage-like cells in relation to cell activation. *Int. Immunopharmacol.*, **2**, 69-82.

Carr, D.B. and Sesack, S.R. (2000) GABA-containing neurons in the rat ventral tegmental area project to the prefrontal cortex. *Synapse*, **38**, 114-123.

Carta, G., Nava, F. and Gessa, G.L. (1998). Inhibition of hippocampal acetylcholine release after acute and repeated Δ^9-tetrahydrocannabinol in rats. *Brain Res.*, **809**, 1-4.

Castaneda, E., Moss, D.E., Oddie, S.D. and Whishaw, I.Q. (1991). THC does not affect striatal dopamine release: microdialysis in freely moving rats. *Pharmacol. Biochem. Behav.*, **40**, 587-591.

Caterina, M.J. (2003). Vanilloid receptors take a TRP beyond the sensory afferent. *Pain*, **105**, 5-9.

Caterina, M.J. and Julius, D. (2001). The vanilloid receptor: a molecular gateway to the pain pathway. *Annu, Rev, Neurosci.*, **24**, 487–517.

Caterina, M.J., Schumacher, M.A., Tominaga, M., Rosen, T.A., Levine, J.D. and Julius, D. (1997). The capsaicin receptor: a heat activated ion channel in the pain pathway. *Nature*, **389**, 816–824.

Catterall, W.A., Perez-Reyes, E., Snutch, T.P. and Striessnig, J. (2005). International Union of Pharmacology. XLVIII. Nomenclature and structure-function relationships of voltage-gated calcium channels. *Pharmacol. Rev.*, **57**, 411-425.

Caulfield, M.P. and Brown, D.A. (1992). Cannabinoid receptor agonists inhibit Ca current in NG108-15 neuroblastoma cells via a Pertussis toxin-sensitive mechanism. *Br. J. Pharmacol.*, **106**, 231-232.

Chakrabarti, A., Onaivi, E.S. and Chaudhuri, G. (1995). Cloning and sequencing of a cDNA encoding the mouse brain-type cannabinoid receptor protein. *DNA Sequence*, **5**, 385–388.

Chang, H.T. and Kitai, S.T. (1985). Projection neurons of the nucleus accumbens: an intracellular labeling study. Brain Res., **347**, 112-116.

Chang, K.J., Miller, R.J. and Cuatrecasas, P. (1978). Interaction of enkephalin with opiate receptors in intact cultured cells. *Mol. Pharmacol.*, **14**, 961-970.

Chaperon, F., Soubrie, P., Puech, A.J. and Thiebot, M.H. (1998). Involvement of central cannabinoid (CB_1) receptors in the establishment of place conditioning in rats. *Psychopharmacology (Berl.)*, **135**, 324–332.

Cheer, J.F., Kendall, D.A., Mason, R. and Marsden, C.A. (2003). Differential cannabinoid-induced electrophysiological effects in rat ventral tegmentum. *Neuropharmacology*, **44**, 633-641.

Chemin, J., Monteil, A., Perez-Reyes, E., Nargeot, J. and Lory, P. (2000). Direct inhibition of T-type calcium channels by the endogenous cannabinoid anandamide. *EMBO J.*, **20**, 7033–7040.

Chemin, J., Nargeot, J. and Lory, P. (2002). Neuronal T-type alpha 1H calcium channels induce neuritogenesis and expression of high-voltage-activated calcium channels in the NG108-15 cell line. *J. Neurosci.*, **22**, 6856–6862.

Chen, J., Marmur, R., Pulles, A., Paredes, W. and Gardner, E.L. (1993). Ventral tegmental microinjection of Δ^9-tetrahydrocannabinol enhances ventral tegmental somatodendritic dopamine levels but not forebrain dopamine levels: evidence for local neural action by marijuana's psychoactive ingredient. *Brain Res.*, **621**, 65-70.

Chen, J.P., Paredes, W., Li, J., Smith, D., Lowinson, J. and Gardner, E.L. (1990). Δ^9-tetrahydrocannabinol produces naloxone-blockable enhancement of presynaptic basal dopamine efflux in nucleus accumbens of conscious, freely-moving rats as measured by intracerebral microdialysis. *Psychopharmacology (Berl.)*, **102**, 156-162.

Chen, J.P., Paredes, W., Lowinson, J.H. and Gardner, E.L. (1991). Strain-specific facilitation of dopamine efflux by Δ^9-tetrahydrocannabinol in the nucleus accumbens of rat: an in vivo microdialysis study. *Neurosci. Lett.*, **129**, 136-180.

Cherubini, E. and North, R.A. (1985). Mu and kappa opioids inhibit transmitter release by different mechanisms. *Proc. Natl. Acad. Sci. U.S.A.*, **82**, 1860-1863.

Childers, S.R., Sexton, T. and Roy, M.B. (1994). Effects of anandamide on cannabinoid receptors in rat brain membranes. *Biochem. Pharmacol.*, **47**, 711-715.

Christopoulos, A., Coles, P., Lay, L., Lew, M.J. and Angus, J.A. (2001). Pharmacological analysis of cannabinoid receptor activity in the rat vas deferens. *Br. J. Pharmacol.*, **132**, 1281–1291.

Cichewicz, D.L. (2004). Synergistic interactions between cannabinoid and opioid analgesics. *Life Sci.*, **74**, 1317– 1324.

Civelli, O., Bunzow, J.R., Grandy, D.K., Zhou, Q.Y. and Van Tol, H.H. (1991). Molecular biology of the dopamine receptors. *Eur. J. Pharmacol.*, **207**, 277-286.

Colquhoun, L.M. and Patrick, J.W. (1997). Pharmacology of neuronal nicotinic acetylcholine receptor subtypes. *Adv. Pharmacol.*, **39**, 191-220.

Connor, M., and Christie, M.J. (1999). Opioid receptor signaling mechanisms. *Clin. Exp. Physiol. Pharmacol.*, **26**, 493-499.

Corbett, A.D., Paterson, S.J. and Kosterlitz, H.W. (1993). Selectivity of ligands for opioid receptors. In: *Handbook Exp. Pharmacol.*, (ed. Herz, A.) pp. 645–679. Berlin: Springer-Verlag.

Costa, M., Brookes, S.J., Steele, P.A., Gibbins, I., Burcher, E. and Kandiah, C.J. (1996). Neurochemical classification of myenteric neurons in the guinea-pig ileum. *Neuroscience*, **75**, 949–967.

Coutts, A.A., Brewster, N., Ingram, T., Razdan, R.K. and Pertwee, R.G. (2000). Comparison of novel cannabinoid partial agonists and SR141716A in the guinea-pig small intestine. *Br. J. Pharmacol.*, **129**, 645–652.

Coutts, A.A., Irving, A.J., Mackie, K., Pertwee, R.G. and Anavi-Goffer, S. (2002). Localisation of cannabinoid CB_1 receptor immunoreactivity in the guinea pig and rat myenteric plexus. *J. Comp. Neurol.*, **448**, 410-422.

Coutts, A.A. and Pertwee, R.G. (1997). Inhibition by cannabinoid receptor agonists of acetylcholine release from the guinea-pig myenteric plexus. *Br. J. Pharmacol.*, **121**, 1557-1566.

Coutts, A.A. and Pertwee, R.G. (1998). Evidence that cannabinoid-induced inhibition of electrically evoked contractions of the myenteric plexus--longitudinal muscle preparation of guinea-pig small intestine can be modulated by Ca^{2+} and cAMP. *Can. J. Physiol. Pharmacol.*, **76**, 340-346.

Cortright, D.N., Crandall, M., Sanchez, J.F., Zou, T., Krause, J.E. and White, G. (2001). The tissue distribution and functional characterization of human VR1. *Biochem. Biophys. Res. Commun.*, **281**, 1183-1189.

Cowie, A.L., Kosterlitz, H.W. and Watt, A.J. (1968). Mode of action of morphine-like drugs on autonomic neuroeffectors. *Nature*, **220**, 1040-1042.

Cox, B.M. and Weinstock, M. (1966). The effect of analgesic drugs on the release of acetylcholine from electrically stimulated guinea-pig ileum. *Br. J. Pharmacol.*, **27**, 81-92.

Dale, D. (1914). Hydrogen ion concentrations limiting automaticity in different regions of the frog's heart. *J. Physiol.* **47**, 493-508.

Deadwyler, S.A., Hampson, R.E., Mu, J., Whyte, A. and Childers, S. (1995). Cannabinoids modulate voltage sensitive potassium A-current in hippocampal neurons via a cAMP-dependent process. *J. Pharmacol. Exp. Ther.*, **273**, 734-743.

Del Castillo, J. and Katz, B. (1955). Production of membrane potential changes in the frog's heart by inhibitory nerve impulses. *Nature*, **175**, 1035.

DeMuth, D.G., Gkoumassi, E., Droge, M.J., Dekkers, B.G., Esselink, H.J., van Ree, R.M., Parsons, M.E., Zaagsma, J., Molleman, A. and Nelemans, S.A. (2005). Arachidonic acid mediates non-capacitative calcium entry evoked by CB_1-cannabinoid receptor activation in DDT1 MF-2 smooth muscle cells. *J. Cell. Physiol.*, **205**, 58-67.

DeMuth, D., Parsons, M. and Molleman, A. (2004). Cannabinoid-mediated inhibition of nicotinic ACh currents in myenteric neurons. 14th ICRS symposium, pp. 59.

De Petrocellis, L., Bisogno, T., Maccarrone, M., Davis, J.-B., Finazzi-Agro, A. and Di Marzo, V. (2001). The activity of anandamide at vanilloid VR1 receptors requires facilitated transport across the cell membrane and is limited by intracellular metabolism. *J. Biol. Chem.*, **276**, 12856–12863.

Derkinderen, P., Ledent, C., Parmentier, M. and Girault, J.A. (2001). Cannabinoids activate p38 mitogen-activated protein kinases through CB_1 receptors in hippocampus. *J. Neurochem.*, **77**, 957– 960.

Derkinderen, P., Toutant, M., Burgaya, F., Le Bert, M., Siciliano, J.C., de Franciscis, V., Gelman, M. and Girault, J.A. (1996). Regulation of a neuronal form of focal adhesion kinase by anandamide. *Science*, **273**, 1719-1722.

Derocq, J.M., Jbilo, O., Bouaboula, M., Segui, M., Clere, C. and Casellas, P. (2000). Genomic and functional changes induced by the activation of the peripheral cannabinoid receptor CB_2 in the promyelocytic cells HL-60. Possible involvement of the CB_2 receptor in cell differentiation. *J. Biol. Chem.*, **275**, 15621-15628.

Derocq, J.M., Segui, M., Marchand, J., Le Fur, G. and Casellas, P. (1995). Cannabinoids enhance human B-cell growth at low nanomolar concentrations. *FEBS Lett.*, **369**, 177-82.

Devane, W.A., Dysarz, F.A. 3rd, Johnson, M.R., Melvin, L.S. and Howlett, A.C. (1988). Determination and characterization of a cannabinoid receptor in rat brain. *Mol. Pharmacol.,* **34**, 605-613.

Devane, W.A., Hanus, L., Breuer, A., Pertwee, R.G., Stevenson, L.A., Griffin, G., Gibson, D., Mandelbaum, A., Etinger, A. and Mechoulam, R. (1992) Isolation and structure of a brain constituent that binds to the cannabinoid receptor. *Science,* **258**, 1946–1949.

Devi, L.A. (2001). Heterodimerization of G-protein-coupled receptors: pharmacology, signaling and trafficking. *Trends Pharmacol. Sci.*, **22**, 532-537.

De Vries, T.J., Homberg, J.R., Binnekade, R., Raaso, H. and Schoffelmeer, A.N. (2003). Cannabinoid modulation of the reinforcing and motivational properties of heroin and heroin-associated cues in rats. *Psychopharmacology (Berl.),* **168**, 164–169.

Dewey, W.L., Martin, B.R. and May, E.L. (1984). Cannabinoid stereoisomers: pharmacological effects, in *Handbook of Stereoisomers: Drugs in Psychopharmacology (Berl.),* (Smith DF, ed) pp 317–326, CRC Press, Boca Raton, FL.

Diaz-Laviada, I. and Ruiz-Llorente, L. (2005). Signal transduction activated by cannabinoid receptors. *Mini reviews in medicinal chemistry*. **5**, 619-630.

Di Marzo, V., Bisogno, T., Melck, D., Ross, R., Brockie, H., Stevenson, L., Pertwee, R. and De Petrocellis, L. (1998). Interactions between synthetic vanilloids and the endogenous cannabinoid system. *FEBS Lett.*, **436**, 449-454.

Di Marzo, V., Breivogel, C.S., Tao, Q., Bridgen, D.T., Razdan, R.K., Zimmer, A.M., Zimmer, A. and Martin, B.R. (2000). Levels, metabolism, and pharmacological activity of anandamide in CB_1 cannabinoid receptor knockout mice: evidence for non-CB_1, non-CB_2 receptor-mediated actions of anandamide in mouse brain. *J. Neurochem.*, **75**(6), 2434-2444.

Di Marzo, V., Fontana, A., Cadas, H., Schinelli, S., Cimino, G., Schwartz, J.C. and Piomelli, D. (1994). Formation and inactivation of endogenous cannabinoid anandamide in central neurons. *Nature,* **372**, 686-691.

Di Toro, R., Campana, G., Sciarretta, V., Murari, G. and Spampinato, S. (1998). Regulation of delta opioid receptors by Δ^9-tetrahydrocannabinol in NG108-15 hybrid cells. *Life Sci.*, **63**, 197-204.

Dogiel, A.S. (1899). Űber den Bau der Ganglien in den Geflechten des Darmes und der Gallenblase des Menschen und der Säugethiere. *Arch. Anat. Physiol. Leipzig., Anat. Abt., Jg.*, 130–158.

Dolphin, A.C. (2006). A short history of voltage-gated calcium channels. *Br. J. Pharmacol.*, **147**, S56-S62.

Drmota, T., Greasley, P. and Groblewski, T. (2004). AstraZeneca, assignee. Screening assays for cannabinoid-ligand-type modulators of GPR55. WIPO patent 074 844.

Duncan, M., Ho, W., Shariat, N., Pittman, Q.J., Mackie, K., Patel, K.D. and Sharkey, K.A. (2005). Distribution of the CB_2 receptor in enteric nerves of the rat ileum. 15th Annual Symposium on the Cannabinoids, Burlington, Vermont, International Cannabinoid Research Society, page 159.

Duncan, M., Pittman, Q.J., Mackie, K., Patel, K.D. and Sharkey, K.A. (2006). LPS treatment upregulates CB_2 receptors in the enteric nervous system of the rat ileum. 16th Annual Symposium on the Cannabinoids, Burlington, Vermont, International Cannabinoid Research Society, page 58.

Dunlap, K. and Fischbach, G.D. (1978). Neurotransmitters decrease the calcium component of sensory neurone action potentials. *Nature*, **276**, 837-9.

Egan, T.M. and North, R.A. (1981). Both μ and δ opiate receptors exist on the same neuron. *Science*, **214**, 923-924.

Egertová, M. and Elphick, M.R. (2000). Localisation of cannabinoid receptors in the rat
brain using antibodies to the intracellular C-terminal tail of CB_1. *J. Comp. Neurol.*, **422**, 159–171.

Eglen, R.M. (2001). Muscarinic receptors and gastrointestinal tract smooth muscle function. *Life Sci.*, **68**, 2573-2578.

Ehrenpreis, S., Sato, T., Takayanagi, I., Comaty, J.E. and Takagi, K. (1976). Mechanism of morphine block of electrical activity in ganglia of Auerbach's plexus. *Eur. J. Pharmacol.*, **40**, 303-309.

Eissenstat, M.A., Bell, M.R., D'Ambra, T.E., Alexander, E.J., Daum, S.J., Ackerman, J.H., Gruett, M.D., Kumar, V., Estep, K.G., Olefirowicz, E.M., Wetzel, J.R., Alexander, M.D., Weaver, J.D., Haycock, D.A., Luttinger, D.A., Casiano, F.M., Chippari, S.M., Kuster, J.E., Stevenson, J.I. and Ward S.J. (1995). Aminoalkylindoles: structure-activity relationships of novel cannabinoid mimetics. *J. Med. Chem.*, 38, 3094–3105.

Ehlert, F.J. (2003). Contractile role of M2 and M3 muscarinic receptors in gastrointestinal, airway and urinary bladder smooth muscle. *Life Sci.*, **74**, 355-366.

ElSohly, M.A. (2002). Chemical constituents of cannabis. In: Cannabis and Cannabinoids. Pharmacology, Toxicology and Therapeutic Potential, (ed. Grotenhermen, F. and Russo, E.), pp. 27–36. Haworth Press, New York.

Evans, G.J. and Morgan, A. (2003). Regulation of the exocytotic machinery by cAMP-dependent protein kinase: implications for presynaptic plasticity. *Biochem. Soc. Trans.*, **31**, 824-827.

Evans, R. M., Scott, R. H. and Ross, R. A. (2004). Multiple actions of anandamide on neonatal rat cultured sensory neurones. *Br, J, Pharmacol.*, **141**, 1223–1233.

Fan, P. (1995). Cannabinoid agonists inhibit the activation of 5-HT_3 receptors in rat nodose ganglion neurons. *J. Neurophysiol.*, **73**, 907-910.

Faubert, B.L. and Kaminski, N.E. (2000). AP-1 activity is negatively regulated by cannabinol through inhibition of its protein components, c-fos and c-jun. *J. Leukoc. Biol.*, **67**, 259-266.

Fearon, I. M., Zhang, M., Vollmer, C. and Nurse, C. A. (2003). GABA mediates autoreceptor feedback inhibition in the rat carotid body via presynaptic $GABA_B$ receptors and TASK-1. *J. Physiol. (Lond.),* **553**, 83–94.

Felder, C.C., Briley, E.M., Axelrod, J., Simpson, J.T., Mackie, K. and Devane, W.A. (1993). Anandamide, an endogenous cannabimimetic eicosanoid, binds to the cloned human cannabinoid receptor and stimulates receptor-mediated signal transduction. *Proc. Natl. Acad. Sci. U.S.A.,* **90**, 7656-7660.

Felder, C.C., Joyce, K.E., Briley, E.M., Glass, M., Mackie, K.P., Fahey, K.J., Cullinan, G.J., Hunden, D.C., Johnson, D.W., Chaney, M.O., Koppel, G.A. and Brownstein, M. (1998). LY320135, a novel cannabinoid CB_1 receptor antagonist, unmasks coupling of the CB_1 receptor to stimulation of cAMP accumulation. *J. Pharmacol., Exp. Ther.*, **284**, 291–297.

Felder, C.C., Joyce, K.E., Briley, E.M., Mansouri, J., Mackie, K., Blond, O.. Lai, Y.. Ma, A.L. and Mitchell, R.L. (1995). Comparison of the pharmacology and signal transduction of the human cannabinoid CB_1 and CB_2 receptors. *Mol. Pharmacol.,* **48**, 443-450.

Felder, C.C., Veluz, J.S., Williams, H.L., Briley, E.M. and Matsuda, L.A. (1992). Cannabinoid agonists stimulate both receptor- and non-receptor-mediated signal transduction pathways in cells transfected with and expressing cannabinoid receptor clones. *Mol. Pharmacol.,* **42**, 838-845.

Filipeanu, C.M., Dick de Zeeuw, S. and Nelemans, A. (1997). Δ^9-Tetrahydrocannabinol

activates $[Ca^{2+}]_i$ increases partly sensitive to capacitative store refilling. *Pflugers Arch.*, **336**, R1– R7.

Fimiani, C., Mattocks, D., Cavani, F., Salzet, M., Deutsch, D.G., Pryor, S., Bilfinger, T.V. and Stefano, G.B. (1999). Morphine and anandamide stimulate intracellular calcium transients in human arterial endothelial cells: coupling to nitric oxide release. *Cell. Signal.*, **11**, 189–193.

Franco, R., Costa, M. and Furness, J.B. (1979). Evidence for the release of endogenous substance P from intestinal nerves. *Naunyn-Schmiedebergs Arch. Pharmacol.*, **306**, 195-201.

Frederickson, R.C., Hewes, C.R. and Aiken, J.W. (1976). Correlation between the in vivo and an in vitro expression of opiate withdrawal precipitated by naloxone: their antagonism by l-(-)-Δ^9-tetrahydrocannabinol. *J. Pharmacol. Exp. Ther.*, **199**, 375-384.

French, E.D. (1997b). Δ^9-Tetrahydrocannabinol excites rat VTA dopamine neurons through activation of cannabinoid CB_1 but not opioid receptors. *Neurosci. Lett.*, **226**, 159-162.

French, E.D., Dillon, K. and Wu, X. (1997a). Cannabinoids excite dopamine neurons in the ventral tegmentum and substantia nigra. *Neuroreport*, **8**, 649-652.

Gaddum, J.H. and Picarelli, Z.P. (1957). Two kinds of tryptamine receptors. *Br. J. Pharmacol.*, **12**, 323-328.

Gainetdinov, R.R., Sotnikova, T.D. and Caron, M.G. (2002). Monoamine transporter pharmacology and mutant mice. *Trends Pharmacol. Sci.*, **23**, 367-373.

Galiègue, S., Mary, S., Marchand, J., Dussossoy, D., Carriere, D., Carayon, P., Bouaboula, M., Shire, D., Le Fur, G. and Casellas, P. (1995). Expression of central and peripheral cannabinoid receptors in human immune tissues and leukocyte subpopulations. *Eur. J. BioChem.*, **232**, 54-61.

Gainetdinov, R.R., Sotnikova, T.D. and Caron, M.G. (2002). Monoamine transporter pharmacology and mutant mice. *Trends Pharmacol. Sci.*, **23**, 367-373.

Galligan, J.J. (1999). Nerve terminal nicotinic cholinergic receptors on excitatory motoneurons in the myenteric plexus of guinea pig intestine. *J. Pharmacol. Exp. Ther.*, **291**, 92-98.

Galligan, J.J. and Bertrand, P.P. (1994). ATP mediates fast synaptic potentials in enteric neurons. *J. Neurosci.*, **14**, 7563-7571.

Galligan, J.J. and North, R.A. (1991). Opioid, 5-HT_{1A} and α_2 receptors localized to subsets of guinea-pig myenteric neurons. *J. Auton. Nerv. Syst.*, **32**, 1-11.

Galligan, J.J. and North, R.A. (2004). Pharmacology and function of nicotinic acetylcholine and P2X receptors in the enteric nervous system. *Neurogastroenterol. Motil.*, **16**, 64-70.

Gaoni, Y. and Mechoulam, R. (1964). Isolation, structure and partial synthesis of an active constituent of hashish. *J. Am. Chem. Soc.*, **86**, 1646–1647.

Garcia, D.E., Brown, S., Hille, B. and Mackie, K. (1998). Protein kinase C disrupts cannabinoid actions by phosphorylation of the CB_1 cannabinoid receptor. *J. Neurosci.*, **18**, 2834-2841.

Gardner, E.L. and Vorel, S.R. (1998). Cannabinoid transmission and reward-related events. *Neurobiol. Dis.*, **5**, 502-533.

Gardener, M. J., Johnson, I. T., Burnham, M. P., Edwards, G., Heagerty, A. M. and Weston, A. H. (2004). Functional evidence of a role for two-pore domain potassium channels in rat mesenteric and pulmonary arteries. *Br. J. Pharmacol.*, **142**, 192–202.

Gebremedhin, D., Lange, A.R., Campbell, W.B., Hillard, C.J. and Harder, D.R. (1999). Cannabinoid CB_1 receptor of cat cerebral arterial muscle functions to inhibit L-type Ca^{2+} channel current. *Am. J. Physiol. (Lond.),* **276**, H2085–H2093.

Gérard, C.M., Mollereau, C., Vassart, G. and Parmentier, M. (1991). Molecular cloning of a human cannabinoid receptor which is also expressed in testis. *Biochem. J.*, **279**, 129-134.

Gessa, G.L., Casu, M.A., Carta, G. and Mascia, M.S. (1998). Cannabinoids decrease acetylcholine release in the medial-prefrontal cortex and hippocampus, reversal by SR 141716A. *Eur. J. Pharmacol.,* **355**, 119-124.

Gifford, A.N. and Ashby, C.R. Jr. (1996). Electrically evoked acetylcholine release from hippocampal slices is inhibited by the cannabinoid receptor agonist, WIN 55212-2, and is potentiated by the cannabinoid antagonist, SR 141716A. *J. Pharmacol. Exp. Ther.,* **277**, 1431-1436.

Gifford, A.N., Samiian, L., Gatley, S.J. and Ashby, C.R. Jr. (1997). Examination of the effect of the cannabinoid receptor agonist, CP 55,940, on electrically evoked transmitter release from rat brain slices. *Eur. J. Pharmacol.,* **324**, 187-192.

Gifford, A.N., Bruneus, M., Gatley, S.J. and Volkow, N.D. (2000). Cannabinoid receptor-mediated inhibition of acetylcholine release from hippocampal and cortical synaptosomes. *Br. J. Pharmacol.,* **131**, 645-650.

Gintzler, A.R. and Scalisi, J.A. (1982). Effects of opioids on noncholinergic excitatory responses of the guinea-pig isolated ileum: inhibition of release of enteric substance P. *Br. J. Pharmacol.*, **75**, 199-205.

Glass, M., Dragunow, M. and Faull, R.L.M. (1997). Cannabinoid receptors in the human brain: a detailed anatomical and quantitative autoradiographic study in the fetal, neonatal and adult human brain. *Neuroscience,* **77**, 299–318.

Glass, M. and Felder, C.C. (1997). Concurrent stimulation of cannabinoid CB_1 and dopamine D_2 receptors augments cAMP accumulation in striatal neurons: evidence for a G_s linkage to the CB_1 receptor. *J. Neurosci.,* **17**, 5327-5333.

Glass, M. and Northup, J.K. (1999). Agonist selective regulation of G proteins by cannabinoid CB_1 and CB_2 receptors. *Mol. Pharmacol.,* **56**, 1362-1369.

Gómez del Pulgar, T., Velasco, G. and Guzman, M. (2000). The CB_1 cannabinoid receptor is coupled to the activation of protein kinase B/Akt. *Biochem. J.*, **347**, 369-373.

Gong, J.P., Onaivi, E.S., Ishiguro, H., Liu, Q.R., Tagliaferro, P.A.. Brusco, A. and Uhl, G.R. (2006). Cannabinoid CB_2 receptors: immunohistochemical localization in rat brain. *Brain Res.,* **1071**, 10-23.

Gonsiorek, W., Lunn, C., Fan, X., Narula, S., Lundell, D. and Hipkin, R.W. (2000). Endocannabinoid 2-arachidonyl glycerol is a full agonist through human type 2 cannabinoid receptor: antagonism by anandamide. *Mol. Pharmacol.,* **57**, 1045–1050.

Greenamyre, J.T., Young, A.B. and Penney, J.B. (1984). Quantitative autoradiographic distribution of L-[^{3}H]glutamate-binding sites in rat central nervous system. *J. Neurosci.,* **4**, 2133–2144.

Griffin, G., Atkinson, P.J., Showalter, V.M., Martin, B.R. and Abood, M.E. (1998). Evaluation of cannabinoid receptor agonists and antagonists using the guanosine-5'-O-(3-[^{35}S]thio)-triphosphate binding assay in rat cerebellar membranes. *J. Pharmacol. Exp. Ther.,* **285**, 553-560.

Griffin, G., Fernando, S.R., Ross, R.A., McKay, N.G., Ashford, M.L., Shire, D., Huffman, J.W., Yu, S., Lainton, J.A. and Pertwee, R.G. (1997). Evidence for the presence of CB_2-like cannabinoid receptors on peripheral nerve terminals. *Eur. J. Pharmacol.,* **339**, 53-61.

Griffin, G., Tao, Q. and Abood, M.E. (2000). Cloning and pharmacological characterization of the rat CB_2 cannabinoid receptor. *J. Pharmacol. Exp. Ther.*, **292**, 886–894.

Grinspoon, L. and Bakalar, J.B. (1993). In: *Marihuana the Forbidden Medicine*, Yale University Press.

Groenewegen, H.J. and Russchen, F.T. (1984). Organization of the efferent projections of the nucleus accumbens to pallidal, hypothalamic, and mesencephalic structures: a tracing and immunohistochemical study in the cat. *J. Comp. Neurol.*, **223**, 347-367.

Guo, J. and Ikeda, S.R. (2004). Endocannabinoids modulate N-type calcium channels and G-protein-coupled inwardly rectifying potassium channels via CB_1 cannabinoid receptors heterologously expressed in mammalian neurons. *Mol. Pharmacol.*, **65**, 665-674.

Gurney, A. M., Osipenko, O. N., MacMillan, D., McFarlane, K. M., Tate, R. J. and Kempsill, F. E. (2003). Two-pore domain K channel, TASK-1, in pulmonary artery smooth muscle cells. *Circ. Res.*, **93**, 957–964.

Guzmán, M. and Sánchez, C. (1999). Effects of cannabinoids on energy metabolism. *Life Sci.*, 65, 657-664.

Guzmán, M., Galve-Roperh, I. and Sánchez, C. (2001). Ceramide: a new second messenger of cannabinoid action. *Trends Pharmacol Sci.*, **22**, 19-22.

Hájos, N. and Freund, T.F. (2002). Distinct cannabinoid sensitive receptors regulate hippocampal excitation and inhibition. *Chem. Phys. Lipids*, **121**, 73-82.

Hájos, N., Ledent, C. and Freund, T.F. (2001). Novel cannabinoid-sensitive receptor mediates inhibition of glutamatergic synaptic transmission in the hippocampus. *Neuroscience*, **106**, 1-4.

Hall, W., Degenhardt, L. and Teesson, M. (2004). Cannabis use and psychotic disorders: an update. *Drug Alcohol Rev.*, **23**, 433-443.

Hamill, O.P., Marty, A., Neher, E., Sakmann, B. and Sigworth, F.J. (1981). Improved patch-clamp techniques for high-resolution current recording from cells and cell-free membrane patches. *Pflugers Arch.*, **391**, 85-100.

Hamprecht, B. (1977). Structural, electrophysiological, biochemical, and pharmacological properties of neuroblastoma-glioma cell hybrids in cell culture. *Int. Rev. Cytol.*, **49**, 99-170.

Hampson, A.J., Bornheim, L.M., Scanziani, M., Yost, C.S., Gray, A.T., Hansen, B.M., Leonoudakis, D.J. and Bickler, P.E. (1998). Dual effects of anandamide on NMDA receptor-mediated responses and neurotransmission. *J. Neurochem.*, **70**, 671-676.

Hampson, R.E., Mu, J., Deadwyler, S.A. (2000). Cannabinoid and kappa opioid receptors reduce potassium K current via activation of G_s proteins in cultured hippocampal neurons. *J. Neurophysiol.,* **84**, 2356-2364.

Hanani, M., Ermilov, L.G., Schmalz, P.F., Louzon, V., Miller, S.M. and Szurszewski, J.H. (1998). The three-dimensional structure of myenteric neurons in the guinea-pig ileum. *J. Auton. Nerv. Syst.*, **71**, 1-9.

Hanus, L., Abu-Lafi, S., Fride, E., Breuer, A., Vogel, Z., Shalev, D.E., Kustanovich, I. and Mechoulam, R. (2001). 2-Arachidonyl glyceryl ether, an endogenous agonist of the

cannabinoid CB_1 receptor. *Proc. Natl. Acad. Sci. U.S.A.,* **98**, 3662–3665.

Hejazi, N., Zhou, C., Oz, M., Sun, H., Ye, J., and Zhang, L. (2006). Delta-9-tetrahydrocannabinol and endogenous cannabinoid anandamide directly potentiate the function of glycine receptors. *Mol. Pharmacol.* **69**, 991–997.

Henderson, G. and McKnight, A.T. (1997). The orphan opioid receptor and its endogenous ligand--nociceptin/orphanin FQ. *Trends Pharmacol. Sci.*, **18**, 293-300.

Henry, D.J. and Chavkin, C. (1995). Activation of inwardly rectifying potassium channels (GIRK1) by co-expressed rat brain cannabinoid receptors in *Xenopus* oocytes. *Neurosci. Lett.*, **186**, 91-94.

Herkenham, M., Lynn, A.B., Johnson, M.R., Melvin, L.S., de Costa, B.R. and Rice, K.C. (1991). Characterization and localization of cannabinoid receptors in rat brain: a quantitative in vitro autoradiographic study. *J. Neurosci.,* **11**, 563–583.

Herkenham, M., Lynn, A.B., Little, M.D., Johnson, M.R., Melvin, L.S., de Costa, B.R. and Rice, K.C. (1990) Cannabinoid receptor localization in brain. *Proc. Natl. Acad. Sci. U.S.A.,* **87**, 1932-1936.

Herlitze, S., Garcia, D.E., Mackie, K., Hille, B., Scheuer, T. and Catterall, W.A. (1996). Modulation of Ca^{2+} channels by G-protein beta gamma subunits. *Nature,* **380**, 258-262.

Hescheler, J., Rosenthal, W., Trautwein, W. and Schultz, G. (1987). The GTP-binding protein, G_o, regulates neuronal calcium channels. *Nature*, **325**, 445-447.

Hilgemann, D. W., Feng, S. and Nasuhoglu, C. (2001). The complex and intriguing lives of PIP2 with ion channels and transporters. Sci. STKE, **111**, RE19.

Hillard, C.J., Manna, S., Greenberg, M.J., Dicamelli, R., Ross, R.A., Stevenson, L.A., Murphy, V., Pertwee, R.G. and Campbell, W.B. (1999). Synthesis and characterization of potent and selective agonists of the neuronal cannabinoid receptor (CB_1). *J. Pharmacol. Exp. Ther.,* **289**, 1427–1433

Hine, B., Torrelio, M. and Gershon, S. (1975). Interactions between cannabidiol and Δ^9-THC during abstinence in morphine-dependent rats. *Life Sci.*, **17**, 851-857.

Hirst, G.D., Holman, M.E. and Spence, I. (1974). Two types of neurones in the myenteric plexus of duodenum in the guinea-pig. *J. Physiol. (Lond.),* **236**, 303-326.

Hirst, R.A. and Lambert, D.G. (1995). Do SHSY5Y human neuroblastoma cells express cannabinoid receptors? *Biochem. Soc. Trans*. **23,** 418s.

Ho, A., Lievore, A., Patierno, S., Kohlmeier, S.E., Tonini, M. and Sternini, C. (2003). Neurochemically distinct classes of myenteric neurons express the mu-opioid receptor in the guinea pig ileum. *J. Comp. Neurol.*, **458**, 404-411.

Ho, B.Y., Uezono, Y., Takada, S., Takase, I. and Izumi, F. (1999). Coupling of the expressed cannabinoid CB_1 and CB_2 receptors to phospholipase C and G protein-coupled inwardly rectifying K^+ channels. *Receptors Channels*, **6**(5), 363-374.

Ho, B.Y. and Zhao, J. (1996). Determination of the cannabinoid receptors in mouse x rat hybridoma NG108-15 cells and rat GH4Cl cells. *Neurosci. Lett.,* **212**, 123-126.

Hodgkiss, J.P. and Lees, G.M. (1983). Morphological studies of electrophysiologically-identified myenteric plexus neurons of the guinea-pig ileum. *Neuroscience*, **8**, 593-608.

Hohmann, A.G., Briley, E.M. and Herkenham, M. (1999). Pre-and postsynaptic distribution of cannabinoid and μ opioid receptors in rat spinal cord. *Brain Res.*, **822**, 17– 25.

Holzer, P. (1984). Characterization of the stimulus-induced release of immunoreactive substance P from the myenteric plexus of the guinea-pig small intestine. *Brain Res.*, **297**, 127-136.

Hosohata, K., Quock, R.M., Hosohata, Y., Burkey, T.H., Makriyannis, A., Consroe, P., Roeske, W.R. and Yamamura, H.I. (1997a). AM630 is a competitive cannabinoid receptor antagonist in the guinea pig brain. *Life Sci.* **61**, PL115–PL118.

Hosohata, Y., Quock, R.M., Hosohata, K., Makriyannis, A., Consroe, P., Roeske, W.R. and Yamamura, H.I. (1997b). AM630 antagonism of cannabinoid-stimulated [^{35}S]GTPγS binding in the mouse brain. *Eur. J. Pharmacol.*, **321**, R1–R3.

Houser, S.J., Eads, M., Embrey, J.P. and Welch, S.P. (2000). Dynorphin B and spinal analgesia: induction of antinociception by the cannabinoids CP55,940, Δ^9-THC and anandamide. *Brain Res.*, **857**, 337–342.

Howlett, A.C. (1987). Cannabinoid inhibition of adenylate cyclase: relative activity of constituents and metabolites of marihuana. *Neuropharmacology.* **26**, 507-512.

Howlett, A.C., Champion, T.M., Wilken, G.H. and Mechoulam, R. (1990). Stereochemical effects of 11-OH-Δ^8-tetrahydrocannabinol-dimethylheptyl to inhibit adenylate cyclase and bind to the cannabinoid receptor. *Neuropharmacology.* **29**, 161-165.

Howlett, A.C. and Fleming, R.M. (1984). Cannabinoid inhibition of adenylate cyclase. Pharmacology of the response in neuroblastoma cell membranes. *Mol. Pharmacol.*, **26**, 532-538.

Howlett, A.C., Johnson, M.R., Melvin, L.S. and Milne, G.M. (1988). Nonclassical cannabinoid analgetics inhibit adenylate cyclase: development of a cannabinoid receptor model. *Mol. Pharmacol.*, **33**, 297-302.

Howlett, A.C., Qualy, J.M. and Khachatrian, L.L. (1986). Involvement of G_i in the inhibition of adenylate cyclase by cannabimimetic drugs. *Mol. Pharmacol.*, **29**, 307–313.

Huang, C.C., Chen, Y.L., Lo, S.W. and Hsu, K.S. (2002). Activation of cAMP-dependent protein kinase suppresses the presynaptic cannabinoid inhibition of glutamatergic transmission at corticostriatal synapses. *Mol. Pharmacol.*, **61**, 578-585.

Huang, C.-C., Lo, S.-W. and Hsu, K.-S. (2001). Presynaptic mechanisms underlying cannabinoid inhibition of excitatory synaptic transmission in rat striatal neurons. *J. Physiol. (Lond.)*, **532**, 731–748.

Huffman, J.W., Yu, S., Showalter, V., Abood, M.E., Wiley, J.L., Compton, D.R., Martin, B.R., Bramblett, R.D. and Reggio, P.H. (1996). Synthesis and pharmacology of a very potent cannabinoid lacking a phenolic hydroxyl with high affinity for the CB_2 receptor. *J. Med. Chem.*, **39**, 3875-3877.

Hughes, J., Smith, T.W., Kosterlitz, H.W., Fothergill, L.A., Morgan. B.A. and Morris, H.R. (1975). Identification of two related pentapeptides from the brain with potent opiate agonist activity. *Nature*, **258**, 577-580.

Huidobro-Toro, J.P., Zhu, Y.-X., Lee, N.M., Loh, H.H. and Way, E.L. (1984). Dynorphin inhibition of the neurotensin contractile activity on the myenteric plexus. *J. Pharmacol. Exp. Ther.*, **228**, 293-303.

Ikeda, S.R. (1996). Voltage-dependent modulation of N-type calcium channels by G-protein beta gamma subunits. *Nature,* **380**, 255-258.

Ingram, S.L. and Williams, J.T. (1994). Opioid inhibition of I_h via adenylyl cyclase. *Neuron*, **13**, 179-186.

Izzo, A.A., Fezza, F., Capasso, R., Bisogno, T., Pinto, L., Iuvone, T., Esposito, G., Mascolo, N., Di Marzo, V. and Capasso, F. (2001). Cannabinoid CB_1-receptor mediated regulation of gastrointestinal motility in mice in a model of intestinal inflammation. *Br. J. Pharmacol.* **134**, 563-570.

Izzo, A.A., Mascolo, N., Borrelli, F. and Capasso, F. (1998). Excitatory transmission to the circular muscle of the guinea-pig ileum: evidence for the involvement of cannabinoid CB_1 receptors. *Br. J. Pharmacol.*, **124**, 1363-1368.

Izzo, A.A., Mascolo, N., Pinto, L., Capasso, R. and Capasso, F. (1999). The role of cannabinoid receptors in intestinal motility, defaecation and diarrhoea in rats. *Eur. J. Pharmacol.*, **384**, 37-42.

Izzo, A.A., Mascolo, N., Tonini, M. and Capasso, F. (2000a). Modulation of peristalsis by cannabinoid CB_1 ligands in the isolated guinea-pig ileum. *Br. J. Pharmacol.*, **129**, 984-990.

Izzo, A.A., Pinto, L., Borrelli, F., Capasso, R., Mascolo, N. and Capasso, F. (2000). Central and peripheral cannabinoid modulation of gastrointestinal transit in physiological states or during the diarrhoea induced by croton oil. *Br. J. Pharmacol.* **129**, 1627-1632.

Jackson, D.M. and Westlind-Danielsson, A. (1994). Dopamine receptors: molecular biology, biochemistry and behavioural aspects. *Pharmacol. Ther.*, **64**, 291-370.

Jaggar, S.I., Hasnie, F.S., Sellaturay, S. and Rice, A.S. (1998). The anti-hyperalgesic actions of the cannabinoid anandamide and the putative CB_2 receptor agonist palmitoylethanolamide in visceral and somatic inflammatory pain. *Pain*, **76**, 189-199.

Jan, L.Y. and Jan, Y.N. (1997). Receptor-regulated ion channels. *Curr. Opin. Cell. Biol.*, **9**, 155-160.

Jan, T.R. and Kaminski, N.E. (2001). Role of mitogen-activated protein kinases in the differential regulation of interleukin-2 by cannabinol. *J. Leukoc. Biol.*, **69**, 841-849.

Jaques, R. (1969). Morphine as inhibitor of prostaglandin El in the isolated guinea-pig intestine. *Experientia*, **25**, 1059-1060.

Járai, Z., Wagner, J.A., Varga, K., Lake, K.D., Compton, D.R., Martin, B.R., Zimmer, A.M., Bonner, T.I., Buckley, N.E., Mezey, E., Razdan, R.K., Zimmer, A. and Kunos, G. (1999). Cannabinoid-induced mesenteric vasodilation through an endothelial site distinct from CB_1 or CB_2 receptors. *Proc. Natl. Acad. Sci. U.S.A.*. **96**, 14136-14141.

Jeon, Y.J., Yang, K.H., Pulaski, J.T. and Kaminski, N.E. (1996). Attenuation of inducible nitric oxide synthase gene expression by Δ9-tetrahydrocannabinol is mediated through the inhibition of nuclear factor-κB/Rel activation. *Mol. Pharmacol.*, **50**, 334-341.

Johns, A. (2001). Psychiatric effects of cannabis. *Br. J. Psychiatry*. **178**, 116-122.

Johnson, M.R. and Melvin, L.S. (1986). The discovery of nonclassical cannabinoid analgetics, in *Cannabinoids As Therapeutic Agents* (Mechoulam R, ed) pp 121–145,CRC Press, Boca Raton, FL.

Johnson, P.J., Bornstein, J.C., Yuan, S.Y. and Furness, J.B. (1996). Analysis of contributions of acetylcholine and tachykinins to neuro-neuronal transmission in motility reflexes in the guinea-pig ileum. *Br. J. Pharmacol.*, **118**, 973-983.

Johnson, S.W. and North, R.A. (1992). Two types of neurone in the rat ventral tegmental area and their synaptic inputs. *J. Physiol. (Lond.)*, **450**, 455-468.

Justinova, Z., Tanda, G., Redhi, G.H. and Goldberg, S.R. (2003). Self-administration of delta-9-tetrahydrocannabinol (THC) by drug naive squirrel monkeys. *Psychopharmacology (Berl.),* **169**, 135–140.

Justinova, Z., Tanda, G., Munzar, P. and Goldberg, S.R. (2004). The opioid antagonist naltrexone reduces the reinforcing effects of Delta-9-tetrahydrocannabinol (THC) in squirrel monkeys. *Psychopharmacology (Berl.),* **173**, 186–194.

Karras, P.J. and North, R.A. (1981). Acute and chronic effects of opiates on single neurons of the myenteric plexus. *J. Pharmacol. Exp. Ther.*, **217**, 70-80.

Katz, B. (1949). Les constantes électriques de la membrane du muscle. *Archs. Sci. Physiol.*, **3**, 285–299

Kelley, B.K. and Thayer, S.A. (2004). Δ-9-Tetrahydrocannabinol antagonizes endocannabinoid modulation of synaptic transmission between hippocampal neurons in culture. *Neuropharmacology*, **46**, 709-715.

Kim, H.I., Kim, T.H., Shin, Y.K., Lee, C.S., Park, M. and Song, J.H. (2005). Anandamide suppression of Na^+ currents in rat dorsal root ganglion neurons. *Brain Res.*, **1062**, 39-47.

Kirchgessner, A.L. and Liu, M.T. (1998). Immunohistochemical localization of nicotinic acetylcholine receptors in the guinea pig bowel and pancreas. *J. Comp. Neurol.*, **390**, 497-514.

Klee, W.A. and Nirenberg, M.A. (1974). A neuroblastoma times glioma hybrid cell line with morphine receptors. *Proc. Natl. Acad. Sci. U.S.A.*, **71**, 3474-3477.

Kobayashi, Y., Arai, S., Waku, K. and Sugiura, T. (2001). Activation by 2-arachidonylglycerol, an endogenous cannabinoid receptor ligand, of p42/44 mitogen-activated protein kinase in HL-60 cells. *J. Biochem.*, **129**, 665-669.

Kojima, Y., Takahashi, T., Fujina, M. and Owyang, C. (1994). Inhibition of cholinergic transmission by opiates in ileal myenteric plexus is mediated by kappa receptor. Involvement of regulatory inhibitory G protein and calcium N-channels. *J. Pharmacol. Exp. Ther.*, **268**, 965-970.

Kollarik, M., Undem, B.J. (2004). Activation of bronchopulmonary vagal afferent nerves with bradykinin, acid and vanilloid receptor agonists in wild-type and TRPV1-/- mice. *J. Physiol. (Lond.),* **555**, 115-123.

Kortenkamp, A. and Altenburger, R. (1998). Synergisms with mixtures of xenoestrogens: a reevaluation using the method of isoboles. *Sci. Total. Environ.* **221**, 59-73.

Kosterlitz, H.W. and Robinson, J.A. (1957). Inhibition of the peristaltic reflex of the isolated guinea-pig ileum. *J. Physiol. (Lond.)*, **136**, 249-262.

Kosterlitz, H.W. and Robinson, J.A. (1958). The inhibitory action of morphine on the contraction of the longitudinal muscle coat of the isolated guinea-pig ileum. *Br. J. Pharmacol.*, **13**, 296-303.

Kotlikoff, M.I., Dhulipala, P. and Wang, Y.X. (1999). M_2 signaling in smooth muscle cells. *Life Sci.* **64**, 437-442.

Kunze, W.A., Bornstein, J.C., Furness, J.B., Hendriks, R. and Stephenson, D.S. (1994). Charybdotoxin and iberiotoxin but not apamin abolish the slow after-hyperpolarization in myenteric plexus neurons. *Pflugers Arch.,* **428**, 300-306.

Kunze, W.A., Clerc, N., Furness, J.B. and Gola, M. (2000). The soma and neurites of primary afferent neurons in the guinea-pig intestine respond differentially to deformation. *J. Physiol. (Lond.),* **526**, 375-385.

Kunze, W.A., Furness, J.B. and Bornstein, J.C. (1993). Simultaneous intracellular recordings from enteric neurons reveal that myenteric AH neurons transmit via slow excitatory postsynaptic potentials. *Neuroscience*, **55,** 685–694.

Lacey, M.G., Mercuri, N.B. and North, R.A. (1987). Dopamine acts on D_2 receptors to increase potassium conductance in neurones of the rat substantia nigra zona compacta. *J. Physiol. (Lond.)*, **392**. 397-416.

Lambert, D.M. and Di Marzo, V. (1999). The palmitoylethanolamide and oleamide enigmas: are these two fatty acid amides cannabimimetic? *Curr. Med. Chem.*, **6**, 757-773.

Lambert, D.M., DiPaolo, F.G., Sonveaux, P., Kanyonyo, M., Govaerts, S.J., Hermans, E., Bueb, J., Delzenne, N.M. and Tschirhart, E.J. (1999). Analogues and homologues of N-palmitoylethanolamide, a putative endogenous CB_2 cannabinoid, as potential ligands for the cannabinoid receptors. *Biochim. Biophys. Acta.*, **1440,** 266-274.

Lambert, D.M., Vandevoorde, S., Jonsson, K.O. and Fowler, C.J. (2002). The palmitoylethanolamide family: a new class of anti-inflammatory agents? *Curr. Med. Chem.*, **9**, 663-674.

Landsman, R.S., Makriyannis, A., Deng, H., Consroe, P., Roeske, W.R. and Yamamura, H.I. (1998). AM630 is an inverse agonist at the human cannabinoid CB_1 receptor. *Life Sci.* **62**, PL109–PL113.

Law, P.Y., Koehler, J.E. and Loh, H.H. (1982). Comparison of opiate inhibition of adenylate cyclase activity in neuroblastoma N18tG2 and neuroblastoma x glioma NG108-15 hybrid cell lines. *Mol. Pharmacol.*, **21**, 483-491.

Ledent, C., Valverde, O., Cossu, G., Petitet, F., Aubert, J.F., Beslot, F., Bohme, G.A., Imperato, A., Pedrazzini, T., Roques, B.P., Vassart, G., Fratta, W. and Parmentier, M.

(1999). Unresponsiveness to cannabinoids and reduced addictive effects of opiates in CB_1 receptor knockout mice. *Science*, **283**, 401-404.

Legendre, P. (2001). The glycinergic inhibitory synapse. *Cell. Mol. Life Sci.*, **58**, 760–793.

Lester, H. A., Dibas, M. I., Dahan, D. S., Leite, J. F. and Dougherty, D. A. (2004). Cys-loop receptors: new twists and turns. *Trends Neurosci.*, **27**, 329–336.

Lin, S.Y., Khanolkar, A.D., Fan, P., Goutopoulos, A., Qin, C., Papahadjis, D. and Makriyannis, A. (1998). Novel analogues of arachidonylethanolamide (anandamide): affinities for the CB_1 and CB_2 cannabinoid receptors and metabolic stability. *J. Med. Chem.*, **41**, 5353–5361.

Little, P.J., Compton, D.R., Johnson, M.R., Melvin, L.S. and Martin, B.R. (1988). Pharmacology and stereoselectivity of structurally novel cannabinoids in mice. *J. Pharmacol. Exp. Ther.*, **247**, 1046–1051.

Liao, C., Zheng, J., David, L.S. and Nicholson, R.A. (2004). Inhibition of voltage-sensitive sodium channels by the cannabinoid 1 receptor antagonist AM 251 in mammalian brain. *Basic Clin. Pharmacol. Toxicol.*, **94**, 73-78.

Liu, J., Gao, B., Mirshahi, F., Sanyal, A.J., Khanolkar, A.D., Makriyannis, A. and Kunos, G. (2000). Functional CB_1 cannabinoid receptors in human vascular endothelial cells. *Biochem. J.*, **346**, 835-40.

Lo, Y. K., Chiang, H. T. and Wu, S. N. (2003). Effect of arvanil (N-arachidonoylvanillyl-amine), a nonpungent anandamide-capsaicin hybrid, on ion currents in NG108-15 neuronal cells. *Biochem. Pharmacol.*, **65**, 581–591.

Logothetis, D.E., Kurachi, Y., Galper, J., Neer, E.J. and Clapham, D.E. (1987). The beta gamma subunits of GTP-binding proteins activate the muscarinic K^+ channel in heart. *Nature*, **325**, 321-326.

López-Redondo, F., Lees, G.M. and Pertwee, R.G. (1997). Effects of cannabinoid receptor ligands on electrophysiological properties of myenteric neurones of the guinea-pig ileum. *Br. J. Pharmacol.*, **122**, 330-334.

Lord, J.A., Waterfield, A.A., Hughes, J. and Kosterlitz, H.W. (1977). Endogenous opioid peptides: multiple agonists and receptors. *Nature*, **267**, 495-499.

Lozovaya, N., Yatsenko, N., Beketov, A., Tsintsadze, T., and Burnashev, N. (2005). Glycine receptors in CNS neurons as a target for nonretrograde action of cannabinoids. *J. Neurosci.*, **25**, 7499–7506.

Luetje, C.W. and Patrick, J. (1991). Both alpha- and beta-subunits contribute to the agonist sensitivity of neuronal nicotinic acetylcholine receptors. *J. Neurosci.*, **11**, 837-845.

Lukyanetz, E.A. (1998). Diversity and properties of calcium channel types in NG108-15 hybrid cells. *Neuroscience*, **87**, 265-274.

Lynch, J. W. (2004). Molecular structure and function of the glycine receptor chloride channel. *Physiol. Rev.*, **84**, 1051−1095.

Lynn, A.B. and Herkenham, M. (1994). Localization of cannabinoid receptors and nonsaturable high-density cannabinoid binding sites in peripheral tissues of the rat: implications for receptor-mediated immune modulation by cannabinoids. *J. Pharmacol. Exp. Ther.*, **268**, 1612-1623.

Maccarrone, M., Bari, M., Lorenzon, T., Bisogno, T., Di Marzo, V. and Finazzi-Agro, A. (2000). Anandamide uptake by human endothelial cells and its regulation by nitric oxide. *J. Biol. Chem.*, **275**, 13484–13492.

Mackie, K., Devane, W.A. and Hille, B. (1993). Anandamide, an endogenous cannabinoid, inhibits calcium currents as a partial agonist in N18 neuroblastoma cells. *Mol. Pharmacol.*, **44**, 498–503.

Mackie, K. and Hille, B. (1992). Cannabinoids inhibit N-type calcium channels in neuroblastoma-glioma cells. *Proc. Natl. Acad. Sci. U.S.A.*, **89**, 3825-3829.

Mackie, K., Lai, Y., Westenbroek, R. and Mitchell, R. (1995). Cannabinoids activate an

inwardly rectifying potassium conductance and inhibit Q-type calcium currents in AtT20 cells transfected with rat brain cannabinoid receptor. *J. Neurosci.,* **15**, 6552–6561.

MacLennan, S.J., Reynen, P.H., Kwan, J. and Bonhaus, D.W. (1998). Evidence for inverse agonism of SR141716A at human recombinant cannabinoid CB_1 and CB_2 receptors. *Br. J. Pharmacol.,* **124**, 619–622.

Madden, D. R. (2002). The structure and function of glutamate receptor ion channels. *Nat. Rev. Neurosci.*, **3**, 91−101.

Mahmoudian, M. (1997). The cannabinoid receptor: computer-aided molecular modeling and docking of ligand. *J. Mol. Graph. Model.*, **15**, 149-153.

Mailleux, P., Parmentier, M. and Vanderhaeghen, J.-J. (1992). Distribution of cannabinoid receptor messenger RNA in the human brain: an *in situ* hybridization histochemistry with oligonucleotides. *Neurosci. Lett.,* **143**, 200–204.

Mailleux, P. and Vanderhaeghen, J.J. (1992). Distribution of neuronal cannabinoid receptor in the adult rat brain: a comparative receptor binding radioautography and in situ hybridization histochemistry. *Neuroscience*, **48**, 655-668.

Maingret, F., Patel, A. J., Lazdunski, M. and Honore, E. (2001). The endocannabinoid anandamide is a direct and selective blocker of the background $K(^{+})$ channel TASK-1. *EMBO J.*, **20**, 47−54.

Mang, C.F., Erbelding, D. and Kilbinger, H. (2001). Differential effects of anandamide on acetylcholine release in the guinea-pig ileum mediated via vanilloid and non-CB_1 cannabinoid receptors. *Br. J. Pharmacol.*, **134**, 161-167.

Mansour, A., Khachaturian, H., Lewis, M.E., Akil, H. and Watson, S.J. (1988). Anatomy of CNS opioid receptors. *Trends Neurosci.*, **11**, 308-314.

Manzanares, J., Corchero, J., Romero, J., Fernandez-Ruiz, J.J., Ramos, A. and Fuentes, J.A. (1999). Pharmacological and biochemical interactions between opioids and
cannabinoids. *Trends Pharmacol. Sci.*, **20**, 287–294.

Mathon, D.S., Kamal, A., Smidt, M.P. and Ramakers, G.M. (2003). Modulation of cellular activity and synaptic transmission in the ventral tegmental area. *Eur. J. Pharmacol.*, **480**, 97-115.

Martin, B.M., Stevenson, L.A., Pertwee, R.G., Breivogal, C.S., Williams, W., Mahadevan, A. and Razdan, R. (2002). Agonists and silent antagonists in a series of cannabinoid sulfonamides. 12th Annual Symposium on the Cannabinoids, Burlington, Vermont, International Cannabinoid Research Society, page 2.

Martin, W.R. (1979). History and development of mixed opioid agonists, partial agonists and antagonists. *Br. J. Clin. Pharmacol.*, **7**, 273S-279S.

Mas-Nieto, M., Pommier, B., Tzavara, E.T., Caneparo, A., Da Nascimento, S., Le Fur, G., Roques, B.P. and Noble, F. (2001). Reduction of opioid dependence by the CB_1 antagonist SR141716A in mice: evaluation of the interest in pharmacotherapy of opioid addiction. *Br. J. Pharmacol.*, **132**, 1809–1816.

Massi, P., Vaccani, A., Romorini, S. and Parolaro, D. (2001). Comparative characterization in the rat of the interaction between cannabinoids and opiates for their immunosoppressive and analgesic effects. *J. Neuroimmunol.*, **117**, 116–124.

Mathison, R., Ho, W., Pittman, Q.J., Davison, J.S. and Sharkey, K.A. (2004). Effects of cannabinoid receptor-2 activation on accelerated gastrointestinal transit in lipopolysaccharide-treated rats. *Br. J. Pharmacol.*, **142**, 1247-1254.

Matsuda, L.A., Bonner, T.I. and Lolait, S.J. (1993). Localization of cannabinoid receptor messenger RNA in rat brain. *J. Comp. Neurol.*, **327**, 535–550.

Matsuda, L.A., Lolait, S.J., Brownstein, M.J., Young, A.C. and Bonner, T.I. (1990). Structure of a cannabinoid receptor and functional expression of the cloned cDNA. *Nature,* **346**, 561-564.

McAllister, S.D., Griffin, G., Satin, L.S. and Abood, M.E. (1999). Cannabinoid receptors can activate and inhibit G protein-coupled inwardly rectifying potassium channels in a *Xenopus* oocyte expression system. *J. Pharmacol. Exp. Ther.*, **291**, 618-626.

McFadzean, I. and Docherty, R.J. (1989). Noradrenaline- and Enkephalin-Induced Inhibition of Voltage-Sensitive Calcium Currents in NG108-15 Hybrid Cells. *Eur. J. Neurosci.*, **1**, 141-147.

McKinney, M.K. and Cravatt, B.F. (2005). Structure and function of fatty acid amide hydrolase. *Annu. Rev. BioChem.*, **74**, 411-432.

Mechoulam, R. (1986). Interview with Prof. Raphael Mechoulam, codiscoverer of THC. Interview by Stanley Einstein. *Int. J. Addict.* **21**, 579-87.

Mechoulam, R., Ben-Shabat, S., Hanus, L., Ligumsky, M., Kaminski, N.E., Schatz, A.R., Gopher, A., Almog, S., Martin, B.R., Compton, D.R., Pertwee, R.G., Griffin, G., Bayewitch, M., Barg, J. and Vogel, Z. (1995). Identification of an endogenous 2-monoglyceride, present in canine gut, that binds to cannabinoid receptors. *Biochem. Pharmacol.*, **50**, 83–90.

Mechoulam, R. and Gaoni, Y. (1967). The absolute configuration of Δ^1-tetrahydrocannabinol, the major active constituent of hashish. *Tetrahedron Lett.*, **12**, 1109-1111.

Melvin, L.S., Milne, G.M., Johnson, M.R., Subramaniam, B., Wilken, G.H. and Howlett, A.C. (1993). Structure-activity relationships for cannabinoid receptor-binding and analgesic activity: studies of bicyclic cannabinoid analogs. *Mol. Pharmacol.*, **44**, 1008–1015.

Mezey, E., Toth, Z.E., Cortright, D.N., Arzubi, M.K., Krause, J.E., Elde, R., Guo, A., Blumberg, P.M. and Szallasi, A. (2000). Distribution of mRNA for vanilloid receptor subtype 1 (VR1), and VR1-like immunoreactivity, in the central nervous system of the rat and human. *Proc. Natl. Acad. Sci. U.S.A.*, **97**, 3655-3660.

Milligan, G. (2004). G protein-coupled receptor dimerization: function and ligand pharmacology. *Mol. Pharmacol.*, **66**, 1-7.

Molina-Holgado, F., Lledó, A. and Guaza, C. (1997). Anandamide suppresses nitric oxide and TNF-γ responses to Theiler's virus or endotoxin in astrocytes. *Neuroreport*, **8**, 1929–1933.

Molleman, A. (2003). *Patch Clamping: An Introductory Guide to Patch Clamp Electrophysiology*, John Wiley and Sons Ltd.

Mombouli, J.-V., Schaeffer, G., Holzmann, S., Kostner, G.M. and Graier, W.F. (1999).

Anandamide-induced mobilization of cytosolic Ca^{2+} in endothelial cells. *Br. J. Pharmacol.*, **126**, 1593–1600.

Mu, J., Zhuang, S.Y., Kirby, M.T., Hampson, R.E. and Deadwyler, S.A. (1999). Cannabinoid receptors differentially modulate potassium A and D currents in hippocampal neurons in culture. *J. Pharmacol. Exp. Ther.*, **291**(2), 893-902.

Mu, J., Zhuang, S.-Y., Hampson, R.E. and Deadwyler, S.A. (2000). Protein kinase dependent phosphorylation and cannabinoid receptor modulation of potassium A current (I_A) in cultured rat hippocampal neurons. *Pflugers Arch.*, 439, 541– 546.

Munro, S., Thomas, K.L. and Abu-Shaar, M. (1993). Molecular characterization of a peripheral receptor for cannabinoids. *Nature,* **365**(6441), 61-65.

Murthy, K.S. and Makhlouf, G.M. (1997). Differential coupling of muscarinic M_2 and M_3 receptors to adenylyl cyclases V/VI in smooth muscle. Concurrent M_2-mediated inhibition via $G_{\alpha i3}$ and M_3-mediated stimulation via $G_{\beta\gamma q}$. *J. Biol. Chem.*, **272**, 21317-21324.

Nauta, W.J., Smith, G.P., Faull, R.L. and Domesick, V.B. (1978). Efferent connections and nigral afferents of the nucleus accumbens septi in the rat. *Neuroscience*, **3**, 385-401.

Nava, F., Carta, G., Battasi, A.M. and Gessa, G.L. (2000). D_2 dopamine receptors enable Δ^9-tetrahydrocannabinol induced memory impairment and reduction of hippocampal extracellular acetylcholine concentration. *Br. J. Pharmacol.,* **130**, 1201-1210.

Navarro, M., Carrera, M.R., Fratta, W., Valverde, O., Cossu, G., Fattore, L., Chowen, J.A., Gomez, R., del Arco, I., Villanua, M.A., Maldonado, R., Koob, G.F. and Rodriguez de Fonseca, F. (2001). Functional interaction between opioid and cannabinoid receptors in drug self-administration. *J. Neurosci.*, **21**, 5344-5350.

Navarro, M., Fernandez-Ruiz, J.J., de Miguel, R., Hernandez, M.L., Cebeira, M. and Ramos, J.A. (1993). An acute dose of Δ^9-tetrahydrocannabinol affects behavioral and neurochemical indices of mesolimbic dopaminergic activity. *Behav. Brain Res.*, **57**, 37-46.

Neher, E. and Sakmann, B. (1976). Single-channel currents recorded from membrane of denervated frog muscle fibres. *Nature*, **260**, 799-802.

Netzeband, J.G., Conroy, S.M., Parsons, K.L. and Gruol, D.L. (1999). Cannabinoids enhance NMDA-elicited Ca^{2+} signals in cerebellar granule neurons in culture. *J. Neurosci.*, **19**, 8765–8777.

Nicholson, R.A., Liao, C., Zheng, J., David, L.S., Coyne, L., Errington, A.C., Singh, G. and Lees, G. (2003). Sodium channel inhibition by anandamide and synthetic cannabimimetics in brain. *Brain Res.*, **978**, 194–204.

Nishi, S. and North, R.A. (1973). Intracellular recording from the myenteric plexus of the guinea-pig ileum. *J. Physiol. (Lond.),* **231**, 471-491.

Nishizaki, T., Matsuoka, T., Nomura, T. and Sumikawa, K. (1998). Modulation of ACh receptor currents by arachidonic acid. *Mol. Brain Res.,* **57**, 173-179.

North, R.A., Katayama, Y. and Williams, J.T. (1979). On the mechanism and site of action of enkephalin on single myentenic neurons. *Brain Res.*, **165**, 67-78.

North, R.A. and Tokimasa, T. (1987). Persistent calcium-sensitive potassium current and the resting properties of guinea-pig myenteric neurones. *J. Physiol. (Lond.),* **386**, 333-353.

North, R.A. and Tonini, M. (1977). The mechanism of narcotic analgesics in the guinea-pig ileum. *Br. J. Pharmacol.*, **61**, 541-549.

North, R.A. and Williams, J.T. (1977). Extracellular recording from the guinea-pig myenteric plexus and the action of morphine. *Eur. J. Pharmacol.*, **45**, 23-33.

Nye, J.S., Seltzman, H.H., Pitt, C.G. and Snyder, S.H. (1985). High-affinity cannabinoid binding sites in brain membranes labeled with [^{3}H]-5'-trimethylammonium delta 8-tetrahydrocannabinol. *J. Pharmacol. Exp. Ther.,* **234**, 784-791.

O'Shaughnessy, W.B. (1839). On the Preparation of the Indian Hemp or Gunja. *Transactions of the Medical and Physical Society of Bengal*, 421-461

Offertáler, L., Mo, F.M., Batkai, S., Liu, J., Begg, M., Razdan, R.K,. Martin, B.R., Bukoski, R.D. and Kunos, G. (2003). Selective ligands and cellular effectors of a G protein-coupled endothelial cannabinoid receptor. *Mol. Pharmacol.*, **63**, 699-705.

Oliver, D., Lien, C. C., Soom, M., Baukrowitz, T., Jonas, P. and Fakler, B. (2004). Functional conversion between A-type and delayed rectifier K^+ channels by membrane lipids. *Science*, **304**, 265−270.

Oz, M. (2006). Receptor-independent effects of endocannabinoids on ion channels. *Curr. Pharm. Des.* **12**, 227-239.

Oz, M., Jackson, S., Woods, A., Morales, M. and Zhang, L. (2005). Additive effects of endogenous cannabinoid anandamide and ethanol on alpha7-nicotinic acetylcholine receptor-mediated responses in *Xenopus* oocytes. *J. Pharmacol. Exp. Ther.*, **313**, 1272−1280.

Oz, M., Ravindran, A., Diaz-Ruiz, O., Zhang, L. and Morales, M. (2003). The endogenous cannabinoid anandamide inhibits α_7 nicotinic acetylcholine receptor-mediated responses in *Xenopus* oocytes. *J. Pharmacol. Exp. Ther.*, **306**, 1003-1010.

Oz, M., Tchugunova, Y. and Dunn, S. M. J. (2000). Endogenous cannabinoid anandamide directly inhibits voltage-dependent calcium fluxes in rabbit T-tubule membrane preparations. *Eur. J. Pharmacol.*, **404**, 13−20.

Oz, M., Zhang, L. and Morales, M. (2002). Endogenous cannabinoid, anandamide acts as a non-competitive inhibitor on 5-HT_3 receptor-mediated responses in *Xenopus* oocytes. *Synapse*, **46**, 150−156.

Oz, M., Zhang, L., Ravindran, A., Morales, M. and Lupica, C.R. (2004). Differential effects of endogenous and synthetic cannabinoids on α_7-nicotinic acetylcholine receptor-mediated responses in Xenopus *oocytes*. *J. Pharmacol. Exp. Ther.*, **310**, 1152-1160.

Pacheco, M., Childers, S.R., Arnold, R., Casiano, F. and Ward, S.J. (1991). Aminoalkylindoles: actions on specific G-protein-linked receptors. *J. Pharmacol. Exp. Ther.*, **257**, 170–183.

Pacheco, M.A., Ward, S.J. and Childers, S.R. (1993). Identification of cannabinoid receptors in cultures of rat cerebellar granule cells. *Brain Res.*, **603**, 102-110.

Pan, X., Ikeda, S.R. and Lewis, D.L. (1996). Rat brain cannabinoid receptor modulates
N-type Ca^{2+} channels in a neuronal expression system. *Mol. Pharmacol.*, **49**, 707–714.

Pan, X., Ikeda, S.R. and Lewis, D.L. (1998). SR 141716A acts as an inverse agonist to increase neuronal voltage-dependent Ca^{2+} currents by reversal of tonic CB_1 cannabinoid receptor activity. *Mol. Pharmacol.*, **54,** 1064–1072.

Parsons, S.M., Prior, C. and Marshall, I.G. (1993). Acetylcholine transport, storage, and release. *Int. Rev. Neurobiol.*, **35**, 279-390.

Pate, D.W. (1999). Anandamide structure-activity relationships and mechanisms of action on intraocular pressure in the normotensive rabbit model. Department of Pharmaceutical Chemistry, University of Kuopio, Finland.

Patel, S. and Hillard, C.J. (2003). Cannabinoid-induced Fos expression within A10 dopaminergic neurons. *Brain Res.*, **963**, 15-25.

Paton, W.D. (1957). The action of morphine and related substances on contraction and on acetylcholine output of coaxially stimulated guinea-pig ileum. *Br. J. Pharmacol.*, **12**, 119-127.

Paton, W.D. and Zar M.A. (1968). The origin of acetylcholine released from guinea-pig intestine and longitudinal muscle strips. *J. Physiol. (Lond.),* **194**, 13-33.

Pennartz, C.M., Boeijinga, P.H., Kitai, S.T. and Lopes da Silva, F.H. (1991). Contribution of NMDA receptors to postsynaptic potentials and paired-pulse facilitation in identified neurons of the rat nucleus accumbens in vitro. *Exp. Brain Res.*, **86**, 190-198.

Perrier, J. F., Alaburda, A. and Hounsgaard, J. (2003). 5-HT_{1A} receptors increase excitability of spinal motoneurons by inhibiting a TASK-1-like K^+ current in the adult turtle. *J. Physiol. (Lond.),* **548**, 485–492.

Pertwee, R.G. (1997). Pharmacology of cannabinoid CB_1 and CB_2 receptors. *Pharmacol. Ther.,* **74**, 129-180.

Pertwee, R.G. (1999). Pharmacology of cannabinoid receptor ligands. *Curr. Med. Chem.*, **6**, 635–664.

Pertwee, R.G. (2001). Cannabinoids and the gastrointestinal tract. *Gut.* **48**, 859-867.

Pertwee, R.G. (2004). Novel pharmacological targets for cannabinoids. *Curr. NeuroPharmacol.*, **2**(1), 9-30.

Pertwee, R.G. (2005). Inverse agonism and neutral antagonism at cannabinoid CB_1 receptors. *Life Sci.* **76**, 1307-1324.

Pertwee, R.G. (2005). Pharmacological actions of cannabinoids. *Handb. Exp. Pharmacol.*, **168,** 1-51.

Pertwee, R.G., Fernando, S.R., Nash, J.E. and Coutts, A.A. (1996). Further evidence for the presence of cannabinoid CB_1 receptors in guinea-pig small intestine. *Br. J. Pharmacol.*, **118**, 2199-2205.

Pertwee, R.G., Griffin, G., Fernando, S.R., Li, X., Hill, A. and Makriyannis, A. (1995). AM630, a competitive cannabinoid receptor antagonist. *Life Sci.*, **56**, 1949-1955.

Pertwee, R.G., Stevenson, L.A., Elrick, D.B., Mechoulam, R. and Corbett, A.D. (1992). Inhibitory effects of certain enantiomeric cannabinoids in the mouse vas

deferens and the myenteric plexus preparation of guinea-pig small intestine. *Br. J. Pharmacol.*, **105**, 980-984.

Pfaffinger, P.J., Martin, J.M., Hunter, D.D., Nathanson, N.M. and Hille, B. (1985) GTP-binding proteins couple cardiac muscarinic receptors to a K channel. *Nature*, **317**, 536-538.

Pierce, K.L., Premont, R.T. and Lefkowitz, R.J. (2002). Seven-transmembrane receptors. *Nat. Rev. Mol. Cell Biol.*, **3**, 639-650.

Pistis, M., Porcu, G., Melis, M., Diana, M. and Gessa, G.L. (2001). Effects of cannabinoids on prefrontal neuronal responses to ventral tegmental area stimulation. *Eur. J. Neurosci.*, **14**, 96-102.

Poling, J. S., Rogawski, M. A., Salem, N. and Vicini, S. (1996). Anandamide, an endogenous cannabinoid inhibits Shaker-related voltage-gated K^+ channels. *Neuropharmacology*, **35**, 983–991.

Poonyachoti, S., Kulkarni-Narla, A. and Brown, D.R. (2002). Chemical coding of neurons expressing δ- and μ-opioid receptor and type I vanilloid receptor immunoreactivities in the porcine ileum. *Cell. Tissue Res.*, **307**, 23–33.

Porter, A.C., Sauer, J.M., Knierman, M.D., Becker, G.W., Berna, M.J., Bao, J., Nomikos, G.G., Carter, P., Bymaster, F.P., Leese, A.B. and Felder, C.C. (2002).

Characterization of a novel endocannabinoid, virodhamine, with antagonist activity at the CB_1 receptor. *J. Pharmacol. Exp. Ther.*, **301**, 1020-1024.

Prevot, V., Rialas, C.M., Croix, D., Salzet, M., Dupouy, J.-P., Poulain, P., Beauvillain, J.-C. and Stefano, G.B. (1998). Morphine and anandamide coupling to nitric oxide stimulates GnRH and CRF release from rat median eminence: neurovascular regulation. *Brain Res.*, **790**, 236–244.

Price, T. J., Patwardhan, A., Akopian, A. N., Hargreaves, K. M. and Flores, C. M. (2004). Cannabinoid receptor-independent actions of the aminoalkylindole WIN55,212-2 on trigeminal sensory neurons. *Br. J. Pharmacol.*, **142**, 257−266.

Pryor, G.T., Larsen, F.F., Husain, S. and Braude, M.C. (1978). Interactions of Δ^9-tetrahydrocannabinol with d-amphetamine, cocaine, and nicotine in rats. *Pharmacol. Biochem. Behav.*, **8**, 295-318.

Reynolds, J.R. (1890). Therapeutic Uses and Toxic Effects of Cannabis Indica, *Lancet*, **1**, 637-638.

Revuelta, A.V., Moroni, F., Cheney, D.L. and Costa, E. (1978). Effect of cannabinoids on the turnover rate of acetylcholine in rat hippocampus, striatum and cortex. *Naunyn Schmiedebergs Arch. Pharmacol.*, **304**, 107-110.

Rhee, M.H., Vogel, Z., Barg, J., Bayewitch, M., Levy, R., Hanus, L., Breuer, A. and Mechoulam, R. (1997). Cannabinol derivatives: binding to cannabinoid receptors and inhibition of adenylylcyclase. *J. Med. Chem.,* **40**, 3228-3233.

Rinaldi-Carmona, M., Barth, F., Heaulme, M., Shire, D., Calandra, B., Congy, C., Martinez, S., Maruani, J., Neliat, G., Caput, D., Ferrarab, P., Soubriéa, P., Brelièrea, J.C. and Le Fura, G. (1994). SR141716A, a potent and selective antagonist of the brain cannabinoid receptor. *FEBS Lett.,* **350**. 240-244.

Rinaldi-Carmona, M., Barth, F., Millan, J., Derocq, J.-M., Casellas, P., Congy, C., Oustric, D., Sarran, M., Bouaboula, M., Calandra, B., Portier, M., Shire, D., Brelière, J.-C. and Le Fur, G. (1998). SR 144528, the first potent and selective antagonist of the CB_2 cannabinoid receptor. *J. Pharmacol. Exp. Ther.,* **284**, 644–650.

Robbe, D., Alonso, G., Duchamp, F., Bockaert, J. and Manzoni, O.J. (2001). Localization and mechanisms of action of cannabinoid receptors at the glutamatergic synapses of the mouse nucleus accumbens. *J. Neurosci.*, **21**, 109-116.

Robbe, D., Kopf, M., Remaury, A., Bockaert, J. and Manzoni, O.J. (2002). Endogenous cannabinoids mediate long-term synaptic depression in the nucleus accumbens. *Proc. Natl. Acad. Sci. U.S.A.*, **99**, 8384-8388.

Roberts, J.C., Davis, J.B. and Benham, C.D. (2004). [^{3}H]Resiniferatoxin autoradiography in the CNS of wild-type and TRPV1 null mice defines TRPV1 (VR-1) protein distribution. *Brain Res.*, **995**, 176-183.

Roberts, L.A., Christie, M.J. and Connor, M. (2002). Anandamide is a partial agonist at native vanilloid receptors in acutely isolated mouse trigeminal sensory neurons. *Br. J. Pharmacol.*, **137**, 421-428.

Robson, P. (2001). Therapeutic aspects of cannabis and cannabinoids. *Br. J. Psychiatry*, **178**, 107–115.

Rodriguez De Fonseca, F., Fernandez-Ruiz, J.J., Murphy, L.L., Cebeira, M., Steger, R.W., Bartke, A. and Ramos, J.A. (1992). Acute effects of Δ^9-tetrahydrocannabinol on dopaminergic activity in several rat brain areas. *Pharmacol. Biochem. Behav.*, **42**, 269-275.

Rodriguez, J.J., Mackie, K. and Pickel, V.M. (2001). Ultrastructural localization of the CB_1 cannabinoid receptor in μ-opioid receptor patches of the rat Caudate putamen nucleus. *J. Neurosci.*, **21**, 823-833.

Ross, R.A., Brockie, H.C., Fernando, S.R., Saha, B., Razdan, R.K. and Pertwee R.G. (1998). Comparison of cannabinoid binding sites in guinea-pig forebrain and small intestine. *Br. J. Pharmacol.*, **125**, 1345-1351.

Ross, R.A., Gibson, T.M., Brockie, H.C., Leslie, M., Pashmi, G., Craib, S.J., Di Marzo, V. and Pertwee, R.G. (2001). Structure-activity relationship for the endogenous cannabinoid, anandamide and certain of its analogues at vanilloid receptors in transfected cells and vas deferens. *Br. J. Pharmacol.*, **132**, 631–640.

Ross, R.A., Gibson, T.M., Stevenson, L.A., Saha, B., Crocker, P., Razdan, R.K. and Pertwee, R.G. (1999). Structural determinants of the partial agonist-inverse agonist properties of 6'-azidohex-2'-yne-delta8-tetrahydrocannabinol at cannabinoid receptors. *Br. J. Pharmacol.,* **128**, 735-743.

Roth, S.H. (1978). Stereospecific presynaptic inhibitory effect of Δ^9-tetrahydrocannabinol on cholinergic transmission in the myenteric plexus of the guinea pig. *Can. J. Physiol. Pharmacol.,* **56**, 968-975.

Rueda, D., Navarro, B., Martinez-Serrano, A., Guzman, M. and Galve-Roperh, I. (2002). The endocannabinoid anandamide inhibits neuronal progenitor cell differentiation through attenuation of the Rap1/B-Raf/ERK pathway. *J. Biol. Chem.*, **277**, 46645-46650.

Rugiero, F., Gola, M., Kunze, W.A., Reynaud, J.C., Furness, J.B. and Clerc, N. (2002). Analysis of whole-cell currents by patch clamp of guinea-pig myenteric neurones in intact ganglia. *J. Physiol. (Lond.),* **538**, 447-463.

Rugiero, F., Mistry, M., Sage, D., Black, J.A., Waxman, S.G., Crest, M., Clerc, N., Delmas, P. and Gola, M. (2003). Selective expression of a persistent tetrodotoxin-resistant Na^+ current and NaV1.9 subunit in myenteric sensory neurons. *J. Neurosci.*, **23**, 2715-2725.

Sade, H., Muraki, K., Ohya, S., Hatano, N. and Imaizumi, Y. (2006). Activation of large-conductance Ca^{2+} activated K^+ channels by cannabinoids. *Am. J. Physiol. Cell. Physiol.*, **290**, C77–C86.

Salio, C., Fischer, J., Franzoni, M.F., Mackie, K., Kaneko, T. and Conrath, M. (2001). CB_1-cannabinoid and μ-opioid receptor co-localization on postsynaptic target in the rat dorsal horn. *Neuroreport*, **12**, 3689–3692.

Sánchez, C., Galve-Roperh, I., Canova, C., Brachet, P. and Guzman, M., (1998a). Δ^9-Tetrahydrocannabinol induces apoptosis in C6 glioma cells. *FEBS Lett.*, **436**, 6–10.

Sánchez, C., Galve-Roperh, I., Rueda, D. and Guzman, M. (1998b). Involvement of sphingomyelin hydrolysis and the mitogen activated protein kinase cascade in the Δ^9-tetrahydrocannabinol-induced stimulation of glucose metabolism in primary astrocytes. *Mol. Pharmacol.*, **54**, 834–843.

Sánchez, M.G., Ruiz-Llorente, L., Sanchez, A.M. and Diaz-Laviada, I., (2003). Activation of phosphoinositide 3-kinase/PKB pathway by CB_1 and CB_2 cannabinoid receptors expressed in prostate PC-3 cells. Involvement in Raf-1 stimulation and NGF induction. *Cell. Signal.*, **15**, 851– 859.

Sanchez, J.F., Krause, J.E. and Cortright, D.N. (2001). The distribution and regulation of vanilloid receptor VR1 and VR1 5' splice variant RNA expression in rat. *Neuroscience*, **107**, 373-381.

Savinainen, J.R., Jarvinen, T., Laine, K. and Laitinen, J.T. (2001). Despite substantial degradation, 2-arachidonoylglycerol is a potent full efficacy agonist mediating CB_1 receptor-dependent G-protein activation in rat cerebellar membranes. *Br. J. Pharmacol.*, **134**, 664–672.

Savinainen, J.R., Kokkola, T., Salo, O.M., Poso, A., Jarvinen, T. and Laitinen, J.T. (2005). Identification of WIN55212-3 as a competitive neutral antagonist of the human cannabinoid CB_2 receptor. *Br. J. Pharmacol.*, **145**, 636-645.

Sawyer, G.W., Lambrecht, G. and Ehlert, F.J. (2000). Functional role of muscarinic M_2 receptors in alpha,beta-methylene ATP induced, neurogenic contractions in guinea-pig ileum. *Br. J. Pharmacol.*, **129**, 1458-1464.

Sawzdargo, M., Nguyen, T., Lee, D.K., Lynch, K.R., Cheng, R., Heng, H.H., George, S.R. and O'Dowd, B.F. (1999). Identification and cloning of three novel human G protein-coupled receptor genes GPR52, PsiGPR53 and GPR55: GPR55 is extensively expressed in human brain. *Brain Res. Mol. Brain Res.*, **64**, 193-198.

Schatz, A.R., Lee, M., Condie, R.B., Pulaski, J.T. and Kaminski, N.E. (1997). Cannabinoid receptors CB_1 and CB_2: a characterization of expression and adenylate cyclase modulation within the immune system. *Toxicol. Appl. Pharmacol.*, **142**, 278–287.

Schaumann, W. (1955). The paralysing action of morphine on the guinea-pig ileum. *Br. J. Pharmacol.*, **10**, 456-461.

Schaumann, W. (1957). Inhibition by morphine of the release of acetylcholine from the intestine of the guinea-pig. *Br. J. Pharmacol.*, **12**, 115-118.

Schweitzer, P. (2000). Cannabinoids decrease the K^+ M-current in hippocampal CA1 neurons. *J. Neurosci.* **20**, 51– 58.

Selley, D.E., Stark, S., Sim, L.J. and Childers, S.R. (1996). Cannabinoid receptor stimulation of guanosine-5'-O-(3-[^{35}S]thio)triphosphate binding in rat brain membranes. *Life Sci.,* **59**, 659–668.

Shapira, M., Gafni, M. and Sarne, Y. (1998). Independence of, and interactions between, cannabinoid and opioid signal transduction pathways in N18TG2 cells. *Brain Res.*, **806**, 26-35.

Shapira, M., Vogel, Z. and Sarne, Y. (2000). Opioid and cannabinoid receptors share a common pool of GTP-binding proteins in cotransfected cells, but not in cells which endogenously coexpress the receptors. *Cell. Mol. Neurobiol.*, **20**, 291-304.

Shen, M. and Thayer, S.A. (1998). The cannabinoid agonist WIN55,212-2 inhibits calcium channels by receptor-mediated and direct pathways in cultured rat hippocampal neurons. *Brain Res.,* **783**, 77– 84.

Shiamsue, K., Urushidani, T., Hagiwara, M. and Nagao, T. (1996). Effects of anandamide and arachidonic acid on specific binding of (+)-PN200-110, diltiazem

and (−)-desmethoxyverapamil to L-type Ca^{2+} channel. *Eur. J. Pharmacol.*, **296**, 347–350.

Shim, J.Y., Welsh, W.J. and Howlett, A.C. (2003). Homology model of the CB_1 cannabinoid receptor: sites critical for nonclassical cannabinoid agonist interaction. *Biopolymers*, **71**, 169-189.

Shire, D., Calandra, B., Rinaldi-Carmona, M., Oustric, D., Pessègue, B., Bonnin-Cabanne, O., Le Fur, G., Caput, D. and Ferrara, P. (1996). Molecular cloning, expression and function of the murine CB_2 peripheral cannabinoid receptor. *Biochim. Biophys. Acta.* **1307**, 132–136.

Shire, D., Carillon, C., Kaghad, M., Calandra, B., Rinaldi-Carmona, M., Le Fur, G., Caput, D. and Ferrara, P. (1995). An amino-terminal variant of the central cannabinoid

receptor resulting from alternative splicing. *J. Biol. Chem.*, **270**, 3726–3731.

Showalter, V.M., Compton, D.R., Martin, B.R. and Abood, M.E. (1996). Evaluation of binding in a transfected cell line expressing a peripheral cannabinoid receptor (CB_2): identification of cannabinoid receptor subtype selective ligands. *J. Pharmacol. Exp. Ther.*, **278**, 989-999.

Slipetz, D.M., O'Neill, G.P., Favreau, L., Dufresne, C., Gallant, M., Gareau, Y. Guay, D., Labelle, M. and Metters, K.M. (1995). Activation of the human peripheral

cannabinoid receptor results in inhibition of adenylyl cyclase. *Mol. Pharmacol.*, **48**, 352–361.

Smart, D., Gunthorpe, M.J., Jerman, J.C., Nasir, S., Gray, J., Muir, A.I., Chambers, J.K., Randall, A.D. and Davis, J.B. (2000). The endogenous lipid anandamide is a full agonist at the human vanilloid receptor (hVR1). *Br. J. Pharmacol.*, **129**, 227-230.

Sones, W.R., Parsons, M.E. and Molleman, A. (2006). Cannabinoid modulation of voltage-gated calcium channels in guinea-pig myenteric neurons. 16th Annual Symposium on the Cannabinoids, Burlington, Vermont, International Cannabinoid Research Society, page 182.

Spanagel, R. and Weiss, F. (1999). The dopamine hypothesis of reward: past and current status. *Trends Neurosci.*, **22**, 521-527.

Starodub, A.M. and Wood, J.D. (1999). Selectivity of omega-CgTx-MVIIC toxin from Conus magus on calcium currents in enteric neurons. *Life Sci.*, **64**, 305-310.

Stefano, G.B., Liu, Y. and Goligorsky, M.S. (1996). Cannabinoid receptors are coupled to nitric oxide release in invertebrate immunocytes, microglia and human monocytes. *J. Biol. Chem.*, **271**, 19238–19242.

Stefano, G.B., Salzet, M., Magazine, H.I. and Bilfinger, T.V. (1998). Antagonism of LPS and IFN-γ induction of iNOS in human saphenous vein endothelium by

morphine and anandamide by nitric oxide inhibition of adenylate cyclase. *J. Cardiovasc. Pharmacol.*, **31**, 813–820.

Stefano, G.B., Salzet, B., Rialas, C.M., Pope, M., Kustka, A., Neenan, K., Pryor, S. and Salzet, M. (1997a). Morphine- and anandamide-stimulated nitric oxide production inhibits presynaptic dopamine release. *Brain Res.*, **763**, 63–68.

Stefano, G.B., Salzet, B. and Salzet, M. (1997b). Identification and characterization of the leech CNS cannabinoid receptor: coupling to nitric oxide release. *Brain Res.*, **753**, 219–224.

Steffens, M., Zentner, J., Honegger, J. and Feuerstein, T.J. (2005). Binding affinity and agonist activity of putative endogenous cannabinoids at the human neocortical CB_1 receptor. *Biochem. Pharmacol.*, **69**, 169-178.

Steffensen, S.C., Svingos, A.L., Pickel, V.M. and Henriksen, S.J. (1998). Electrophysiological characterization of GABAergic neurons in the ventral tegmental area. *J. Neurosci.*, **18**, 8003-8015.

Sternini, C., Patierno, S., Selmer, I.S. and Kirchgessner, A. (2004). The opioid system in the gastrointestinal tract. *Neurogastroenterol. Motil.*, **16**, 3-16.

Sternini, C., Spann, M., Anton, B., Keith, D.E. Jr, Bunnett, N.W., von Zastrow, M., Evans. C, and Brecha, N.C. (1996). Agonist-selective endocytosis of μ opioid receptor by neurons in vivo. *Proc. Natl. Acad. Sci. U.S.A.*, **93**, 9241–9246.

Sternini, C., Spann, M. and De Giorgio, R. (1995). Cellular localization of the mu opioid receptor in the rat enteric nervous system. *Analgesia*, **1**, 762–765.

Storr, M., Gaffal, E., Saur, D., Schusdziarra, V. and Allescher, H.D. (2002). Effect of cannabinoids on neural transmission in rat gastric fundus. *Can. J. Physiol. Pharmacol.*, **80**, 67-76.

Straiker, A., Stella, N., Piomelli, D., Mackie, K., Karten, H.J. and Maguire, G. (1999). Cannabinoid CB_1 receptors and ligands in vertebrate retina: localisation and function of an endogenous signalling system. *Proc. Natl. Acad. Sci. U.S.A.*, **96**, 14565–14570.

Straiker, A. and Sullivan, J.M. (2003). Cannabinoid receptor activation differentially modulates ion channels in photoreceptors of the tiger salamander. *J. Neurophysiol.*, **89**, 2647-2654.

Sugiura, T., Kondo, S., Kishimoto, S., Miyashita, T., Nakane, S., Kodaka, T., Suhara, Y., Takayama, H. and Waku, K. (2000). Evidence that 2-arachidonoylglycerol but not N-palmitoylethanolamine or anandamide is the physiological ligand for the cannabinoid CB_2 receptor: comparison of the agonistic activities of various cannabinoid receptor ligands in HL-60 cells. *J. Biol. Chem.*, **275**, 605–612.

Sugiura, T., Kodaka, T., Kondo, S., Nakane, S., Kondo, H., Waku, K., Ishima, Y., Watanabe, K., Yamamoto, I. (1997). Is the cannabinoid CB_1 receptor a 2-

arachidonoylglycerol receptor? Structural requirements for triggering a Ca^{2+} transient in NG108-15 cells. *J. BioChem.*, **122**, 890-895.

Sugiura, T., Kodaka, T., Kondo, S., Tonegawa, T., Nakane, S., Kishimoto, S., Yamashita, A. and Waku, K. (1996). 2-Arachidonoylglycerol, a putative endogenous cannabinoid receptor ligand, induces rapid, transient elevation of intracellular free Ca^{2+} in neuroblastoma x glioma hybrid NG108-15 cells. *Biochem. Biophys. Res. Commun.*, **229**, 58-64.

Sugiura, T., Kodaka, T., Nakane, S., Miyashita, T., Kondo, S., Suhara, Y., Takayama, H., Waku, K., Seki, C., Baba, N. and Ishima, Y. (1999). Evidence that the cannabinoid CB_1 receptor is a 2-arachidonoylglycerol receptor: structure-activity relationship of 2-arachidonoylglycerol ether-linked analogues and related compounds. *J. Biol. Chem.*, **274**, 2794–2801.

Sugiura, T., Kondo, S., Sukagawa, A., Nakane, S., Shinoda, A., Itoh, K., Yamashita, A. and Waku, K. (1995). 2-Arachidonoylglycerol: a possible endogenous cannabinoid receptor ligand in brain. *Biochem. Biophys. Res. Commun.*, **215**, 89–97.

Sun, H., Hejazi, N., Oz, M., and Zhang, L. (2005). Endogenous and exogenous cannabinoids potentiate glycine receptor-mediated responses through a CB receptor independent mechanism in *Xenopus* oocytes. *Soc. Neurosci. Abst.*, **742**.2.

Szabo, B., Muller, T. and Koch, H. (1999). Effects of cannabinoids on dopamine release in the corpus striatum and the nucleus accumbens in vitro. *J. Neurochem.*, **73**, 1084-1089.

Szabo, B., Siemes, S. and Wallmichrath, I. (2002). Inhibition of GABAergic neurotransmission in the ventral tegmental area by cannabinoids. *Eur. J. Neurosci.*, **15**, 2057-2061.

Szerb, J.C. (1982). Correlation between acetylcholine release and neuronal activity in the guinea-pig ileum myenteric plexus: effect of morphine. *Neuroscience*, **7**, 327-340.

Tanda, G. and Goldberg, S.R. (2003). Cannabinoids: reward, dependence, and underlying neurochemical mechanisms-a review of recent preclinical data. *Psychopharmacology (Berl.),* **169**, 115-134.

Tanda, G., Munzar, P. and Goldberg, S.R. (2000). Self-administration behavior is maintained by the psychoactive ingredient of marijuana in squirrel monkeys. *Nat. Neurosci.*, **3**, 1073–1074.

Tanda, G., Pontieri, F.E. and Di Chiara, G. (1997). Cannabinoid and heroin activation of mesolimbic dopamine transmission by a common μ_1 opioid receptor mechanism. *Science*, **276**, 2048-2050.

Tao, Q. and Abood, M.E. (1998). Mutation of a highly conserved aspartate residue in the second transmembrane domain of the cannabinoid receptors, CB_1 and CB_2, disrupts G-protein coupling. *J. Pharmacol. Exp. Ther.*, **285**, 651–658.

Tao, Q., McAllister, S.D., Andreassi, J., Nowell, K.W., Cabral, G.A., Hurst, D.P., Bachtel, K., Ekman, M.C., Reggio, P.H. and Abood, M.E. (1999). Role of a conserved lysine residue in the peripheral cannabinoid receptor (CB_2): evidence for subtype specificity. *Mol. Pharmacol.*, **55**, 605-613.

Thorpe, K. and Robb, P. (2006). Extent and trends. In: *Crime in England and Wales 2005/06*, (ed. Walker, A., Kershaw, C. and Nicholas, S.) pp. 13-33, Home Office statistical bulletins.

Tognetto, M., Amadesi, S., Harrison, S., Creminon, C., Trevisani, M., Carreras, M., Matera, M., Geppetti, P. and Bianchi, A. (2001). Anandamide excites central terminals of dorsal root ganglion neurons via vanilloid receptor-1 activation. *J. Neurosci.*, **21**, 1104–1109.

Tominaga, M., Caterina, M.J., Malmberg, A.B., Rosen, T.A., Gilbert, H., Skinner, K., Raumann, B.E., Basbaum, A.I. and Julius, D. (1998). The cloned capsaicin receptor integrates multiple pain-producing stimuli. *Neuron*, **21**, 531–543

Trendelenburg P. (1917). Physiologische und pharmakologische Versuche uber die Dunndarmperistaltik. *Arch. Exp. Pathol. Pharmakol.*, **81**, 55-129.

Tripathi, H.L., Vocci, F.J., Brase, D.A. and Dewey, W.L. (1987). Effects of cannabinoids on levels of acetylcholine and choline and on turnover rate of acetylcholine in various regions of the mouse brain. *Alcohol Drug Res.*, 7, 525-532.

Tsou, K., Brown, S., Saňudo-Peňa, M.C., Mackie, K. and Walker, J.M. (1998). Immunohistochemical distribution of cannabinoid CB_1 receptors in the rat central nervous system. *Neuroscience,* **83**, 393–411.

Tsunoo, A., Yoshii, M. and Narahashi, T. (1986). Block of calcium channels by enkephalin and somatostatin in neuroblastoma-glioma hybrid NG108-15 cells. *Proc. Natl. Acad. Sci. U.S.A.*, **83**, 9832-9836.

Turkanis, S.A., Karler, R. and Partlow, L.M. (1991a). Differential effects of Δ^9-tetrahydrocannabinol and its 11-hydroxy metabolite on sodium current in neuroblastoma cells. *Brain Res.*, **560**, 245-250.

Turkanis, S.A., Partlow, L.M. and Karler, R. (1991b) Delta-9-tetrahydrocannabinol depresses inward sodium current in mouse neuroblastoma cells. *Neuropharmacology*, **30**, 73-77.

Twitchell, W., Brown, S. and Mackie, K. (1997). Cannabinoids inhibit N- and P/Q type calcium channels in cultured rat hippocampal neurones. *J. Neurophysiol.*, **78**, 43-50.

Ueda, N. and Yamamoto, S. (2000). Anandamide amidohydrolase (fatty acid amide hydrolase). *Prostaglandins Leukot. Essent. Fatty Acids*, **66**, 19-28.

Valjent, E., Mitchell, J.M., Besson, M.J., Caboche, J. and Maldonado. R. (2002). Behavioural and biochemical evidence for interactions between Δ^9-tetrahydrocannabinol and nicotine. *Br. J. Pharmacol.*, **135**, 564-578.

Valk, P., Verbakel, S., von Lindern, M., Lowenberg, B. and Delwel, R. (2000). Enhancement of erythropoietin-stimulated cell proliferation by Anandamide correlates with increased activation of the mitogen-activated protein kinases ERK1 and ERK2. *Hematol. J.*, **1**, 254-263.

Vallone, D., Picetti, R. and Borrelli, E. (2000). Structure and function of dopamine receptors. *Neurosci. Biobehav. Rev.*, **24**, 125-132.

Van den Bossche, I. and Vanheel, B. (2000). Influence of cannabinoids on the delayed rectifier in freshly dissociated smooth muscle cells of the rat aorta. *Br. J. Pharmacol.*, **131**, 85–93.

Van Sickle, M.D., Duncan, M., Kingsley, P.J., Mouihate, A., Urbani, P., Mackie, K., Stella, N., Makriyannis, A., Piomelli, D., Davison, J.S., Marnett, L.J., Di Marzo, V., Pittman, Q.J., Patel, K.D. and Sharkey, K.A. (2005). Identification and functional characterization of brainstem cannabinoid CB_2 receptors. *Science*, **310**, 329-332.

Varvel, S.A., Cichewicz, D.L. and Lichtman, A.H. (2004). Interactions between cannabionoids and opioids. In: *Recent Advances in Pharmacology and Physiology of Cannabinoids*, (ed. Tibor, W.) pp. 157– 182, Kerala, India Research Signpost Trivandrum-695 023.

Vasquez, C., Navarro-Polanco, R.A., Huerta, M., Trujillo, X., Andrade, F., Trujillo-Hernandez, B. and Hernandez, L. (2003). Effects of cannabinoids on endogenous K^+ and Ca^{2+} currents in HEK293 cells. *Can. J. Physiol. Pharmacol.*, **81**, 436–442.

Velasco, G., Galve-Roperh, I., Sanchez, C., Blazquez, C., Haro, A. and Guzman, M. (2005). Cannabinoids and ceramide: two lipids acting hand-by-hand. *Life Sci.*, **77**, 1723-1731.

Venance, L., Sagan, S. and Giaume, C. (1997). (R)-methanandamide inhibits receptor-induced calcium responses by depleting internal calcium stores in cultured astrocytes. *Pflugers Arch.*, **434**, 147-149.

Viganò, D., Rubino, T. and Parolaro, D. (2005). Molecular and cellular basis of cannabinoid and opioid interactions. *Pharmacol. Biochem. Behav.*, **81**, 360-368.

Vizi, E.S. and Bartho, L. (1985). Presynaptic modulation by noradrenaline and an opioid of the substance P-induced release of ^{3}H-acetylcholine from the myenteric plexus. *Reg. Peptides*, **12**, 317-325.

Vizi, E.S., Ono, K., Adam-Vizi, V., Duncalf, D. and Foldes. F.F. (1984). Presynaptic inhibitory effect of Met-enkephalin on ^{14}C-acetylcholine release from the myenteric plexus and its interaction with muscarinic negative feedback inhibition. *J. Pharmacol. Exp. Ther.*, **230**, 493-499.

Vogalis, F., Harvey, J.R. and Furness, J.B. (2003). PKA-mediated inhibition of a novel K^+ channel underlies the slow after-hyperpolarization in enteric AH neurons. *J. Physiol.* **548**, 801-814.

Vogel, Z., Barg, J., Levy, R., Saya, D., Heldman, E. and Mechoulam, R. (1993). Anandamide, a brain endogenous compound, interacts specifically with cannabinoid receptors and inhibits adenylate cyclase. *J. Neurochem.*, **61**, 352-355.

Welch, S.P., Huffman, J.W. and Lowe, J. (1998). Differential blockade of the antinociceptive effects of centrally administered cannabinoids by SR141716A. *J. Pharmacol. Exp. Ther.*, **286**, 1301–1308.

Wenger, T., Ledent, C., Csernus, V. and Gerendai, I. (2001). The central cannabinoid receptor inactivation suppresses endocrine reproductive functions. *Biochem. Biophys. Res. Commun.*, **284**, 363–368.

Wartmann, M., Campbell, D., Subramanian, A., Burstein, S.H. and Davis, R.J. (1995). The MAP kinase signal transduction pathway is activated by the endogenous cannabinoid anandamide. *FEBS Lett.*, **359**, 133-136.

White, T.D. (1982). Release of ATP from isolated myenteric varicosities by nicotinic agonists. *Eur. J. Pharmacol.*, **79**, 333-334.

Williams, J.T., Christie, M.J. and Manzoni, O. (2001). Cellular and synaptic adaptations mediating opioid dependence. *Physiol. Rev.*, 81, 299–343.

Williamson, S., Pompolo, S. and Furness, J.B. (1996). GABA and nitric oxide synthase immunoreactivities are colocalized in a subset of inhibitory motor neurons of the guinea-pig small intestine. *Cell Tissue Res.*, **284,** 29–37.

Wright, K.L., Duncan, M. and Sharkey, K.A. (2008). Cannabinoid CB_2 receptors in the gastrointestinal tract; a regulatory system in states of inflammation. *Br. J. Pharmacol.*, **153**, 263−270.

Yagasaki, O., Takai, M. and Yanagiya, I. (1981). Acetylcholine release from the myenteric plexus of guinea-pig ileum by prostaglandin E1. *J. Pharm. Pharmacol.*, **33**, 521-525.

Yau, W.M., Dorsett, J.A. and Youther, M.L. (1986). Inhibitory peptidergic neurons: functional difference between somatoatatin and enkephalin in myenteric plexus. *Am. J. Physiol.*, **250**, G60-G63.

Yau, W.M., Lingle, P.F. and Youther, M.L. (1983b). Interaction of enkephalin and caerulein on guinea pig small intestine. *Am. J. Physiol.*, **244**, G65-G70.

Yau, W.M., Verdun, P.R. and Youther, M.L. (1983a). Neurotenain: a modulator of enteric cholinergic neurons in the guinea pig small intestine. *Eur. J. Pharmacol.*, **95**. 253-258.

Yunker, A.M. and Galligan, J.J. (1996). Endogenous NO inhibits NANC but not cholinergic neurotransmission to circular muscle of guinea pig ileum. *Am. J. Physiol. (Lond.),* **271**, G904-G912.

Zadina, J.E., Hackler, L., Ge, L.J. and Kastin, A.J. (1997). A potent and selective endogenous agonist for the -opiate receptor. *Nature*, **386**, 499–502.

Zhou, X., Ren, J., Brown, E., Schneider, D., Caraballo-Lopez, Y. and Galligan, J.J. (2002). Pharmacological properties of nicotinic acetylcholine receptors expressed by guinea pig small intestinal myenteric neurons. *J. Pharmacol. Exp. Ther.,* **302**, 889-897.

Zholos, A.V., Baidan, L.V. and Wood, J.D. (2002). Sodium conductance in cultured myenteric AH-type neurons from guinea-pig small intestine. *Auton. Neurosci.*, **96**, 93-102.

Zoratti, C., Kipmen-Korgun, D., Osibow, K., Malli, R. and Graier, W.F. (2003). Anandamide initiates Ca^{2+} signalling via CB_2 receptor linked to phospholipase C in calf pulmonary endothelial cells. *Br. J. Pharmacol.,* **140**, 1351–1362.

Zygmunt, P.M., Petersson, J., Andersson, D.A., Chuang, H., Sorgard, M., Di Marzo, V., Julius, D. and Hogestatt, E.D. (1999). Vanilloid receptors on sensory nerves mediate the vasodilator action of anandamide. *Nature,* **400**, 452-457.